Duchenne Muscular Dystrophy: RNA-based therapeutics and microRNA biology

Thomas C. Roberts

Thesis submitted for the degree of Doctor of Philosophy

Department of Physiology, Anatomy and Genetics, University of Oxford

Oriel College

17 September 2012

Declaration

The work presented in this thesis was undertaken at the Department of Physiology, Anatomy and Genetics, University of Oxford, between 2008 and 2011. All work presented is my own with the following exceptions. The microRNA microarray study was performed in collaboration with Edvard Smith and Emelie Blomberg at the Department of Laboratory Medicine, Karolinska Institutet, Sweden (section 3.2.1). Peptide-PMO conjugates were produced by Thibault Coursindel in the laboratory of Mike Gait at the MRC Laboratory of Molecular Biology in Cambridge. The Pip6e-PMO study was performed in collaboration with other members of the Wood laboratory; Caroline Godfrey, Graham McClorey and Corinne Betts (section 3.2.4). This work has not been submitted for any other degree at this university or any other institute of learning.

Acknowledgements

I am grateful for a Medical Research Council (MRC) doctoral training award which funded this DPhil. Additionally, this work was funded by the Muscular Dystrophy Campaign (MDC), Association Français contre les Myopathies (AFM) and a seed grant from ISIS Innovation.

In particular, I would like to thank Professor Matthew Wood. I could not have asked for a more supportive and encouraging PI. I am truly grateful for the friendly and open atmosphere that he has fostered in his laboratory, and the freedom he has granted me to pursue my ideas.

Graham McClorey has been an excellent supervisor and has spent much time discussing this work with me and helping to refine this thesis. Samir EL Andaloussi has taught me very much about oligonucleotides and his advice and discussion have greatly advanced this work. I am also grateful for the opportunity to work alongside Yiqi Seow and Chris Sibley, who set an incredibly high standard for what a student can accomplish during a DPhil.

I would like to thank my collaborators:
Edvard Smith, Emelie Blomberg, Mike Gait, Thibault Coursindel, Caroline Godfrey, Graham McClorey, Corrine Betts and Kevin Morris.

Especially I would like to those who helped me with accommodation when I was in San Diego; Kevin and Paula Morris, Stuart and Katie Knowling, Amanda Ackley and Per Johnsson.

I would also like to thank all the fantastic people at the Wood lab and our friends for their intellectual support and excellent company. Especially, I thank Graham McClorey, Janine Scholefield, Tom Merritt, Lydia Alvarez-Erviti, Miguel Varela, Suzan Hammond, Taeyoung Koo, Helen Curtis, Chris Sibley, Yiqi Seow, Samir EL Andaloussi, Martina Halleger, Mary McMenamin, Caroline Godfrey, Corrine Betts, Andrew Douglas, Lauren Watson, Sarah Williams, Sara Ahmadi, Imre Mäger, Fiona Lee, Liz Thomas, Caz Woffindale, Aisling O'Loughlin, Pieter Vader, Jinguan Li, Alex Wyatt, Aurélie Goyenvalle, Anthony Walsh and Akshay Bareja.

Lastly I would like to thank my family and Charlotte for their love and support over last few years.

Abstract

Duchenne muscular dystrophy (DMD) is a progressive muscle wasting disorder caused by absence of functional dystrophin protein. This thesis describes investigations into the role of small non-coding RNAs in both DMD pathology, and as potential therapeutic molecules.

MicroRNAs (miRNAs) are a class of small RNAs that regulate gene expression and are implicated in wide-ranging cellular processes and pathological conditions. This study has compared differential miRNA expression in proximal and distal limb muscles, diaphragm, heart and serum in the *mdx* dystrophic mouse model relative to wild-type controls. Global transcriptome analysis revealed muscle-specific patterns of differential miRNA expression as well as commonalities between tissues, including previously identified dystromirs. miR-1, miR-133a and miR-206 were found to be highly abundant in *mdx* serum, suggesting that these miRNAs are promising disease biomarkers. Indeed, the relative serum levels of these miRNAs were normalised in response to peptide-PMO mediated dystrophin restoration therapy. This study has revealed further complexity in the miRNA transcriptome of the *mdx* mouse, an understanding of which will be valuable for the development of novel DMD therapeutics and for monitoring their efficacy.

Myostatin is a secreted growth factor that negatively regulates muscle mass and is therefore a potential pharmacological target for the treatment of muscle wasting disorders such as DMD. This study describes a novel myostatin inhibition approach in which small interfering RNAs (siRNAs) complementary to a promoter-associated transcript induce

transcriptional gene silencing (TGS) in cultured myotubes. Silencing was sensitive to treatment with the histone deacetylase inhibitor Trichostatin A, and the silent state chromatin mark H3K9me2 was enriched at the myostatin promoter following siRNA transfection, suggesting epigenetic remodelling underlies the silencing effect. These observations suggest that long-term epigenetic silencing may be feasible for myostatin and that TGS is a promising novel therapeutic strategy for the treatment of muscle wasting disorders.

The work in this thesis therefore demonstrates the potential of small RNAs as therapeutic agents and as disease biomarkers in the context of DMD.

List of Abbreviations

2′-OMe	2′-O-methyl RNA
2′-O-MOE	2′-O-methoxyethyl RNA
5-azaC	5′-azacytidine
AAV	Adeno-Associated Virus
ACTB	β-Actin
Acvr2b	Activin Receptor Type IIb
AGO1	Argonaute 1
AGO2	Argonaute 2
agRNA	antigene RNA
ANOVA	Analysis Of Variance
AMO	Anti-microRNA Oligonucleotide
APC	Antigen Presenting Cell
asRNA	antisense RNA
BDNF	Brain Derived Neurotrophic Factor
BMD	Becker Muscular Dystrophy
bp	base pair
CCR5	C-C chemokine receptor type 5
cDNA	Complementary DNA
ChIP	Chromatin Immunoprecipitation
CK	Creatine Kinase
CLL	Chromic Lymphocytic Leukemia (CLL) and
CRC	Colorectal Cancer
Ct	Cycle threshold
DAPC	Dystrophin Associated Protein Complex
DAPI	4',6-diamidino-2-phenylindole
DM	Differentiation Medium
DMEM	Dulbecco's Modified Eagle's Media
DBTSS	Database of Transcription Start Sites
DGCR8	DiGeorge Syndrome critical Region 8
DGC	Dystrophin Associated Glycoprotein Complex
DMD	Duchenne Muscular Dystrophy
DNMT3A	DNA (cytosine-5-)-methyltransferase 3 α
EEF1A1	Eukaryotic Elongation Factor 1α
EZH2	Enhancer of Zeste Homologue 2
FBS	Fetal Bovine Serum
FDR	False Discovery Rate
Fst	Follistatin
FLRG	Follistatin-Related Gene
GASP-1	Growth Differentiation Factor Associated Protein-1)
GDF-8	Growth and Differentiation Factor 8 (Mstn)
GDF-11	Growth and Differentiation Factor 11
gDNA	genomic DNA
GM	Growth Medium

HITS-CLIP	High Throughput Sequencing of RNA Molecules-Cross-linking Immunoprecipitation
H3K9me2	di-methylated histone H3 lysine 9
H3K27me3	tri-methylated histone H3 lysine 27
HCV	Hepatitis C Virus
HDAC	Histone Deacetylase
HIV	Human Immunodeficiency Virus
HMT	Histone Methyltransferase
ICV	Intracerebroventricular
Ig	Immunoglobulin
Il-6	Interleukin-6
lncRNA	long non-coding RNA
lincRNA	long intergenic non-coding RNA
LTR	Long Terminal Repeat
LAP	(myostatin) Latency Associated Peptide
LNA	Locked Nucleic Acid
LPS	Lipopolysaccharide
Luc	Firefly Luciferase
MB	Myoblast
MIAME	Minimum Information About a Microarray Experiment
MIQE	Minimum Information for publication of Quantitative real-time PCR Experiments
miRISC	RISC containing miRNA
miRNA	microRNA
miRNA*	miRNA minor species
mRNA	messenger RNA
Mstn	Myostatin
MT	Myotube
NAT	Natural Antisense Transcript
ncRNA	non-coding RNA
nNOS	neuronal Nitric Oxide Synthase
NO	Nitric Oxide
nPTB	neuronal Polypyrimidine Tract Binding protein
ns	not significant
NTC	No Template Control
Oas1b	2′,5′ oligoadenylate synthase 1b
PAGE	Polyacrylamide Gel Electrophoresis
PAX3	Paired Box Proteins 3
PAX7	Paired Box Proteins 7
PBS	Phosphate Buffered Saline
PCR	Polymerase Chain Reaction
PGR	Progesterone Receptor
PI3K	Phosphoinositide-3-Kinase
PLAU	Plasminogen Activator, Urokinase
Ppib	Peptidylprolyl isomerase B (Cyclophilin B)
PMO	Phosphordiamidate Morpholino Oligonucleotide

PNA	Peptide Nucleic Acid
PPMO	Peptide- Phosphordiamidate Morpholino Oligonucleotide
PRC2	Polycomb Repressive Complex 2
pre-miRNA	precursor-microRNA
pri-miRNA	primary-microRNA
pRNA	promoter associated-RNA
PS RNA	Phosphorothioate RNA
PTEN	Phosphatase and Tensin homolog
PTGS	Post-Transcriptional Gene Silencing
RISC	RNA Induced Silencing Complex
RIP	RNA Immunoprecipitation
RITS	RNA Induced Transcriptional Silencing Complex
RLuc	Renilla Luciferase
RNA	Ribonucleic Acid
RNAa	RNA activation
RNAi	RNA interference
RNAPII	RNA Polymerase II
RT	Reverase Transcription
RT-qPCR	Reverse Transcriptase - Quantitative PCR
SD	Standard Deviation
SEM	Standard Error of the Mean
siRNA	small interfereing RNA
shRNA	short hairpin RNA
snRNA	small nuclear RNA
SRF	Serum Response Factor
TA	Tibialis Anterior
TGF-β	Transforming Growth Factor-β
TGS	Transcriptional Gene Silencing
TGA	Transcriptional Gene Activation
T_m	melting Temperature
TRBP	TAR RNA Binding Protein 2
TSA	Trichostatin A
TSS	Transcription Start Site
TXNIP	Thioredoxin-Interacting Protein
UBC	Ubiquitin C
UTR	Untranslated Region
VEGFA	Vascular Endothelial Growth Factor
WT	Wild-Type

List of Figures

List of Tables

Table of Contents

1 Introduction

1.1 Duchenne Muscular Dystrophy

Duchenne muscular dystrophy (DMD) is an X-linked, recessive, fatal disorder caused by loss-of-function mutations in the *DMD* gene [1,2]. DMD is the most common muscular dystrophy and affects 1 in 3,500 live male births. Disease progression is characterised by progressive myofibre degeneration, muscle wasting, fibrosis and loss of ambulation. Degeneration of cardiac muscle and the diaphragm result in cardiac and/or respiratory failure with subsequent fatality in the second or third decade of life. The much less severe myopathy, Becker muscular dystrophy (BMD), is also caused by *DMD* mutations. In BMD, mutations result in in-frame, internally deleted dystrophin transcripts which are translated into a truncated dystrophin protein which retains partial functionality [3].

The *DMD* gene, located on the X chromosome, is ~2.4 megabases in size and therefore the largest protein-coding gene in the human genome. The spliced full-length dystrophin mRNA is ~14 kb and consists of 79 exons [4]. A number of dystrophin protein isoforms are encoded by this locus although here we shall be concerned only with the largest isoform (427 kDa) which is involved in DMD pathophysiology [5]. Dystrophin protein is comprised of four main regions. (a) The N-terminal domain binds to cytoskeletal F-actin [6]. (b) The central rod domain binds actin [7] and neuronal nitric oxide synthase (nNOS) [8]. Four hinge regions in the rod domain contribute to the flexibility of the dystrophin protein [9]. (c) The cystein-rich domain binds to β-dystroglycan at the sarcolemma [10]. (d) The C-terminal domain binds α-, β- and γ-syntrophins [11–13]. Dystroglycan and syntrophin proteins make additional protein-protein contacts and consequently,

dystrophin acts as an organizing centre for the dystrophin-associated protein complex (DAPC, also known as the dystrophin-associated glycoprotein complex, DGC) at the sarcolemma [14]. The DAPC has been implicated in signaling functions [15].

Dystrophin is localised to the sarcolemma of muscle fibres where it acts as a mechanical link between the actin cytoskeleton and the extracellular matrix and, as such, is important for the transmission of contractile force [16,17]. Similarly, it has also been proposed that dystrophin acts as a shock absorber due to the elastic nature of the central rod domain in order to protect against contraction-induced stress [18]. Loss of functional dystrophin at the sarcolemma and concomitant DAPC disruption leads to wide ranging cellular pathologies. These include; myofibre necrosis, impaired signaling activities (e.g. NO) [19,20], loss of sarcolemmal integrity [21–23], irregular calcium homeostasis [21,24–26], increased oxidative stress [27], chronic cycles of degeneration and regeneration leading to satellite cell depletion [28] and inflammation [29].

The *mdx* mouse is the most widely used animal model of DMD and as such is the focus of much of the work presented in this thesis. A single nucleotide polymorphism in exon 23 of the murine *Dmd* gene results in a premature termination codon leading to a truncated and non-functional dystrophin protein [30]. Although the *mdx* mouse exactly copies the genetic defect leading to DMD, *mdx* mice show less severe pathology than DMD patients.

1.2 Therapeutic Approaches to DMD

1.2.1 Conventional Pharmacology

As DMD is characterised by a wide range of pathological processes there are a multitude of potential pharmacological targets. For example, drugs which reduce inflammation or fibrosis may slow disease progression. Corticosteroids such as prednisone and deflazacort have been shown to be effective in the treatment of DMD patients and are the only drugs currently in clinical use [31,32]. Long-term administration of these drugs has been shown to prolong ambulation by two years and to reduce scoliosis [33], although their mechanisms of action are not well understood. Additionally, many patients discontinue corticosteroid treatment due to unwanted side-effects which include weight gain, hypertension and behavioural problems [34]. An alternative pharmacological approach is to restore dystrophin expression by promoting ribosomal read-through of premature termination codons using compounds such as the aminoglycoside antibiotic Gentamicin and the synthetic compound Ataluren (PTC124). 10-15% of DMD patients have mutations that induced premature termination of translation and so are amenable to a read-through approach [3,35]. These compounds work by inducing incorporation of an amino acid at a stop codon thereby continuing translation of the dystrophin mRNA. Efficacy of these drugs has been limited in clinical trials with a maximum of ~20% dystrophin restoration observed [36,37]. Results with Gentamicin have been highly variable, with some patients showing no dystrophin restoration. Furthermore, a recent trial of Ataluren in DMD and BMD patients was discontinued as insufficient improvement in a test of muscle function was attained. Consequently, pharmacological treatments for DMD are currently insufficient.

1.2.2 Cell Therapy

Cell therapy is the delivery of cells to treat a disease. In the case of DMD, injection of cells carrying the wild-type dystrophin gene complements dystrophin deficiency in dystrophic patients or animal models. The delivered cells differentiate to form new dystrophin-positive muscle fibres and thus restore function to diseased muscle. One approach to DMD cell therapy is myoblast transplantation. Myoblasts are derived from healthy donors and expanded in cell culture before being re-introduced into diseased tissue. Although initial pre-clinical studies showed promise [38], myoblast transplantation in patients has been less successful [39]. Injected myoblasts tend to fuse with myofibres at the site of injection and so systemic delivery of myoblasts has so far not been possible. In addition, as myoblasts are derived from a donor they are allogenic and therefore delivery must be accompanied by immune suppression in order to avoid rejection of the transplanted cells. An alternative to myoblast transplantation is the use of stem cells. A number of different types of stem cell have the potential to adopt a myogenic differentiation program. These include muscle-derived stem cells [40], muscle side-population cells [41,42], mesoangioblasts [43,44] and CD133+ progenitor cells [45,46]. An advantage of these types of therapies is that the transplanted stem cells do not accumulate at the site of injection and so can be delivered systemically.

1.2.3 Gene Therapy

Gene therapy is the delivery of nucleic acids to treat or manage disease. This includes classical gene replacement approaches whereby an exogenous transgene encoded by a plasmid or virus is administered to complement a deficiency in an endogenous gene and

RNA-based approaches such as gene silencing and splice modulation. As such, much of the work presented in this thesis falls into this latter category.

1.2.4 Gene Replacement Therapy

Classical gene therapy approaches to DMD have focused on the delivery of either full-length dystrophin cDNA (~13kb) or internally deleted forms of dystrophin; minidystrophin (~6 kb) [47] and microdystrophin (~4 kb) [48]. A major advantage of the latter form of truncated dystrophin is that they are small enough to be delivered by adeno-associated virus (AAV) which shows good muscle tropism. Transgenic animals expressing these three forms of dystrophin on a dystrophin null background show histological improvement, improved muscle function and restoration of the DAPC at the sarcolemma of muscle fibres [49,50]. However, internally deleted forms of dystrophin were not as effective as full length dystrophin in ameliorating dystrophic pathology.

Although adenoviral vectors have the capacity to deliver full length dystrophin, their poor muscle tropism and the high prevalence of anti-viral antibodies in the general population mean they are unlikely to be effective gene therapy vectors for DMD. Conversely, AAV vectors have been used to deliver truncated dystrophin cDNAs in mice, dogs and non-human primates successfully [47,51–53]. However, an anti-viral response was observed in the canine model and dystrophin restoration in the non-human primate model was reduced following a second administration of the AAV vector. Furthermore, in a human trial of AAV-delivered microdystrophin a T-cell response against dystrophin epitopes was detected which limited the effectiveness of dystrophin restoration [54].

1.2.5 Exon Skipping

Exon skipping therapy (also called splice correction) is an RNA-based approach whereby expressed or synthetic oligonucleotides influence pre-mRNA splicing patterns. In the case of DMD, exons containing disease-causing mutations can be alternatively spliced so as to generate an in-frame transcript lacking one or more exons. Oligonucleotides act to mask splicing signals at a desired exon and thereby 'hide' that exon from the splicing machinery. The exon is subsequently removed by splicing along with the adjacent introns. This results in an internally deleted dystrophin protein molecule that retains partial functionality. Whereas the N- and C-terminal domains of dystrophin are required for functionality, the rod domain of dystrophin consists of many redundant domains. Indeed, a BMD patient has been reported who lacks exons 17-48 and has only very mild symptoms [55]. Consequently, the loss of one or more exons in the rod domain is frequently well tolerated with only a minimal loss of dystrophin protein function. The exon skipping approach can thus be thought of as inducing a BMD-like phenotype. Clinical trials have so far been promising using 2′-O-methyl phosphorothioate and phosphorodiamidate morpholino oligonucleotides (PMOs) that target exon 51 of the human dystrophin mRNA [56,57] and further trials are currently underway. Skipping exon 51 would result in restoration of the dystrophin mRNA reading frame in as many as 13% of patients [3]. As PMOs are uncharged molecules they can be conjugated to cationic cell penetrating peptides in order to improve cellular uptake and confer targeting to muscle tissues. Pre-clinical studies in *mdx* mice have shown that peptide-PMO (PPMO) conjugates are highly effective at restoring dystrophin protein in skeletal muscle and, more recently, in the heart [58,59]. An alternative delivery approach is to utilise

AAV vectors to deliver expressed exon skipping effectors. The U1 and U7 small nuclear RNA (snRNA) molecules are modified so that they target a mutant exon. AAV1 delivery of U7 and U1 snRNA genes targeting *Dmd* exon 23 in the *mdx* mouse have been shown to induce dystrophin restoration lasting 3 months [60] and 1 year [61] after injection respectively. Whereas AAV vectors enable long-term dystrophin restoration following a single injection, repeat administration of these viral vectors is problematic as discussed above.

A multi-exon skipping approach in which multiple exons are skipped is a possible alternative approach that may be able to treat a large number of patients. A bioinformatics study of potential single- and multi-exon skipping strategies predicted that as many as 63% of DMD patients could be treated by skipping of exons 45 to 55 [62]. However, attempts to achieve multi-exon skipping experimentally in cell culture have shown only minimal success as multiple different alternative dystrophin isoforms are generated with only a minority having the desired exon 45-55 deletion. Current exon-skipping technologies are therefore not sufficient to induce efficient multi-exon skipping [63].

1.2.6 Utrophin Up-Regulation

Utrophin (dystrophin-related protein) is a close homologue of dystrophin (80% identical sequence) that is expressed in skeletal muscle early during development but in adult myofibres is restricted primarily to the neuromuscular and myotendinous junctions [64]. It has been proposed that expression of utrophin could compensate for dystrophin loss as it is up-regulated in the muscle of DMD patients and *mdx* mice [65,66]. Similarly, transgenic over-expression of utrophin in *mdx* mice ameliorates the dystrophic phenotype

[67], whereas mice in which both dystrophin and utrophin are absent (double knock-out, *dko* mice) exhibit much more severe pathology than *mdx* mice and rarely live beyond three months [68]. Pre-clinical studies of utrophin up-regulation are promising [69–71] although these strategies have so far been unable to completely restore the wild-type phenotype [72].

1.3 Myostatin

Myostatin (Mstn) or growth differentiation factor-8 (GDF-8) is an endogenous, secreted protein from the transforming growth factor-β (TGF-β) superfamily that negatively regulates skeletal muscle growth and differentiation [73]. Myostatin knock-out mice are significantly larger (2-3 fold) than wild-type animals and exhibit widespread skeletal muscle hyperplasia and hypertrophy [73,74]**.** Conversely, transgenic mice over-expressing myostatin show the reverse phenotype of reduced musculature and myofibre size [75]. Loss of function or deletion mutations in the myostatin gene result in increased musculature (the double-muscling phenotype) in cattle (Belgian Blue and Piedmontese) with a 20% increase in muscle mass [76–78]. Similarly, a child presenting with severe muscular hypertrophy was found to have inactivating mutations in both myostatin alleles [79]**.** In addition to conservation of function between cattle, mice and humans, sequence comparison shows that the C-terminal, biologically active region of myostatin is conserved between humans and mice [73,78]**.** These observations led to the suggestion that myostatin blockade might be of therapeutic benefit with respect to muscle wasting disease such as DMD.

1.3.1 Myostatin Pathway

The 1.6 kb myostatin promoter contains conserved muscle specific transcription factor binding sites and consequently myostatin is expressed almost exclusively in skeletal muscle [80]. The 3.1 kb myostatin mRNA transcript encodes a 55 kDa propeptide which is cleaved to generate the 20.5 kDa mature protein which subsequently homodimerises. Myostatin exhibits several features typical of TGF-β superfamily members. The 55 kDa immature translated myostatin consists of a 24 amino acid N-terminal signal sequence which targets myostatin for secretion, the latency associated peptide (LAP) and the C-terminal mature myostatin peptide. A dibasic proteolytic processing/cleavage site (with amino acid sequence RSRR at position 240-243) resides between the LAP and mature myostatin. The mature myostatin peptide contains 9 conserved cysteine residues with defined spacings that form a disulphide bonded cysteine-knot structure when two mature peptides dimerise. [73]. The myostatin dimer circulates in the blood in complex with the LAP and other regulatory factors including FLRG (follistatin-related gene) and GASP-1 (growth differentiation factor associated protein-1) which inhibit myostatin signaling function [81,82]. Myostatin is believed to be activated through proteolytic cleavage of the LAP by a BMP/tolloid family metalloproteinase which causes the myostatin/LAP complex to dissociate [83]. Activated myostatin binds to the activin receptor IIB (Acvr2b or ActRIIB) which subsequently heterodimerises with a co-receptor (activin receptor type IIa) and initiates an intracellular signaling cascade. As a result, Smad2 and Smad3 become phosphorylated and complex with Smad4. The Smad complex translocates to the nucleus where it regulates a battery of genes [84–86] (**Fig. 1.1**).

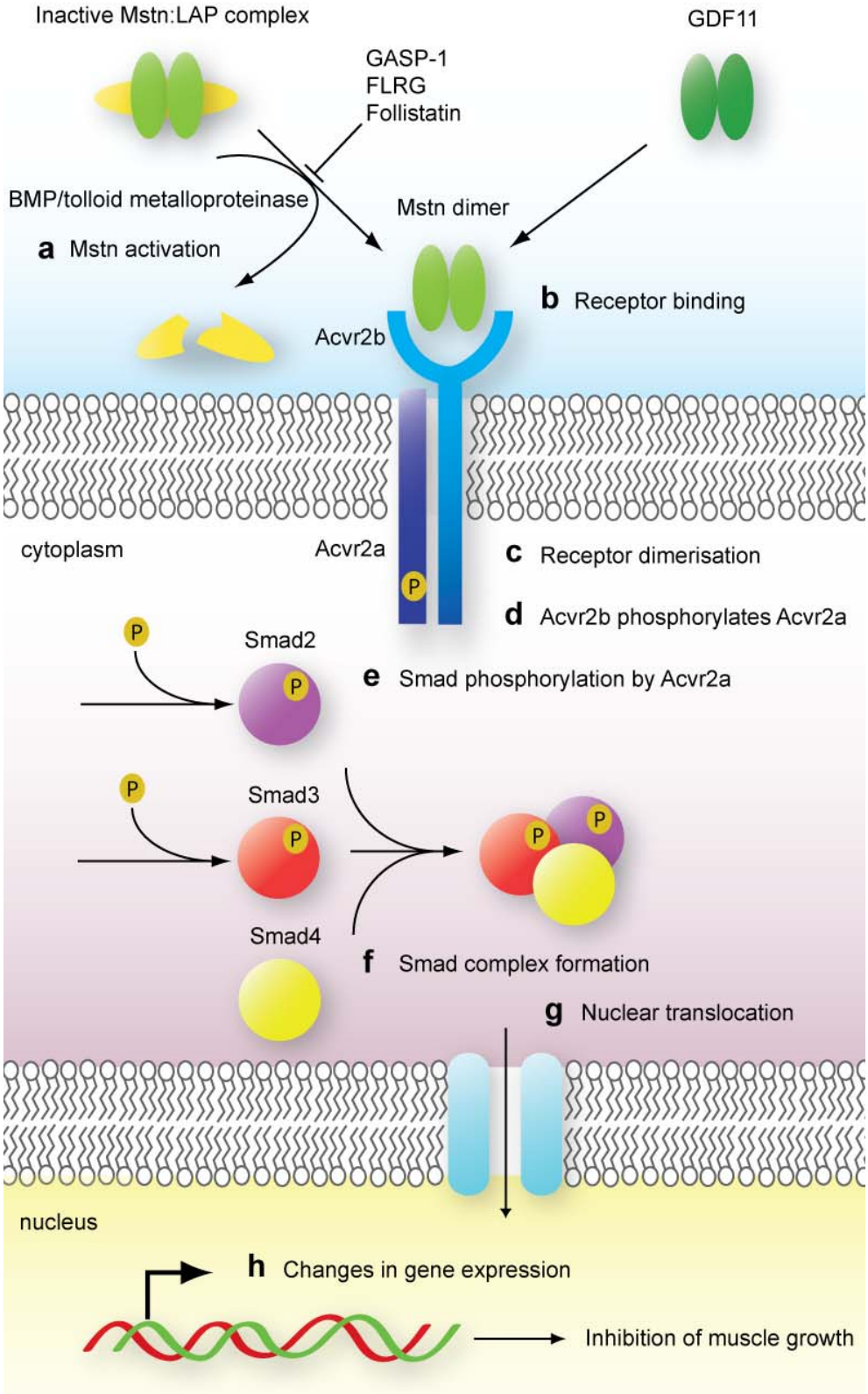
Inactive Mstn:LAP complex
GDF11
GASP-1
FLRG
Follistatin
BMP/tolloid metalloproteinase
Mstn dimer
a Mstn activation
b Receptor binding
Acvr2b
cytoplasm
Acvr2a
c Receptor dimerisation
d Acvr2b phosphorylates Acvr2a
P
Smad2
e Smad phosphorylation by Acvr2a
Smad3
Smad4
f Smad complex formation
g Nuclear translocation
nucleus
h Changes in gene expression
Inhibition of muscle growth

Figure 1.1 The myostatin pathway.

Myostatin circulates in the blood in an inactive complex with latency associated peptide (LAP). (a) Myostatin is activated by proteolytic cleavage of LAP by a member of the BMP/tolloid family metalloproteinase. GASP-1 antagonises myostatin signaling by blocking the site of proteolysis. (b) The active myostatin dimer binds to the activin receptor type IIb (Acvr2b). Other ligands also signal through Acvr2b (e.g. GDF11). (c) Acvr2b dimerises with Acvr2a. (d) Acvr2b phosphorylates Acvr2a. (e) Acvr2a phosphorylates Smad2 and Smad3. (f) Phosphorylated Smad2 and Smad3 form a complex with Smad4. (g) The Smad complex translocates to the nucleus and (h) facilitates changes in gene expression. The net effect of these changes is to signal withdrawal from the cell cycle, promotion of differentiation and inhibition of myocyte proliferation.

1.3.2 Myostatin Inhibition

A number of studies have demonstrated both increased musculature and functional improvement in animal models (specifically the *mdx* mouse model of DMD) upon inhibition of myostatin [87–92]. Transgenic mice lacking both myostatin and dystrophin show both increased musculature and functional improvement in strain gauge and grip strength performance relative to *mdx* mice. Histological assessment of these animals shows reduced replacement of myofibres with fatty and fibrotic tissue indicating reduced myofibre degeneration [93]. In addition, myostatin blockade has also been shown to be associated with reduced fibrosis and fat deposition [93], reduced necrosis [87] and the stimulation of satellite cell proliferation [94–97]. The latter point is somewhat contentious, as Amthor *et al.* recently demonstrated that satellite cells elicit little or no influence on hypertrophy in the case of loss of myostatin in an *in vitro* model [98]. This is potentially beneficial as it had been previously suggested that continuous myocyte proliferation as a consequence of myostatin blockade might result in depletion of the satellite cell pool and exacerbate disease pathology.

Consequently, a myostatin blockade strategy may be able to reverse some of the disease pathophysiology in the absence of effective treatments for the underlying dystrophinopathies in DMD and BMD or may serve as an adjuvant therapy in combination with putative gene replacement/exon skipping strategies in the future. Although current therapeutics research has focused on DMD, myostatin blockade could be of potential clinical benefit in other muscle wasting diseases e.g. sarcopenia, age-related muscular atrophy, HIV/cancer associated cachexia.

1.4 Small RNA-Mediated Post-Transcriptional Gene Silencing

1.4.1 RNA Interference

RNA interference (RNAi), also known as post-transcriptional gene silencing (PTGS), is a homology-dependent gene silencing pathway in which small RNA effector molecules induce either degradation of mRNA transcripts or repression of mRNA translation. Endogenous RNAi is primarily mediated through the microRNA pathway (discussed in more detail below). RNAi has been used extensively in the study of gene function and holds much promise as a therapy for a wide-range of diseases. Typically, small interfering RNAs (siRNAs) are used to elicit RNAi. siRNAs are double stranded RNA molecules ~21 bp in length. The archetypal siRNA consists of 19 bp of double stranded sequence with two nucleotide 3′ single-stranded RNA or DNA overhangs. One strand of an siRNA is incorporated into the RNA binding protein AGO2, the so called 'catalytic engine of RNAi', and a component of the RNA induced silencing complex (RISC) [99,100]. RISC is then guided by the siRNA to complementary mRNA transcripts in the cytoplasm. The target transcript is then catalytically cleaved by the 'slicer' activity of the RISC component Argonaute 2 (AGO2) [101] at a position 10 nucleotides from the 5′ end of the siRNA. The effect of silencing by PTGS is short-lived, typically declining over a period of ~7 days with peak silencing observed between 24 and 72 hours in cell culture experiments [102,103]. Silencing is also dependent on the abundance of siRNA molecules, the concentration of which is reduced by the activity of cellular RNases and diluted by successive rounds of cell division.

1.4.2 MicroRNA

MicroRNAs (miRNAs) are small RNA sequences (21-23 nucleotides) that are endogenous RNAi effectors [104]. Typically, miRNAs are derived from longer primary-miRNA (pri-miRNA) transcripts that are transcribed by RNA polymerase II (RNAPII). Pri-miRNAs can either be intergenic non-coding transcripts or the mRNAs of protein-coding genes (with the miRNA sequences contained within one or more introns). Pri-miRNA transcripts are progressively processed by the Drosha/DGCR8 complex (in the nucleus) and then Dicer (in the cytoplasm) to generate the precursor-miRNA (pre-miRNA) hairpin and mature miRNA species respectively. Following Dicer cleavage, one strand of the miRNA hairpin is loaded into AGO2. The mature miRNA sequence (analogous to one strand of an siRNA) guides RISC to its mRNA targets in the cytoplasm where it binds, typically in the 3′ untranslated (UTR) region, to form an imperfect duplex and induce translational repression and/or mRNA decay [105–108] (**Fig. 1.2**). Similarly, miRNAs with complete sequence complementarity to an mRNA can act like siRNAs and induce 'slicing' of the target transcript as opposed to translational repression or slicer-independent mRNA decay [109]. As miRNAs can induce silencing with only partial complementarity to a target transcript (i.e. multiple mRNA:miRNA mismatches are tolerated) each miRNA can bind to multiple mRNA targets. Similarly, each mRNA 3′ UTR contains multiple potential miRNA binding sites. Consequently, miRNAs can act as master regulators of gene expression by regulating families of transcripts with related functions [110]. Individual miRNAs have been implicated in a wide variety of physiological and pathophysiological processes and, as such, are potential pharmacological targets [111].

1.4.3 MicroRNA Theraeutics

In instances when the activity of a miRNA is a causitive factor in pathology, strategies which antagonise miRNA activity are desirable. These fall in to two broad categories; (1) small oligonucleotide miRNA inhibitors and (2) expressed miRNA sponges. Conversely, miRNA replacement therapy can be utilised to correct a miRNA deficiency, or to modulate an endogenous protective pathway (**Fig. 1.2**).

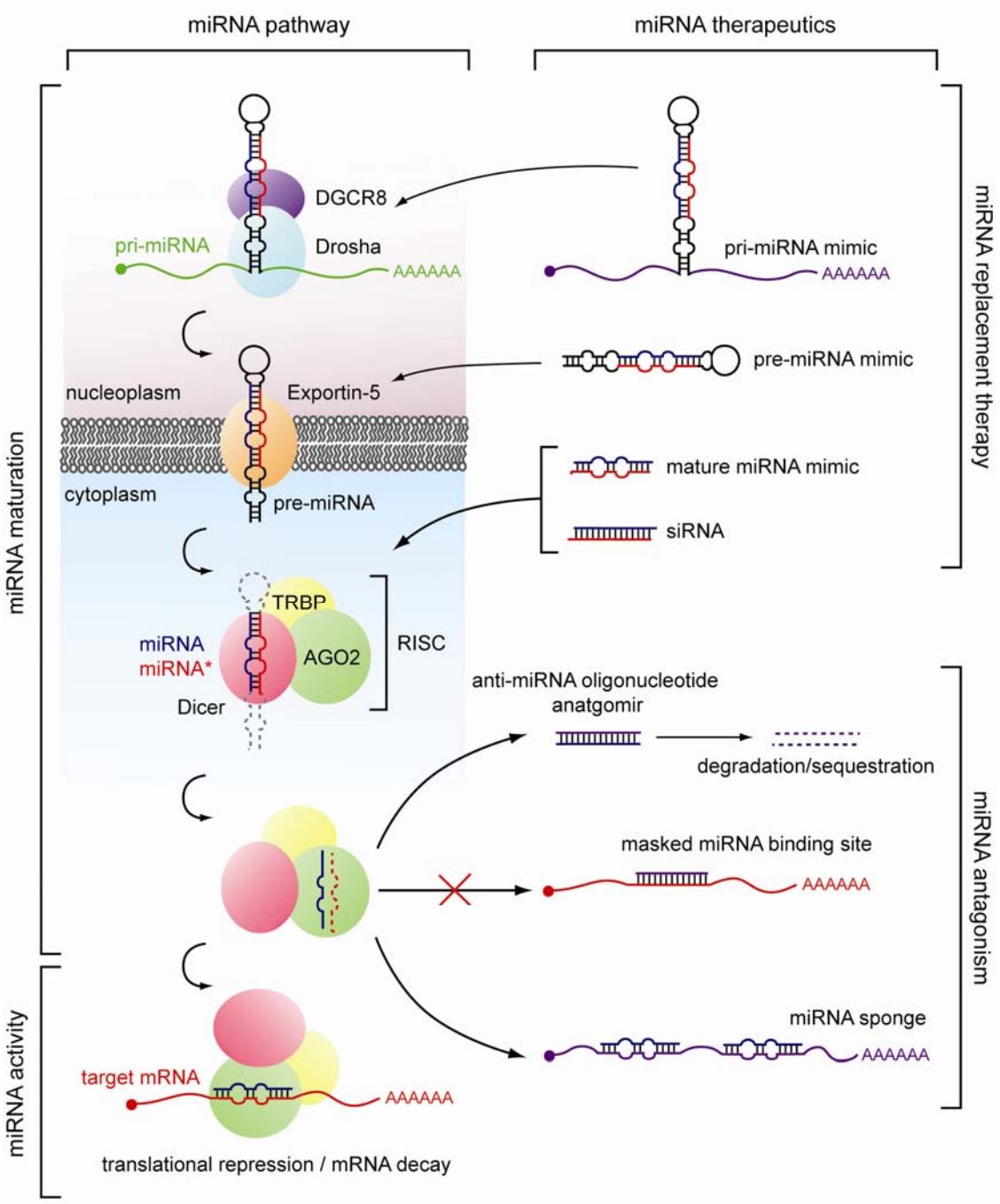
miRNA pathway
miRNA therapeutics
DGCR8
Drosha
pri-miRNA
AAAAAA
pri-miRNA mimic
AAAAAA
pre-miRNA mimic
nucleoplasm
Exportin-5
cytoplasm
pre-miRNA
mature miRNA mimic
siRNA
miRNA replacement therapy
miRNA maturation
TRBP
miRNA
miRNA*
AGO2
RISC
Dicer
anti-miRNA oligonucleotide
anatgomir
degradation/sequestration
masked miRNA binding site
AAAAAA
miRNA sponge
AAAAAA
miRNA antagonism
target mRNA
AAAAAA
translational repression / mRNA decay
miRNA activity

Figure 1.2 The microRNA pathway and targets for therapeutic intervention.

Schematic showing the miRNA pathway whereby primary miRNA (pri-miRNA) transcripts are progressively processed to generate the mature miRNA species. Firstly, a complex of Drosha and DGCR8 (DiGeorge Syndrome critical Region 8) cleaves the pri-miRNA transcript to produce the precursor miRNA (pre-miRNA) in the nucleus. Export of the pre-miRNA hairpin from the nucleus is facilitated by Exportin-5. In the cytoplasm, the pre-miRNA is cleaved by Dicer generating a ~21 basepair RNA duplex. Dicer is part of the RNA induced silencing complex (RISC) along with Argonaute 2 (AGO2) and TAR RNA Binding Protein 2 (TRBP). One strand of the duplex is loaded into AGO2 and the other strand (labelled miRNA*) is subsequently degraded. RISC is then guided to complementary target mRNAs and induces translational repression or mRNA decay. Approaches for miRNA replacement therapy and miRNA antagonism are indicated. miRNA mimics enter the miRNA pathway at various stages. Expressed pri-miRNA and pre-miRNA mimics enter at the Drosha and Dicer clevage steps respectively. Conversely, mature miRNA mimics (either bulged duplexes or completely complementary small interefering RNAs, siRNAs) enter RISC directly without prior processing. Anti-miRNA oligonucleotides or antagomirs bind to mature miRNA species in the cytoplasm and induce degradation or sequestration of the target miRNA. Similarly, oligonucleotides can bind to target mRNAs and mask a miRNA binding site. Expressed miRNA sponges are transcripts containing multiple miRNA binding sites which compete with endogenous mRNAs for miRNA binding.

1.4.4 MicroRNA Antagonism

There are numerous examples of miRNAs that promote pathology in human disease and are consequently therapeutic targets. For example, many viruses express specific miRNA genes [112], or are dependent upon host cell miRNAs for viral replication [113]. One promising application of miRNA inhibition is in the treatment of cancer, as miRNA-mediated gene regulation has been implicated in tumorigenesis and metastasis [114]. For example, inhibition of miR-10b in a mouse mammary tumor model resulted in a reduction in lung metastasis [115]. Anti-miRNA technologies are currently the most advanced miRNA-based therapeutic strategy with the most commonly used approach being anti-miRNA oligonucleotides (AMOs). These are single-stranded oligonucleotides consisting of the reverse complement sequence of a target miRNA that function by either degrading or sequestering the target miRNA. Alternatively, oligonucleotides complementary to target mRNAs block miRNA binding at individual recognition sites [116]. This target masking strategy allows for the inhibition of specific miRNA:mRNA interactions.

AMOs contain extensive chemical modification to both the oligonucleotide backbone (e.g. phosphorothioate linkages) and the ribose sugar (e.g. substitution at the 2′-hydroxl with O-methyl or O-methoxyethyl groups) in order to improve nuclease stability, reduce clearance and increase bioavailability. The incorporation of locked nucleic acid, LNA, bases results in an increase in the T_m of AMOs and favours binding to RNA over DNA [117]. Similarly, the nucleic acid analogue; peptide nucleic acid (PNA) has also been utilised to antagonise miRNA activity [118,119]. The conjugation of AMOs with

lipophilic moieties, such as cholesterol in the case of antagomirs, results in improved cellular uptake [120,121] (**Fig. 1.3**). At the time of writing the most advanced anti-miRNA therapy is currently in Phase IIa clinical trials. Miravirsen, developed by Santaris Pharma A/S to treat chronic Hepatitis C Virus (HCV) infection, is a 15mer LNA-modified phosphorothioate antisense oligonucleotide inhibitor of miR-122. Endogenous miR-122 is required for HCV viral replication [113] and antagonism of this miRNA was shown to reduce viremia in a chronically infected chimpanzee model with no evidence of toxicity [122].

The effects of AMOs are transient as they are dependent on the presence of the effector molecule. Consequently, expressed miRNA decoys or sponges have been developed in order to elicit longer-term miRNA inhibition [123]. These virus or plasmid-encoded transcripts contain multiple miRNA target sites and compete with endogenous target mRNAs for miRNA binding. miRNA sponges have been used successfully to inhibit miR-9 in highly malignant 4T1 cells leading to suppression of metastasis [124]. Expressed miRNA inhibitors are an alternative therapeutic modality to the use of AMOs although, as they will likely require viral vector-mediated delivery *in vivo*, they are subject to the limitations and risks associated with classical gene therapy [125].

miRNA inhibition strategies are not limited to diseases in which aberrant miRNA expression is a causative factor in the pathology. In the case of DMD, loss of function mutations in the gene which encodes the dystrophin protein leads to progressive muscle weakness and are ultimately fatal. miR-31 is highly up-regulated in dystrophic muscle

and acts to suppress translation of dystrophin mRNA. This interaction is clinically relevant as the activity of miR-31 limits the efficacy of efforts to restore dystrophin protein expression by exon skipping therapy. Inhibition of miR-31 using a miRNA sponge in combination with exon skipping was shown to be more effective at restoring dystrophin than exon skipping alone [126]. This study demonstrates that modulating miRNA activity can be an effective means of boosting the expression of therapeutically relevant genes.

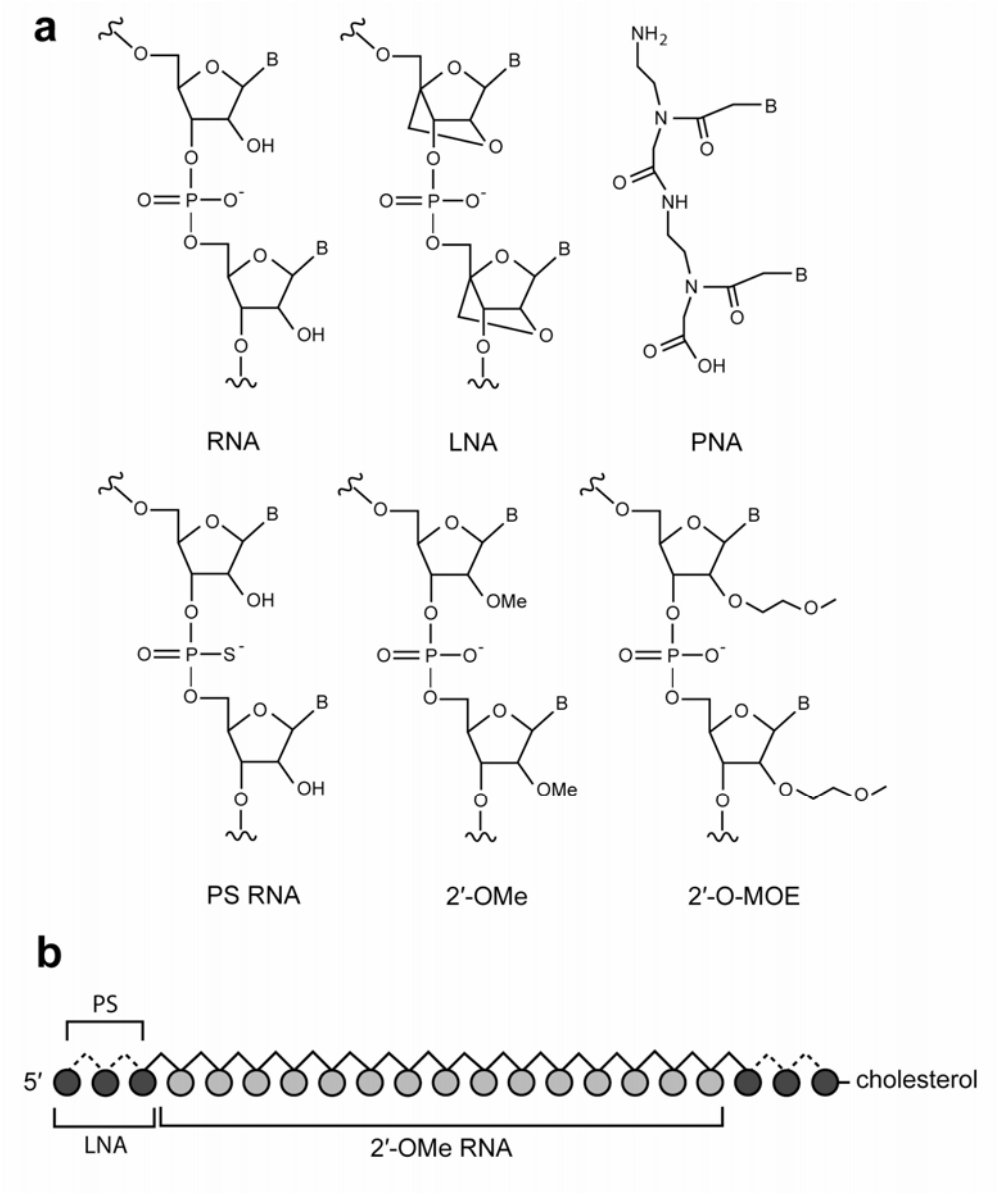
a
RNA
LNA
PNA
PS RNA
2′-OMe
2′-O-MOE
b
PS
5′
cholesterol
LNA
2′-OMe RNA

Figure 1.3 Chemistry of anti-miRNA oligonucleotides.

(a) Examples of nucleic acid chemistries utilised in anti-miRNA oligonucleotides; RNA, locked nucleic acid (LNA), peptide nucleic acid (PNA), phosphorothioate RNA (PS RNA), and RNA with O-methyl (2′-OMe) or O-methoxyethyl (2′-O-MOE) substitutions at the 2′ carbon of the ribose sugar. (b) Design of a generic antagomir. Nucleotides have O-methyl modifications at the 2′ position (light grey circles). The terminal nucleotides are LNA chemistry (dark grey circles) with phosphorothioate (PS) backbones (dotted lines). Additionally, the oligonucleotide has a cholesterol group conjugated to the 3′ terminus.

1.4.5 MicroRNA Replacement Therapy

MicroRNA mimics are synthetic or expressed oligonucleotides that mimic the function of endogenous miRNAs. As miRNA expression is frequently dysregulated in tumors [127] and some miRNAs have been shown to have tumor suppressive functionality [128], miRNA mimics are potential anti-cancer therapeutics. For example, adenovirus-mediated delivery of an expressed miR-26a mimic resulted in inhibition of tumor progression in a murine hepatocellular carcinoma model [129]. Conversely, miRNA mimics can be used to modulate pathophysiological processes. miR-29 is known to regulate fibrosis by suppressing the expression of collagens, fibrillins and elastin [130]. miR-29 expression is reduced in dystrophic muscle leading to fibrogenesis in DMD. Consequently, treatment with a synthetic miR-29 mimic was capable of reducing fibrosis and improving pathology in the *mdx* mouse [131].

Considering that AMOs are required only to bind mature single stranded miRNAs with high affinity and specificity there are relatively few constraints on what chemical modifications can be incorporated in oligonucleotide design. Conversely, synthetic miRNA mimics have much more stringent requirements on chemical composition as RISC incorporation, which is essential for function, is sensitive to backbone chemistry. Synthetic miRNA mimics must primarily consist of RNA nucleotides with relatively few chemical modifications tolerated. As such, the development of therapeutic miRNA mimics has lagged behind that of anti-miRNA technology. Additionally, the delivery of synthetic miRNA mimics is subject to the same delivery obstacles as small interfering RNAs (siRNAs) (reviewed here [132]).

1.4.6 MicroRNA-Mediated Transgene Inactivation

Classical gene therapy typically involves the delivery of DNA encoding a therapeutic transgene to treat or manage disease. Transgene expression in professional antigen-presenting cells (APCs) can lead to immune-related vector clearance and consequently limit therapeutic efficacy. To address this problem, Brown *et al.* engineered a lentiviral vector expressing a GFP reporter to contain miRNA target sites complementary to miR-142-3p (which is highly expressed in immune cells) in its 3′ UTR. This strategy restricted GFP expression to non-hematopoietic cells and resulted in stable transgene expression in the desired target tissues [133]. A similar approach has been used with respect to adenovirus-mediated oncolytic virotherapy for cancer. In this case, high expression levels of the adenoviral E1A protein in hepatocytes results in acute liver toxicity. To abrogate this toxicity, miRNA target sites for a liver-specific miRNA, miR-122, were inserted in the 3′ UTR of the viral transgene. Mice treated with these miRNA-restricted adenoviral vectors showed reduced viral replication in the liver and almost no liver toxicity [134]. Thus, by taking advantage of endogenous miRNA regulation, the expression of therapeutic transgenes can be fine-tuned to minimise toxic off-target effects.

1.4.7 MicroRNAs in Muscle Biology

Many miRNAs show tissue-specific expression [135] and a number of miRNAs are primarily expressed in skeletal and cardiac muscle, some of which have been implicated in muscle physiology (so-called 'myomirs'). The myomirs miR-1, miR-133 and miR-206 are the best studied. These miRNAs are generally regarded as 'muscle specific' as they are almost exclusively found in adult skeletal and cardiac muscle and have been implicated in the regulation of muscle physiology through the regulation of their cognate mRNA targets [136,137]. miR-1 and miR-133 are found within miRNA clusters at two genomic loci in the mouse genome; miR-133a-1 and miR-1-2 on chromosome 2 and miR-133a-2 and miR-1-1 on chromosome 18. These loci produce polycistronic primary-miRNA transcripts which encode both mature miRNAs. The miR-1/miR-133a promoter on chromosome 2 has been shown to drive skeletal and cardiac muscle specific expression of a DsRed reporter gene [136]. Conversely, expression of miR-206 is restricted to skeletal muscle [137]. miR-206 is transcribed with miR-133b on a single primary transcript (miR-133b differs from miR-133a by one nucleotide at the 3′ end) [137].

In the C2C12 murine myoblast cell line (which faithfully replicates skeletal muscle differentiation by forming multinucleated myotubes when cultured in reduced serum conditions) the expression of these myomirs correlates well with differentiation. miR-1, miR-133 and miR-206 are present at low levels or undetectable in undifferentiated C2C12 myoblasts but are up-regulated upon differentiation [138]. A similar correlation between myogenesis and myomir expression was also observed in myoblasts derived

from human foetal tissue [139]. Expression of these myomirs is thus indicative of commitment to a myogenic differentiation program.

Transcription of muscle-specific miRNAs has been shown to be regulated by transcription factors involved in muscle growth and development [140–142]. For example, serum response factor (SRF) (with the coactivator myocardin) activates miR-1/miR-133 expression [143]. SRF is itself regulated by miR-133 and therefore forms a negative feedback loop controlling expression of miR-1/miR-133 polycistrons [144]. Similarly, ChIP-on-chip analysis has shown that the muscle-specific transcription factors MyoD and myogenin bind to myomir promoters in differentiated C2C12 cells [140].

Despite their common biosynthetic origins, the mature species of miR-1 and miR-133 promote opposing biological functions. miR-1 promotes myogenesis (differentiation) whereas miR-133 represses myogenesis and promotes proliferation of progenitor cells. Over-expression of miR-1 in C2C12 cells leads to enhanced myogenesis as exemplified by up-regulated myogenic factors (i.e. MyoD, Mef2 and skeletal α-actin) whereas over-expression of miR-133 results in the inhibition of myogenesis (i.e. reduced levels of myogenin and myosin heavy chain, MHC) and increased proliferation [137,144]. Conversely, antagonising miR-1 activity slows differentiation whereas inhibiting miR-133 promotes differentiation [144]. Transgenic over-expression of miR-1 in mouse heart results in premature differentiation characterised by reduced mitotic activity (without apoptosis) leading to developmental arrest at E13.5 [143]. Similarly, forced expression of miR-1 in HeLa (non-muscle) cells alters their transcriptional profile to become more

muscle-like [145]. However, miR-133 has been shown to repress the splicing factor neuronal polypyrimidine tract-binding protein (nPTB) and thus influencing alternative splicing of multiple other mRNAs. Consequently, upon miR-133 up-regulation, a cell will adopt a muscle-specific pattern of splicing indicative of myogenic differentiation [138]. This suggests that miR-133 can promote both myoblast proliferation and differentiation to some extent.

The histone deacetylase HDAC4 epigenetically suppresses a number of genes that are required for myogenesis [146]. miR-1 represses expression of HDAC4 which de-represses myogenic factors such as Mef2. miR-1 has also been shown to promote differentiation of cardiac myocytes through regulation of the phosphatase and tensin homolog (PTEN)/Akt pathway [147].

miR-206 is related to miR-1 as 18 out of 21 nucleotides (including the seed sequence) are identical. Perhaps unsurprisingly, miR-206 acts in a similar manner to miR-1 by regulating many of the same target mRNAs and thereby promoting differentiation [148]. However, miR-206 knock-out mice do not appear to show a defect in myogenesis suggesting there is a degree of functional redundancy between these myomirs [149]. miR-1 and miR-206 both act to suppress the paired box proteins PAX3 and PAX7 which are expressed in satellite cells where they act to inhibit terminal differentiation [150–152]. miR-206 has also been shown to regulate expression of the p180 subunit of DNA polymerase α, thereby inhibiting DNA synthesis and promoting cell cycle withdrawal (and subsequently differentiation) [137]. Interestingly, miR-206 has also been shown to

repress expression of the therapeutically relevant genes; utrophin and follistatin-like 1 (a component of the myostatin pathway) [153]. The potential therapeutic relevance of these myomirs is exemplified in a recent study in which local injection of double-stranded miR-1, miR-133 and miR-206 mimics improved muscle regeneration in rat skeletal muscle injury model [154].

Other miRNAs have also been found to be implicated in muscle processes. miR-181 is required for terminal differentiation of myoblasts [155]. miR-181 represses expression of Hox-A11 (which is an inhibitor of differentiation). Similarly, the muscle–enriched miR-486 promotes differentiation through regulation of the phosphoinositide-3-kinase (PI3K)/Akt pathway [156]. Conversely, miR-155 inhibits differentiation by repressing MEF2A expression. As myoblasts progressively differentiate miR-155 expression decreases [157].

1.5 Small RNA-Mediated Transcriptional Modulation

The utility of small RNAs to modulate the transcription of specific target genes in mammalian cells is an exciting recent development with implications for our understanding of endogenous transcriptional control, the development of novel RNA-based therapeutics and the study of gene function. Both transcriptional gene silencing (TGS) and transcriptional gene activation (TGA) have been reported. TGS is a potent and specific RNA-mediated, homology-dependent gene silencing pathway in which small RNA molecules homologous to gene promoters either induce epigenetic changes at the targeted locus, or sterically inhibit procession of RNA polymerase, thus achieving silencing at the transcriptional level. Conversely, small RNAs targeting promoters can also induce transcriptional gene activation (TGA). Although the mechanistic details of this process are less well understood, several reports suggest that TGA is operative through targeting of promoter overlapping antisense RNA transcripts which leads to the reversal of endogenous epigenetic silencing. Non-coding RNA transcripts appear to be involved in both transcriptional silencing and activation processes.

1.5.1 Mechanisms of Transcriptional Gene Silencing

Although TGS is relatively well understood in *Schizosaccharomyces pombe*, *Drosophila* and *Arabidopsis* (reviewed in refs. [158–161]), until recently it was not known to occur in mammals. Multiple studies now show that small RNAs complementary to target promoters silence gene expression at the level of transcription. Two competing models have emerged to explain these observations. In the RNA:RNA model, the small RNA effector molecule targets a sense promoter-associated RNA (pRNA) and recruits an epigenetic remodelling complex to the target promoter in order to induce heterochromatin formation and promoter DNA methylation. Conversely, the RNA:DNA model posits that the small RNA effector molecule interacts directly with chromosomal DNA. The binding of small RNAs to DNA occurs either by DNA:DNA:RNA triplex formation or by binding to single-stranded sequences that are susceptible to transient melting, most notably at the site of transcription initiation where RNA Polymerase II (RNAPII) mediates local DNA unwinding. Although these two models were initially in competition, it now seems that both models may be true under different specific circumstances. Here we refer to silencing by the RNA:RNA model as Epigenetic-TGS and silencing by the RNA:DNA model as Antigene-TGS.

1.5.1.1 Epigenetic-TGS

Epigenetics is the study of mitotically and meiotically heritable changes in gene expression that are not coded in the DNA itself [162]. Here we are primarily concerned with two kinds of epigenetic modification. (1) Direct chemical modification of DNA nucleotides. Specifically, methylation of cytosine at CpG dinucleotides, which is associated with gene silencing in mammals. (2) Post-translational modifications of

accessory proteins that regulate the accessibility of DNA to the transcriptional machinery. Eukaryotic genomic DNA is packaged with histone proteins to form the dynamic polymer chromatin. Genomic DNA wraps around a histone protein octamer in 1.67 superhelical turns to form a structure called a nucleosome. The N-terminal tails of histones H3 and H4 protrude from the nucleosome core structure and undergo extensive post-translational modification. The pattern of histone tail modifications regulates the transition between transcriptionally active (euchromatin) and the transcriptionally silent (heterochromatin) conformations and is known as the histone code. For example, the methylation of lysine 9 (H3K9me2) and lysine 27 (H3K27me3) on the N-terminal tail of histone H3 results in chromatin compaction which reduces the accessibility of DNA to transcription factors and RNA polymerase [163]. Consequently, the histone code greatly expands the information content of the genome [164]. The dual mechanisms of DNA methylation and silent state chromatin formation are functionally linked such that methylation of histone H3K9 directs DNA methylation (as in the case of pericentromeric chromatin) [165] and conversely, the Polycomb protein Enhancer of Zeste Homologue 2 (EZH2) (which tri-methylates H3K27) has been shown to directly influence DNA methylation [166]. The patterns of CpG methylation and histone tail modifications are inherited as somatic cells divide and, in some cases, in the germ line [167].

Epigenetic-TGS (RNA:RNA model) is a homology-dependent gene silencing pathway in which small RNA effector molecules targeting low-copy-number promoter transcripts recruit the RNA Induced Transcriptional Silencing (RITS) to the target promoter. RITS acts to induce silent state chromatin formation and, in some cases, *de novo* promoter

DNA methylation. These epigenetic modifications at the target promoter potentially result in long-term, stable gene silencing (**Fig. 1.4**). The first study to report small RNA-mediated TGS by Morris *et al.* showed that targeting the Eukaryotic Elongation Factor 1α (*EEF1A1*) promoter with a small interfering RNA (siRNA) resulted in silencing of both an integrated GFP transgene driven by the *EEF1A1* promoter and endogenous *EEF1A1* expression. Silencing was sensitive to the histone deacetylase inhibitor trichostatin A (TSA) and the DNA methyltransferase inhibitor 5′-azacytidine (5-azaC) which implied that epigenetic remodeling at the *EEF1A1* promoter was responsible for the observed silencing effect. Methylation of the *EEF1A1* promoter was also detected by methyl specific digestion [168]. Subsequent studies showed that treatment with promoter-targeting siRNAs results in enrichment of the silent state chromatin modifications H3K9me2 and H3K27me3 as measured by chromatin immunoprecipitation (ChIP) both for *EEF1A1* [169] and for other promoters (**Table 1.1**).

The induction of targeted epigenetic changes enables long-term therapeutic gene silencing. To this end, Hawkins *et al.* showed that targeting the Ubiquitin C (*UBC*) promoter for 2-3 days with a tetracycline induced shRNA was sufficient to induce long-term gene silencing (~30 days) [170]. Similarly, Suzuki *et al.* showed that transient transfection of an siRNA targeting the HIV-1 5′ LTR was able to suppress HIV replication for 31 days in the HeLa-derived MAGIC-5 cells [171] and, building on this work, Yamagishi *et al.* were able to silence HIV mRNA transcription and viral replication for up to 1 year using a retrovirus-expressed shRNA in a T-cell line (Molt-4)

[172]. Collectively, these studies suggest that long-term, targeted gene suppression by TGS may be possible in a therapeutic context.

Cytosine methylation has been reported in the case of a number of mammalian promoters targeted for epigenetic-TGS [168,170,173–175]. Conversely, other studies have shown that TGS can occur in the absence of DNA methylation [176]. A study by Kim *et al.* demonstrated TGS of transforming growth factor β receptor II (*Tgfbr2*) in rat hepatic stellate cells (SBC10) following lentiviral transduction. Short hairpin RNAs (shRNAs) targeting the *Tgfbr2* promoter induced dense methylation of CpGs and non-CpG cytosines. DNA methylation and silencing were alleviated in the presence of 5-azaC and the strength of silencing was found to correlate with the degree of promoter methylation. *Tgfbr2* inhibition was only observed 7 days after transduction suggesting that promoter DNA methylation is a pre-requisite for silencing [173]. This relatively late appearance of DNA methylation may explain some of the discrepancies between studies. Alternatively, it may be that persistent targeting is required to induce DNA methylation as an shRNA, but not an equivalent siRNA, induced cytosine methylation at the *Tgfbr2* promoter [173]. Conversely, Ting *et al.* showed that siRNAs targeting the *CDH1* promoter (E-cadherin) induced TGS in the absence of promoter methylation as demonstrated by bisulfite sequencing. In addition, the same effect could be reproduced in cells deficient in the *de novo* DNA methylation machinery suggesting that DNA methylation is not required for TGS [176]. Taken together, these studies suggest that there is redundancy between the epigenetic mechanisms of TGS (i.e. heterochromatin formation and promoter DNA

methylation). Consequently, the ability to induce targeted promoter methylation may be cell-type dependent or gene specific.

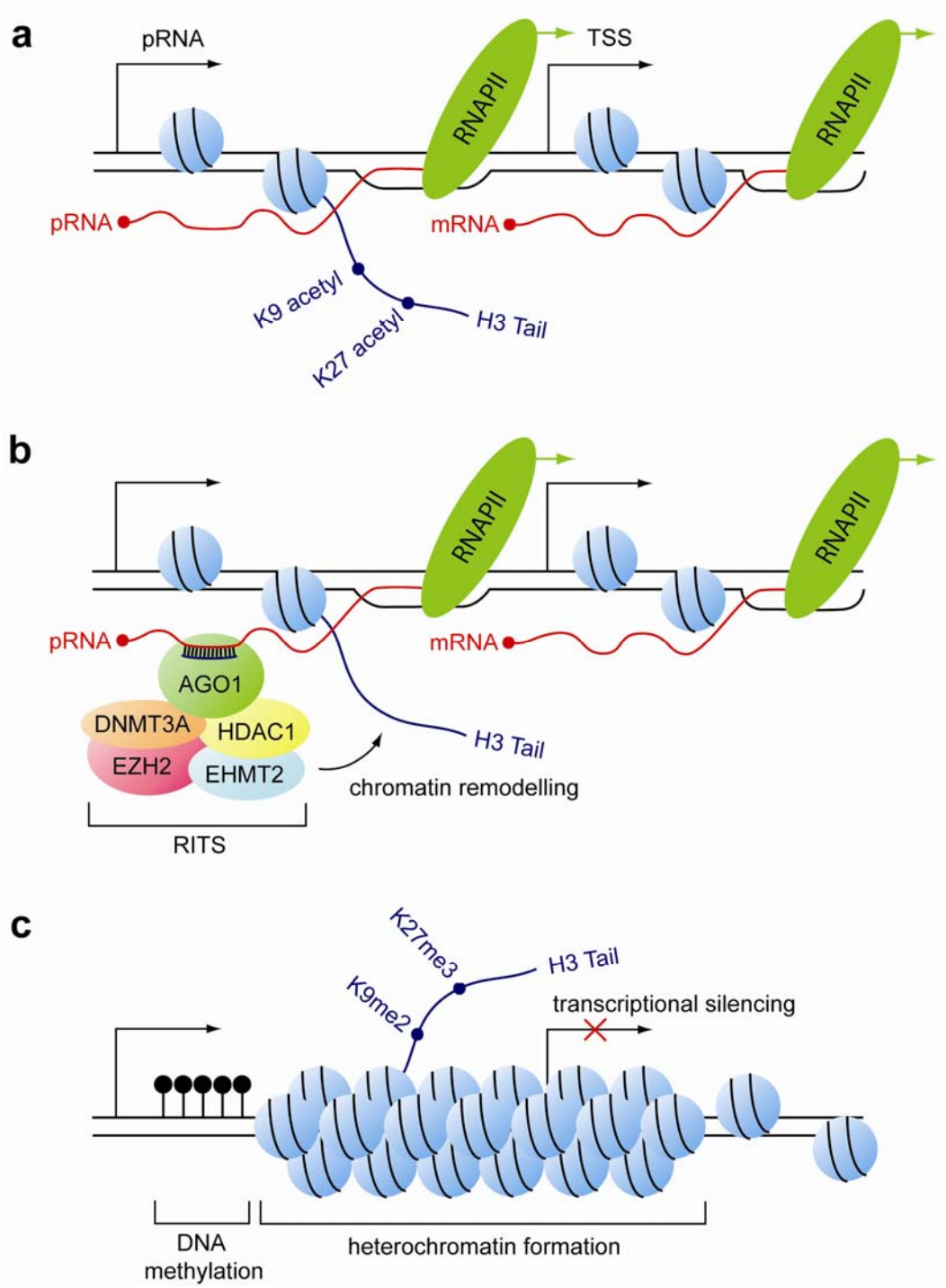
a
pRNA
TSS
RNAPII
RNAPII
pRNA
mRNA
K9 acetyl
K27 acetyl
H3 Tail
b
RNAPII
RNAPII
pRNA
mRNA
AGO1
DNMT3A
HDAC1
EZH2
EHMT2
H3 Tail
chromatin remodelling
RITS
c
K27me3
H3 Tail
K9me2
transcriptional silencing
DNA
methylation
heterochromatin formation

Figure 1.4 A Model of Transcriptional Gene Silencing In Mammalian Cells.

(a) Promoter-associated RNA (pRNA) is transcribed from the promoter region of a hypothetical gene locus upstream of the transcription start site (TSS). (b) A promoter-targeting siRNA or antisense RNA recruits the RNA-induced transcriptional silencing complex (RITS) which includes a histone deacetylase (HDAC1), a histone methyltransferase (EZH2) and a *de novo* DNA methyltransferase (DNMT3A) to the targeted promoter. (c) Replacement of H3K9 and H3K27 acetyl groups with di- and tri-methyl modifications (and in some cases methylation of promoter DNA) results in transcriptional silencing of the target locus.

1.5.1.1.1 RITS Components

The RITS complex which facilitates epigenetic-TGS is analogous to RISC that is involved in post-transcriptional gene silencing (and contains the RNA binding protein, Argonaute 2 (AGO2)) [101,177]. In *Arabidopsis* and fission yeast, Argonaute proteins are involved in TGS and constitute part of the RITS complex. Notably, in *S. pombe* the RITS complex contains Argonaute 1 (AGO1) [178,179]. These observations led researchers to hypothesise a role for AGO1 in mammalian TGS. Subsequently, Kim *et al.* showed that the presence of AGO1 is required for TGS in HEK293T cells [180]. AGO1, a close homologue of AGO2, lacks the catalytic amino acid residues (the DDH motif [181]) required for 'slicer' functionality and thus does not cleave target RNA [182]. However, several studies have detected enrichment of AGO2 at the promoters of genes targeted for TGS by ChIP and the RISC component TRBP was enriched at the *RASSF1A* promoter following treatment with a promoter-targeting siRNA suggesting the involvement of other components of the RNAi machinery in mammalian TGS [180]. Initiation of TGS requires the deacetylation of histone N-terminal tails. The involvement of histone deacetylases (HDACs) has been demonstrated indirectly through sensitivity of silencing to treatment with TSA and directly through ChIP and RNAi depletion experiments [170,183]. Similarly, the histone methyltransferases (HMTs); EHMT2 (formerly G9a) and EZH2, which methylate H3K9 and H3K27 respectively, have been similarly implicated in mammalian TGS [170,180]. The *de novo* DNA methyltransferase DNMT3A co-immunoprecipitates with H3K27me3 [169], HDAC1 [184,185], the histone methyltransferases SUV39H [186] and EZH2 [187], in addition to binding siRNAs *in vitro* [188]. Furthermore, inhibition of DNA methyltransferases by treatment with 5-azaC

or an siRNA against DNMT3A abrogates TGS [170,174,176,189,190]. Expression of DNMT1 was required for maintenance of long-term silencing [170].

1.5.1.1.2 Promoter-Associated RNA

Next generation sequencing and RNA tiling array technologies have revealed that transcription from mammalian genomes is much more prevalent than once thought [191,192]. Transcription is observed in both sense and antisense orientations and divergent transcription is frequently observed at promoters [193–196]. Non-coding RNA (ncRNA) transcripts that overlap the 5′ and 3′ termini of genes have been described previously as promoter-associated RNAs and termini-associated RNAs respectively [197]. Furthermore, depletion of the exonucleolytic RNA exosome reveals ubiquitous unstable promoter-associated transcripts [198]. Han *et al.* showed the existence of a pRNA at the *EEF1A1* promoter which was spliced and polyadenylated and could be considered an mRNA transcript with an extended 5′ untranslated region (5′-UTR). The EEF1A1 pRNA could be recovered after streptavidin pull down when HEK293T cultures were treated with a biotinylated siRNA, thus demonstrating direct physical association between the TGS effector siRNA and the pRNA target transcript [199]. Epigenetic-TGS has been shown to be dependent on the presence of pRNA for a number of different promoters as determined by antisense oligonucleotide and RNAi depletion experiments (**Table 1.1**). There are several examples of pRNAs acting as *cis*-regulatory elements that influence the transcription of their respective downstream promoters [200–202]. As such, pRNAs may directly associate with the chromatin from which they are transcribed. Alternatively, pRNAs may be indirectly tethered to their respective promoter chromatin by association with RNAPII rather than by direct binding to chromatin. In either case the

pRNA is retained in the proximity of the promoter for the downstream gene and acts as an ‘RNA signature’ for the associated locus.

promoter	effector	cell line	evidence	ref
EEF1A1	siRNA	HEK293FT	TSA/5-azaC sensitive. Promoter methylation. H3K9me2 enrichment. pRNA dependence.	[168,169,199]
RASSF1A	shRNA (stable transfection)	HeLa	AGO1, EZH2 and TARBP2 enrichment. Promoter methylation.	[180,189]
CCR5	siRNA	HEK293T	H3K9me2, AGO1 enrichment. Promoter methylation.	[180]
CDH1	siRNA	HCT116, MCF-7	H3K9me2 enrichment. Silencing in methylation deficient cell line. No promoter methylation.	[176]
UBC	siRNA shRNA (stable transfection)	HEK293GT	H3K9me2, H3K7me3, AGO1 enrichment. G9a, DNMT3A, HDAC1 and AGO1 dependence. pRNA dependence. Promoter methylation.	[170]
Tgfbr2	shRNA (lentiviral transduction)	SBC10	5-aza-dC sensitivity. Promoter methylation.	[173]
HIV1 5′ LTR	siRNA asRNA shRNA (retroviral transduction)	MAGIC-5, IG5, TZMb1	H3K9me2, H3K27me3, HDAC1 enrichment. Reduced NF-κB and Sp1 binding. TSA, α-amanitin sensitive. Promoter methylation. Ago1, DNMT3a and HDAC1 dependent.	[169,183,171,175,172]
	siRNA miRNA	HEK293, TZMb1	TSA sensitive. HDAC1 enrichment.	[203]
SIV 5′ LTR	siRNA	MAGIC-5, CEMx174	H3K9me2, H3K27me3 enrichment. 5-azaC and TSA sensitive.	[204]
PLAU	siRNA	PC3, DU145	Promoter methylation. TSA/5-azaC sensitive.	[174]
VEGFA	shRNA	C166, Intramuscular injection	H3K9me2, H3K27me3 and nucleosome enrichment.	[205]
Txnip	siRNA (combination of two)	retinal EC, Intravitreal injection	Reduced association of p300 suggesting closed chromatin formation.	[206]
HPV16 E6/E7	siRNA	SiH3, CaSki Intratumoral injection	H3k9me3 enrichment. No promoter methylation detected.	[207–209]
IL2	shRNA	jurkat	Promoter methylation. 5-azaC sensitivity. Loss of H3Ac.	[210]

ENOS	siRNA (19 and 27nt)	HAEC	cDNA microarray confirms specificity of silencing.	[211]
β-actin-Ig-μ minigene	proposed endogenous siRNA	HeLa	H3Kme enrichment. Sodium butyrate and TSA sensitive. Sensitive to 3′hExo.	[212]
RD-INK4/ARF	siRNA	HEK293T	H3K9me3, AGO1/AGO2 enrichment. pRNA dependent.	[213,214]
MTAP	shRNA	MEF		[213]
CDKN2A (p16)	siRNA	HEK293T	H3K9me3 enrichment.	[215]
RUNX3	shRNA (stable transfection)	SGC7901	Not 5-azaC sensitive.	[216]
MYC	siRNA shRNA (stable transfection)	MCF-7, SiHa, Caco-2, U87MG	Promoter methylation. 5-azaC sensitive.	[190]
CDKN1A (p21)	tiRNA mimic	MCF-7, THP-1	Loss of CTCF binding.	[217]
PGR	siRNA	T47D, MCF-7	H3K27me3 enrichment. Loss of RNAPII.	[218]
FN1	siRNA	Hep3B, HeLa	H3K9me2, H3K27me3, enrichment. TSA, 5-aza-dC, BIX sensitive. AGO1, AGO2, HP1α dependent.	[219]
POLR3D	miR-320	HEK293	H3K27me3, AGO1, EZH2 enrichment.	[220]
HOXD4	siRNA miR-10a	MCF-7, MDA-MB-231, MCF10A, HepG2, HeLa, A549	H3K27me3 enrichment. Dicer, AGO1, AGO3 dependent. Promoter methylation. pRNA involvement. 5azaC sensitive.	[221]
TBCEL	miR-17-5p miR-20a	HCT116	AGO1/AGO2 enrichment.	[215]
RASA2	miR-17-5p miR-20a	HCT116	AGO1/AGO2 enrichment.	[215]
RHPN2	miR-17-5p miR-20a	HCT116	AGO1/AGO2 enrichment.	[215]
WHSC1	miR-17-5p miR-20a	HCT116	AGO1 enrichment.	[215]
CDCA8	miR-let-7f	WI38	H3K27me3, AGO2 enrichment.	[222]
CDC2	miR-let-7f	WI38	H3K27me3, AGO2 enrichment.	[222]

Table 1.1 Studies Reporting Epigenetic-TGS.

Studies in which small RNA-based effectors silence gene expression with associated epigenetic changes. 'Enrichment' and 'Loss of' indicates that the described proteins were enriched or reduced at the effector target site as measured by chromatin immunoprecipitation. 'Dependent' indicates that the reported effect was abolished or reduced when the described genes were down-regulated by siRNAs or antisense oligonucleotides. 'Sensitive' indicates that the reported effect was abolished or reduced when cultures were treated with the chemical inhibitors described (i.e. TSA and sodium butyrate (inhibitors of histone deacetylases), 5-azaC and 5-aza-dC (inhibitors of DNA methyltransferases), BIX (inhibitor of histone methyltransferases specifically targeting H3K9) and 3′hExo (digests siRNAs).

1.5.1.1.3 Non-Promoter-Targeting TGS

Several studies have demonstrated TGS or TGS-like effects through targeting non-promoter regions and these are noteworthy 'exceptions that prove the rule'. The observation that siRNAs can direct promoter chromatin remodelling raises the question as to whether similar effects can be seen in non-promoter regions. Several studies have now shown that this is the case. A study by Bühler *et al.* showed that a small RNA species produced from intron 4 of an Immunoglobulin (Ig) minigene driven by the β-actin (*ACTB*) promoter induced transcriptional silencing in HeLa cells [212]. Enrichment of methylated H3K9 was observed at the minigene promoter and the silencing was sensitive to treatment with TSA and sodium butyrate suggesting the involvement of histone deacetylases. Interestingly, a neomycin resistance gene found on the same plasmid as the Ig minigene was also silenced. This suggested that the induced heterochromatic region had spread upstream from the small RNA target site in intron 4 to silence the minigene promoter and the upstream neomycin cassette.

In some cases, non-promoter transcripts may be present in close proximity to promoters as a result of the formation of higher order chromatin structures [223]. A recent study by Yue *et al.* showed that the human progesterone receptor (*PGR*) could be silenced by siRNAs that target downstream of the 3′ terminus of the gene and are therefore not complementary to either the mRNA or the promoter. Chromosome conformation capture (3C) analysis showed that the locus formed a gene loop structure whereby the promoter region and the 3′ terminal region were found to be in close proximity in three-dimensional space. Additionally, ncRNA species were identified at both termini and were

found to associate with AGO2 as determined by RNA immunoprecipitation (RIP) and ChIP. Consequently, the siRNA was indirectly targeting the *PGR* promoter through interaction with a promoter-proximal ncRNA [224].

Epigenetic control of splicing has also been shown in a study by Alló *et al.* In this case, an intron-targeting siRNA induced local heterochromatin formation within the coding region of the fibronectin gene (*FN1*) and consequently influenced alternative splicing [219]. The formation of a local closed chromatin region resulted in slowed RNAPII procession and preferential inclusion of an alternatively spliced exon proximal to the siRNA target site.

1.5.1.2 Antigene-TGS

Antigene-TGS (RNA:DNA model) is the use of oligonucleotides to inhibit transcription through direct interaction of the effector molecule with chromosomal DNA by either DNA:DNA:oligonucleotide triplex formation or by the oligonucleotide binding to exposed single stranded DNA (e.g. at the transcription start site, TSS) [225,226]. The effector oligonucleotide acts to sterically hinder RNA polymerase procession and consequently induce transcriptional gene silencing. Janowski *et al.* showed that siRNAs (which they term antigene RNAs (agRNAs) as they are designed to target DNA) that target the transcription start site of the *PGR* B-promoter induce transcriptional inhibition. Functional agRNAs were found to overlap the -9 to +2 region that was predicted to form an open complex during transcription initiation. This region constitutes an oligonucleotide target site where the two strands of DNA are transiently separated in order to permit transcription initiation. Inhibition by agRNAs was highly potent with an IC50 of 2.5 nM and similar results were seen in the case of the Major Vault Protein (*MVP*), the Androgen Receptor (*AR*) and Cyclooxygenase-2 (*COX2*) genes indicating the effect is observable for TATA-containing and TATA-less promoters. No promoter DNA methylation was observed (up to 5 days post transfection) for any of these genes studied [227]. Similarly, for an agRNA targeting just upstream of PGR TSS (-26 to -7) no TSA [228] or 5-azaC [227] sensitivity, DNA methylation or substantial changes in histone H3K4, H3K9 or H3K27 methylation were observed [227]. Taken together these results suggest a non-epigenetic mechanism of silencing. PNA [229], LNA [230,231] and other chemically modified mixmer oligonucleotides [232] were also shown to silence *PGR* in a similar manner.

Similar results were reported in a study by Napoli *et al.* who targeted the transcription start site of the *MYC* promoter with an siRNA [233] (**Table 1.2**). Interestingly, this study also showed that the presence of a promoter transcript was required for silencing. The role of this transcript in this mechanism of silencing is unclear. Despite early reports of antigene-TGS failing to show any evidence of epigenetic involvement in silencing, a recent study targeting the *PGR* promoter did show enrichment of silent state chromatin modifications [224]. Additionally, the expression of AGO2 was shown to be required for *PGR* silencing which points towards an RNA:RNA interaction [234]. Consequently, the degree to which agRNAs target chromosomal DNA or RNA remains an open question.

promoter	effector	cell line	evidence	ref
PGR	agRNA agPNA agLNA agENA	T47D	Not TSA sensitive. No histone changes. No promoter methylation. AGO1 and AGO2 dependent. AGO1 and AGO2 enrichment. AGO1 and AGO2 associate with a PGR antisense transcript as measured by RIP. Conflicting evidence of epigenetic changes [224].	[227,229,228, 235,232,230, 231]
AR	agRNA agLNA agENA	T47D	AGO1 and AGO2 dependent. No promoter methylation.	[227,228,231]
MVP	agRNA	T47D		[227]
COX2	agRNA	T47D		[227]
HTT	agRNA	T47D	AGO1 and AGO2 dependent.	[228]
MYC	siRNA	PC3, DU145 and LNCaP	No histone changes. pRNA dependent.	[233]
HPA	siRNA shRNA	PC3 EJ SGC-7901	Loss of RNAPII, TFIIB No histone changes or DNA methylation detected. AGO1 and AGO2 dependent.	[236]

Table 1.2 Studies Reporting Antigene-TGS.

Studies in which small RNA-based effectors targeted to transcription start sites silence gene expression in the absence of epigenetic changes. 'Enrichment' and 'Loss of' indicates that the described proteins were enriched or reduced at the effector target site as measured by chromatin immunoprecipitation. 'Dependent' indicates that the reported effect was abolished or reduced when the described genes were down-regulated by siRNAs or antisense oligonucleotides. 'Sensitive' indicates that the reported effect was abolished or reduced when cultures were treated with the chemical inhibitors described (i.e. TSA (inhibitor of histone deacetylases).

1.5.2 Transcriptional Gene Activation

Small RNAs have also been shown to activate gene expression (**Table 1.3**). Although some groups have termed this phenomenon RNA activation (RNAa), here we use the term transcriptional gene activation (TGA) as recent reports suggest that the effect is closely related to epigenetic-TGS. The first evidence that small RNAs could activate gene transcription came from the Functional Annotation of the Mammalian Genome (FANTOM) consortium [195]. Pairs of overlapping sense and antisense transcripts were identified and targeted with siRNAs and both concordant (i.e. both transcripts were silenced) and discordant (i.e. the target transcript was silenced but the expression of the overlapping transcript increased) modes of regulation were observed. Separately, Li *et al.* showed that siRNAs targeting the *CDH1* (E-cadherin) promoter induced sequence specific, long-lasting (~13 days) gene activation in human cells. 2-10 fold induction was observed and 1 nM siRNA was sufficient to induce silencing. RNAi experiments demonstrated that AGO2 was indispensable for gene activation and silencing was associated with a loss of H3K9 methylation. Similarly, *CDKN1A* (p21) and *VEGFA* (vascular endothelial growth factor A) could also be activated following transient transfection with promoter-targeting RNA duplexes [237]. Morris *et al.* investigated these results further and demonstrated that siRNAs targeting the p21 promoter induced PTGS of an antisense transcript leading to gene activation through the reversal of an endogenous TGS mechanism. In this case the antisense transcripts themselves were shown to be directing epigenetic silencing [238] (**Fig. 1.5**). Similarly, Modarresi *et al.* have shown that targeting an antisense RNA overlapping the *Bdnf* (brain-derived neurotrophic factor) gene using antisense oligonucleotide gapmers (which degrade the

target RNA) results in abrogation of epigenetic silencing with consequent gene activation [239].

promoter	effector	cell line	comments	ref
CD97	siRNA	Hepa1-6		[195]
CDH1	siRNA	PC-3, DU-145, 5637, COS1, WES, MCF-7, MDA-MB-453	AGO2 dependent.	[237,240–242]
CDKN1A	siRNA	PC-3, Hela, COS1, WES, MCF-7	Bidirectional transcription regulates silencing and activation	[237,238,241]
PR	siRNA	TF7D, MCF-7	AGO2 enrichment. AGO2 dependent.	[235,243]
MVP	siRNA	MCF-7		[243]
LDLR	siRNA	HepG2		[244]
VEGFA	siRNA shRNA (lentiviral tranduction)	Hela, COS1, WES, CCSMC, C166, IM injection	*In vivo* transcriptional up-regulation.	[205,237,241,245]
IL10	siRNA	THP1	Enhancer targeting.	[246]
IL24	miR-205	PC3		[247]
IL32	miR-205	PC3		[247]
CDH1	miR-373	PC3		[248]
CSDC2	siRNA	PC3, HCT116		[248]
OCT4	siRNA	MCF-7		[249]
BDNF	siRNA antagoNAT	N2a HEK293T ICV injection	Loss of H3K27me3, EZH2. *In vivo* transcriptional up-regulation.	[239]
GDNF	antagoNAT	HEK293T		[239]
EPHB2	antagoNAT	HEK293T		[239]
p53	siRNA	COS1, WES		[241]
PAR4	siRNA	WES		[241]
NKX3-1	siRNA	COS1, WES		[241]
Ccnb1	siRNA miR-744 miR-1186 miR-366d-3p	NIH/3T3, TRAMP C1	H3K4me3, RNAPII, AGO1 enrichment.	[241,250]
CXCR4	siRNA	Primary rat stem cells		[241]
KLF4	siRNA	DuPro, PC3, DU145		[251]
NANOG	siRNA	NCCIT		[252]
WT1	siRNA	HepG2		[253]

Table 1.3 Studies Reporting TGA.

Studies in which small RNA-based effectors induce transcriptional gene activation. 'Enrichment' and 'Loss of' indicates that the described proteins were enriched or reduced at the effector target site as measured by chromatin immunoprecipitation. 'Dependent' indicates that the reported effect was abolished or reduced when the described genes were down-regulated by RNA interference. 'Sensitive' indicates that the reported effect was abolished or reduced when cultures were treated with the chemical inhibitors described (i.e. TSA (inhibitor of histone deacetylases)). 'antagoNAT' refers to anti-natural antisense transcript oligonucleotides (i.e. LNA gapmers and LNA mixmers).

Building on previous work targeting the *PGR* promoter, the Corey lab demonstrated that when the sequence of a silencing siRNA was shifted by a single nucleotide, it induced potent and specific activation of PGR mRNA and protein expression in T47D and MCF7 breast cancer cells. Importantly, *PGR* is differentially expressed in these two cell lines. In T47D cells, which express high levels of PGR, gene activation was relatively modest. However, in MCF7 cells, which express low levels of PGR, the observed activation was as much as 18 fold. These results suggest that the gene activation is dependent on cellular context and that cells that already express the targeted gene at high levels may be less susceptible to TGA. Gene activation was reversed by treatment with TSA and resulted in reduced H3K9 and H3K14 acetylation and increased di- and tri-methylation of H3K4 implicating chromatin conformation changes in gene activation. Similarly, a 4 fold induction in *MVP* gene expression was observed following treatment with siRNAs [243]. Further work showed that antisense transcripts overlapping the *PGR* promoter are the targets for activating siRNAs. These antisense transcripts are spliced, polyadenylated, span a 70,000 kb region of genomic DNA and are present at levels 10 to 1,000 fold lower than the PGR mRNA. Direct association of the siRNAs was determined by biotin pull down, and pan-Argonaute RIP showed recruitment of AGO to the antisense RNA [234]. A combination of RNAi depletion and RIP for all 4 human AGO proteins demonstrated that AGO2 is involved in siRNA-mediated *PGR* transcriptional silencing and activation [237].

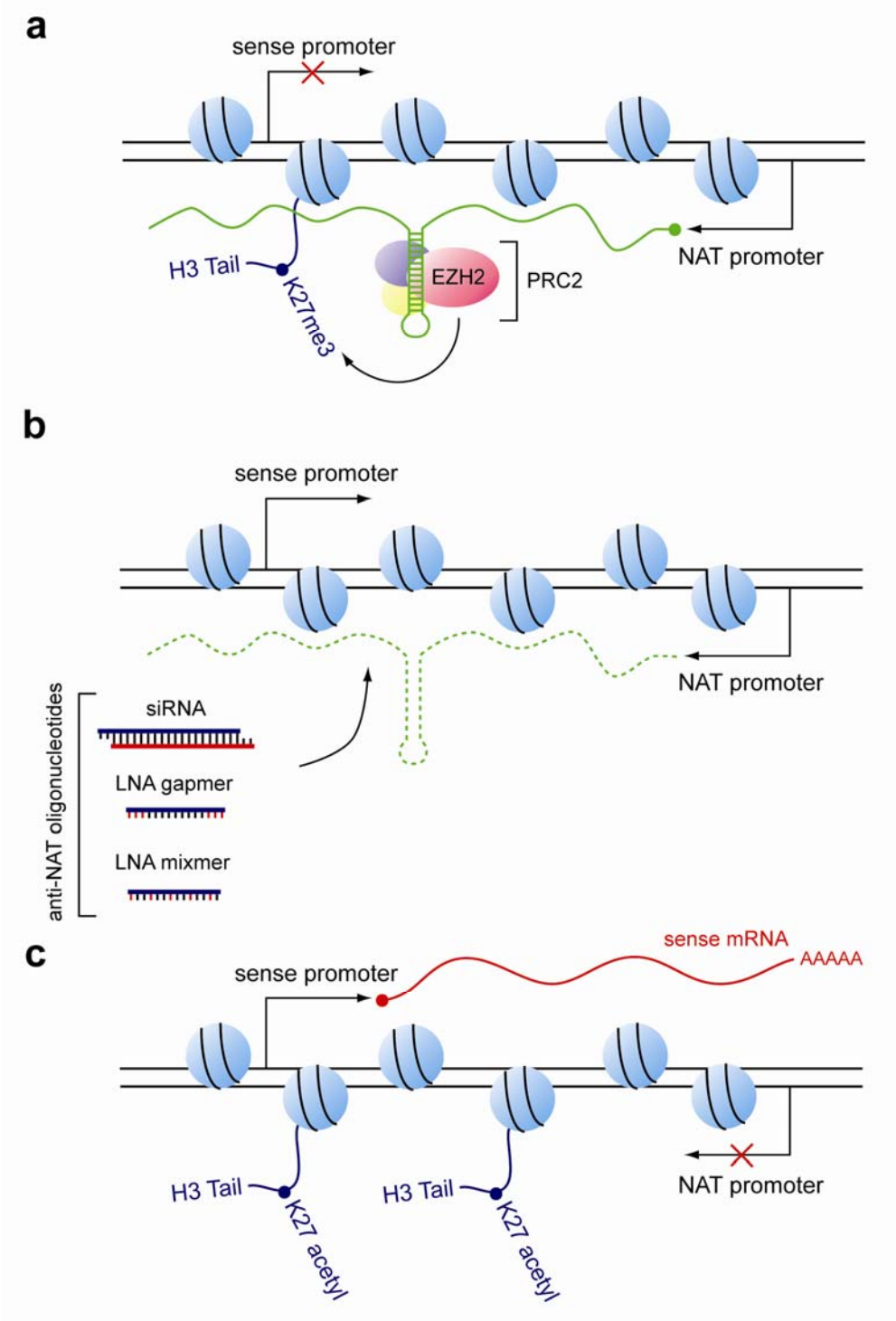
a
sense promoter
H3 Tail
K27me3
EZH2
PRC2
NAT promoter
b
sense promoter
NAT promoter
anti-NAT oligonucleotides
siRNA
LNA gapmer
LNA mixmer
c
sense mRNA
AAAAA
sense promoter
H3 Tail
K27 acetyl
H3 Tail
K27 acetyl
NAT promoter

Figure 1.5 A Model of Transcriptional Gene Activation in Mammalian Cells.

(a) A natural antisense transcript (NAT) directs epigenetic silencing at a hypothetical promoter through recruitment of the Polycomb Repressive Complex 2 (PRC2) which contains the histone methyltransferase Enhancer of Zeste 2 (EZH2). (b) Targeting the NAT with siRNAs or antisense oligonucleotides (e.g. LNA gapmers/mixmers) alleviates endogenous epigenetic repression and results in transcriptional activation.

1.5.3 The Practical Application of Transcriptional Modulation

Methods for facilitating epigenetic-TGS and TGA are discussed here [254] and the use of agRNAs and agPNAs here [255]. Typically, the target gene promoter is targeted within 200 bp upstream of the transcription start site. Some studies have specifically targeted CpG dinucleotides [204]. There is, as yet, no consensus on TGS/TGA effector design criteria as some researchers have utilised conventional siRNA design rules [237] to good effect, whereas other have shown highly functional siRNAs that score poorly [171] based on Reynolds criteria [256].

Small-RNA mediated transcriptional modulation requires delivery to the nucleus which can be achieved in a number of ways. In actively cycling cells it is likely that dissolution of the nuclear membrane during cell division is sufficient to allow small RNA effector molecules to enter the nucleus. Similarly, lentiviral transduction facilitates nuclear membrane permeabilisation [257]. Generally, mammalian TGS studies have used relatively high (>50nM) siRNA concentrations, presumably in order to achieve effective nuclear concentrations of siRNA. This suggests that, in the absence of a dedicated nuclear-targeting strategy, nuclear delivery may be achieved through passive diffusion from the cytoplasm to the nucleus (thus high oligonucleotide concentrations in the cytoplasm are required). Nuclear targeting has also been achieved through non-covalent complexing of siRNA with nuclear-targeting peptides such as MPG [169,258].

TGS/TGA can be induced by small interfering RNA (siRNA) molecules or viral/plasmid expressed short hairpin RNA (shRNA) precursors [189]. The siRNA antisense strand

alone is sufficient to induce TGS [169] and, to this end, ~21mer expressed antisense RNAs (asRNAs) have also been shown to induce TGS [169,175]. The use of expressed asRNAs may be preferable to shRNAs in two respects. Firstly, there is no corresponding sense strand to mediate off-target effects, and secondly, transcription alone generates the mature antisense species in the nucleus, whereas shRNAs must be transcribed, exported, diced and imported back into the nucleus for functionality.

Recently, Hwang *et al.* demonstrated that a hexanucleotide motif is sufficient to direct miR-29b to the nucleus. The same nuclear-targeting effect was observed when the sequence was incorporated into a synthetic siRNA targeting luciferase [259]. The potential for this sequence motif to direct siRNAs to the nucleus may be highly useful in the design of TGS effectors. However, a word of caution is warranted as Liao *et al.* detected no nuclear enrichment of RNAs carrying the hexanucleotide motif using a deep sequencing approach [260].

Chemical modification of TGS/TGA effector oligonucleotides offers a potential means of enhancing nuclear delivery. For example, phosphorothioate-substituted oligonucleotides are primarily located in the nucleus following transient transfection [261]. Similarly, a recent study has shown that chemical addition of a 2,2,7-trimethylguanosine cap to antisense oligonucleotides improves their nuclear accumulation [262]. These simple modifications may enhance nuclear delivery, although it remains to be seen as to whether chemical alteration reduces the functionality of the TGS/TGA effector molecule.

1.5.4 Potential for Off-Target Effects

The main technologies utilised to induce TGS and TGA (primarily siRNAs and shRNAs) are chemically identical to those used for conventional RNAi and so can potentially mediate similar off-target effects. Indeed, the requirement for high concentrations of siRNA to induce TGS/TGA means that potential off-target effects must be considered carefully [169,258]. siRNAs completely or partially complementary to non-target mRNAs will induce mRNA slicing or translational repression respectively [263]. Furthermore, siRNAs and shRNAs can, in some circumstances, induce non-specific gene silencing by activation of the interferon response [264,265]. The presence of long double-stranded RNA [266], specific immunostimulatory sequence motifs [267,268] or 5′-triphosphates that result from *in vitro* transcribed RNAs [269] are markers of viral infection and so have the potential to induce the interferon response. As with conventional RNAi, care must be taken to avoid these immunostimulatory effects when designing oligonucleotides for TGS/TGA.

Weinberg *et al.* showed that an asRNA targeting the HIV-1 5′-LTR, which activated expression of proviral mRNA transcription, was actually functioning via the off-target down-regulation of a general transcriptional suppressor [270]. This study indicates that care must be taken to validate the specificity of interactions in studies of transcriptional modulation. Similarly, a study by Moses *et al.* showed that intended transcriptional gene silencing of *VEGFA* was, in fact, a sequence-dependent off-target effect [271]. This study also provided evidence that TGS in a previous report [169] may also be due to non-specific effects. The authors emphasised the need to mutate the small RNA target

sequence within the targeted promoter as a means of ensuring specificity. However, experiments of this type, whilst potentially informative, suffer from two technical difficulties. Firstly, mutations in the promoter sequence may adversely affect target gene transcription. And secondly, cloning the target promoter upstream of reporter genes may result in loss of endogenous ncRNA regulation and thereby not accurately model the transcriptional landscape of the target gene.

Conversely, a thorough study by Suzuki *et al.* showed highly specific TGS of HIV-1 replication by a promoter-targeting shRNA. Scrambled and mismatched controls did not suppress viral transcription, and other genes involved in viral entry showed no change in expression. Furthermore, the shRNA failed to silence HIV-2 (which does not contain the complementary shRNA target site) and genes with similar regulatory elements in their promoters (i.e. NF-κB binding sites) were similarly unaffected. Additionally, no interferon induction was observed. Taken together this study shows that sequence-specific on-target TGS is possible in the case of HIV-1 with no observed off-target effects [272].

One strategy to enhance the potency of conventional PTGS is to utilise a pool of siRNAs (typically 2-4) targeting different regions of the target mRNA, so called combinatorial RNAi. This approach has the advantage of exhibiting high levels of knockdown with minimal off-target effects as the siRNAs converge on the same target mRNA but are individually at relatively low concentration. To this effect, Ting *et al.* showed that combining two promoter-targeting siRNAs induced higher levels of knockdown relative

to treatment with each individual siRNA alone [176]. This suggests that combinatorial TGS may be a means of maximising potency while minimising off-target effects.

Heterochromatin has been shown to propagate following induction by small RNA effectors [183]. Spreading of heterochromatin to upstream genes has been observed in at least one report of mammalian TGS [212]. This presents an additional source of potential off-target effects as heterochromatin spreading may result in the silencing of genes adjacent to the target locus. In addition, small RNAs with complementarity to non-target promoters may mediate off-target TGS and/or TGA. Equally, siRNAs intended to silence genes by RNAi may potentially elicit off-target TGS/TGA effects.

1.5.5 Therapeutic Applications of Transcriptional Modulation

1.5.5.1 Human Immunodeficiency Virus

The Human Immunodeficiency Virus (HIV) is a particularly promising target for gene silencing therapies. PTGS has been utilised to target the HIV RNA genome and transcribed viral mRNA in order to inhibit viral replication. The high rate of viral turnover and the error prone nature of HIV reverse transcriptase contribute to the rapid accumulation of escape mutants to conventional small molecule inhibitor drugs and RNA interference effectors [273–275]. von Elje *et al.* showed that the ability of HIV to accumulate escape mutations was restricted by targeting shRNAs to conserved regions of the viral genome [276]. Consequently, nucleic acid based therapeutics are a promising anti-HIV approach as modifying effector molecules to account for escape mutants is relatively trivial. A combination therapy whereby multiple gene silencing approaches target several viral genes may limit the capacity of the virus to mutate, analogous with highly active antiretroviral therapy [277]. TGS offers an additional advantage by silencing the integrated proviral DNA, therefore inhibiting the viral lifecycle before the reverse transcription stage and thus limiting the possibility of escape mutations occurring [171]. An alternative anti-viral strategy is to target host factors that are required for viral replication or entry, as these are not subject to the same evolutionary pressure as viral genomes. For example, Kim et al showed that the HIV-1 co-receptor CCR5 promoter is amenable to silencing by TGS [180].

One of the first reports of HIV TGS was by Suzuki *et al.* who utilised 21nt duplex siRNAs targeting tandem NF-κB motifs in the U3 region of the HIV-1 5′-LTR.

Transfection in MAGIC-5 cells (CCR5-CXCR4 expressing Hela/CD4+ cell line infected with HIV) resulted in LTR cytosine methylation and the suppression of viral replication for at least 30 days [171]. Four LTR-targeting duplexes were found to induce differential CpG methylation with the degree and density of methylation correlating with the strength of viral suppression. Two subsequent studies showed that (1) treatment with an LTR-targeting siRNA was accompanied by sustained recruitment of RITS components AGO1 and HDAC1, enrichment of the silent chromatin modification H3K9me2 and rearrangement of nucleosome positioning around the transcription start site within the integrated provirus [183], and (2) that viral suppression could be maintained for up to one year [172]. The same group also showed inhibition of simian immunodeficiency virus (SIVmac251) replication mediated by siRNAs targeting the 5′-LTR upstream of the transcription start site in two cell lines (MAGIC-5 and CEMx174 (human lymphoid cells)). The silencing effect induced DNA methylation, enrichment of H3K9me2 and H3K27me3 and was partially reversed by treatment with TSA and 5-azaC.[204]

In parallel, Weinberg *et al.* used asRNAs targeting the U3 region of HIV-1 5′-LTR in IG5 cells (which contain an integrated tat-inducible firefly luciferase transgene driven by the HIV-1 5′-LTR [278]). asRNAs were found to be comparable to equivalent double-stranded siRNAs and directed H3K27 tri-methylation in a RNAPII dependent manner [169]. Building on this work, Turner *et al.* developed a mobilisation-competent lentiviral system to express these HIV-targeting asRNAs. Suppression of viral replication was observed for up to one month and TGS verified by nuclear run-on analysis, enrichment of silent state chromatin modifications and CpGs methylation at the HIV-1 5′-LTR. In

addition silencing was found to be dependent on the presence AGO1, HDAC1 and DNMT3A [175].

1.5.5.2 Cancer

Cancer refers to a broad group of diseases characterised by the formation of masses of cells that have lost cell cycle regulation and thus divide uncontrollably (i.e. tumors). Tumorigenesis is a multi-step process in which the various cellular mechanisms that restrain cell proliferation are progressively lost [279]. Activating mutations in oncogenes (i.e. genes which promote proliferation) leading to ectopic expression is one such step. Conversely, loss-of-function mutation or epigenetic silencing of tumor suppressor genes (i.e. genes which act to protect against cancer progression) are common features of many tumors. The silencing of oncogenes and activation of tumor suppressor genes, by TGS and TGA respectively, have thus been the focus of numerous transcriptional modulation studies [174,176,180,189,190,207,213–216,237,238,243,280].

One promising anti-cancer TGS target is the plasminogen activator, urokinase (*PLAU*), a gene involved in tumor invasion and metastasis. DNA demethylation at the *PLAU* promoter leads to increased *PLAU* expression which is observed in many cancers and correlates with poor survival [281]. In a study by Pulukuri and Rao, PC3 cells were transfected with siRNAs that target the *PLAU* promoter and implanted into immunodeficient mice. (The lung is a common metastatic site of prostate cancers and implantation of PC3 human prostate cancer cells into mice induces lung metastasis). Mice implanted with *PLAU* promoter-targeting siRNA treated cells showed long-term *PLAU* silencing, suppressed primary tumor growth and reduced lung metastasis relative to those

implanted with control siRNA treated cells [174]. This *ex vivo* study provided the first evidence that TGS may be a relevant therapeutic strategy *in vivo*.

1.5.5.3 Transcriptional Modulation *in vivo*

To date, four studies have demonstrated transcriptional modulation *in vivo*. A landmark study by Turunen *et al.* demonstrated both TGS and TGA of *Vegfa* following lentiviral delivery of shRNAs in a mouse hindlimb ischemia model [205]. Inhibition of *Vegfa* has the potential to suppress metastasis by inhibiting tumor vascularisation, whereas activation of *Vegfa* could be used to promote neovascularisation as a therapy for myocardial or peripheral ischemias [282]. The silencing shRNA induced reductions in H3K4 methylation and acetylation, and increases in methylation of H3K9 and H3K27 consistent with epigenetic silencing. Conversely, treatment with the activating shRNA resulted in an increase in H3K4 tri-methylation and reductions in H3K9 and H3K27 methylation consistent with transcriptional activation [205]. Other *in vivo* TGS studies have utilised local injections of promoter-targeting siRNAs against the human papillomavirus (HPV) E6/E7 and thioredoxin-interacting protein (*Txnip*) promoters to induce *in vivo* TGS in mouse xenograft tumors [280] and rat retina [206] respectively, although these reports did not include investigations of epigenetic remodelling. More recently, *in vivo* TGA of *Bdnf* was shown by intracerebroventricular (ICV) injection of siRNAs and antisense oligonucleotides (which they term antagoNATs) in mouse brain. The oligonucleotides targeted a natural antisense transcript which overlaps with the *Bdnf* locus and recruits Ezh2. Following treatment, a loss of H3K27me3 and Ezh2 was observed at the *Bdnf* promoter by ChIP [239].

1.5.6 Endogenous Epigenetic Modulation

The observation that exogenously introduced small RNAs can utilise cellular machinery to induce epigenetic changes in gene expression implied that microRNAs (miRNAs) might be endogenous epigenetic triggers of epigenetic silencing. Kim *et al.* utilised a bioinformatic search for miRNA target sites in human promoters 200 bp upstream of the transcription start site and 10 completely complementary miRNA target sites were identified. One candidate, miR-320, was found to target the *POLR3D* promoter and induced transcriptional gene silencing including promoter enrichment of AGO1, EZH2 and H3K27me3. Low levels of sense transcription were also detected at *POLR3D* promoter [220]. Conversely, Place *et al.* showed miR-373 induces activation of *CDH1* and *CSDC2* (cold-shock domain-containing protein C2) in PC3 cells [248]. Gene activation was induced by both mature miR-373 and expressed pre-miR-373 synthetic double-stranded RNA mimics, was Dicer-dependent and resulted in enrichment of RNAPII at the *CDH1* and *CSDC2* promoters. Interestingly, a miRNA with only partial complementarity to its target promoters has also been shown to induce TGA suggesting there may be numerous endogenous transcriptional modulation events [247]. These studies suggest new functions for miRNAs in the regulation of mammalian transcription in addition to PTGS by transcript degradation and translational repression.

1.5.6.1 Long Non-Coding RNAs

lncRNAs are a heterogeneous group of RNA transcripts >200 nucleotides in length with low protein coding potential that are processed in similar ways to mRNAs (i.e. the majority are spliced and many are polyadenylated). lncRNAs can be sense or antisense transcripts with respect to a neighbouring protein-coding gene locus, intron-derived, the products of divergent bidirectional transcription or reside in the space between genes (i.e. long intergenic non-coding RNAs, lincRNAs). (**Fig. 1.6a**) Many lncRNAs show distinct spatial, temporal, cell-type specific and sub-cellular specific expression patterns suggesting that their transcription is tightly regulated and therefore unlikely to be transcriptional 'noise' [191,283,284]. In addition many lncRNAs show a high degree of evolutionary conservation consistent with biological function [285]. lncRNAs have been implicated in a wide variety of cellular processes and are therefore potential drug targets.

Similarly, there are clear parallels between small RNA-mediated transcriptional regulation and gene regulation by lncRNAs. For example, Yu *et al.* identified an antisense transcript at the p15 promoter. Over-expression of portions of the p15 antisense RNA led to silent state chromatin formation and long-term gene silencing of the p15 tumor suppressor. Levels of the antisense RNA were also found to be inversely correlated with p15 expression in a variety of cancers. Silencing was reversed by treatment with TSA and 5-azaC. The same effect was also observed in a Dicer-deficient cell line, suggesting that the antisense RNA is not processed into smaller siRNA effectors [286].

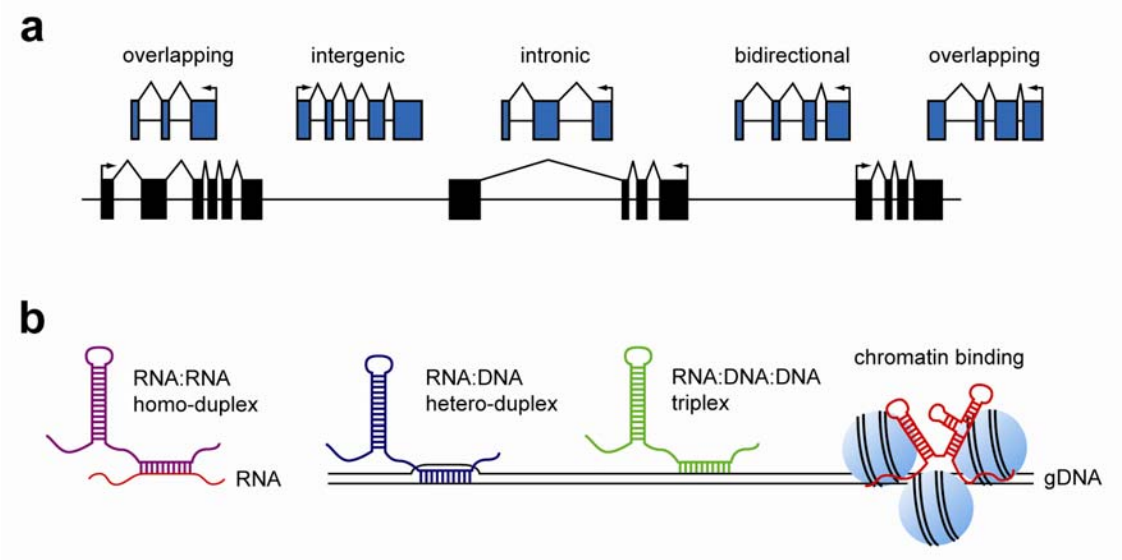

Figure 1.6 Genomic organisation and function of lncRNAs.

(a) Genomic organisation of lncRNAs (blue) with respect to protein coding genes (black). Arrows indicate the direction of transcription. lncRNAs can be partially or completely overlapping with protein coding genes, reside within introns (intronic) or the space between genes (intergenic), or result from bidirectional transcription at promoters. (b) lncRNAs can interact with other RNA molecules (RNA:RNA homo-duplex), transient single-stranded genomic DNA (gDNA) regions (RNA:DNA hetero-duplex), form RNA:DNA:DNA triplexes with gDNA or fold into secondary structures which can directly bind to chromatin.

1.5.6.2 lncRNA Function

lncRNAs primarily act as adaptors that mediate interactions between chromatin, proteins and other RNAs. Two properties of lncRNA molecules enable them to function in this manner. Firstly, they can bind to DNA or other RNA molecules by (a) complementary Watson-Crick base-pairing to form hetero- or homo-duplexes, (b) formation of DNA:DNA:RNA triplexes by Hoogstein and reverse Hoogstein base-pairing, or (c) by direct RNA recognition of chromatin surface features [287]. Secondly, the inherent flexibility of RNA permits the formation of complex secondary structures that can function as binding domains for proteins or small molecules (**Fig. 1.6b**). The combination of these properties enables a much wider range of functions than is possible with miRNAs. Additionally, lncRNAs may also contain multiple binding modules allowing for complex, multi-functional interactions.

Arguably the most exciting role of lncRNAs is as epigenetic regulators of gene expression. lncRNAs form riboprotein complexes where the ncRNA acts as a guide that targets chromatin modifying activities or transcription factors to specific genomic loci. For example, RepA ncRNA (derived form the 5′ region of Xist transcript) binds PRC2 (Polycomb Repressive Complex 2) and guides it to induce H3K27 tri-methylation and heterochromatin formation at the *Xist* promoter. This event initiates the process of X-chromosome inactivation [202]. Similarly, in the case of rRNA genes, a promoter-associated RNA transcript forms a triplex structure at the rRNA promoter and recruits DNMT3B (DNA (cytosine-5-)-methyltransferase 3 β) in order to induce promoter DNA methylation and transcriptional gene silencing [200,288]. Thus RepA and the rDNA

promoter transcript act as guides for epigenetic modifiers in *cis* (i.e. influencing neighbouring genes). Conversely, lncRNAs can also function as guides in *trans* (i.e. affecting distal genes). For example, lincRNA-p21 is able to guide epigenetic remodelling at multiple genomic loci via recruitment of hnRNP-k [289].

lncRNAs can also act as RNA scaffolds that remain associated with a chromatin locus and recruit multiple epigenetic modifiers. As a result, complex changes in chromatin states can be dynamically coordinated in response to external signals. The lncRNA *HOTAIR*, which is transcribed from the *HOXC* cluster, binds to the *HOXD* cluster. HOTAIR associates with the polycomb repression complex PRC2 at its 5′ region [290] and a complex containing LSD1, CoREST, and REST at its 3′ region [291]. Consequently, the activities of these two complexes (i.e. tri-methylation of H3K27 and demethylation of H3K4 respectively) are coordinated in order to induce transcriptional silencing. Similarly, scaffold lncRNAs transcribed from pericentromeric satellite regions have been shown to associate with SUMOlated-heterochromatin protein 1 (HP1) which induces further recruitment of additional HP1 molecules and transcriptional silencing [292]. The epigenetic silencing complexes SMCX and PRC1, and the epigenetic activating complex WDR5/MLL have also been shown to associate with lncRNAs [293,294].

Recently, it was shown that lncRNAs can influence the sub-nuclear localisation of genomic loci. The lncRNA TUG1 was shown to bind methylated Pc2 (a polycomb component) and thereby direct the accompanying genomic DNA to polycomb bodies

where it is epigenetically silenced. Conversely, unmethylated Pc2 was bound by another lncRNA, MALAT1 (also known as NEAT2), which resulted in localisation to interchromatin granules (ICGs) which are associated with active transcription [295]. Thus, post-translational modification of a non-histone protein is capable of influencing the sub-nuclear localisation of chromatin through interactions with lncRNAs.

lncRNAs also act as 'riboregulator' decoys by binding and sequestering proteins (e.g. transcription factors and chromatin modifiers) or other RNAs. For example, the lncRNA Gas-5 (growth arrest-specific 5) forms an RNA secondary structure that binds to the DNA binding domain of glucocorticoid receptor (GR) and prevents it from interacting with its DNA target sites, thus repressing GR activity [296]. Additionally, lncRNAs have been shown to act as endogenous miRNA sponges [297,298] or to mask miRNA binding sites on target mRNAs [299]. Similarly, MALAT1 alters the sub-nuclear localisation of the splicing factor SR through sequestration in nuclear speckles [300,301].

lncRNAs also exert non-epigenetic effects on gene expression. Transcription of upstream lncRNA genes is sufficient, in some cases, to inhibit transcription of downstream genes – a phenomenon known as transcriptional interference [302]. In the case of the dihydrofolate reductase (*DHFR*) locus, a 5′ sense promoter RNA forms a direct association with *DHFR* promoter DNA in order to inhibit transcription (in addition to acting as a decoy for the basal transcription factor TFIIB) [201].

Where overlapping bidirectional transcription occurs, there is potential for hybridisation between the pair of sense and antisense transcripts. In the case of β-secretase (*BACE1*), a gene involved in the pathophysiology of Alzheimer's disease (AD), a 3′ overlapping antisense RNA (BACE1-AS) forms an RNA duplex with the BACE1 mRNA leading to stabilisation and increased β-secretase expression [303,304]. Additionally, the formation of double-stranded RNA as a result of overlapping transcription can form substrates for Dicer leading to the production of endogenous-small interfering RNAs (endo-siRNAs) capable of silencing complementary target mRNAs [305,306]. Mechanisms of lncRNA action are summarised in **Fig. 1.7**.

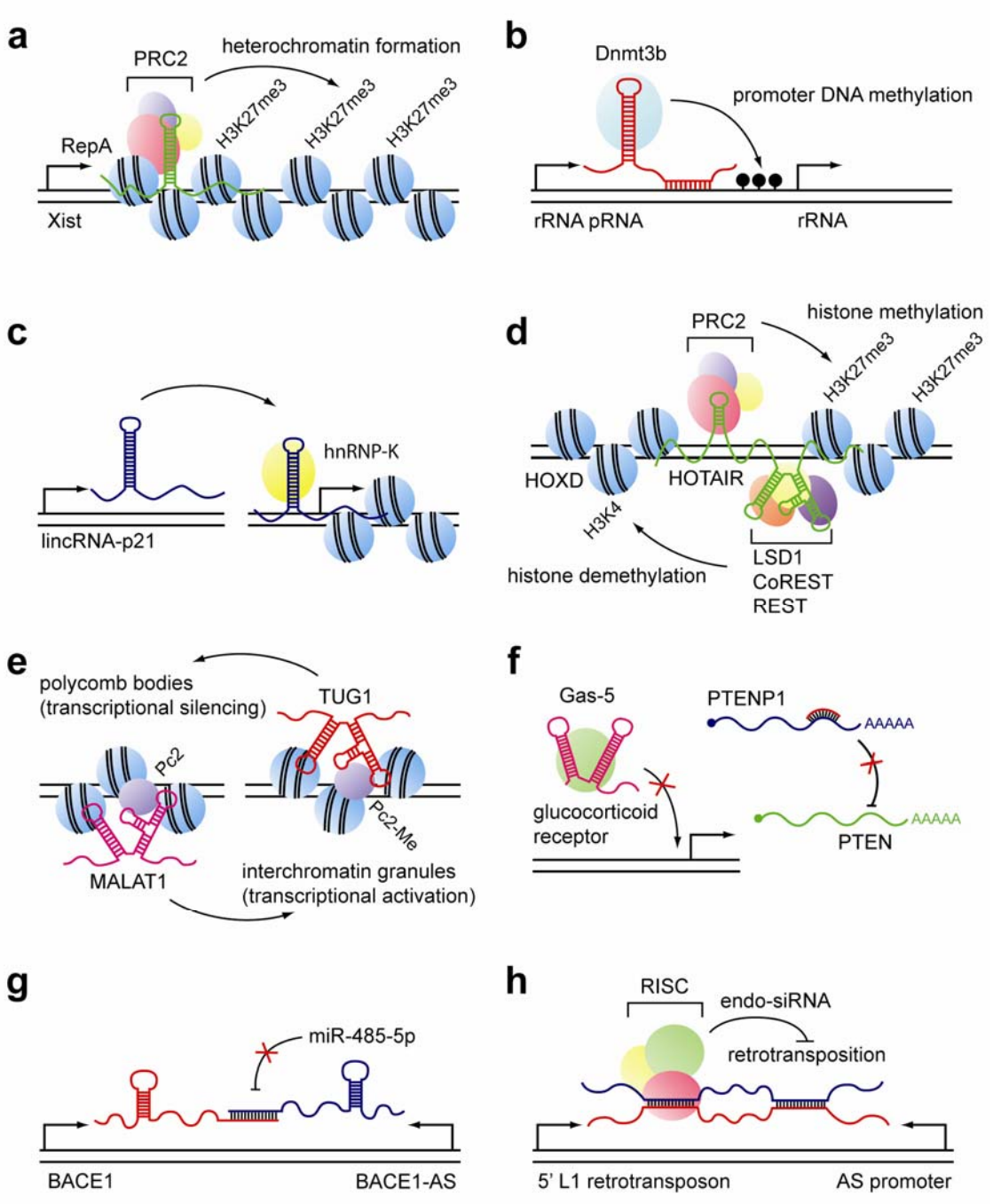
a
PRC2
heterochromatin formation
H3K27me3
H3K27me3
H3K27me3
RepA
Xist
b
Dnmt3b
promoter DNA methylation
rRNA pRNA
rRNA
c
hnRNP-K
lincRNA-p21
d
PRC2
histone methylation
H3K27me3
H3K27me3
HOXD
HOTAIR
H3K4
histone demethylation
LSD1
CoREST
REST
e
polycomb bodies
(transcriptional silencing)
TUG1
Pc2
Pc2-Me
MALAT1
interchromatin granules
(transcriptional activation)
f
Gas-5
PTENP1
AAAAA
glucocorticoid
receptor
AAAAA
PTEN
g
miR-485-5p
BACE1
BACE1-AS
h
RISC
endo-siRNA
retrotransposition
5' L1 retrotransposon
AS promoter

Figure 1.7 Mechanisms of gene regulation by lncRNAs.

lncRNAs can act as guides for chromatin modifying activities or transcription factors in *cis*; (a) RepA guides PRC2 to the *Xist* locus resulting in H3K27 tri-methylation and heterochromatin formation. (b) An rRNA promoter-associated RNA guides Dnmt3b to the rRNA promoter resulting in hypermethylation of the rRNA promoter and gene silencing. In addition rRNA pRNA also forms a triplex structure with the rRNA promoter. lncRNAs can also act as guides in *trans*; (c) lincRNA-p21 guides hnRNP-K to multiple sites in the genome and initiates gene silencing events. (d) lncRNAs can act as scaffolds for epigenetic modifying complexes. The lncRNA, HOTAIR binds both PRC2 and a complex containing LSD1, CoREST and REST to facilitate coordinated H3K27 tri-methylation and H3K4 demethylation at the *HOXD* locus. (e) Differential binding of lncRNAs TUG1 and MALAT1 to methylated or unmethylated Pc2 targets chromatin to polycomb bodies or interchromatin granules respectively. (f) lncRNAs can also act as riboregulator decoys for transcription factors (e.g. Gas-5 sequesters the glucocorticoid receptor) or miRNAs (e.g. the pseudogene PTENP1 acts as a miRNA sponge to relieve miRNA repression of PTEN). (g) Overlapping lncRNAs can hybridise with complementary mRNAs and stabilise them. In the case of the sense-antisense pair BACE1:BACE1-AS this is, at least in part, achieved by masking a binding site for miR-485-5p in the BACE1 3′ UTR. (h) Bidirectional transcription of lncRNAs can generate substrates for Dicer which are processed into endogenous-siRNAs (endo-siRNAs). These can induce post-transcriptional gene silencing of complementary target RNAs (e.g. endo-siRNAs generated from bidirectional transcription of L1 retrotransposon sites leads to inhibition of retrotransposition).

1.5.6.3 lncRNA in Disease

Considering that lncRNAs are involved in a wide variety of gene regulation processes including epigenetic remodelling and memory, control of transcription and translation [303], cellular differentiation [307,308], X-chromosome inactivation [309], mono-allelic expression of imprinted loci [310] and modulation of splicing [301] to name only a few, it is unsurprising that some lncRNAs are also implicated in human disease. Given that only a small portion of the genome (~1%) codes for protein, the majority of mutations occur in non-coding regions [311]. Consequently, lncRNA mutations and misexpression have been linked to disease [312]. For example, mutations have been identified in lncRNAs transcribed from ultra-conserved regions in patients with chromic lymphocytic leukemia (CLL) and colorectal cancer (CRC) [313]. Similarly, expression of HOTAIR is increased in breast tumors and correlates well with metastasis [314]. Increased levels of HOTAIR result in retargeting of the PRC2 to novel genomic sites with consequent changes in gene expression and increased tumor invasiveness. Similarly, MALAT1 was initially identified due to its association with lung metastasis [315].

In a landmark study by Tufarelli *et al.* an antisense RNA was shown to be the direct cause of α-thalassemia in a patient with a rare chromosome rearrangement. In this instance, the *LUC7L* promoter was found to be translocated immediately downstream of the *HBA2* (α-globin) gene resulting in transcription of a novel antisense RNA through the CpG island in the *HBA2* promoter. This antisense RNA mediates hypermethylation of the CpG island leading to epigenetic silencing of *HBA2* [316]. This study was the first to

demonstrate how misexpression of a non-coding RNA could directly lead to human disease.

A study by Lewejohann *et al.* revealed that mice in which the neuron-enriched ncRNA, *BC1*, was knocked-out showed no obvious physical or neurological defects relative to wild-type controls when under normal laboratory conditions. However, mutant mice exhibited reduced exploratory behaviour, increased anxiety and decreased survival upon reintroduction into a semi-natural outdoor environment [317]. This study raises the possibility that ncRNAs may also be involved in complex behavioral phenotypes in humans, specifically in disorders with cryptic etiologies. Furthermore, the human homologue of *BC1*, *BC200*, is found to be up-regulated in the brains of Alzheimer's disease patients and is mislocalised to neuronal cell bodies instead of dendritic spines, suggesting that it may be involved in disease pathophysiology [318].

1.5.6.4 Crosstalk Between Short and Long RNAs

Whereas the targeting of mRNA sequences with antisense technologies (i.e. siRNAs and antisense oligonucleotides) for post-transcriptional gene silencing is now commonplace, in recent years a number of reports have demonstrated that targeting non-coding regions can also influence gene expression. Specifically, it is now apparent that transcription occurs at many promoters, enhancers and 3′ gene termini [198,319,320], and that these transcripts are targets for therapeutic modulation. As described above, studies targeting promoters with siRNAs reported both gene silencing [168,169,199] and gene activation [237,243,321]. Tentative mechanistic models have been proposed to explain these opposing phenomena [238] and long ncRNAs appear to be involved in both processes.

Sense orientation pRNAs are required for TGS [199]. These rare transcripts may act as *cis*-regulatory sequences that remain bound to the promoter chromatin or, alternatively, they may simply be tethered to the locus by association with RNAPII. There is evidence that unstable pRNAs may exist at the majority of gene loci [198]. Conversely, natural antisense transcripts (NATs) are RNA transcripts which overlap a sense protein-coding gene and often act to regulate the associated loci through the recruitment of histone modifying complexes and induction of transcriptional silencing. Targeting these NATs with siRNAs or antisense oligonucleotides (also known as antagoNATs [239]) results in loss of this epigenetic silencing and consequently, transcriptional gene activation (TGA) of the sense gene [237–239,321]. It has since been demonstrated that miRNAs can also act to regulate transcription by TGS and TGA, suggesting that crosstalk between short and long ncRNA activities is an endogenous mechanism of gene regulation [220,248,322]. As a result, the use of anti-miRNA oligonucleotides may also be able to disrupt endogenous networks of epigenetic regulation.

Small RNA-mediated transcriptional regulation permits both silencing and activation of therapeutic target genes. Targeting promoter proximal transcripts or natural antisense transcripts allows for gene-specific epigenetic manipulation with numerous potential therapeutic applications. The majority of transcriptional modulation studies have focused on the silencing of the HIV-1 provirus [169,171,175,183], silencing of oncogenes [174,176,190] and the activation of tumor suppressors [237,238] although theoretically any gene can be targeted. Recent studies targeting vascular endothelial growth factor (*Vegfa*) [205] and brain-derived neurotrophic factor (*Bdnf*) [239] have reported TGS and

TGA *in vivo* suggesting that these are plausible therapeutic strategies. The ability to regulate genes at the epigenetic level has several advantages over conventional RNAi and antisense oligonucleotide approaches (which regulate gene expression at the post-transcriptional level). Epigenetic modifications are stable and heritable, meaning that long-term silencing can be achieved through a single treatment (or short course of treatments) [172,175,323]. Repeat administration is not required as the silencing or activation effects are not dependent on the presence of effector molecules. Consequently, off-target effects are minimised, saturation of endogenous RNA processing pathways is avoided and the material cost of treatment is greatly reduced.

1.6 Hypotheses

This thesis investigates the following hypotheses:

1. Differential miRNA expression will vary between *mdx* tissues.
2. *mdx* serum miRNA abundance will mirror the expression profile of *mdx* muscle.
3. Serum miRNA abundance will be normalised in response to antisense oligonucleotide-mediated exon skipping therapy in the *mdx* mouse.
4. Small interfering RNA molecules complementary to the myostatin promoter will induce transcriptional gene silencing of myostatin expression.

2 Materials and Methods

2.1 RNA Extraction

Total RNA was extracted by guanidinium thiocyantate-acid-phenol-chloroform extraction using TRIzol reagent as according to manufacturer's instructions (Invitrogen, Paisely, UK). Briefly, 0.25 ml TRIzol was added per well of a 24 well plate. Samples were homogenised and then 50 µl of chloroform was added to each sample. Samples were vortexed for 15 seconds and then incubated for 15 minutes at room temperature. Samples were then centrifuged at 12,000 g for 15 minutes at 4°C. The aqueous phase was collect by careful pipetting and RNA precipitated using 125 µl of isopropanol. 1 µl of RNase-free glycogen (Roche, West Sussex, UK) was added to each sample to maximise RNA recovery. Samples were mixed by brief vortexing and incubated for 10 minutes at room temperature before centrifugation at 12,000 g for 10 minutes at 4°C. Supernatants were discarded and the RNA pellets washed with 0.5 ml of 80% ethanol, vortexed briefly and centrifuged at 7,500 g for 5 minutes at 4°C. Supernatants were discarded and RNA dried at room temperature for 25 minutes. RNA samples were re-dissolved in 15-27 µl DEPC treated water (Fisher Scientific, Loughborough, UK) and stored at -80°. Nucleic acid samples were quantified using a Nanodrop ND 1000 spectrophotometer (Thermo Scientific, Loughborough, UK) and sample purity assessed by calculating A_{260}/A_{280} and A_{260}/A_{230} ratios for each sample (**Fig. 2.1a**). Pure RNA samples have an A_{260}/A_{280} ratio of ~2 and an A_{260}/A_{230} ratio >1.8. Samples with ratios that fell substantially below these crfiteria were re-extracted using the method described above. In addition, RNA integrity was also assessed by separating RNA samples by agarose gel electrophoresis. Samples

were considered to be of high integrity if two clear ribosomal RNA bands were present (18S and 28S) in an approximate ratio of 1:2 (**Fig. 2.1b**).

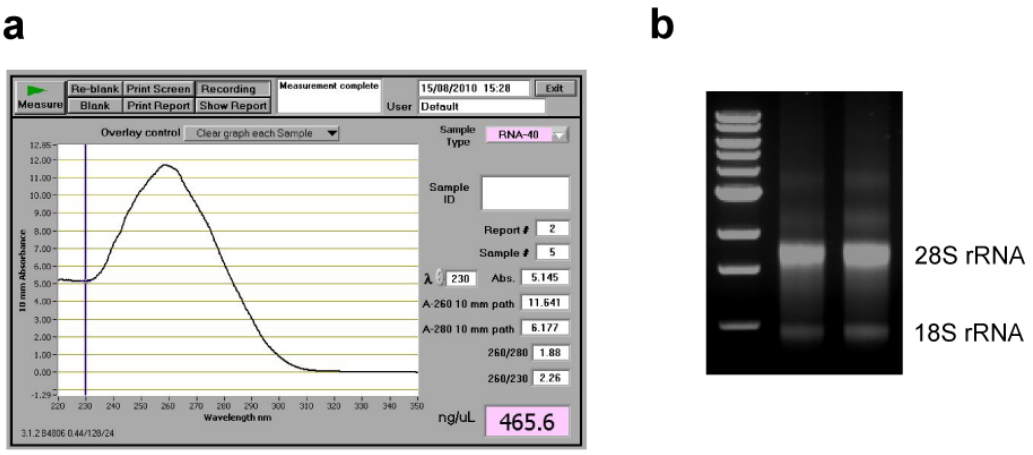

Figure 2.1 Assessment of RNA quality and integrity.

(a) Typical nanodrop trace showing a highly pure RNA sample. (b) Two RNA samples were separated by agarose gel electrophoresis, stained with ethidium bromide and visualised using a UV transilluminator. Two clear bands are visible which correspond to 28S and 18S ribosomal RNAs indicating high RNA integrity.

2.2 Preparation of Animal Tissues for Microarray Analysis

All animal experiments were carried out in the Biomedical Sciences Unit, University of Oxford in accordance to procedures authorised by the UK Home Office. Male C57/B10 and *mdx* mice (n=4) were sacrificed at eight weeks of age. Whole blood was extracted using Microvette CB300 capillary serum collection tubes (Sarstedt Ltd, Leicester, UK) and dissection was performed immediately after. The heart, quadriceps femoris, tibialis anterior, diaphragm and triceps were dissected and snap frozen in liquid nitrogen-cooled isopentane. Samples were homogenised using Precellys 24 ball bearing-based tissue grinder (Bertin Technologies, Paris, France) and RNA extracted using TRIzol reagent (Invitrogen) as according to manufacturer's instructions. Genomic DNA was removed by DNase I treatment with the TURBO DNA-*free* kit (Ambion, Warrington, UK) where appropriate. To extract total RNA from serum whole blood samples were placed at 4°C for 2 hours and then centrifuged at 13,000 rpm for 5 minutes in a bench top microcentrifuge. The serum supernatant was retained and stored at -80°C until ready for use. Total RNA was extracted from serum using TRIzol LS reagent (Invitrogen) as according to manufacturer's instructions. RNase-free glycogen (Roche) was used as carrier to improve extraction efficiency.

2.3 Peptide-Conjugate Preparation and Injection

Pip6e peptide (Ac-RXRRBRRXYRFLIRXRBRXRB-OH, with X = aminohexanoyl, B = β-Alanine) was synthesized by standard Fmoc chemistry and purified by reverse-phase HPLC. The PMO (5'-GGCCAAACCTCGGCTTACCTGAAAT) was purchased from Gene Tools LLC (Philomath, OR). Pip6e was then conjugated to the PMO through an

amide linkage at the 3′ end of the PMO, followed by purification by cation exchange HPLC, desalted and analysed by MALDI-TOF MS. Pip6e-PMO was dissolved in sterile water and filtered through a 0.22 μm cellulose acetate membrane before use. Pip6e-PMO conjugate was prepared in sterile saline for intravenous injection (in a total volume of 160 μl). Under isoflurane anaesthesia, 12.5 mg/kg of Pip6e-PMO was administered via the tail vein of 12 week old male *mdx* mice (n=4).

2.4 MicroRNA Microarray Analysis

Implementation and analysis of miRNA microarray experiments were designed to comply with the minimum information about a microarray experiment (MIAME) guidelines [324]. Each RNA sample was analysed using the Agilent 2100 Bioanalyzer (Agilent Technologies, Wokingham, UK) to assess RNA quality. 1 μg of total RNA was run for each of the 24 samples on Affymetrix GeneChip® miRNA 2.0 arrays (Affymetrix, Santa Clara, CA) (based on miRBase v15). Labeling and hybridisation were performed according to standard Affymetrix protocols at the Affymetrix Core facility BEA, Bioinformatics and Expression Analysis, at Novum, Huddinge, Sweden. The processing and data analyses were performed in Affymetrix miRNA QCTool as well as in DNA-Chip Analyzer (dChip) and Excel. The analysis was done according to the following workflow; BC-CG background adjustment, Quantile normalisation and Median Polish summarisation. Since the miRNA 2.0 array covers 131 organisms only *Mus musculus* transcripts were selected. Group comparisons were performed in dChip software (www.dchip.org). The criterion for differentially expressed transcripts was set to $p<0.05$ (unpaired, two-tailed t-test). For each comparison, transcripts with false detection signals in at least three of four replicates were removed. False Discovery Rate (FDR)

estimations were performed by calculating q-values (*qvalue* R package) from the p-value lists. The q-value of a test measures the proportion of false positives incurred when calling that test significant.

Array data were curated so as to remove ambiguous probe sets and 'dead' miRNAs. The array data discussed in this publication have been deposited in the NCBI Gene Expression Omnibus [325] and are accessible through GEO Series accession number GSE36257 (http://www.ncbi.nlm.nih.gov/geo/query/acc.cgi?acc=GSE36257).

2.5 MicroRNA Quantification by Small RNA TaqMan RT-qPCR

In order to validate the array results reverse transcriptase quantitative polymerase chain reaction (RT-qPCR) was performed using Small RNA TaqMan Assays (Applied Biosystems) as according to manufacturer's instructions. All RT-qPCR studies were designed to comply with the Minimum Information for publication of Quantitative real-time PCR Experiments (MIQE) guidelines where applicable or practical [326,327]. Briefly, 5 ng of total RNA was reverse transcribed using the TaqMan MicroRNA Reverse Transcription Kit (Applied Biosystems) using miRNA-specific stem-loop RT primers as according to manufacturer's instructions. For primary miRNA assays, samples were treated to remove genomic DNA using the Ambion TURBO DNA-*free* kit as according to manufacturer's instructions. 500 ng of DNase-treated total RNA were reverse transcribed using the High Capacity cDNA Synthesis Kit (Applied Biosystems) as according to manufacturer's instructions. qPCR analysis was performed on a StepOne Plus real-time thermocycler (Applied Biosystems) using TaqMan Gene Expression Mastermix (Applied Biosystems). Universal cycling conditions were used (95°C for 10

minutes (hotstart) and then 40 cycles of 95°C for 15 seconds, 60°C for 1 minute). For small RNA assays 1.33 µl of RT reaction were used in each qPCR reaction. For primary miRNA assays 2 µl of RT reaction were used for each qPCR reaction. All primer/probe assays are listed in **Table 2.1**. For mature miRNA assays data were analysed using the Pfaffl method [328]. Gene-of-interest expression was normalised to miR-16 expression for tissue samples and miR-223 expression for serum samples as this miRNA has previously been used as a reference miRNA in a study of serum dystromirs in DMD patients [329]. miR-223 expression was highly stable across all experimental samples (mean Ct = 25.47, SD = 0.28). For primary miRNA assays data were analysed using relative standard curve method and gene-of-interest expression normalised to PpiB expression.

miRNA	Assay ID
miR-1	002222
miR-16	000391
miR-21	000397
miR-29c	000587
miR-31	000185
miR-34c	000428
miR-133a	002246
miR-146b	001097
miR-199a-3p	002304
miR-206	000510
miR-221	000524
miR-223	002295
pri-miR-31	Mm03306874_pri
pri-miR-34c	Mm03306660_pri
pri-206	Mm03306546_pri
PpiB	Mm00478295_m1

Table 2.1 List of RT-qPCR assays used in this study.

2.6 Determination of Exon Skipping by RT-PCR

In order to assess the degree of exon skipping in treated *mdx* muscles, 400 ng of total RNA was used as a template in a 50µl Reverse Transcriptase-Polymerase Chain Reaction (RT-PCR) using the GeneAmp RNA PCR kit (Applied Biosystems). RT-PCR of the dystrophin transcript was performed under the following conditions; 95°C for 20s, 58°C for 60s and 72°C for 120s for 30 cycles using the following primers: DysEx20Fo (5′–CAGAATTCTGCCAATTGCTGAG) and DysEx26Ro (5′–TTCTTCAGCTTGTGTCATCC). 2 µl of this reaction was used as a template for nested amplification using Amplitaq Gold (Applied Biosystems) under the following conditions; 95°C for 20s, 58°C for 60s and 72°C for 120s for 22 cycles using the following primers: DysEx20Fi (5′–CCCAGTCTACCACCCTATCAGAGC) and DysEx26Ri (5′–CCTGCCTTTAAGGCTTCCTT). PCR products were analysed on 2% agarose gels.

2.7 Western Blotting

Cryosectioned muscle samples were homogenised in lysis buffer (75 mM Tris-HCl (pH 6.5), 10% Sodium Dodecyl Sulphate (SDS) and 5% 2-mercaptoethanol). Samples were heated at 100°C for 3 minutes before centrifugation and removal of supernatant. Protein levels were determined by Bradford assay (Sigma-Aldrich, Dorset, UK) against bovine serum albumin standards. 15 µg of protein was separated by SDS-polyacrylamide gel electrophoresis on 3-8% Tris-Acetate gels (Novex, Invitrogen). Proteins were electroblotted onto a PVDF membrane and probed for dystrophin using the DYS1 monoclonal antibody (Novocastra, Leica Microsystems, Milton Keynes, UK). An anti-vinculin monoclonal antibody (hVIN-1 (V-9131) Sigma) was used as a loading control as

described previously [330]. A goat anti-mouse antibody conjugated to an infra-red dye (IRDye 800CW 926-32210D) (LI-COR Biosciences UK Ltd, Cambridge) was used as a secondary antibody. Western blots were imaged and analysed using the Odyssey Fc Imaging System (LI-COR Biosciences UK Ltd).

2.8 Immunohistochemistry

Transverse sections of TA muscle (8μm) were collected onto superfrost slides (VWR, Leicestershire, UK). Slides were air dried and soaked in phosphate buffered saline (PBS) for 10 minutes before being incubated in 20% FBS and 20% normal goat serum for 2 hours. A simultaneous staining protocol was then performed with primary antibodies against dystrophin (rabbit polyclonal antibody, Abcam ab15277) and Laminin α-2 chain (rat monoclonal antibody, Sigma L0663) (20% normal goat serum; 2 hours) and secondary antibodies Alexa Fluor® 488 (goat anti-rat IgG) and Alexa Fluor® 594 (goat anti-rabbit IgG) (1 hour). Slides were mounted with Vectashield Hard Set mounting medium (with DAPI) (Vector Laboratories Ltd, Peterborough, UK). All dilutions and washes were performed with PBS and incubations were performed at room temperature. Images were viewed by epifluorescence using a Leica DM IRB microscope and digitally captured using Axiovision software (Carl Zeiss MicroImaging GmbH, Jena, Germany). Treated muscle sections were compared to samples from untreated age and sex matched *mdx* and C57BL10 mice (n=4).

2.9 Directional RT-PCR

Total RNA was extracted from C2C12 myotubes using TRIzol reagent (Invitrogen) as according to the manufacturer's protocol and DNase treated using the TURBO DNase-

free kit (Ambion/Applied Biosystems). 1 μg of total RNA was then reverse transcribed using SuperScript III RT (Invitrogen). In order to differentiate between sense and antisense transcripts cDNA synthesis was primed with either MstnPro-Rev (5′-AGCTTGCCCTCGACTGTAAC) or MstnPro-Fwd (5′-TCCAAGTGGCTTTTTATATTCCA) respectively. Following reverse transcription, polymerase chain reaction (PCR) was performed with both primers and the amplification products analysed by agarose gel electrophoresis. Mock reverse transcription controls (RT-) were performed to demonstrate that product amplification was not due to genomic DNA contamination. PCR products were gel extracted and sequenced to confirm identity.

2.10 Small Interfering RNA

siRNAs were produced by *in vitro* transcription using the Silencer^{TM} siRNA construction kit (Ambion) as according to manufacturer's instructions or by chemical synthesis (Eurogentec, Seraing, Belgium). For Silencer^{TM} siRNAs double-stranded T7 promoter templates were prepared and the sense and antisense RNA strands generated by separate *in vitro* transcription reactions. These reactions were combined to hybridise the siRNA strandes and then treated with DNAse to remove the template and RNase to generate 3′ siRNA overhangs. Unincorporated nucleotides were removed by column clean-up (**Fig. 2.2**). siRNAs were quantified by nanodrop. Chemically synthesised siRNAs had 3′ dTdT overhangs. siRNAs designed to target the myostatin sense promoter-associated RNA all conform to the AA(N_{19}) pattern. All siRNA sequences used in this study are listed in **Table 2.2**. Unless otherwise stated non-specific control (NS ctrl) refers to 'Control siRNA duplex negative control' (Eurogentec, catalogue #SR-CL000-005). Additionally, an siRNA which targets human C-C chemokine receptor type 5 (CCR5) mRNA was used

as an additional non-specific control produced by *in vitro* transcription. The sequence of the PTGS control siRNA was a kind gift from Luis Garcia.

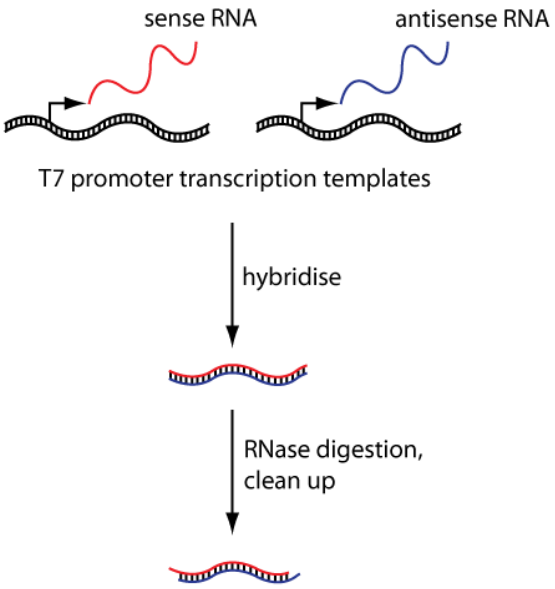

Figure 2.2 Diagram of *in vitro* siRNA synthesis.

Sense and antisense RNAs are produced by separate *in vitro* transcription reactions using double-stranded DNA T7 transcription templates. The two RNA strands are combined and hybridised. 3′ overhangs are generated by RNase digestion and the preparation purified by column clean-up.

	Sequence	Target
siGDF8 antisense	UUACGUUACUAGAGCAUACTT	GTATGCTCTAGTAACGTAA
siGDF8 sense	GUAUGCUCUAGUAACGUACTT	
siMstn-P2 antisense	UUCCAAGUGGCUUUUUAUAUU	AATATAAAAAGCCACTTGGAA
siMstn-P2 sense	UAUAAAAAGCCACUUGUAAUU	
siCCR5 antisense	AAUUAUUCAGGCCAAAGAAUU	AATTCTTTGGCCTGAATAATT
siCCR5 sense	UUCUUUGGCCUGAAUAAUUUU	
siMstn-P1 antisense	UACUGUAUUCCAAGUGGCUUU	AAAGCCACTTGGAATACAGTA
siMstn-P2 sense	GGCCACUUGGAAUAUAGUAUU	
siMstn-P3 antisense	UGAAUCUCGCUGUCAGAGGUU	AACCTCTGACAGCGAGATTCA
siMstn-P3 sense	GCUCUGACAGCGAGAUUUAUU	
siMstn-P4 antisense	ACAGUCGAGGGCAAGCUGAUU	AATCAGCTTGCCCTCGACTGT
siMstn-P4 sense	GCAGCUUGCCCUCGAUUGUUU	
siMM antisense	UUCCAAGUUCGGUUUUAUATT	N/A
siMM sense	UAUAAAACCGAACUUGGAATT	
siScramble antisense	AGUUCUUGUUACUAUCUAGTT	N/A
siScramble sense	CUAGAUAGUAACAAGAACUTT	

Table 2.2 Sequences of siRNAs used in this study.

All sequences are 5′ to 3′.

2.11 Cell Culture

C2C12 mouse myoblasts were maintained in growth media (GM); Dulbecco's Modified Eagle's Media (DMEM) supplemented with 15% fetal bovine serum (FBS) and antibiotic/antimycotic (all Invitrogen) and 5% CO_2. For differentiation, 24 well cell culture plates were coated with 0.02% gelatin (Sigma-Aldrich) and UV sterilised. C2C12 myoblasts were seeded (5 x 10^4 cells/ml) in growth medium and grown overnight. When confluent, the cells were switched to differentiation media (DM); DMEM supplemented with 5% horse serum (Invitrogen) and antibiotic/antimycotic. Cells were cultured in DM for seven days in order to induce differentiation to myotubes.

H2K *mdx* tsA58 mouse myoblasts [331] were cultured in DMEM supplemented with 20% FBS, 2% chick embryo extract (PAA Laboratories Ltd, Yeovil, UK) and 20U ml^{-1} γ-Interferon (Invitrogen) at 33°C and 10% CO_2 When confluent, the H2K *mdx* cells were switched to differentiation medium and switched to 37°C and 5% CO_2 for seven days.

Cells were transfected with RNAiMax (Invitrogen) and INTERFERin (PolyPlus Transfection, Strasbourg, France) were performed as according to manufacturer's instructions. Peptide transfections with PepFect 14 (CePep, Stockholm, Sweden) were performed as follows. Separate peptide and siRNA solutions were prepared in sterile water. The mixes were combined in a ratio of 30:1 (peptide:siRNA), mixed gently and incubated for 30 minutes at 37°C to allow transfection complexes to form. After incubation, the transfection mixtures were diluted in optiMEM (Invitrogen) to a total volume of 0.45ml per well (24 well plate). The media was removed from the C2C12

cultures and the cells washed with PBS (Invitrogen). Transfection complexes in optiMEM were then added to each well as appropriate and the cultures returned to the incubator. After 1 hour the cultures were supplemented with 50 µl FBS and after 24 hours the transfection mixture was removed and replaced with fresh media. For all experiments mock transfections received transfection reagent/peptide only. Dexamethasone, Trichostatin A and Lipopolysaccharide (all Sigma-Aldrich) were added to cell culture medium as appropriate. Cell viability was determined using the MTS assay (Promega, Southampton, UK) as according to manufacturer's instructions.

2.12 mRNA Quantification by RT-qPCR

Reverse Transcriptase-Quantitative Polymerase Chain Reaction (RT-qPCR) was performed as follows. The planning, implementation and reporting of RT-qPCR experiments were designed to comply with the MIQE guidelines [326,327] as much as was possible or appropriate. To generate cDNA 2 µg of high quality total RNA was reverse transcribed using the High-Capacity cDNA Synthesis kit (Applied Biosystems) as according to manufacturer's instructions. 20 µl RT reactions were primed using random primers. Samples were incubated at 25°C for 10 minutes to allow primer extension to occur and then cDNA was reverse transcribed for 2 hours at 37°C. The reaction was terminated at 80°C for 15 minutes. Typically 200 ng cDNA was added to each reaction such that a maximum of 2 µl of RT reaction was added per well. RT-qPCR was performed on a StepOne Plus Real-Time PCR System (Applied Biosystems) using TaqMan Gene Expression Mastermix (Applied Biosystems). Relative quantities of target mRNA were determined using the relative standard curve method. Data were analysed using the StepOne Software v2.1 (Applied Biosystems). Standard curves were produced

from serial dilutions of cDNA reverse transcribed from untreated experimental samples. Universal cycling conditions were used (95°C for 10 minutes (hotstart) and then 40 cycles of 95°C for 15 seconds, 60°C for 1 minute). Typically, gene of interest expression was normalised to β-Actin expression. TaqMan assays were purchased from Applied Biosystems and are listed in **Table 2.3**.

Gene Symbol	Assay ID	Amplicon	Probe	RefSeq
Mstn	Mm01254559_m1*	90bp	**FAM®/MGB**	NM_010834.2
ACTB	Mm00607939_s1*	115bp	**VIC®/MGB**	NM_007393.1
Oas1b	Mm00449297_m1*	63bp	**FAM®/MGB**	NM_001083925.1
Il-6	Mm00446190_m1*	78bp	**FAM®/MGB**	NM_031168.1
Ppib	Mm00478295_m1	82bp	**FAM®/MGB**	NM_011149.2

Table 2.3 RT-qPCR TaqMan Primer/Probe assays used in this study.

2.13 Dual Luciferase Assay

HEK 293 cells were seeded at 50% confluency in 24 well plates and cultured in DMEM (Invitrogen) supplemented with 10% FBS (Gibco) overnight. Each well was co-transfected with 0.25 µg of plasmid DNA and 100 nM of siRNA in complex with Lipofectamine 2000 (Invitrogen) as according to manufacturer's instructions. Cells were harvested 24 hours post transfection and Firefly and Renilla luciferase activities were quantified using the Dual-Luciferase Reporter Assay System (Promega) on a 96 well Victor 3 plate-reader (PerkinElmer Ltd, Beaconsfield, UK).

2.14 Chromatin Immunoprecipitation

Chromatin immunoprecipitation (ChIP) was performed as described previously with several modifications [170]. C2C12 myotubes were cultured in 10 cm dishes and siRNAs transfected with RNAiMax. After 48 hours cells were harvested for ChIP assays. DNA:histone complexes were crosslinked by addition of 37% formaldehyde (Fisher Scientific, Loughborough, UK) (to a final concentration of 1%) to the cell culture media and incubating for 10 minutes at room temperature with shaking. The crosslinking reaction was terminated by adding glycine (Sigma-Aldrich) to a final concentration of 0.125 M with shaking for 5 minutes. Media was then removed and the cells washed with cold PBS containing 1/1000 phenylmethanesulfonylfluoride (PMSF) (Sigma-Aldrich). 4ml of PBS containing 1/1000 PMSF was added to each culture and the cells scraped. The cells were then pelleted, washed with PBS containing 1/1000 PMSF and the pellets flash frozen in liquid nitrogen for future processing.

Cell pellets were resuspended in 200 µl C2C12 Lysis Buffer (1% SDS, 10mM EDTA, 50mM Tris-Hcl pH 8) containing 1/1000 PMSF and incubated on ice for 10 minutes. Nuclei were then pelleted by centrifugation at 5,000 rpm for 5 minutes at 4°C and the supernatant discarded. The pellet was resuspended in 200 µl C2C12 lyis Buffer and 800 µl C2C12 Lysis Dilution Buffer (0.01% SDS, 1.1% Triton-X 100, 1.2 mM EDTA, 16.7 mM Tris-HCl pH 8, 167 mM NaCl) (both containing 1/1000 PMSF), incubated on ice for 10 minutes and then sonicated to an average length of ~200bp using a Misonix S-1000 cup horn sonicator (Misonix, NY,USA) (pulse amplitude setting: 24, 2 pulses, 90 seconds on, 105 seconds off). Sonicated chromatin samples were precleared with 30 µl Protein G Agarose/Salmon Sperm (KPL, MD, USA) and then the samples were aliquoted for each pulldown and a 'No Antibody Control'. DNA and histone complexes and immunoprecipiated with antibodies against H3K9me2 (#07-441, Upstate/Millipore, MA, USA) and H3K27me3 (#97565, Cell Signalling Technologies, MA, USA). 1 µg of each antibody was added to each sample and the volume of sample adjusted to 600 µl with ChIP Lysis Buffer (50 mM Hepes, 140 mM NaCl, 1% Triton-X 100, 0.1% Sodium deoxycholoate) containing 1/1000 PMSF. The samples were incubated overnight at 4°C on a rotating platform.

The following day 30 µl of Protein A Dynabeads (Invitrogen) was added to each sample and incubated on a rotating platform for 15 minutes at room temperature. The tubes were then briefly centrifuged and the beads pulled down using a magnet. The supernatant from the 'No Antobody Control' was transferred to a clean tube for use as an 'Input' sample. All other supernatants were discarded. The beads were then washed three times with

ChIP Lysis Buffer, then with ChIP Lysis High Salt Buffer (50 mM Hepes, 0.5 M NaCl, 1% Triton-X 100, 0.1% Sodium deoxycholate) and finally with ChIP Wash Buffer (10 mM Tris pH 6.7, 250 mM LiCl, 1 mM EDTA, 0.5% Triton-X 100, 0.5% NP-40). Chromatin-antibody complexes were eluted from the beads with 200 µl Elution Buffer (50 mM Tris pH 6.7, 1% SDS, 10 mM EDTA). Eluates were heated at 65°C for 10 minutes and then 1 µl RNaseA (10mg/ml) (Roche) and 20 µl 5M NaCl were added to each sample. Cross-linking was reversed by incubation at 65°C for 5 hours. To digest the protein sample 10 µl 0.5M EDTA, 20 µl 1M Tris-HCl pH 6.5 and 2 µl of Proteinase K (10mg/ml) (Roche) and incubated for 45°C for 45 minutes. DNA was recovered by phenol chloroform extraction and resuspended in 30 µl of nuclease free water. Quantitative PCR was performed on a Mastercycler Realplex real-time thermal cycler (Eppendorf, NY, USA) using KAPA SYBR Fast SYBR mastermix (KAPA Biosystems, MA, USA) and the primers; MstnChIP-Fwd (5′-AGATTCATTGTGGAGCAGGAG) and MstnChIP-Rev (5′-ATATTAGTGCATGTACCGTCCG). The relative standard curve method was used to compare samples and a five fold dilution of input chromatin DNA used to prepare the standard curve. Dissociation curve analysis confirmed that only a single amplification product was generated by the PCR reaction. Sample values were calculated as background subtracted, fraction of input for each experimental group and then normalised to the NS control siRNA group.

2.15 Phenol Chloroform Extraction

DNA samples were purified and concentrated by phenol chloroform extraction and ethanol precipitation. Briefly, one volume of phenol chloroform (pH 7.2) (Ambion) was

added to an equal volume of DNA sample. Samples were mixed by vortexing and centrifuged at 12,000 g for 3 minutes. The upper aqueous phase was transferred to a fresh Eppendorf tube. A second volume of phenol chloroform was added, the sample mixed by vortexing and separated by centrifugation as described above. The aqueous phase was again removed. One volume of chloroform was added, the sample mixed and centrifuged as described above. This step removes phenol contamination. The aqueous phase was removed and DNA precipitated by ethanol precipitation. Briefly, 0.1 volumes of 3M sodium acetate (pH 5.2), 2.5 volumes of ice cold 100% ethanol was added to each sample and mixed by brief vortexing. Samples were incubated at -20°C for at least 1 hour to precipitate DNA. DNA was pelleted by centrifugation at 12,000g for 10 minutes at 4°C. Supernatants were discarded and pellets washed with 75% ethanol. Samples were then centrifuged at 7,500 g for 5 minutes and the supernatants discarded. DNA pellets were air dried for 25 minutes and then resuspended in an appropriate volume of nuclease free H_2O.

2.16 Statistical Analysis for MicroRNA Studies

Individual comparisons between disease and wild-type samples were tested for statistical significance using a two-tailed Student's t test. For comparisons of more than two groups one-way analysis of variance (ANOVA) and Bonferroni correction *post hoc* test were performed using GraphPad Prism 5 (GraphPad Software Inc, La Jolla, CA, USA). Differences were considered significant at p values below 0.05.

2.17 Statistical Analysis for Myostatin Studies

All statistical analysis was performed in SPSS v11.5 (IBM Corporation, NY, USA). Data were assessed for normalcy using the Shapiro-Wilk test and equality of variance by the Levene's test. Significance within a data set was determined by one-way ANOVA (analysis of variance) and significant differences between treatment groups were determined *by post hoc* analysis. The Bonferroni correction or the Games-Howell test were used in the instances of equality and inequality of variance respectively. P values less than 0.05 were considered significant. Unless otherwise indicated all statistical comparisons are made against non-specific control siRNA treated cultures (grey bars).

3 Investigation of Differential MicroRNA Expression in the *mdx* Mouse

3.1 Introduction

DMD pathology and the role of miRNAs in regulating gene expression are discussed in sections 1.1 and 1.4.2 respectively. In DMD, loss of dystrophin protein leads to a range of cellular pathologies. Given the role of miRNAs as regulators of both physiological and pathophysiological processes, it is highly likely that they participate in regulating DMD-associated pathologies. This chapter focuses on differentially expressed miRNAs in the *mdx* mouse model of DMD.

Gene expression profiling has the potential to identify the sequence of events that leads from dystrophin loss to dystrophic pathological processes. The discovery that unique miRNA expression patterns were associated with different tumor types [127] has led to investigation of miRNA profiles in a wide variety of other diseases. Two major miRNA profiling studies have identified differentially expressed miRNAs associated with DMD. However there are considerable differences between the findings of these reports [332,333] (**Table 3.1**). For example, Greco *et al.* showed a ~70 fold increase in miR-31 expression in both *mdx* and human muscle whereas Eisenberg *et al.* did not identify this miRNA as being differentially expressed (in DMD patient biopsies). Conversely, the most differentially expressed miRNA in the Eisenberg study, miR-146b, was not significantly changed in the study by Greco *et al.* The differences in results between these

studies may be due to the methodologies used (microarray and TaqMan array respectively) and the assaying of different muscle groups.

This study has investigated miRNA expression in a range of muscle groups and serum in *mdx* mice compared with age and sex-matched wild-type controls. miRNA microarray technology was utilised to perform an initial comparative miRNA analysis between quadriceps femoris, diaphragm and heart muscles. Array results were validated using small RNA TaqMan assays and the study expanded to include the triceps and tibialis anterior muscles, and serum. This study has focused on a set of 11 miRNAs referred to as 'dystromirs'. This term has been used previously [329] but in this study it is defined more specifically as meaning miRNAs which have been previously found to be differentially expressed in DMD patients and/or dystrophic animal models. The dystromirs relevant to this study are described in **Table 3.2**.

A comprehensive understanding of miRNA expression in the *mdx* mouse is important because; (1) miRNAs are promising biomarkers for non-invasive monitoring of disease progression and response to experimental therapies, (2) it contributes to the understanding of the series of molecular events leading from loss of dystrophin to dystrophic pathology, and (3) it forms the basis for the development of novel miRNA-based therapeutics. The present study is the first to compare differential miRNA expression in the *mdx* heart and diaphragm and has directly compared multiple muscles and serum from the same set of animals. The findings point to an unexpected layer of complexity in the *mdx* mouse miRNA transcriptome.

miRNA	Eisenberg *et al.* 2007		Greco *et al.* 2009	
	miRNA microarray		TaqMan array	
	BMD	DMD	*mdx*	DMD
	various muscles		adductor	various muscles
miR-21		3.1		
miR-31			71.5	20.1
miR-34c			6.6	6.8
miR-146b	11.5	13.0		
miR-199a-3p		3.9		
miR-206			8.8	3.9
miR-221	3.3	2.9		
miR-223			4.0	5.2
miR-1			-2.7	-3.1
miR-29c		-6.2	-6.0	-2.3

Table 3.1 Summary of published DMD related miRNA profiling papers.

The subject of study (i.e. DMD patients, BMD patients or *mdx* mice), methodology and type of muscle studied are indicated. Empty cells indicate that a statistically significant change in miRNA expression was not reported.

miRNA	function	evidence
miR-1	myogenesis	Down-regulated in *mdx* adductor and DMD patients [332]. Down-regulated in *mdx* TA and $CXMD_J$ TA [334]. Down-regulated in *mdx* gastrocnemius [335]. Highly abundant in *mdx* serum and DMD patient serum [329,336]. miR-1 promotes muscle differentiation [136].
miR-133a	myogenesis	Down-regulated in *mdx* TA and $CXMD_J$ TA [334]. Down-regulated in *mdx* gastrocnemius [335]. Highly abundant in *mdx* serum and DMD patient serum [329,336]. miR-133a promotes muscle proliferation [136].
miR-206	myogenesis	Up-regulated in *mdx* adductor and diaphragm and in DMD patients [332,333,337]. Up-regulated in *mdx* TA and down-regulated in $CXMD_J$ TA [334]. Up-regulated in *mdx* gastrocnemius [335]. Highly abundant in *mdx* serum and DMD patient serum [329,336]. miR-206 promotes muscle differentiation [137].
miR-21	fibrosis	Up-regulated in DMD patients [333]. miR-21 promotes fibrosis [338].
miR-29c	fibrosis	Down-regulated in *mdx* adductor and in DMD patients [332,333]. Down-regulated in *mdx* gastrocnemius [335]. miR-29 regulates collagens and elastin [130]. Expression of miR-29 in *mdx* gastrocnemius reduces fibrosis [335].
miR-31	regeneration regulates dystrophin	Up-regulated in *mdx* adductor and DMD patients [332] (most up-regulated miRNA in this study). miR-31 is strongly induced in ischemia damaged myofibres [332]. miR-31 regulates dystrophin expression [126].
miR-34c	regeneration/ degeneration	Up-regulated in *mdx* adductor and DMD patients [332]. miR-34c is strongly induced in ischemia damaged myofibres [332]. miR-34c promotes cell cycle withdrawal and apoptosis [339].
miR-146b	myogenesis	Up-regulated in DMD patients [333] (most up-regulated miRNA in this study). miR-146 promotes proliferation of C2C12 myoblasts [340].
miR-199a-3p	unknown	Up-regulated in DMD patients [333]
miR-221	myogenesis	Up-regulated in DMD patients [333]. miR-221/222 is highly up-regulated in terminally differentiated myoblasts [341].
miR-223	inflammation	Up-regulated in *mdx* adductor and DMD patients [332]. Up-regulated in *mdx* gastrocnemius [335]. Possible immune infiltrate [342].

Table 3.2 Dystromirs of interest in this study.

3.2 Results

3.2.1 MicroRNA Microarray Analysis

To identify differentially expressed mature miRNAs associated with the DMD phenotype, miRNA microarray analysis was performed on quadriceps, diaphragm and cardiac muscles harvested from 8 week old male C57Bl/10 (wild-type) and *mdx* mice. The 8 week timepoint was selected as this is after the initial 'crisis' period of necrosis and before the onset of the majority of secondary pathologies such as inflammation, fibrosis and fat deposition [343,344]. Statistically significant ($p<0.05$) changes in mature miRNA expression were identified across all of the tissues; 188 miRNAs in quadriceps (False Discovery Rate, FDR = 6%), 181 miRNAs in diaphragm (FDR = 5%) and 64 miRNAs in heart (FDR = 26%). Analysis of the full miRNA transcriptome reveals widespread differences between these tissues (**Fig. 3.1a**). More miRNAs were differentially expressed in quadriceps and diaphragm compared to heart, in addition, the observed changes in the heart were generally of lesser magnitude than in quadriceps and diaphragm (**Fig. 3.1b**). Overlap between miRNAs commonly differentially expressed across all three tissues is indicated in the Venn diagram (**Fig. 3.1c**). For each tissue, there was a subset of miRNAs found to be differentially expressed only in that tissue suggesting tissue-specific differences in pathological processes. 18 miRNAs that were significantly differentially expressed in all three tissues are shown graphically in **Fig 3.1d** and fold changes listed in **Table 3.3**. In addition to the dystromirs listed in **Table 3.2,** miR-1944, miR-296-3p and miR-543 showed increased expression, and miR-185, miR-151-5p, miR-151-3p, miR-345-3p, miR-139-5p, miR-143, and miR-378* showed decreased expression in all three *mdx* tissues. To our knowledge these miRNAs listed above have not been previously

identified as differentially expressed in miRNA profiling studies of the *mdx* mouse or dystrophic patients.

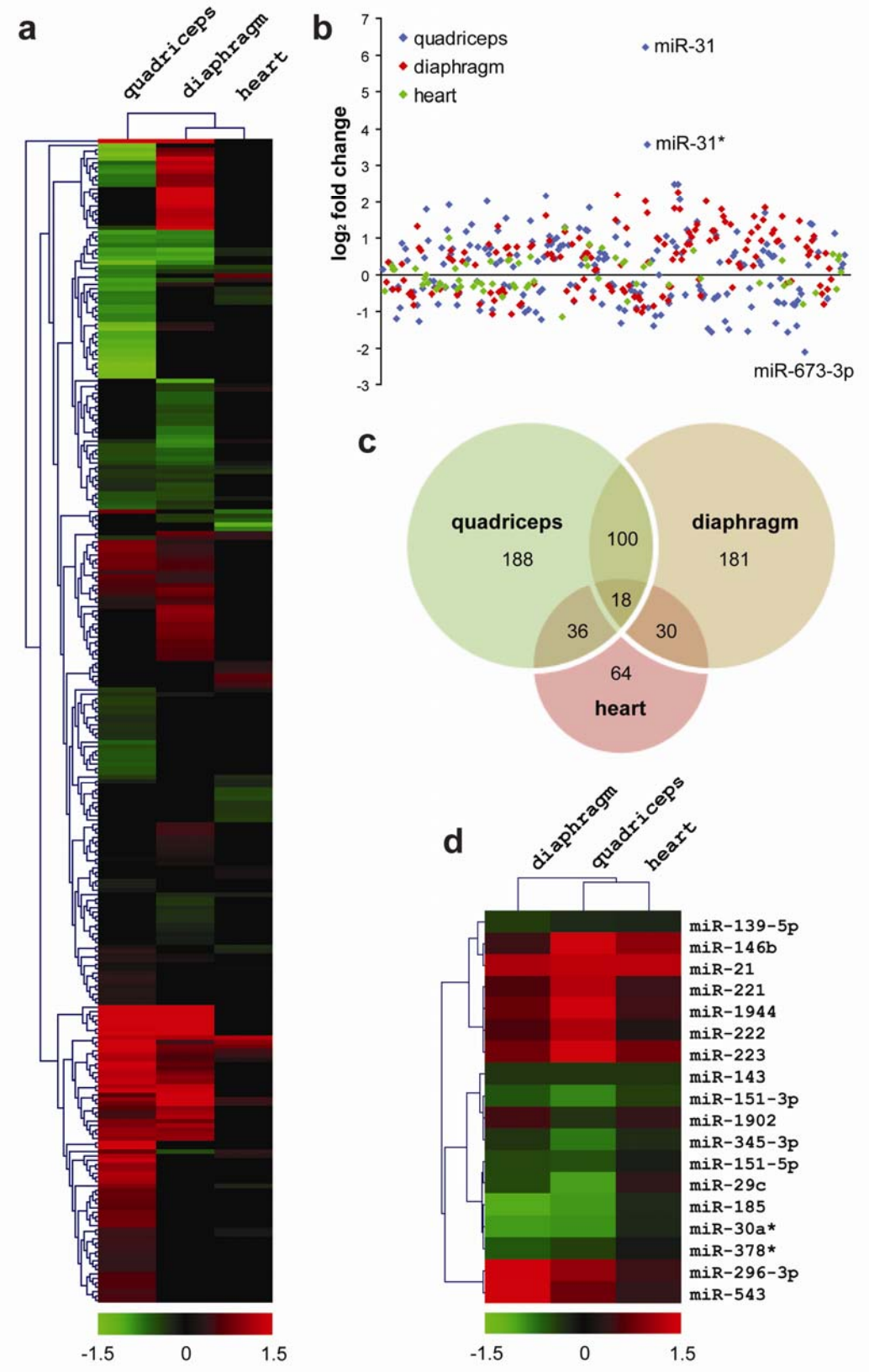
a
quadriceps
diaphragm
heart
-1.5
0
1.5
b
quadriceps
diaphragm
heart
miR-31
miR-31*
log2 fold change
miR-673-3p
c
quadriceps
188
diaphragm
181
heart
64
100
18
36
30
d
diaphragm
quadriceps
heart
miR-139-5p
miR-146b
miR-21
miR-221
miR-1944
miR-222
miR-223
miR-143
miR-151-3p
miR-1902
miR-345-3p
miR-151-5p
miR-29c
miR-185
miR-30a*
miR-378*
miR-296-3p
miR-543
-1.5
0
1.5

Figure 3.1 miRNA transcriptome analysis.

Quadriceps, diaphragm and heart tissue from 8 week old C57/Bl10 (wild-type) and *mdx* mice (n=4) were harvested and miRNA microarray analysis performed. (a) Heatmap of whole miRNA transcriptome of all three tissues for all miRNAs with a statistically significant ($p<0.05$) change in expression between WT and *mdx* mice. (b) Scatter plot showing the relative spread of fold changes across all three tissues. The most up-regulated and most down-regulated miRNAs across all of the arrays are highlighted. (c) Venn diagram showing common changes in miRNA expression between the tissues. (d) Heatmap showing miRNAs with statistically significant expression changes in all three tissues. Hierarchical clustering analysis was used to identify patterns of miRNA expression in the *mdx* quadriceps, diaphragm and heart. Red signifies an increase in expression and green, a decrease in expression. Heatmap scale bars indicate $\log_2$ fold changes.

miRNA	quadriceps			diaphragm			heart		
	fold	p-value	q-value	fold	p-value	q-value	fold	p-value	q-value
miR-139-5p	-1.20	3.270E-03	1.005E-02	-1.32	2.217E-03	8.525E-03	-1.17	3.471E-04	4.362E-02
miR-143	-1.28	5.950E-03	1.365E-02	-1.26	4.527E-03	1.305E-02	-1.27	6.808E-06	2.937E-03
miR-146b	3.78	8.760E-04	4.135E-03	1.38	2.351E-02	3.913E-02	1.99	1.152E-03	6.702E-02
miR-151-3p	-1.79	1.328E-04	1.918E-03	-1.48	1.401E-02	2.702E-02	-1.33	4.437E-03	1.007E-01
miR-151-5p	-1.44	7.052E-04	3.994E-03	-1.39	8.764E-05	1.052E-03	-1.11	6.265E-03	1.010E-01
miR-185	-1.92	1.299E-04	1.918E-03	-2.10	1.486E-04	1.327E-03	-1.20	1.704E-03	7.325E-02
miR-1902	-1.26	3.287E-02	4.226E-02	1.43	1.292E-02	2.532E-02	1.32	1.187E-02	1.284E-01
miR-1944	2.77	7.887E-04	3.994E-03	1.68	1.241E-03	6.060E-03	1.40	8.959E-03	1.152E-01
miR-21	2.45	2.314E-03	7.759E-03	2.26	1.314E-03	6.096E-03	2.40	2.037E-03	7.325E-02
miR-221	2.34	2.036E-04	2.034E-03	1.51	3.400E-05	7.957E-04	1.36	4.348E-04	4.362E-02
miR-222	2.28	1.303E-03	5.331E-03	1.49	1.779E-04	1.431E-03	1.19	6.036E-03	1.010E-01
miR-223	3.58	4.653E-02	5.054E-02	1.76	8.690E-03	1.911E-02	1.77	4.980E-02	2.618E-01
miR-296-3p	2.03	4.925E-02	5.233E-02	2.80	1.255E-04	1.247E-03	1.38	4.116E-02	2.433E-01
miR-29c	-1.97	2.762E-03	8.921E-03	-1.40	2.392E-02	3.913E-02	1.29	3.735E-02	2.427E-01
miR-30a*	-1.87	9.616E-03	1.935E-02	-1.95	4.808E-04	2.827E-03	-1.19	1.944E-02	1.677E-01
miR-345-3p	-1.70	1.040E-03	4.707E-03	-1.26	1.528E-02	2.878E-02	-1.21	1.100E-02	1.284E-01
miR-378*	-1.34	1.869E-02	2.922E-02	-1.49	1.330E-05	5.474E-04	-1.08	1.266E-02	1.284E-01
miR-543	1.72	4.411E-02	4.943E-02	3.02	5.169E-05	9.636E-04	1.31	2.568E-02	1.944E-01

Table 3.3 Table of fold changes, p-values and q-values for differentially expressed miRNAs common to *mdx* quadriceps, diaphragm and heart as measured by miRNA microarray.

The q-value of a test measures the minimum false discovery rate that is incurred when calling that test significicant.

3.2.2 RT-qPCR Validation of Array Data

In order to validate the results of the miRNA microarray, RT-qPCR analysis was performed on the same RNA samples used for the arrays. Small RNA TaqMan assays designed to detect only the mature miRNA species were used for all of the dystromirs in **Table 3.2**. All small RNA TaqMan assays were validated by amplifying serial dilutions of cDNA to produce standard curves. Amplification was linear over the range of cDNA levels tested (**Fig. 3.2**). PCR efficiencies were obtained from the standard curve gradients (**Table 3.4**) and these utilsed to quantify miRNA expression levels as described in materials and methods.

In order to determine if inferences drawn from array data can be applied to other tissues, the study was expanded to include dystromir expression in additional tissues; triceps and tibialis anterior (TA) muscles (**Figs 3.3a-k** and fold changes listed in **Table 3.5**). Serum was also included as changes in serum miRNA abundance have recently been reported in the *mdx* mouse, $CXMD_J$ dog and DMD patients [329,336]. miR-1 and miR-133a were down-regulated or unchanged in all *mdx* muscles whereas in serum both miRNAs were increased by 43.6 fold and 50.6 fold respectively (**Figs. 3.3a,f**). miR-206 was increased in all *mdx* groups measured with a 52.9 fold increase observed in serum (**Fig. 3.3i**). miRNA-21, -31, -34c and -221 were increased in all muscles except the heart (only modest increases were observed in *mdx* serum in each case) (**Figs. 3.3b,d,e,j**). miR-223 was found to be increased in the skeletal muscles but not in the diaphragm, heart or serum (**Fig. 3.3k**). Notably, miR-146b was only significantly increased in *mdx* quadriceps (**Fig.**

3.3g) and similarly, miR-199a-3p was only increased in *mdx* quadriceps and diaphragm (**Fig. 3.3h**).

Generally, the RT-qPCR validation closely matches the miRNA microarray data (**Fig. 3.4a,b** and **Table 3.6**). Hierarchical clustering analysis was used to group fold changes for the respective miRNAs and tissues. As expected, quadriceps, TA and triceps muscles cluster away from diaphragm and heart. Similarly, all the tissues cluster away from serum (**Fig. 3.4b**). In quadriceps and diaphragm, fold changes were highly similar between the two methodologies used (e.g. in the case of miR-31 expression; 70.9 fold by RT-qPCR and 74.3 by microarray) with few exceptions. A number of miRNAs were changed in the same direction between the two methodologies but did not reach significance at the 95% level as measured by RT-qPCR (i.e. miR-1, miR-29c and miR-133a in quadriceps, and miR-29c, miR-146b, miR-199a-3p and miR-223 in diaphragm). Interestingly, miR-1 was significantly decreased in the *mdx* diaphragm as measured by RT-qPCR (-2.27 fold) although its expression was unchanged as measured by microarray. In the heart dataset only miR-206 was significantly increased in *mdx* heart as measured by RT-qPCR but not by microarray. No other miRNAs were significantly changed in *mdx* heart as measured by RT-qPCR.

The expression of one miRNA (miR-29c) did not match the microarray data. According to the miRNA microarray miR-29c was increased in *mdx* heart (1.29 fold, p=0.0373) although the significance corresponds to a false discovery rate of 0.24 and the possibility of a false positive cannot be excluded. Similarly, miR-29c expression was not significantly different as measured by RT-qPCR (**Fig. 3.3c** and **Table 3.5**).

In general, the cycle threshold (Ct) values for all miRNAs measured fell within the range of 20-30 cycles which was comparable to the reference miRNAs (Ct values around 25-26). miR-31 and miR-34c were expressed at low levels (Ct values 30-35) in all the C57 tissues. Raw fluorescence values from the miRNA microarray also indicate low levels of expression for these miRNAs (data not shown). miR-206 was present at very low levels in all of the heart samples (Ct values ~35) which is unsurprising given that expression of miR-206 is generally restricted to skeletal muscle [137].

Interestingly, the abundance of dystromirs in the *mdx* serum did not match the pattern of expression observed in the tissues. This was reflected in the clustering analysis which showed that serum clustered separately from the tissues (**Fig. 3.4b**). In particular, miR-1 and miR-133a were increased in *mdx* serum and were either decreased or unchanged in the *mdx* muscle tissues. Similarly, miR-206 was highly increased in serum but only moderately increased in the muscle tissues. Conversely, miR-31, was increased ~50-70 fold in quadriceps, TA and triceps but was only 2.3 fold increased in serum. Other dystromirs including miR-21, miR-34c, miR-221 and miR-223 followed similar patterns of differential expression between serum and muscle.

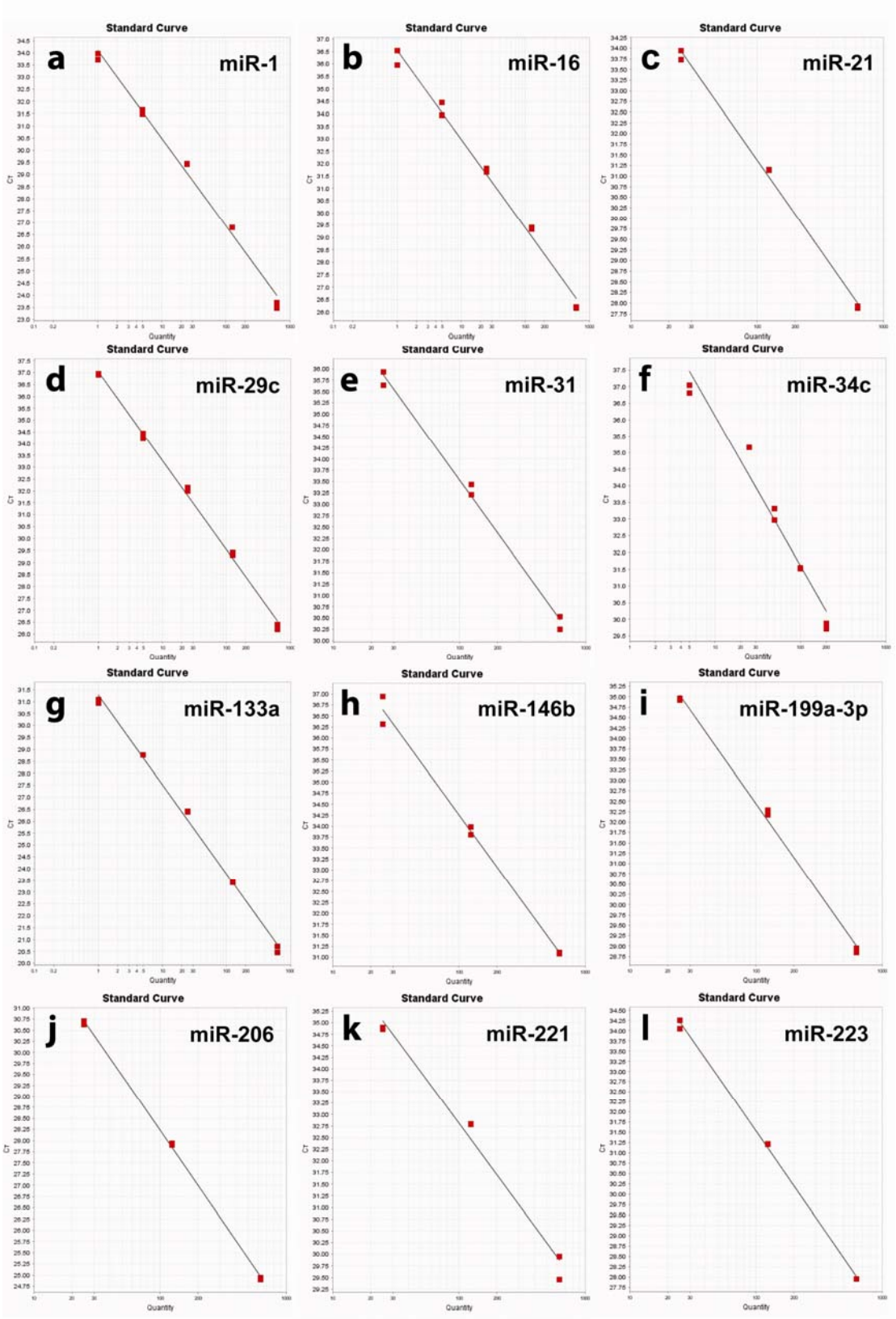
Standard Curve
a
miR-1
b
miR-16
c
miR-21
d
miR-29c
e
miR-31
f
miR-34c
g
miR-133a
h
miR-146b
i
miR-199a-3p
j
miR-206
k
miR-221
l
miR-223
Ct
Quantity

Figure 3.2 Graphs of standard curves for PCR efficiency calculations.

(a) miR-1, (b) miR-16, (c) miR-21, (d) miR-29c, (e) miR-31, (f) miR-34c, (g) miR-133a, (h) miR-146b, (i) miR-199a-3p (j) miR-206, (k) miR-221 and (l) miR-223.

miRNA	gradient	efficiency (%)	R^2
miR-1	-3.617	89.015	0.992
miR-16	-3.568	90.647	0.991
miR-21	-4.244	72.039	0.996
miR-29c	-3.75	84.794	0.997
miR-31	-3.858	81.63	0.994
miR-34c	-4.512	66.587	0.960
miR-133a	-3.75	84.782	0.996
miR-146b	-3.96	78.865	0.993
miR-199a-3p	-4.321	70.377	0.996
miR-206	-4.114	75.016	0.999
miR-221	-3.704	86.184	0.983
miR-223	-4.44	67.977	0.998
pri-miR-31	-3.324	99.918	0.985
pri-miR-34c	-3.447	95.025	0.897
pri-miR-206	-3.373	84.411	0.998
PpiB	-3.447	95.025	0.999

Table 3.4 PCR efficiency determinations for all RT-qPCR assays used in this study. Standard curve gradients, PCR efficiencies and R^2 values are shown. PCR efficiencies were taken into account using the Pfaffl method **[328]** when calculating fold changes between samples.

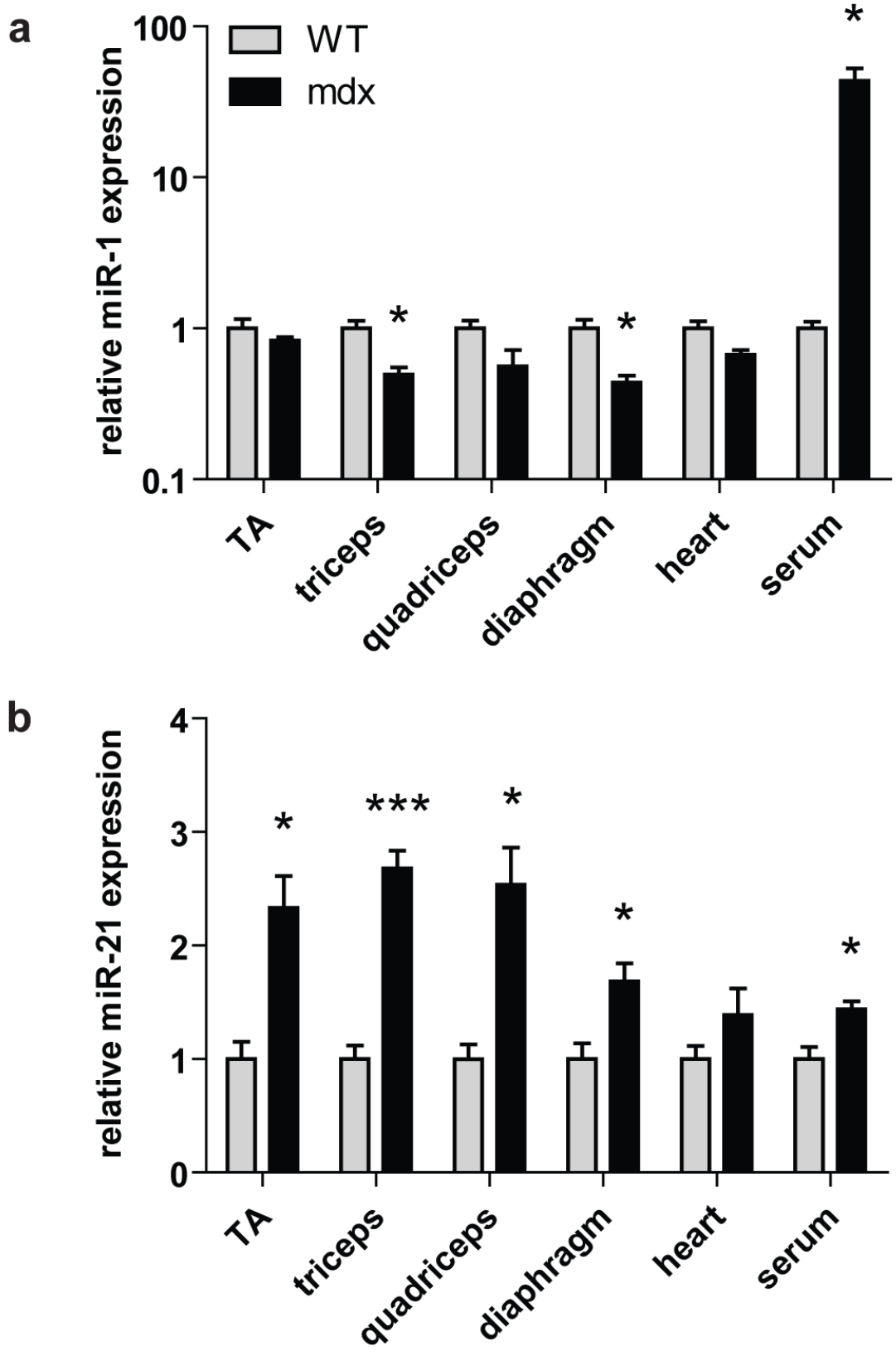
a
100
10
1
0.1
relative miR-1 expression
WT
mdx
*
*
*
TA
triceps
quadriceps
diaphragm
heart
serum
b
4
3
2
1
0
relative miR-21 expression
*
***
*
*
*
TA
triceps
quadriceps
diaphragm
heart
serum

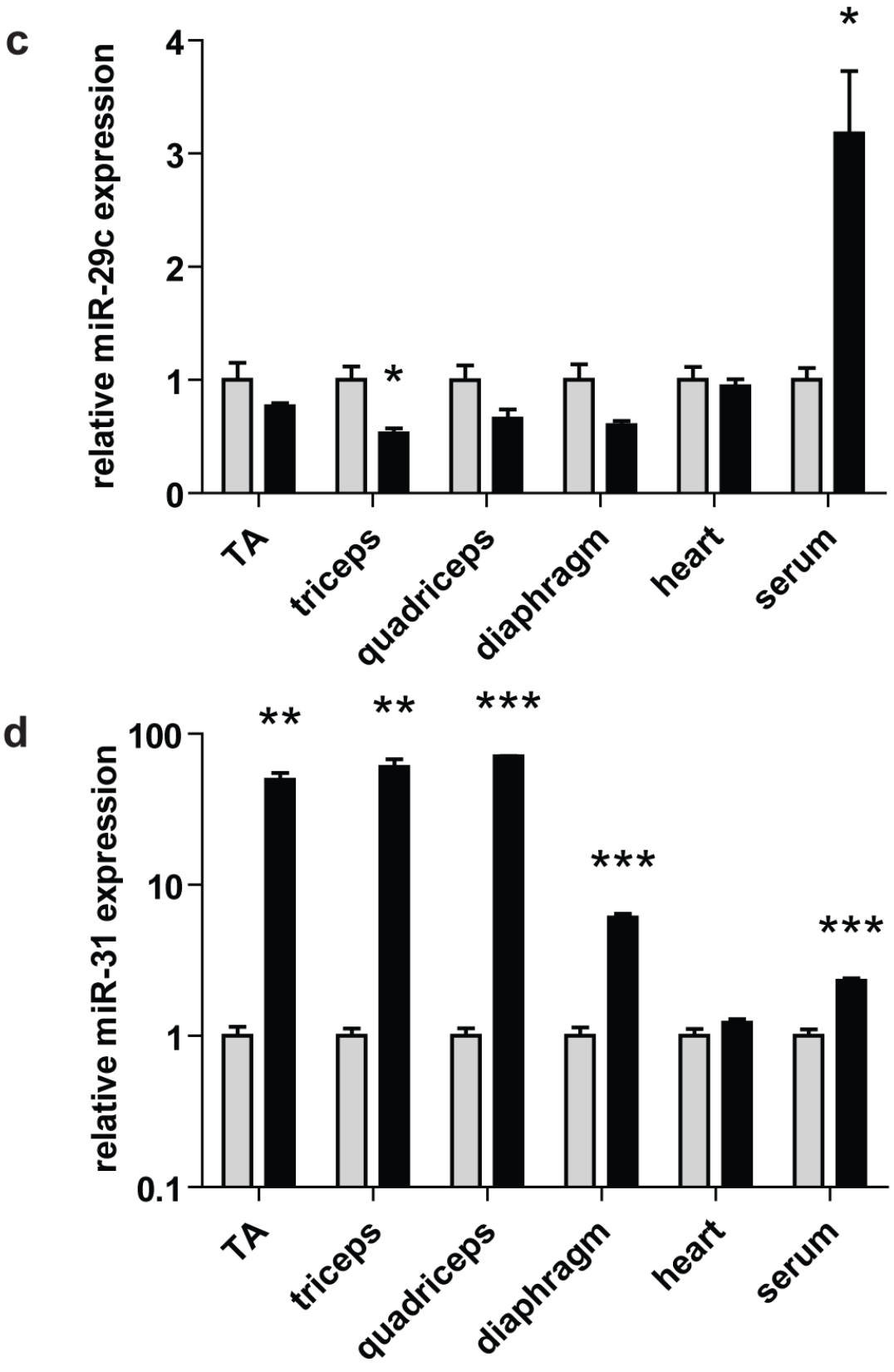
c
relative miR-29c expression
4
3
2
1
0
*
*
TA
triceps
quadriceps
diaphragm
heart
serum
d
relative miR-31 expression
100
10
1
0.1
**
**
***
***
***
TA
triceps
quadriceps
diaphragm
heart
serum

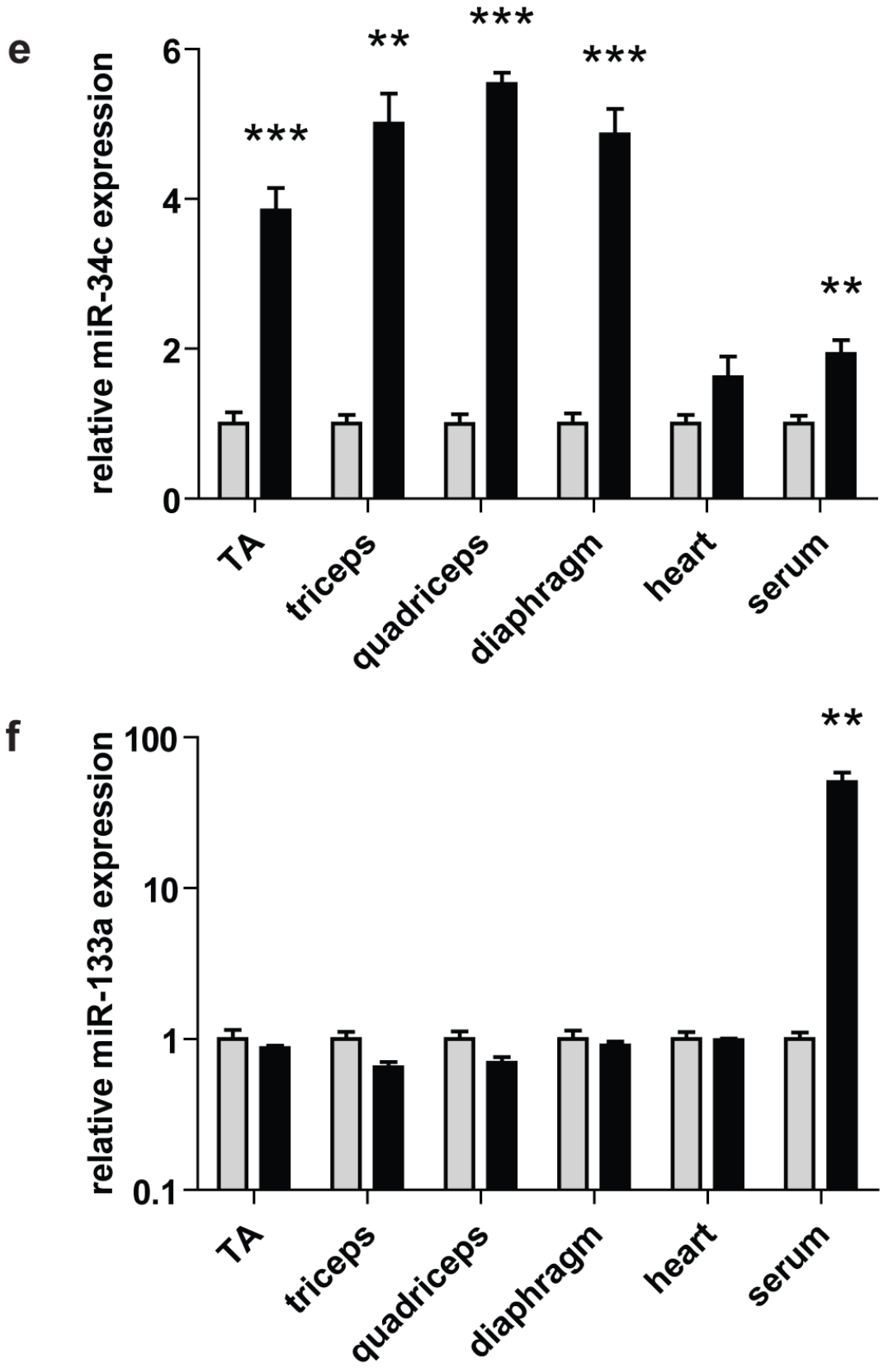
e
relative miR-34c expression
6
4
2
0
***
**
***
***
**
TA
triceps
quadriceps
diaphragm
heart
serum
f
relative miR-133a expression
100
10
1
0.1
**
TA
triceps
quadriceps
diaphragm
heart
serum

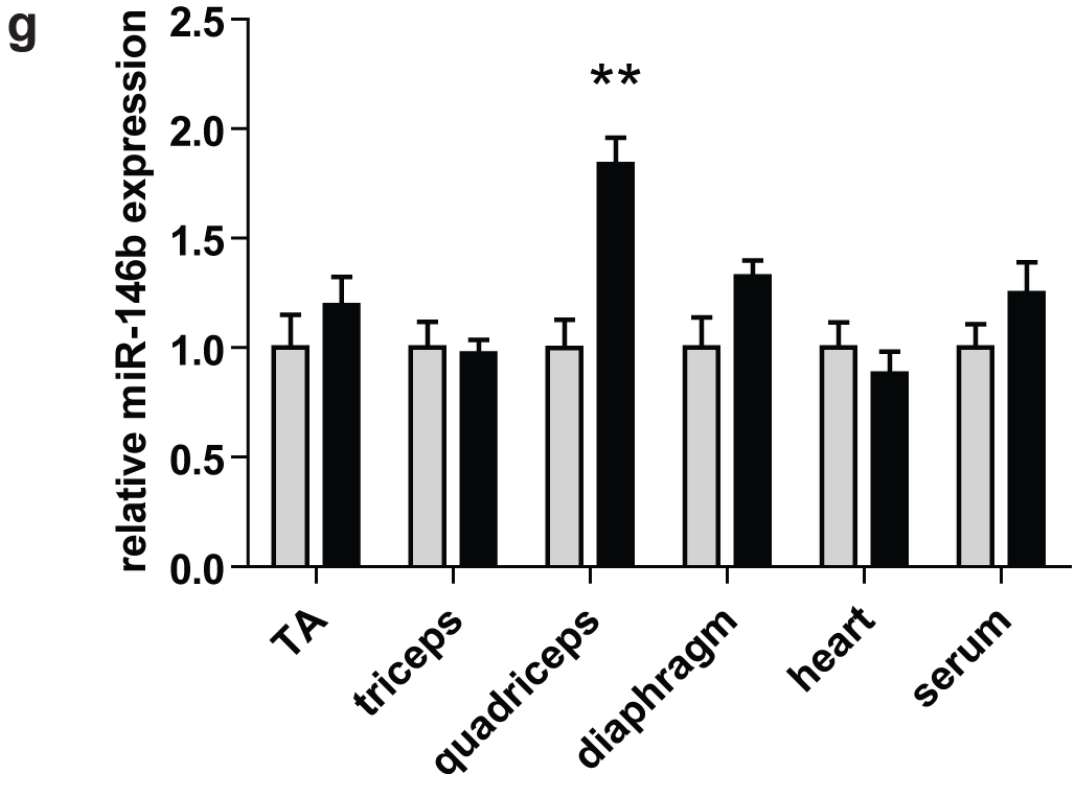
g
relative miR-146b expression
2.5
2.0
1.5
1.0
0.5
0.0
**
TA
triceps
quadriceps
diaphragm
heart
serum

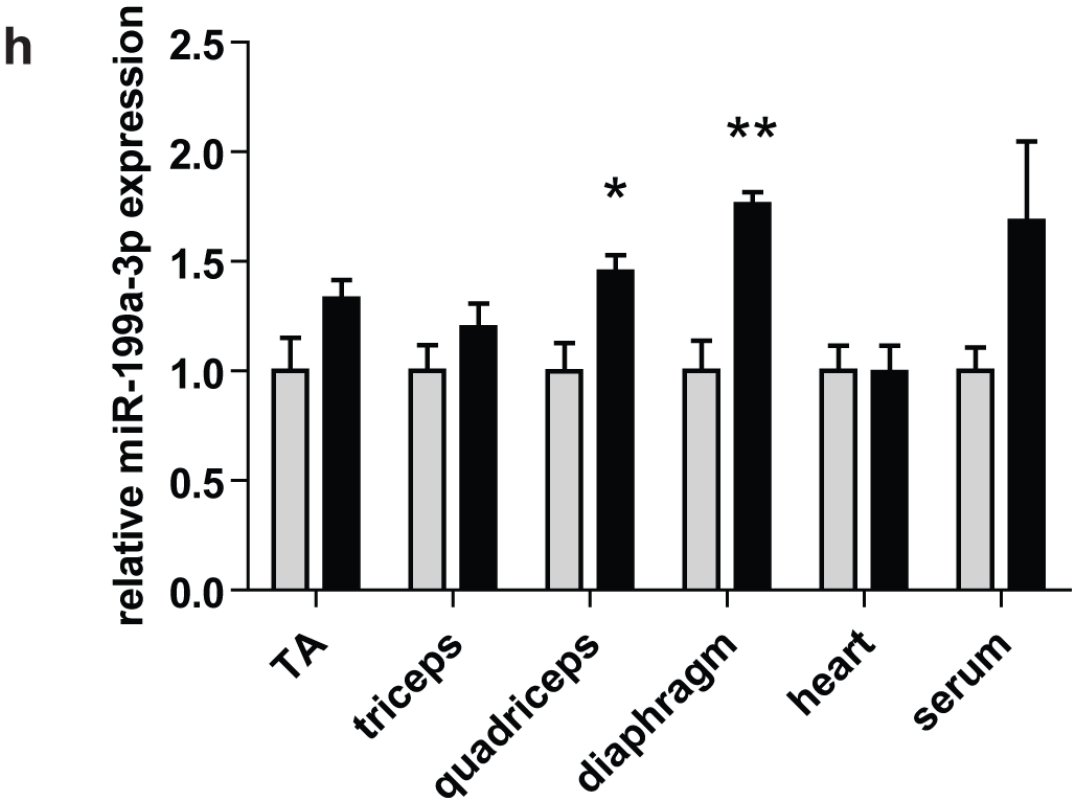
h
relative miR-199a-3p expression
2.5
2.0
1.5
1.0
0.5
0.0
*
**
TA
triceps
quadriceps
diaphragm
heart
serum

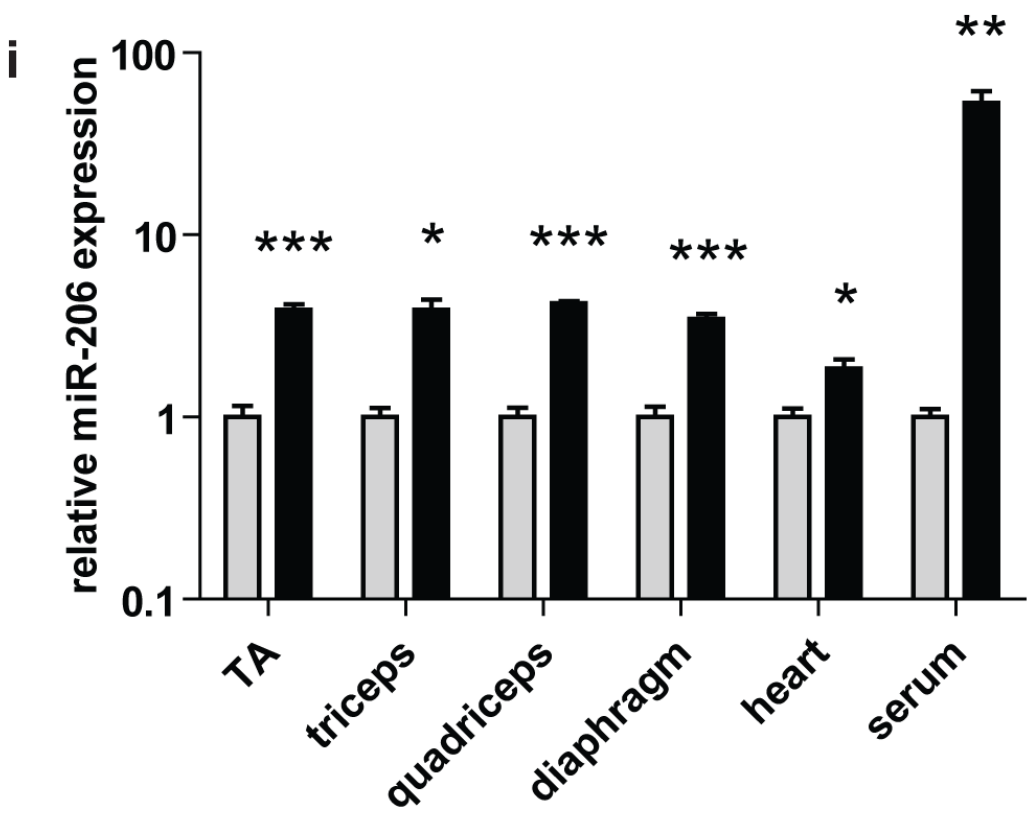
i
relative miR-206 expression
100
10
1
0.1
***
*
***
***
*
**
TA
triceps
quadriceps
diaphragm
heart
serum

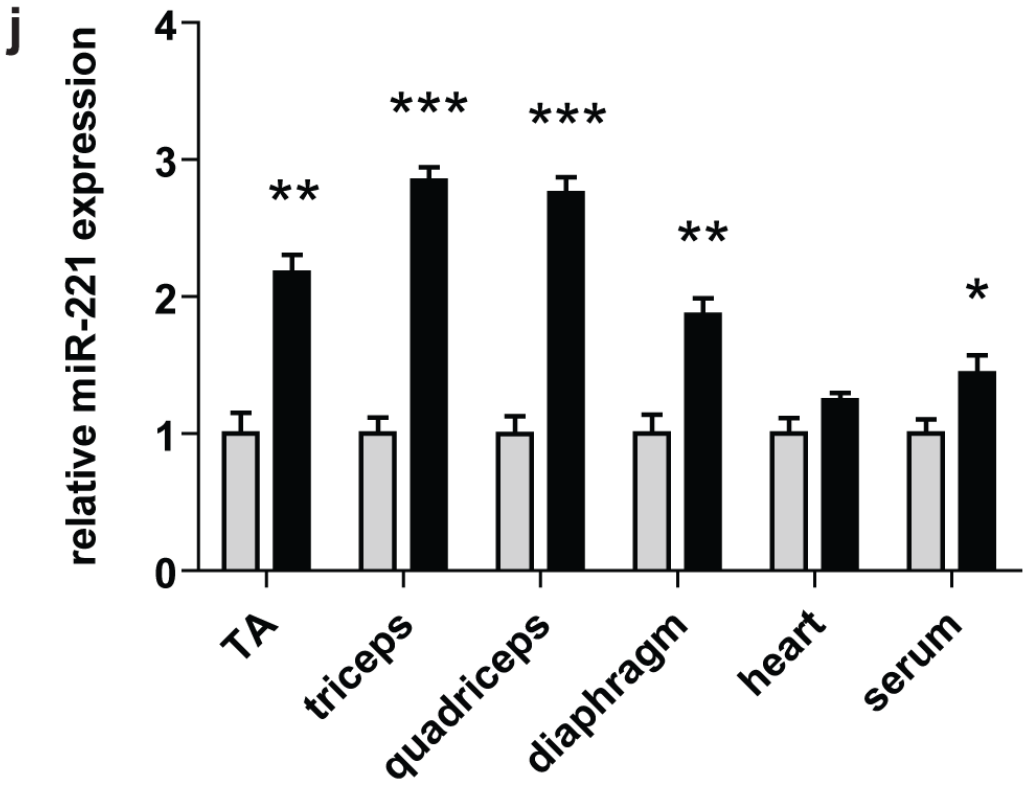
j
relative miR-221 expression
4
3
2
1
0
**
***
***
**
*
TA
triceps
quadriceps
diaphragm
heart
serum

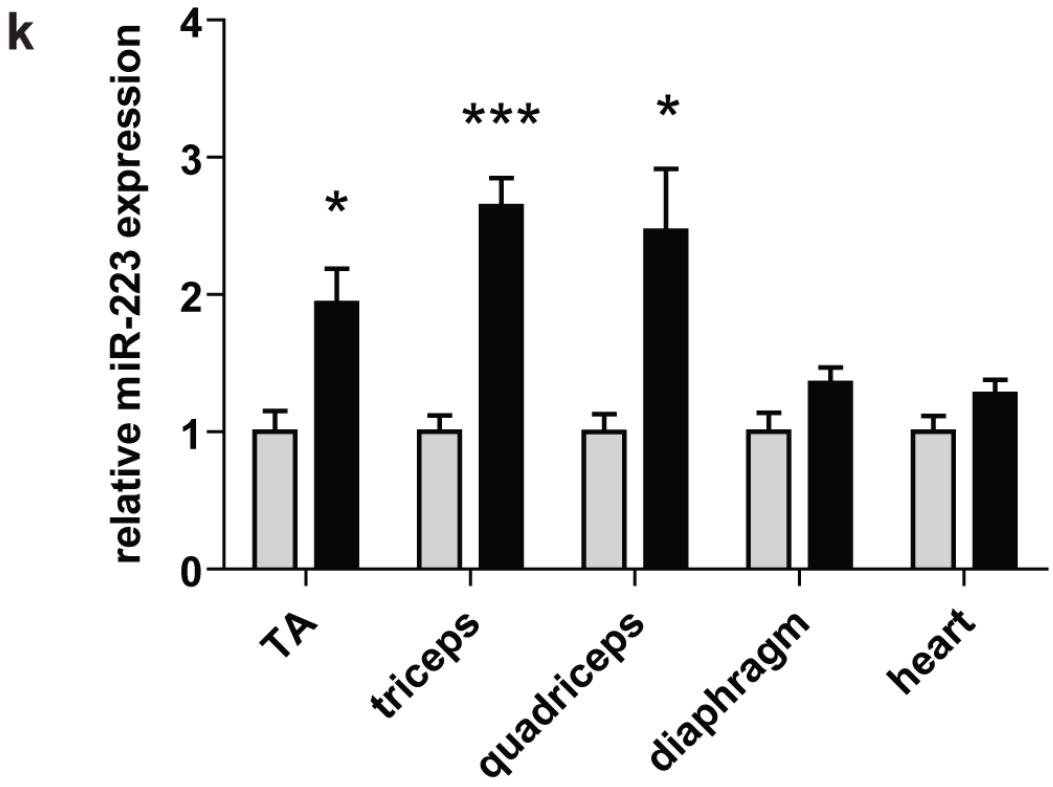

Figure 3.3 RT-qPCR analysis of dystromir expression.

Tibialis anterior (TA), triceps, quadriceps, diaphragm, heart and serum from 8 week old C57/Bl10 (wild type, WT) and *mdx* mice were harvested and small RNA TaqMan reverse transcriptase quantitative polymerase chain reaction (RT-qPCR) performed to determine relative expression of the following dystromirs; (a) miR-1, (b) miR-21, (c) miR-29c, (d) miR-31, (e) miR-34c, (f) miR-133a, (g) miR-146b, (h) miR-199a-3p, (i) miR-206, (j) miR-221, (k) miR-223. Grey bars represent WT samples and black bars represent *mdx* samples. Relative fold changes were determined by the Pfaffl method. Tissue miRNA expression was normalised to miR-16 and serum miRNA expression normalised to miR-223 (consequently serum expression of miR-223 is omitted from panel (k)). All values

are mean + SEM. *p<0.05, **p<0.01, ***p<0.001. For tissue samples n=4. For WT serum n=3 and for *mdx* serum n=4.

	miR-1	miR-21	miR-29c	miR-31	miR-34c	miR-133a	miR-146b	miR-199a-3p	miR-206	miR-221	miR-223
TA	-1.3	2.3	-1.3	49.8	3.8	-1.1	1.2	1.3	3.9	2.2	1.9
triceps	-2.0	2.7	-2.0	60.5	5.0	-1.4	1.0	1.2	3.9	2.8	2.6
quadriceps	-1.7	2.5	-1.4	70.9	5.5	-1.4	1.8	1.5	4.2	2.8	2.5
diaphragm	-2.5	1.7	-1.7	6.1	4.9	-1.1	1.3	1.8	3.5	1.9	1.4
heart	-1.4	1.4	-1.1	1.2	1.6	1.0	-1.1	1.0	1.8	1.2	1.3
serum	43.6	1.4	3.2	2.3	1.9	50.6	1.2	1.7	52.9	1.4	1.0

Table 3.5 Summary of fold changes for all dystromir *mdx* vs wild-type comparisons as measured by small RNA TaqMan RT-qPCR.

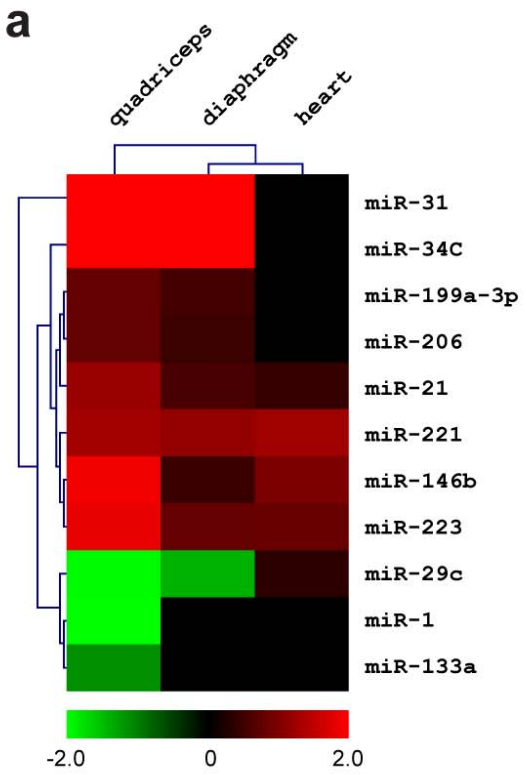
a
quadriceps
diaphragm
heart
miR-31
miR-34C
miR-199a-3p
miR-206
miR-21
miR-221
miR-146b
miR-223
miR-29c
miR-1
miR-133a
-2.0
0
2.0

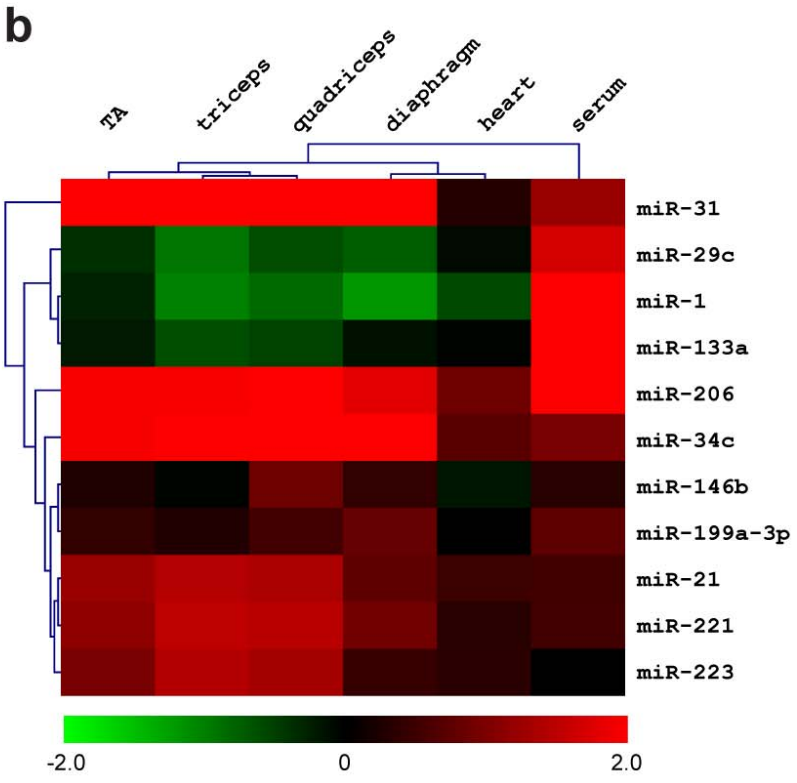
b
TA
triceps
quadriceps
diaphragm
heart
serum
miR-31
miR-29c
miR-1
miR-133a
miR-206
miR-34c
miR-146b
miR-199a-3p
miR-21
miR-221
miR-223
-2.0
0
2.0

Figure 3.4 Heatmaps of *mdx* dystromir expression.

Heatmaps of dystromir expression as determined by (a) miRNA microarray analysis and (b) small RNA TaqMan RT-qPCR. Hierarchical clustering analysis was used to identify patterns of miRNA expression across the *mdx* tissues and serum. Red signifies an increase in expression and green, a decrease in expression. Heatmap scale bars indicate $\log_2$ fold changes.

	quadriceps		diaphragm		heart	
	array	**RT-qPCR**	**array**	**RT-qPCR**	**array**	**RT-qPCR**
miR-1	**-2.31**	-1.79	ns	**-2.27**	ns	-1.50
miR-21	**2.45**	**2.54**	**2.26**	**1.68**	**2.40**	1.39
miR-29c	**-1.97**	-1.51	**-1.40**	-1.67	**1.29**	-1.06
miR-31	**74.30**	**70.93**	**4.00**	**6.09**	ns	1.23
miR-34c	**5.59**	**5.54**	**4.80**	**4.86**	ns	1.62
miR-133a	**-1.13**	-1.43	ns	-1.10	ns	-1.02
miR-146b	**3.78**	**1.84**	**1.38**	1.33	**1.99**	-1.14
miR-199a-3p	**1.74**	**1.45**	**1.46**	1.76	ns	1.00
miR-206	**1.73**	**4.20**	**1.39**	**3.45**	ns	**1.85**
miR-221	**2.34**	**2.76**	**1.50**	**1.87**	**1.36**	1.24
miR-223	**3.58**	**2.46**	**1.76**	1.35	**1.77**	1.28

Table 3.6 Validation of miRNA microarray by small RNA TaqMan RT-qPCR.

Comparison of miRNA microarray and small RNA TaqMan RT-qPCR for dystromirs of interest. Statistically significant ($p<0.05$) fold changes are indicated in bold. 'ns' indicates that expression was not significantly changed in the array dataset.

3.2.3 Transcriptional Dystromir Up-Regulation

Mature miRNAs are derived from hairpin structures residing within long primary transcripts. Often multiple miRNA hairpin structures are found in a single primary transcript, so-called miRNA clusters. After cleavage by Dicer, only one arm of the miRNA hairpin is loaded into the miRISC complex. miRISC loading is asymmetric and depends on the relative thermodynamic stability of the 5′ ends of each strand (i.e. the strand with most unstable 5′ end is preferentially loaded). Inspection of the miRNA microarray data revealed that, in many cases, all of the miRNAs from a primary transcript were concordantly differentially expressed. For example, miR-31 and miR-31* (the minor miRNA species derived from the 3′ arm of the miR-31 hairpin) were both increased in *mdx* quadriceps and diaphragm. Similar results were seen for the major and minor species of other dystromirs; miR-21, miR-146 and miR-199a (**Table 3.7**) and for other non-dystromirs; miR-199b, miR-362, miR-675, miR-501 and miR-532 (data not shown). Similarly, the miRGen resource [345] was utilised to identify miRNA clusters within the mouse genome that are differentially expressed in the *mdx* mouse. Two differentially expressed dystromir-containing clusters were identified; (1) the miR-34 cluster (i.e. mature miR-34c, miR-34c*, miR-34b-5p and miR-34b-3p all up-regulated) and (2) the miR-221/miR-222 cluster (i.e. mature miR-221 and miR-222 up-regulated). A number of other differentially expressed miRNA clusters were identified and are listed in **Table 3.8**. Notably, mature miRNAs from the miR-188/miR-532 and miR-296/miR-298 clusters were concordantly up-regulated in both *mdx* quadriceps and diaphragm.

The miRNA microarray chips also contained probe sets that detect pre-miRNA hairpins. Twelve pre-miRNA hairpins were significantly ($p<0.05$) differentially expressed across all three tissues (**Fig. 3.5a**). Each pre-miRNA was differentially expressed in at least two tissues and two pre-miRNAs, pre-miR-181a-2 and pre-miR-185, were differentially expressed in all three tissues. Expression of both pre-miR-31 and pre-miR-34c was increased in *mdx* quadriceps and diaphragm which matches the observed increases in mature miR-31 and miR-34c species respectively.

Increases in mature miRNA levels could be due to either, (1) enhanced post-transcriptional Drosha/Dicer processing, or (2), up-regulation of the primary miRNA transcript. To discriminate between these possibilities RT-qPCR was performed with primer/probe assays that detect primary-miRNA transcripts for miRs-31, -34c and 206. Statistically significant increases were detected for all three miRNAs in *mdx* quadriceps (**Fig. 3.5b**). The increases in these pri-miRNAs correlated well with their mature miRNA counterparts (correlation coefficient = 0.980). Taken together these data suggest that miR-31, -34c and -206 are up-regulated at the level of transcription.

primary miRNA	tissue/mature miRNA	fold change	p-value	q-value
pri-miR-21	**quadriceps**			
	miR-21	2.4493	2.314E-03	7.759E-03
	miR-21*	1.3913	2.199E-02	3.156E-02
	diaphragm			
	miR-21	2.2591	1.314E-03	6.096E-03
	miR-21*	1.3626	1.443E-02	2.735E-02
pri-miR-31	**quadriceps**			
	miR-31	74.3002	2.731E-06	2.234E-04
	miR-31*	11.8677	1.905E-04	2.034E-03
	diaphragm			
	miR-31	4.0047	7.636E-05	9.998E-04
	miR-31*	3.2380	2.239E-05	7.166E-04
pri-miR-34	**quadriceps**			
	miR-34b-3p	5.5937	1.549E-04	2.034E-03
	miR-34b-5p	1.6915	1.122E-02	2.139E-02
	miR-34c	5.5899	4.341E-05	1.111E-03
	miR-34c*	4.1830	1.374E-03	5.527E-03
	diaphragm			
	miR-34b-3p	3.5178	4.347E-05	8.945E-04
	miR-34b-5p	1.5045	6.034E-03	1.552E-02
	miR-34c	4.8033	2.888E-05	7.957E-04
	miR-34c*	3.4774	1.631E-03	7.339E-03
pri-miR-199a	**quadriceps**			
	miR-199a-3p	1.7414	3.254E-04	2.700E-03
	miR-199a-5p	2.0624	1.627E-05	5.706E-04
	diaphragm			
	miR-199a-3p	1.4592	1.290E-02	2.532E-02
	miR-199a-5p	1.8950	1.091E-04	1.221E-03
pri-miR-221/222	**quadriceps**			
	miR-221	2.3383	2.036E-04	2.034E-03
	miR-222	2.2782	1.303E-03	5.331E-03
	diaphragm			
	miR-221	1.5050	3.400E-05	7.957E-04
	miR-222	1.4887	1.779E-04	1.431E-03
	heart			
	miR-221	1.3596	4.348E-04	4.362E-02
	miR-222	1.1857	6.036E-03	1.010E-01

Table 3.7 Concordantly changed mature dystromirs derived from common primary-miRNA transcripts in *mdx* quadriceps, diaphragm and heart.

miRNA cluster	mature miRNA	fold change	p-value	q-value
miR-188/miR-532	**quadriceps**			
	miR-188-3p	1.2212	1.201E-02	2.216E-02
	miR-188-5p	2.2865	3.339E-02	4.269E-02
	miR-532-3p	1.3996	3.888E-03	1.084E-02
	miR-532-5p	1.4263	1.593E-04	2.034E-03
	diaphragm			
	miR-188-3p	1.5233	1.320E-03	6.096E-03
	miR-188-5p	2.4893	1.604E-06	3.554E-04
	miR-532-3p	2.1782	6.645E-04	3.612E-03
	miR-532-5p	2.3233	6.357E-04	3.522E-03
miR-296/miR-298	**quadriceps**			
	miR-296-3p	2.0259	4.925E-02	5.233E-02
	miR-298	2.7240	4.491E-03	1.167E-02
	diaphragm			
	miR-296-3p	2.7955	1.255E-04	1.247E-03
	miR-298	4.5096	3.366E-05	7.957E-04
miR-23a/ miR-27a/miR-24-2	**quadriceps**			
	miR-23a	1.1932	4.526E-05	1.111E-03
	miR-23b	1.0453	1.900E-02	2.922E-02
	miR-27a	1.4646	3.842E-05	1.111E-03
	miR-27a*	1.3656	2.526E-02	3.463E-02
	miR-24-2*	1.3405	4.360E-02	4.909E-02
miR-212/miR-132	**quadriceps**			
	miR-212	1.7539	2.185E-02	3.156E-02
	miR-132	1.8865	3.823E-03	1.084E-02
miR-337/miR-540/miR-665	**quadriceps**			
	miR-337-5p	-2.1507	3.797E-04	2.824E-03
	miR-540-3p	-1.6626	1.685E-02	2.872E-02
	miR-665	-1.7477	4.509E-02	4.985E-02
miR-411/miR-229	**quadriceps**			
	miR-411	-1.5651	3.637E-02	4.531E-02
	miR-299	-1.8541	4.517E-03	1.167E-02
	miR-299*	-2.4882	2.881E-02	3.852E-02
miR-668/miR-485	**quadriceps**			
	miR-668	-1.3369	8.698E-03	1.794E-02
	miR-485	-2.9339	6.571E-06	3.037E-04
miR-494/miR-679	**diaphragm**			
	miR-494	1.4014	3.591E-05	7.957E-04
	miR-679	1.4012	3.599E-03	1.139E-02
miR-381/miR-487b	**diaphragm**			
	miR-381	4.0546	3.379E-04	2.295E-03
	miR-487b	2.2198	4.176E-03	1.280E-02
miR-181a-1/miR-181b-1	**heart**			
	miR-181a	-1.1496	3.738E-02	2.427E-01
	miR-181b	-1.1949	1.535E-03	7.325E-02
miR-194-2/miR-192	**heart**			
	miR-194	-1.2899	1.176E-02	1.284E-01
	miR-192	-1.2749	3.668E-02	2.427E-01

Table 3.8 Concordantly changed mature miRNAs derived from common miRNA clusters in *mdx* quadriceps, diaphragm and heart.

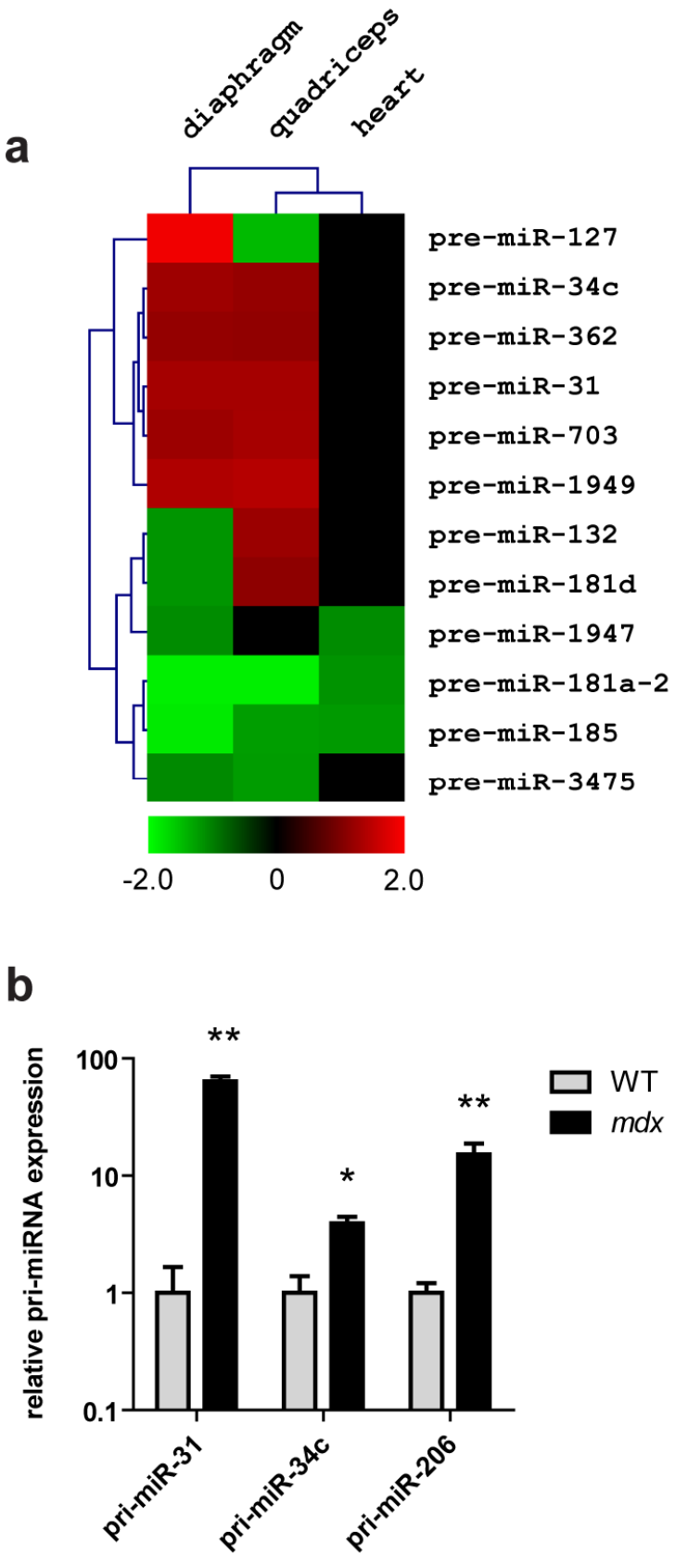
a
diaphragm
quadriceps
heart
pre-miR-127
pre-miR-34c
pre-miR-362
pre-miR-31
pre-miR-703
pre-miR-1949
pre-miR-132
pre-miR-181d
pre-miR-1947
pre-miR-181a-2
pre-miR-185
pre-miR-3475
-2.0
0
2.0
b
relative pri-miRNA expression
100
10
1
0.1
**
*
**
WT
mdx
pri-miR-31
pri-miR-34c
pri-miR-206

Figure 3.5 Differential expression of precursor-miRNAs and primary-miRNAs.

(a) Statistically significant changes in precursor-miRNA (pre-miRNA) expression in *mdx* quadriceps, diaphragm and heart (n=4). Hierarchical clustering analysis was used to identify patterns of pre-miRNA expression in the *mdx* quadriceps, diaphragm and heart. Red signifies an increase in expression and green, a decrease in expression. Heatmap scale bars indicate fold changes. (b) Changes in primary-miRNA expression in *mdx* quadriceps for pri-miR-31, pri-miR-34c and pri-miR-206 as measured by RT-qPCR. Relative values were determined using the relative standard curve method and primary-miRNA expression normalised to PpiB. Values are mean + SEM, n=4, *$p<0.05$, **$p<0.01$.

3.2.4 Pip6e-PMO Treatment Partially Normalises Serum Dystromir Abundance

Circulating miR-1, miR-133a and miR-206 have been proposed as serum biomarkers for the progression of DMD [329,336]. In order to determine if the serum levels of these dystromirs responded to antisense oligonucleotide-mediated exon skipping therapy, twelve-week-old *mdx* mice were treated with a single 12.5 mg/kg tail vein injection of Pip6e-conjugated phosphorodiamidate morpholino oligonucleotide (PMO). (This conjugate is a novel variant of Pip5e-PMO that had previously been demonstrated to induce skipping of exon 23 from the mature dystrophin transcript to restore restoration of dystrophin protein expression and muscle function [59]). Treated mice were harvested two weeks after injection and tibialis anterior, quadriceps, heart and diaphragm muscles collected along with sera. Comparisons were made against age-matched wild-type and non-treated *mdx* controls. Treated animals showed a partial normalisation of the high serum levels of miR-1 (18.1 fold to 3.6 fold), miR-133a (32.3 fold to 3.8 fold) and miR-206 (65.9 fold to 10 fold) observed in the *mdx* mouse (**Figs 3.6a-c**). In all cases serum dystromir abundance was reduced to levels close to wild-type controls. Restoration of dystrophin protein expression by Pip6e-PMO treatment was confirmed in all muscles analysed by immunofluorescence (representative image of restoration in the tibialis anterior shown in **Fig. 3.7**) and by the detection of mature dystrophin transcripts lacking exon 23, as determined by RT-PCR (**Fig. 3.8a**) and western blot (**Fig. 3.8b**).

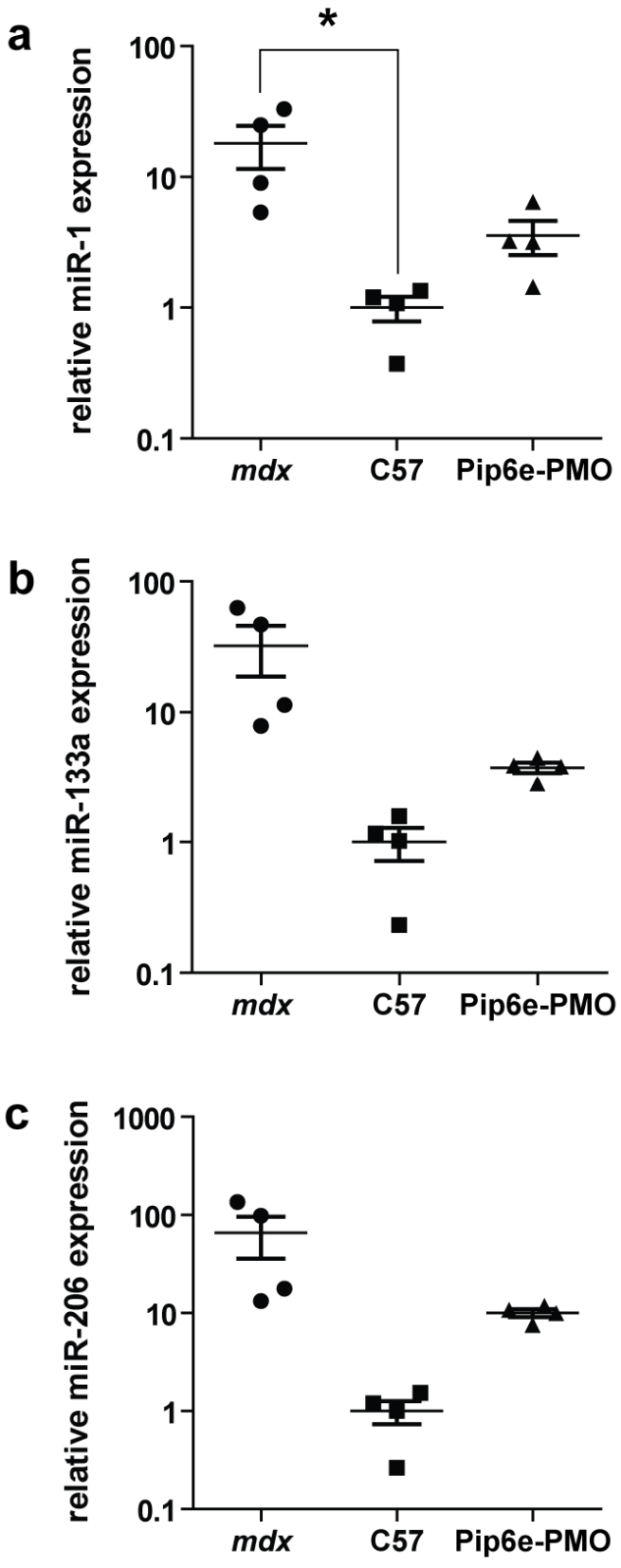
a
*
relative miR-1 expression
100
10
1
0.1
mdx
C57
Pip6e-PMO
b
relative miR-133a expression
100
10
1
0.1
mdx
C57
Pip6e-PMO
c
relative miR-206 expression
1000
100
10
1
0.1
mdx
C57
Pip6e-PMO

Figure 3.6 Pip6e-PMO treatment normalises serum dystromir abundance.

12 week old *mdx* mice were injected with a single 12.5 mg/kg dose of Pip6e-PMO intravenously and harvested 2 weeks later. Serum samples were analysed for the expression of (a) miR-1, (b) miR-133a, and (c) miR-206 by small RNA TaqMan RT-qPCR. miRNA levels were normalised to miR-223 expression and fold changes presented relative to the wild-type C57 average. Values are mean +/- SEM, n=4, *$p<0.05$.

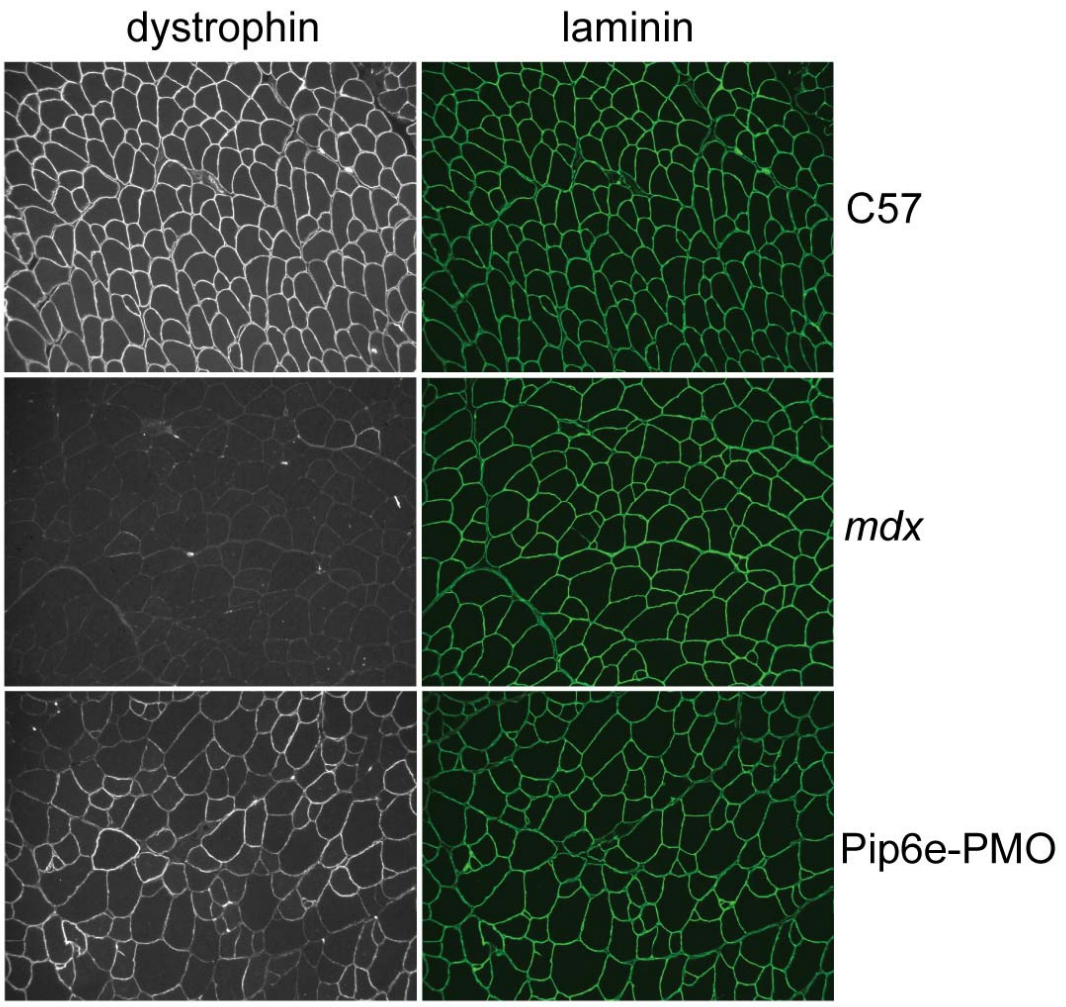

Figure 3.7 Pip6e-PMO treatment restores dystrophin expression in *mdx* tibialis anterior. Representative immunofluorescence images of tibialis anterior muscle showing restoration of dystrophin at the sarcolemma in *mdx* mice following treatment with Pip6e-PMO. Samples were co-stained with laminin to indicate muscle fibres.

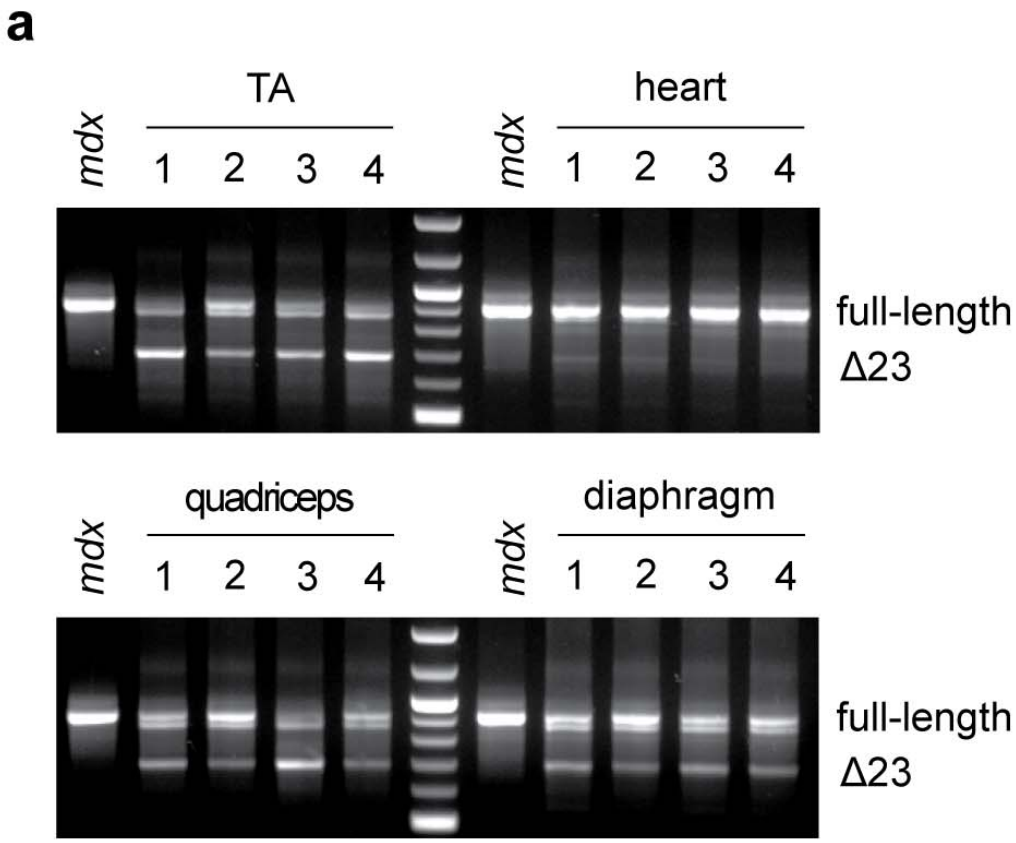
a
TA
heart
mdx
1 2 3 4
mdx
1 2 3 4
full-length
Δ23
quadriceps
diaphragm
mdx
1 2 3 4
mdx
1 2 3 4
full-length
Δ23

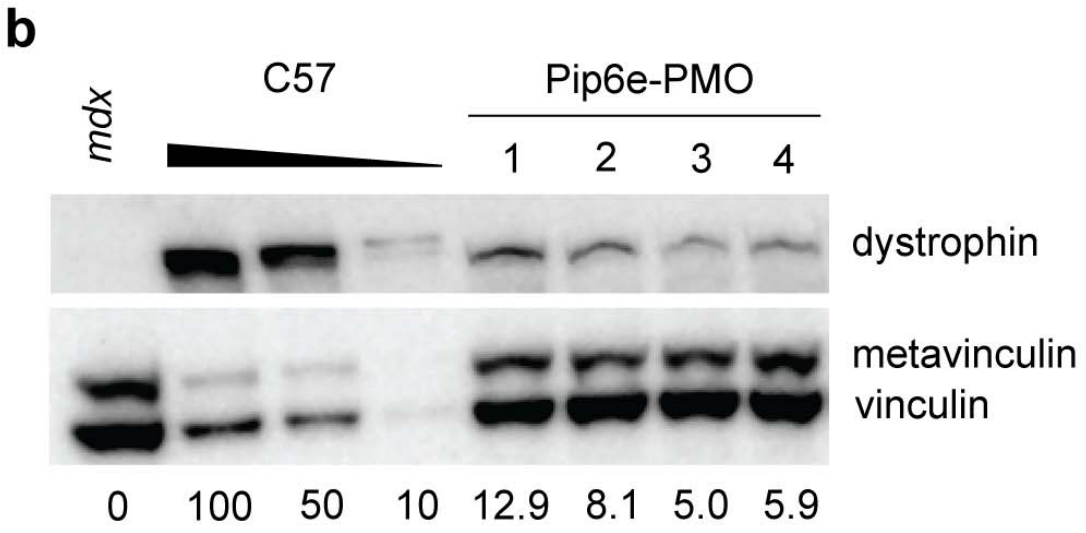
b
C57
Pip6e-PMO
mdx
1 2 3 4
dystrophin
metavinculin
vinculin
0 100 50 10 12.9 8.1 5.0 5.9

Figure 3.8 Pip6e-PMO treatment restores dystrophin mRNA and protein expression.

(a) RT-PCR shows skipping of dystrophin exon 23 in tibialis anterior, heart, quadriceps and diaphragm. (b) Western blot showing restoration of dystrophin protein in tibialis anterior muscles of *mdx* mice treated with Pip6e-PMO. Dystrophin expression was normalised to vinculin protein levels. Dystrophin quantification (as a percentage of C57 control) is indicated underneath each lane.

3.3 Discussion

This study has characterised differential miRNA expression between different muscle groups and serum of the *mdx* mouse. This study is the first to provide a complete profile by microarray analysis of miRNA expression in the *mdx* heart and diaphragm, tissues which are central to the dystrophic pathology and disease progression in DMD patients. The use of miRNA microarray analysis has enabled the detection of the maximum number of miRNAs possible (miRBase v15) whereas TaqMan Array Card technology is limited to 381 miRNA assays. Generally, the *mdx* diaphragm and heart show less differential miRNA expression, both in number of differentially expressed miRNAs and in the magnitude of fold changes, reflecting a lower level of degeneration in the diaphragm and heart in mice of this age. This is consistent with what is already known about the natural history of disease progression [346]. In addition, by assaying different tissues from the same animals this study has shown that there are important differences between the skeletal muscle groups themselves. In general, quadriceps, tibialis anterior and triceps muscles show similar levels of differential dystromir expression. However, significant changes in the expression of miR-146b and miR-199a-3p were not observed in all tissues. (**Figs. 3.3g,h and Table 3.5**). Differential expression between tissues is one explanation for contradictions between previous reports. For example, differential expression of miR-146b has been reported by some investigators [333] but not others [332]. One of the first studies of miRNA expression (also in the 8 week old *mdx* mouse) showed that miR-206 expression was increased in the *mdx* diaphragm but not in the soleus or plantaris muscles [337]. The reported 4.5 fold increase in miR-206 expression in diaphragm is closely matched by our study (4.7 fold increase). However, the previous

study suggested that miR-206 was up-regulated in diaphragm but not in hindlimb on account of the diaphragm being the most severely affected *mdx* muscle. Our results do not support this conclusion as we have detected increased miR-206 expression in two hindlimb *mdx* muscles (tibialis anterior and quadriceps) and in the *mdx* forelimb (triceps). In all of these cases the increase in miR-206 expression is moderately higher than in the diaphragm. To reconcile the differences between these studies, we note that the study by McCarthy *et al.* utilised semi-quantitative PCR and image quantification from PAGE gels, which is a much less quantitative and sensitive methodology than small RNA TaqMan RT-qPCR. Alternatively, a lack of increase in miR-206 expression in the *mdx* soleus and plantaris may represent further complexity in the *mdx* muscle transcriptome.

The most differentially expressed miRNA of all array datasets was miR-31 (~70 fold increase). This is consistent with the study by Greco *et al.* which showed similar magnitude fold change in the adductor muscles of mice of the same age and in DMD patient biopsies (from the quadriceps femoris) [332]. Interestingly, Eisenberg *et al.* did not report miR-31 as being differentially expressed in a microarray study of patients with diverse muscle disorders (including DMD and BMD) [333]. We have observed high levels of miR-31 across all of the skeletal muscles studied. This is encouraging as antagonism of miR-31 activity has recently been proposed as a synergistic therapeutic strategy to exon skipping-mediated dystrophin restoration [126].

Our results are consistent with those reported by Yuasa *et al.* who profiled miR-1, miR-133 and miR-206 in the TA muscle of *mdx* mice and the $CXMD_J$ dystrophic dog model

[334]. Similarly, two recent studies have identified miR-486 as down-regulated in *mdx* skeletal muscle [156,347]. We have confirmed this result as miR-486 expression was reduced 1.3 fold ($p = 0.0002$) in the *mdx* quadriceps dataset only. miR-486 is encoded within the ankyrin gene and has been shown to regulate components of the PTEN/AKT pathway and in doing so influences cell cycle kinetics [347].

In general, microarray and RT-qPCR validation data were in close agreement. Those minor differences observed between the miRNA microarray and RT-qPCR data are likely to be due to the increased sensitivity of the RT-qPCR assays, and to the high false discovery rate in the heart array dataset. Methodological differences may be one reason for some of the variations in dystromir expression reported previously [332,333,337]. We have calculated PCR efficiencies for all of the TaqMan assays used in this study by performing standard curves on serial dilutions of cDNA (**Figs 3.2a-k** and **Table 3.4**). Importantly, in all cases the PCR efficiencies were less than 100%. We therefore utilised the Pfaffl method [328] (which corrects for sub-optimal PCR efficiencies) to calculate relative changes in gene expression as opposed to the Livak ($\Delta\Delta$Ct) method [348] (which assumes 100% PCR efficiency). Not correcting for PCR efficiency results in an overestimation of the differences between samples and underlines the importance of validating assays used in studies of gene expression.

Multiple lines of evidence point to transcriptional up-regulation of dystromirs in the *mdx* mouse. Firstly, mature miRNAs that are derived from the same primary transcript are concordantly differentially expressed. Secondly, increases in the pre-miRNA hairpins are

detected in the case of miR-31 and miR-34c, and lastly, pri-miRNA levels are increased for miR-31, -34c and -206. A previous report has shown that epigenetic silencing is responsible for changes in the expression of certain miRNAs in the *mdx* mouse as a result of impaired nitric oxide signalling and consequent HDAC2 activation [335]. It remains to be seen if a similar mechanism is operative for the dystromirs we have investigated.

Several studies have identified miR-1, miR-133a and miR-206 as being highly enriched (~50 fold) in the serum of *mdx* mice and DMD patients relative to controls [329,336]. Intriguingly, despite the significant up-regulation of these miRNAs in serum, this pattern of expression is not reciprocated in skeletal muscles (i.e. miR-206 is only increased ~4-10 fold and miR-1 and miR-133a are generally decreased or not significantly changed in the skeletal muscles but all three miRNAs are ~50 fold increased in serum). Similarly, the patterns of expression of other dystromirs did not generally correlate between the muscles and serum. This incongruence between the miRNA expression profile of muscle and serum suggests that *mdx*-enriched extracellular miRNAs do not simply 'leak' from damaged muscle due to impaired sarcolemmal integrity; otherwise the serum profile would be expected to reflect the muscle profile. The non-random distribution of extracellular miRNAs suggests that they may constitute a specific biological response. We speculate that miR-1, miR-133a and miR-206 are actively released from dystrophic muscle and are protected from RNase-mediated degradation by either encapsulation in microvesicles [349] or in complex with proteins such as Argonate 2 [350]. We speculate that these extracellular miRNAs function to drive muscle regeneration in response to muscle damage or to the dystrophic condition through cell-to-cell communication.

This study has shown that systemic administration of a single dose of an antisense oligonucleotide-mediated exon skipping therapy resulted in partial normalisation of the circulating dystromirs that are highly enriched in *mdx* serum. This is consistent with a previous report that utilised a virus-mediated exon skipping strategy. The same study also showed that patients with the less severe Becker Muscular Dystrophy (BMD) showed intermediate levels of serum dystromirs between DMD and healthy [329]. These serum dystromirs show promise as disease biomarkers that could be used to non-invasively monitor the effectiveness of experimental therapies in DMD patients. Currently, serum creatine kinase (CK) is used as a biomarker for muscle damage. In contrast to CK, serum miRNAs have been shown to change little in response to exercise [336] and correlate better with disease severity [329]. A possible limitation of this approach is that the levels of serum dystromirs in dystrophic mice and DMD patients are highly variable, as observed here and in a previous study [329]. This variability may mean it is difficult to detect changes in serum miRNA levels due to minor improvements in therapeutic outcomes.

This study has demonstrated muscle-specific changes in miRNA expression and indicates that methodological differences are a plausible explanation for the contradictions between previous miRNA investigations in the *mdx* mouse and DMD patients. The observation that the miRNA expression varies between tissues (even between skeletal muscles) is indicative of differential pathological processes occurring between these tissues. This unexpected level of complexity will need to be considered with regards to the development of novel miRNA-based therapies for treating DMD and the use of serum biomarkers for monitoring the efficacy of experimental treatments.

4 Small RNA-Mediated Epigenetic Myostatin Silencing

4.1 Introduction

The myostatin signaling pathway is a promising pharmacological target for the treatment of muscle wasting conditions such as DMD (see section 1.3.2). Previous studies have demonstrated that the combination of myostatin blockade with dystrophin restoration in *mdx* mice resulted in a greater functional improvement than either treatment alone [351]. Consequently, A number of strategies have been utilised to achieve myostatin blockade including myostatin neutralising antibodies [352], endogenous myostatin antagonists (myostatin propeptide [87], follistatin [89] and soluble Acvr2b (the myostatin receptor [353])), destructive exon skipping [354] and RNA interference (RNAi) [355]. A common limitation of all of these strategies is that they induce transient inhibition of myostatin signalling and so repeat administration would be required for therapy. Whereas the majority of these approaches are experimental, an anti-myostatin antibody developed by Wyeth Pharmaceuticals (Stamulumab) has reached phase I/II clinical trials. However, development of this therapy was discontinued due to a lack of muscle function improvement in treated patients. There is therefore a need to develop novel approaches to targeting the myostatin pathway.

An alternative to the canonical RNAi pathway is transcriptional gene silencing (TGS) [168,170] (discussed in detail in section 1.5.1.1). TGS is a homology-dependent gene silencing pathway mediated by small interfering RNAs (siRNAs), viral/plasmid expressed short hairpin RNAs (shRNAs) [189] or expressed antisense RNAs (asRNAs) [169,175] with complementarity to target gene promoters. These small RNA effector

molecules target low copy-number promoter-associated RNA transcripts [199] in order to recruit chromatin remodelling factors [169] to the complementary promoter and, in some cases, induce promoter DNA methylation [189,199]. As epigenetic changes are stable and heritable, long-term silencing of therapeutically relevant genes may be possible. A number of TGS studies have demonstrated long-term gene silencing in cell culture [170–172,175]. The aim of this work is to demonstrate the feasibility of silencing myostatin expression by TGS. The results of this chapter show that myostatin expression is silenced by a promoter-targeted siRNA and that the silencing involves epigenetic remodelling of the myostatin promoter. This study thus opens up a new therapeutic avenue in the treatment of muscle wasting disorders.

4.2 Results

4.2.1 Detection of Myostatin Promoter-Associated RNA

Previous studies have shown that TGS in mammalian cells requires the presence of promoter RNA transcripts. The database of transcription start sites (DBTSS) [356] and UCSC genome browser [357] resources were used to identify the myostatin transcription start site (TSS). To characterise transcription at the myostatin promoter, directional RT-PCR was performed using primers that amplify a 153 bp region upstream of the annotated TSS in a strand-specific manner (**Fig. 4.1a**). Transcripts were detected in both sense and antisense orientations indicating the presence of promoter-associated RNA at the myostatin promoter. PCR amplicons were sequenced to confirm identity (data not shown). Reverse transcriptase minus (RT-) control PCR reactions failed to amplify ruling out genomic DNA contamination (**Fig. 4.1b**).

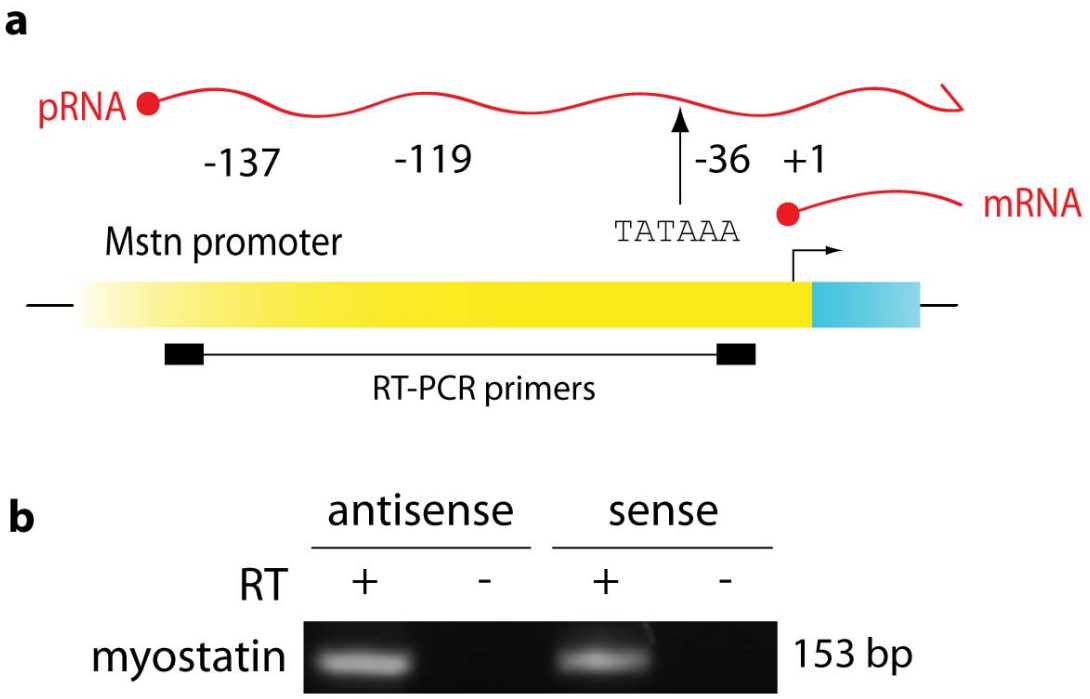

Figure 4.1 Detection of myostatin promoter-associated RNAs.

(a) Schematic of myostatin promoter showing annotated transcription start site and hypothetical promoter-associated RNA transcript (pRNA). Position of TATA box and location of RT-PCR amplicons are indicated. (b) Detection of pRNA at the myostatin promoter in sense and antisense orientations by directional RT-PCR. RT- controls do not amplify indicating no genomic DNA contamination.

4.2.2 RT-qPCR Assay Validation

Preliminary experiments showed that myostatin was expressed at relatively low, but readily detectable, levels in C2C12 myotubes. Consequently, the maximum recommended amount of input total RNA was used in the RT reaction (2 μg) and the maximum amount of RT reaction used in the qPCR reaction (2 μl in a 20 μl reaction). This was to ensure that the myostatin cDNA amplification fell within the Ct range of 25-35. (Statistical power to detect fold changes decreases above 35 cycles). To validate the RT-qPCR assays used in this study, standard curves were produced by two-fold serial dilutions of cDNA from untreated C2C12 cultures and amplified as described in section 2.12 (**Fig. 4.2**). Both assays were linear over the range of input cDNA amounts assayed and did not reach the limit of quantification within the range of values measured for all experiments (Ct standard deviations < 0.5). R^2 values were high (0.998 for Mstn and 0.999 for β-Actin (ACTB)). PCR efficiencies were sub-optimal (82% for Mstn and 84% for ACTB). Consequently, the relative standard curve method [358] was used to compare samples while taking into account PCR inefficiencies. As such, a cDNA standard curve was included on every RT-qPCR plate. The low PCR efficiencies are most likely due to the high input RNA in the RT reaction and/or the presence of RT components in the qPCR reaction leading to a small degree of PCR inhibition.

The Mstn assay was designed to amplify only mature mRNA. This was confirmed by observing that no amplification was detected in RT minus controls (**Fig. 4.3a**). Conversely, the ACTB assay has the potential to amplify genomic DNA. This was confirmed as amplification was detected in the RT minus control for the ACTB assay

(**Fig. 4.3b**). However, ACTB RT minus amplification was ~14 cycles later than RT plus amplification indicating that β-Actin mRNA is over 10,000 fold more abundant than genomic DNA. Genomic DNA was thus not considered to be significantly affecting the results.

Typically β-actin (ACTB) was used to normalise myostatin expression although studies were also performed using peptidylprolyl isomerase B (Ppib) as a reference gene with similar results (data not shown). No template controls (NTCs) were included on every plate analysed. No NTC amplification was observed in any experiment described indicating the absence of contamination of samples or reagents with PCR amplicons.

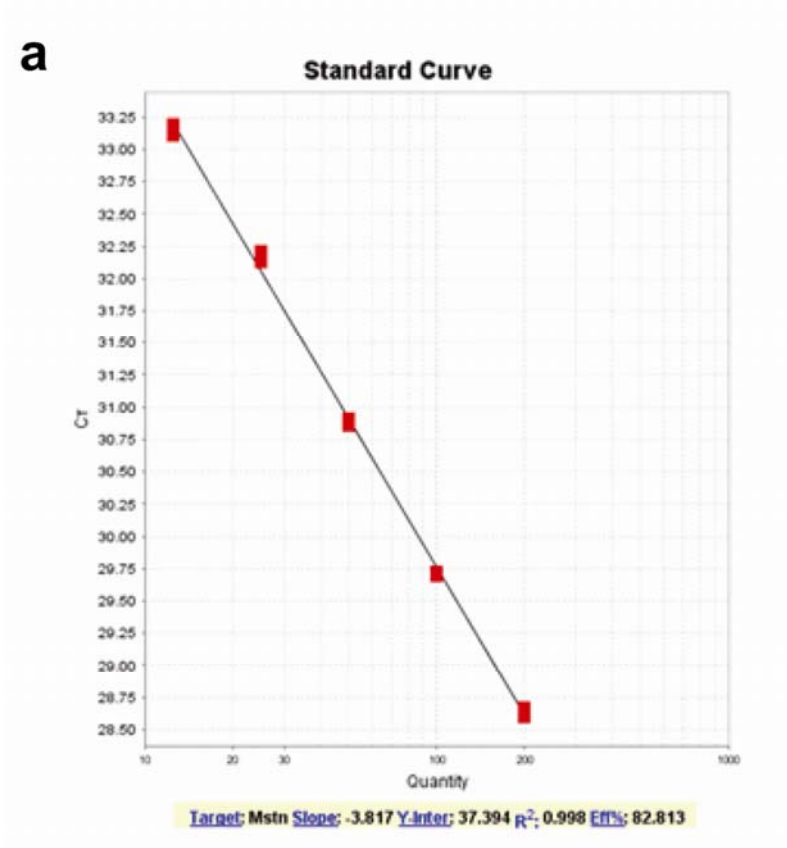
a
Standard Curve
Ct
Quantity
Target: Mstn Slope: -3.817 Y-Inter: 37.394 R2: 0.998 Eff%: 82.813

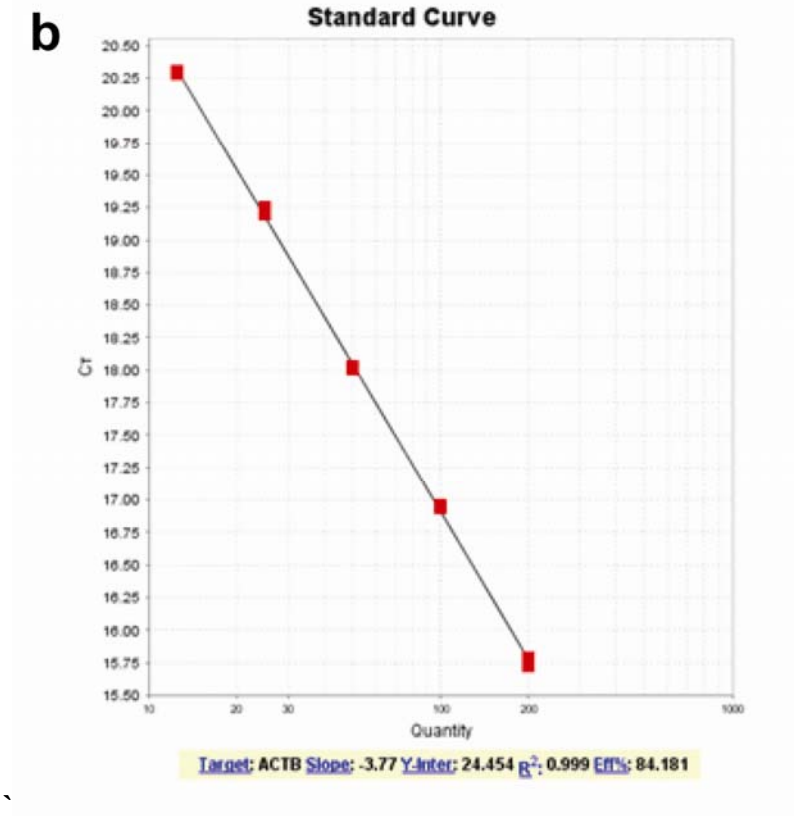
b
Standard Curve
Ct
Quantity
Target: ACTB Slope: -3.77 Y-Inter: 24.454 R2: 0.999 Eff%: 84.181

Figure 4.2 RT-qPCR assay validation.

Standard curves for (a) Mstn, and (b) ACTB RT-qPCR assays. Gradients, y-intercept, PCR efficiency and R^2 values are indicated.

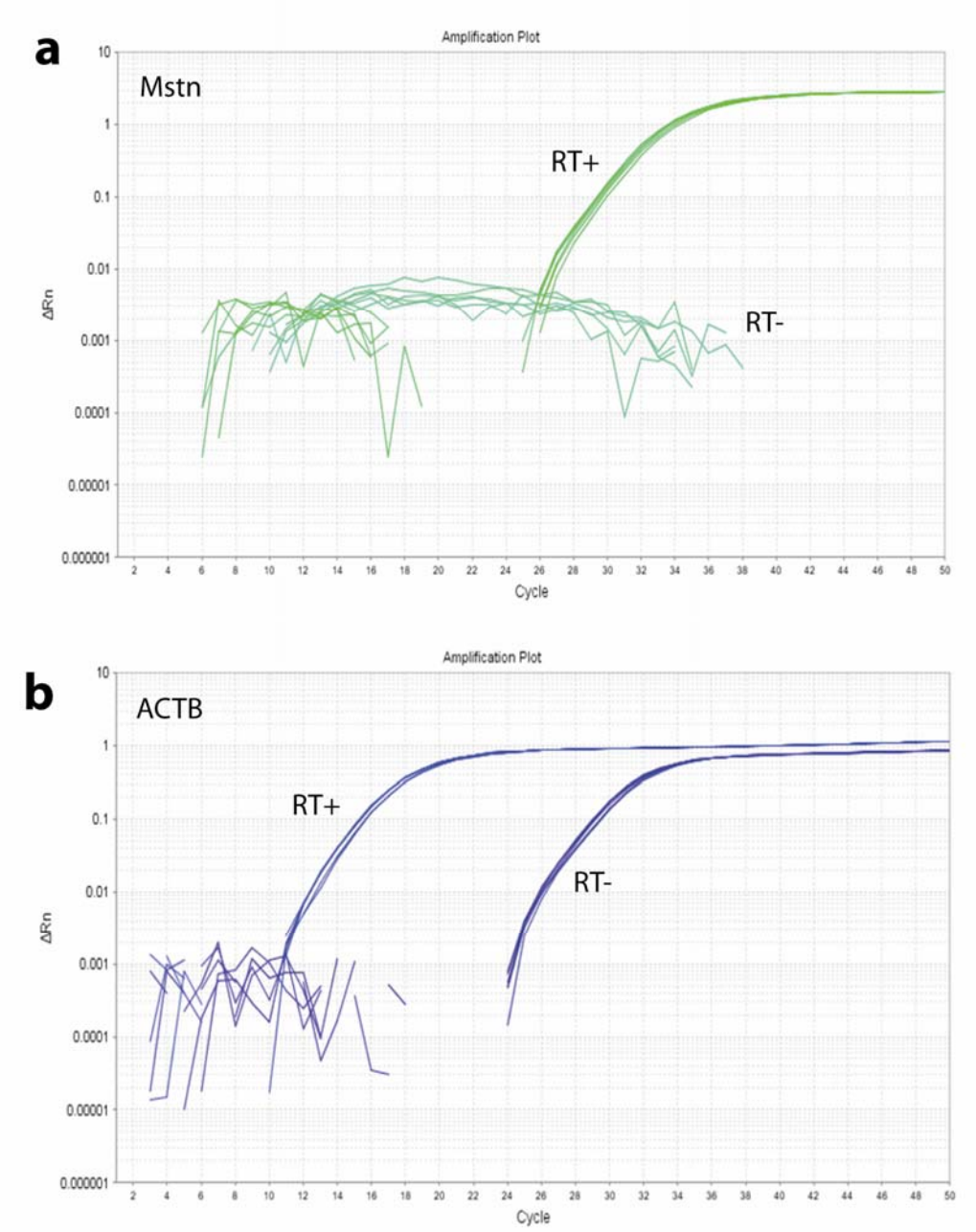

Figure 4.3 Reverse transcriptase minus controls for Mstn and ACTB RT-qPCR assays. RT+ and RT- samples for (a) Mstn and (b) ACTB RT-qPCR assays.

4.2.3 Promoter-Targeting siRNAs Induce Transcriptional Silencing of Myostatin

Four siRNAs targeting the myostatin sense promoter-associated RNA (**Fig. 4.4a**) were synthesised by *in vitro* transcription, transfected into differentiated C2C12 myotube (MT) cultures and myostatin expression assessed by RT-qPCR. An mRNA-targeting siRNA that induces post-transcriptional gene silencing of myostatin was used as a positive control (PTGS control). One siRNA, siMstn-P2, was found to significantly reduce myostatin mRNA levels by 50% (**Fig. 4.4b**). This level of silencing was observed in at least 20 independent transfections under similar conditions (i.e. 100 nM siRNA in differentiated myotube cultures) and found to be highly reproducible (mean knockdown = 48%, SD = 11.5%).

Reduction in myostatin expression was observed relative to two unrelated non-specific control siRNAs (including an *in vitro* transcribed siRNA (siCCR5) which targets the human C-C chemokine receptor type 5) (**Fig. 4.5a**). In addition, transfection with two further control siRNAs; one with the siMstn-P2 sequence scrambled (siScrambled) and the other with the central four nucleotides of siMstn-P2 inverted (siMM), did not significantly reduce myostatin expression (**Fig. 4.5b**). Negligible batch-to-batch variation was observed between different siRNA preparations (**Fig. 4.5c**) and no significant cellular toxicity was observed between any of the siRNA treatments (**Fig. 4.5d**). Myostatin silencing was further confirmed using a chemically synthesised siMstn-P2 (**Fig. 4.6a**). Additionally, promoter-targeted silencing was dose-dependent although significant myostatin knockdown was only observed at siRNA concentrations of 50 nM

and 100 nM (**Fig. 4.6b**). Conversely, maximal silencing by the PTGS control siRNA was observed at 10 nM (data not shown).

Previous studies have suggested that delivery of siRNA to the nucleus is essential to induce TGS and that nuclear targeting peptides were required to facilitate this delivery. [168,169,180]. However, in this study silencing was observed with both conventional, commercially available transfection reagents (INTERFERin and RNAiMax) and with a stearylated transportan-10 derived peptide (PepFect14) that had previously been shown to effectively deliver splice-switching oligonucleotides to the nucleus [359] (**Fig. 4.6c**). Statistically significant knockdown of myostatin was also observed in H2K *mdx* cells (a murine myoblast cell line that carries a mutation in dystrophin exon 23 [331]) indicating that the silencing effect is not restricted to the C2C12 line (**Fig. 4.6d**). Taken together, these data suggest that myostatin is susceptible to siRNA-directed TGS.

Given that TGS and PTGS occur via different mechanisms, we hypothesised that co-transfection of TGS and PTGS siRNAs would act in a combinatorial manner to improve maximal myostatin gene silencing. Transfection of a combination of 50 nM siMstn-P2 and 50 nM PTGS control siRNA was compared against 100 nM of each individual siRNA or a non-specific control siRNA. The combination of the two siRNAs gave the greatest knockdown (87%) (**Fig. 4.6e**).

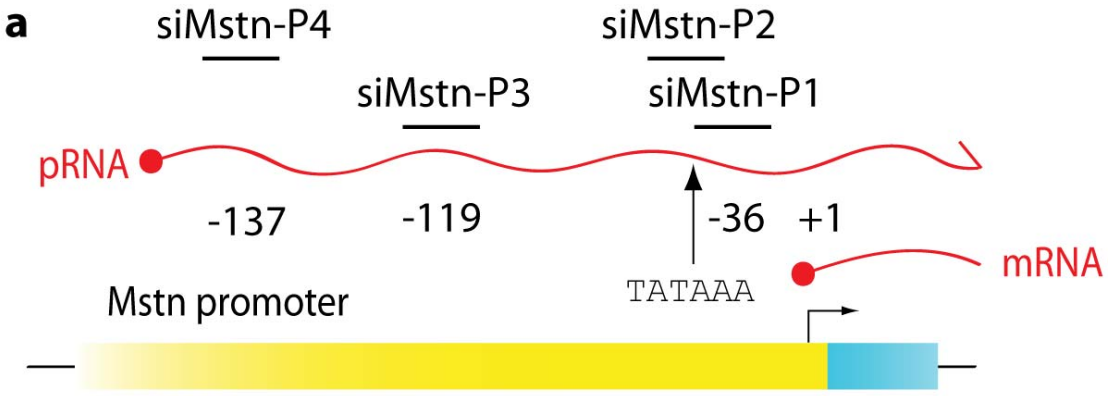
a
siMstn-P4
siMstn-P2
siMstn-P3
siMstn-P1
pRNA
-137
-119
-36
+1
mRNA
TATAAA
Mstn promoter

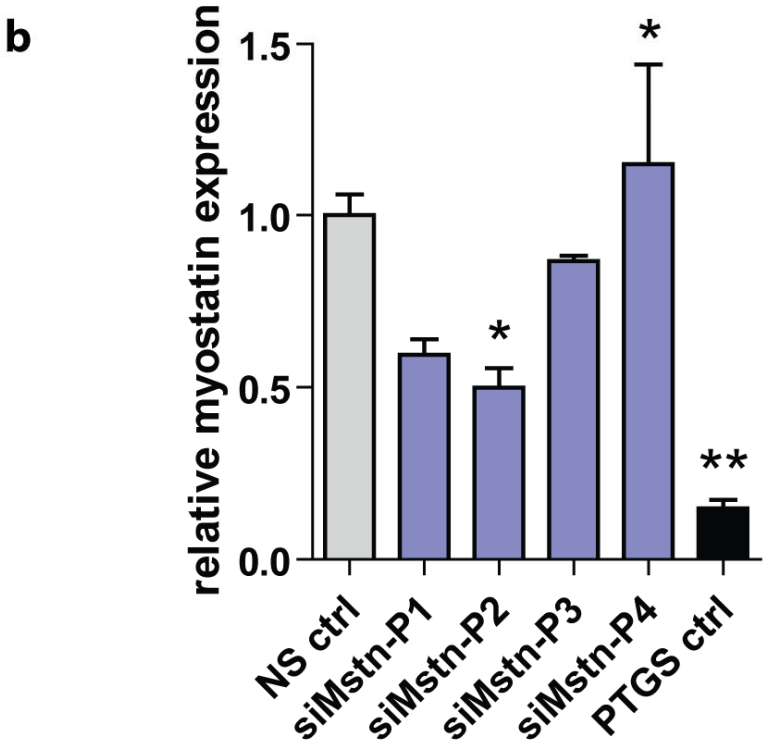
b
relative myostatin expression
1.5
1.0
0.5
0.0
*
*
**
NS ctrl
siMstn-P1
siMstn-P2
siMstn-P3
siMstn-P4
PTGS ctrl

Figure 4.4 Screen of myostatin promoter-targeting siRNAs.

Schematic of myostatin promoter showing annotated transcription start site and hypothetical promoter-associated RNA transcript (pRNA). Position of TATA box and siRNA target sites are indicated. (b) Promoter-targeting siRNAs (blue bars) were transfected in differentiated C2C12 myotubes and myostatin expression assessed by RT-qPCR. Results were normalised to a non-targeting control siRNA (NS ctrl, grey bar) and a coding sequence-targeting siRNA that silences myostatin by post-transcriptional gene silencing (PTGS ctrl, black bar) was used as a positive control for transfection. Values are mean + SEM, n=3, * $p<0.05$, ** $p<0.01$.

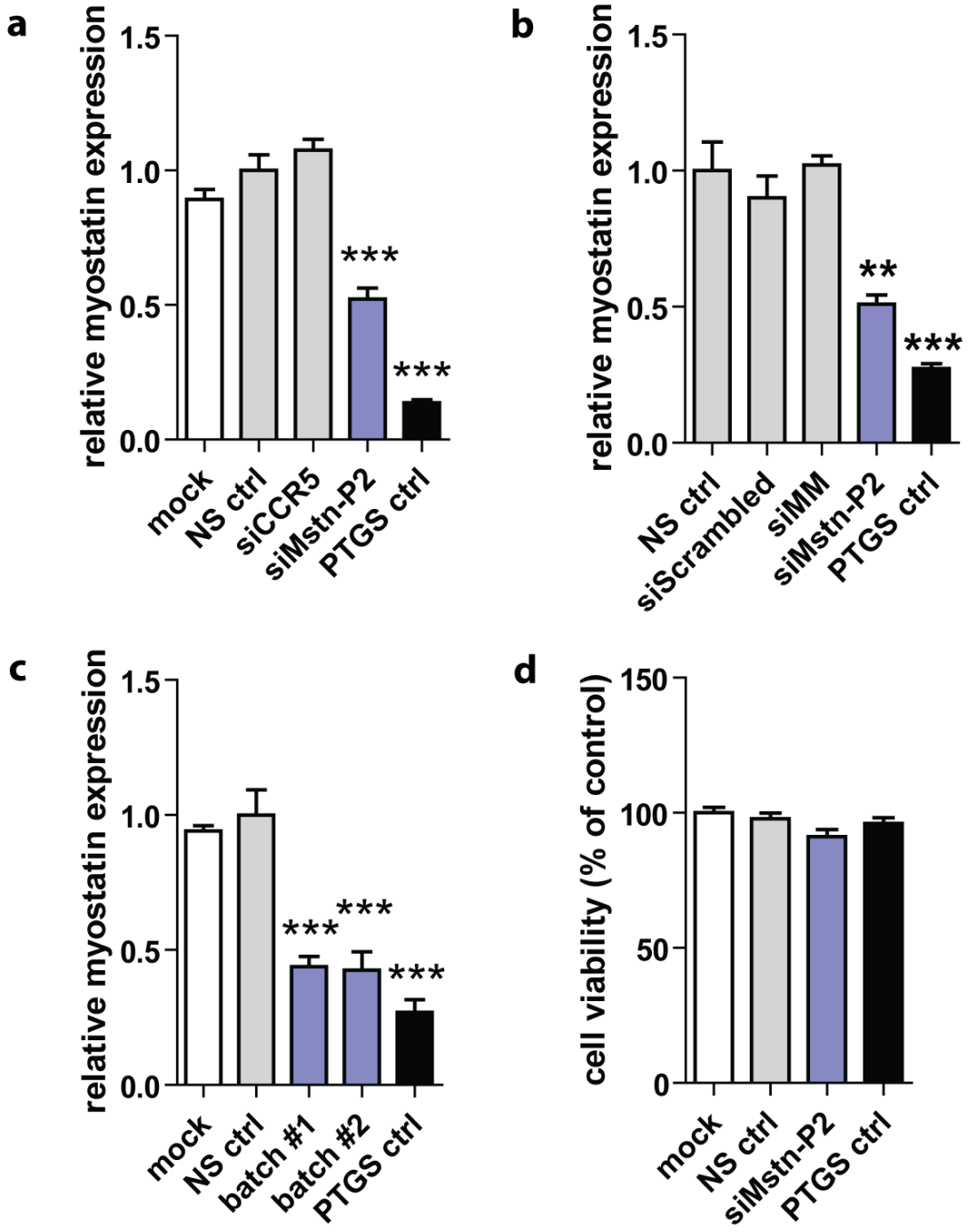
a
relative myostatin expression
1.5
1.0
0.5
0.0
***
***
mock
NS ctrl
siCCR5
siMstn-P2
PTGS ctrl
b
relative myostatin expression
1.5
1.0
0.5
0.0
**
***
NS ctrl
siScrambled
siMM
siMstn-P2
PTGS ctrl
c
relative myostatin expression
1.5
1.0
0.5
0.0
***
***
***
mock
NS ctrl
batch #1
batch #2
PTGS ctrl
d
cell viability (% of control)
150
100
50
0
mock
NS ctrl
siMstn-P2
PTGS ctrl

Figure 4.5 Validation of specific myostatin silencing.

(a) siMstn-P2 knocks down myostatin expression relative to two non-specific siRNA controls; NS ctrl (Eurogentec) and siCCR5 (produced by *in vitro* transcription). There is no significant difference between control siRNA and mock (transfection reagent only) control. (b) siMstn-P2 knocks down myostatin expression relative to a scrambled siMstn-P2 sequence control (siScrambled) and an additional control using the siMstn-P2 sequence with the central four nucleotides inverted (siMM). (c) Comparison of two separate batches of siMstn-P2 produced by *in vitro* transcription on separate days with different siRNA yields. (d) Toxicity of siRNA treatments was assessed by MTS assay. No significant differences were observed between any treatment groups. Values are mean + SEM n=3 for (a) and (b) and n=6 for (c), ** $p<0.01$ *** $p<0.001$.

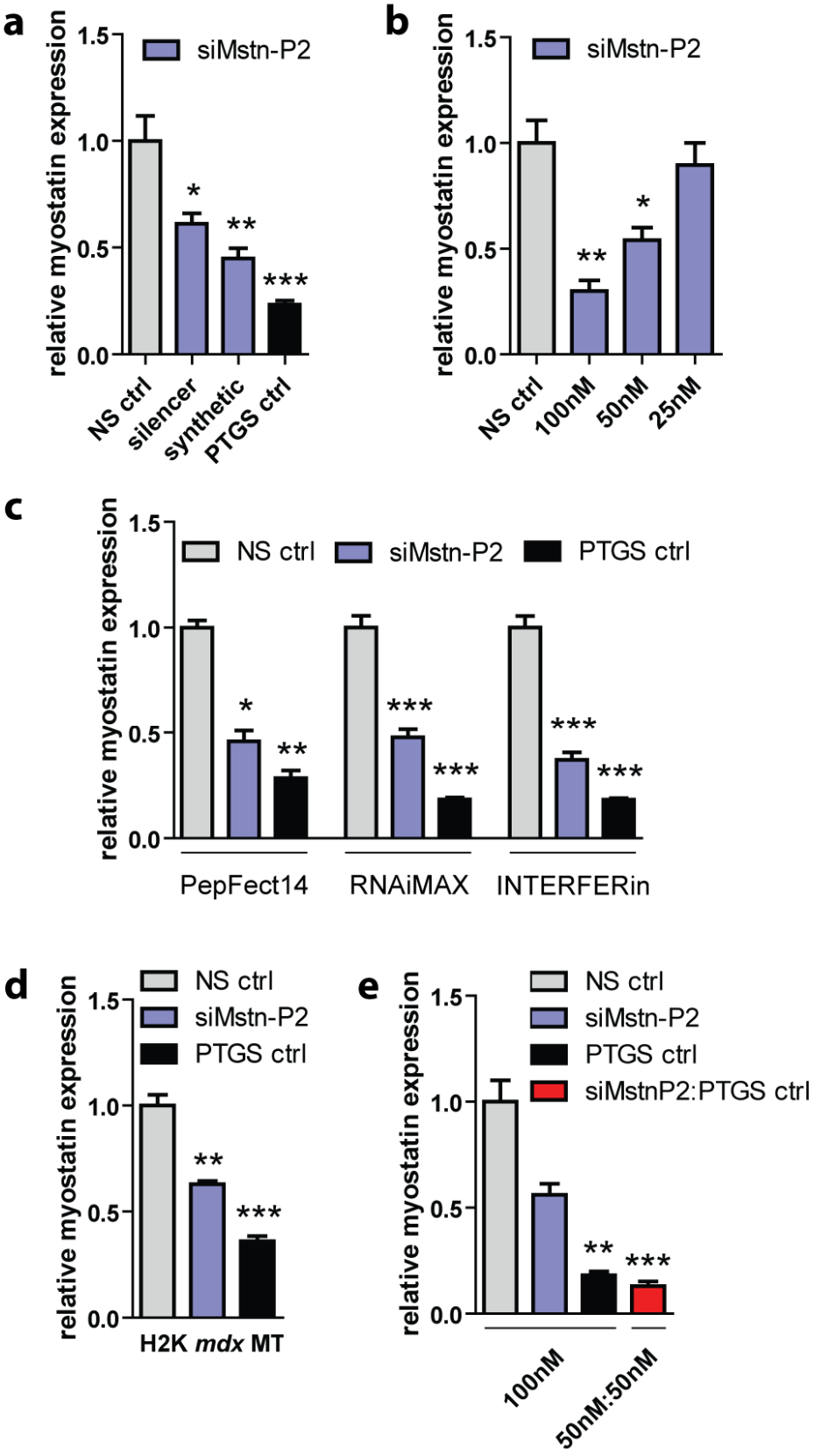
a
relative myostatin expression
1.5
1.0
0.5
0.0
siMstn-P2
*
**
***
NS ctrl
silencer
synthetic
PTGS ctrl
b
relative myostatin expression
1.5
1.0
0.5
0.0
siMstn-P2
**
*
NS ctrl
100nM
50nM
25nM
c
relative myostatin expression
1.5
1.0
0.5
0.0
NS ctrl
siMstn-P2
PTGS ctrl
*
**
***
***
***
***
PepFect14
RNAiMAX
INTERFERin
d
relative myostatin expression
1.5
1.0
0.5
0.0
NS ctrl
siMstn-P2
PTGS ctrl
**
***
H2K mdx MT
e
relative myostatin expression
1.5
1.0
0.5
0.0
NS ctrl
siMstn-P2
PTGS ctrl
siMstnP2:PTGS ctrl
**
***
100nM
50nM:50nM

Figure 4.6 Promoter-targeting siRNAs silence myostatin expression.

(a) C2C12 MT cultures were transfected with *in vitro* transcribed (silencer) and chemically synthesised (synthetic) promoter-targeting siRNAs (siMstn-P2). (b) Dose response of siMstn-P2 over the range of 25-100 nM, (c) H2K *mdx* MT were transfected with siMstn-P2. (d) Similar results are obtained in C2C12 MT cultures independent of transfection reagent used. (e) Transfection of a mixture of 50 nM siMstn-P2 and 50 nM PTGS control results in higher levels of silencing than either siRNA alone at 100 nM. All values are mean + SEM, n=3, * $p<0.05$, ** $p<0.01$, ***$p<0.001$.

4.2.4 Determination of Strand Selection Asymmetry

All siRNAs were designed so as to bias strand selection towards the guide strand by incorporating a mismatched nucleotide into the passenger strand and thermodynamically destabilising the 5′ end of the guide strand [360,361]. This method has been used to maximise siRNA potency. Similarly, asymmetric strand selection is involved in miRNA processing and miRNAs have been shown to be associated with the various human argonautes equally [362], which suggests that the rules that apply to RISC loading in post-transcriptional gene silencing are likely also applicable to RITS loading in transcriptional gene silencing. In order to assess asymmetric strand selection, the target sites complementary to the guide and passenger strands of siMstn-P2 were cloned downstream of the Renilla luciferase (RLuc) transgene in the psiCheck2.2 vector (which also carries a firefly luciferase transgene (Luc)). The luciferase constructs were then co-transfected with siMstn-P2 in HEK293 cells and RLuc activity measured (normalised to Luc expression) (**Fig. 4.7a**). siMstn-P2 was found to down-regulate the sense target of the guide strand by 81% whereas the antisense target of the passenger strand was down-regulated by only 25% (not statistically significant) (**Fig. 4.7b**). These results indicate that siMstn-P2 is capable of post-transcriptional silencing and that the mismatch included in the design of the siRNA successfully biases strand selection towards the guide strand. Strand selection bias is important for minimising off-target effects, particularly in the case of targeting promoters as a passenger strand may interact with transpromoter natural antisense transcripts thereby directing off-target transcriptional gene activation [234,363].

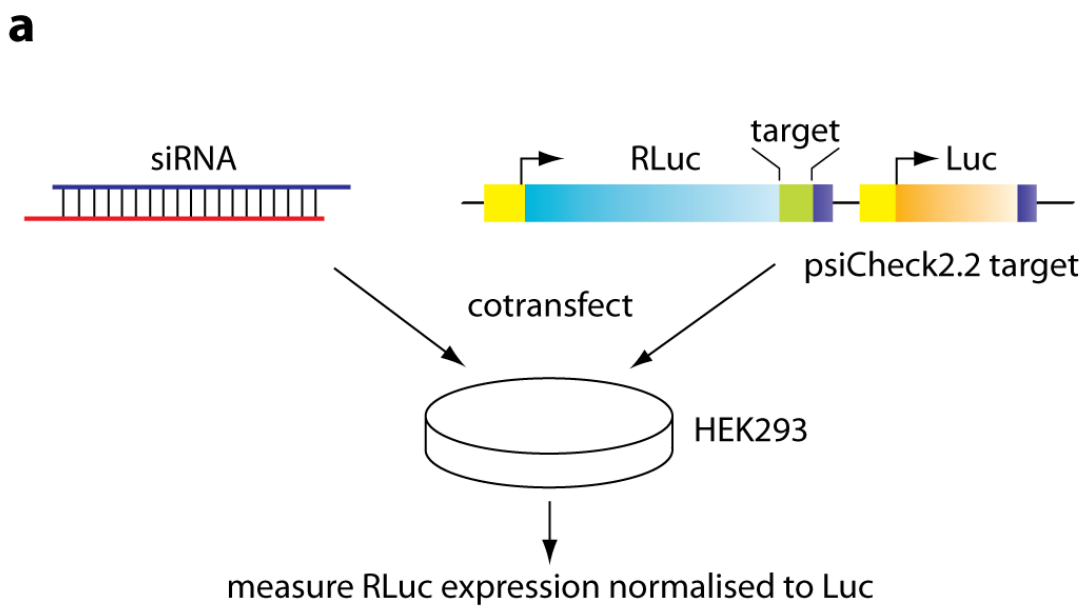
a
siRNA
target
RLuc
Luc
psiCheck2.2 target
cotransfect
HEK293
measure RLuc expression normalised to Luc

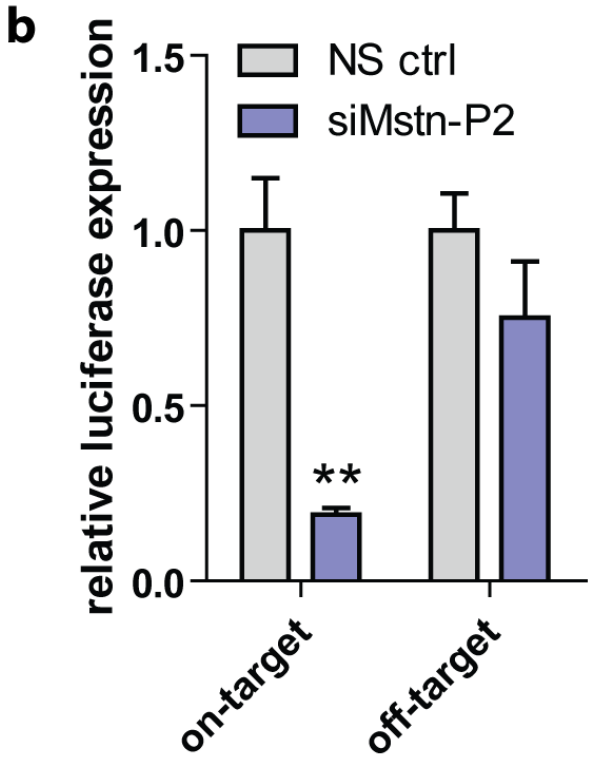
b
relative luciferase expression
1.5
1.0
0.5
0.0
NS ctrl
siMstn-P2
**
on-target
off-target

Figure 4.7 The antisense strand of siMstn-P2 is preferentially loaded into RISC.

(a) Diagram of experimental design. Sense (on-target) and antisense (off-target) target sequences were cloned into the 3′ untranslated region of psiCheck2.2. These constructs were separately cotransfected with siMstn-P2 or non-specific control siRNA in HEK293 cells and renilla and firefly luciferase activities measured 24 hours later. (b) Relative luciferase expression for transfections with the on-target and off-target constructs. Values are mean + SEM, n=3, **p<0.01.

4.2.5 Myostatin Silencing is Independent of Interferon Induction

In contrast with chemically synthesised siRNA molecules, small RNAs generated by *in vitro* transcription from T7 promoters are tri-phosphorylated at the 5′ terminus and therefore have the potential to induce non-specific knockdown by activating the interferon response [269]. In order to investigate this possibility, C2C12 myotube cultures were transfected with all relevant siRNAs. After 48 hours total RNA samples were reverse transcribed and levels of the interferon-induced genes 2′,5′ oligoadenylate synthase 1b (Oas1b) and interleukin-6 (Il-6) by RT-qPCR. Treatment with 15 μg/ml lipopolysaccharide (LPS) was used as a positive control for interferon induction. Statistically significant induction of Oas1b and Il-6 was observed with the *in vitro* transcribed siRNAs (siMstn-P2 and siCCR5) but not with chemically synthesised siRNAs (**Fig. 4.8a,b**). The stability of the reference gene transcript (β-Actin) was unaffected by transfection with *in vitro* transcribed siRNAs (**Fig. 4.8c**). These results indicate that *in vitro* transcribed Silencer^{TM} constructed siRNAs induce expression of interferon-stimulated genes whereas chemically synthesised siRNAs do not.

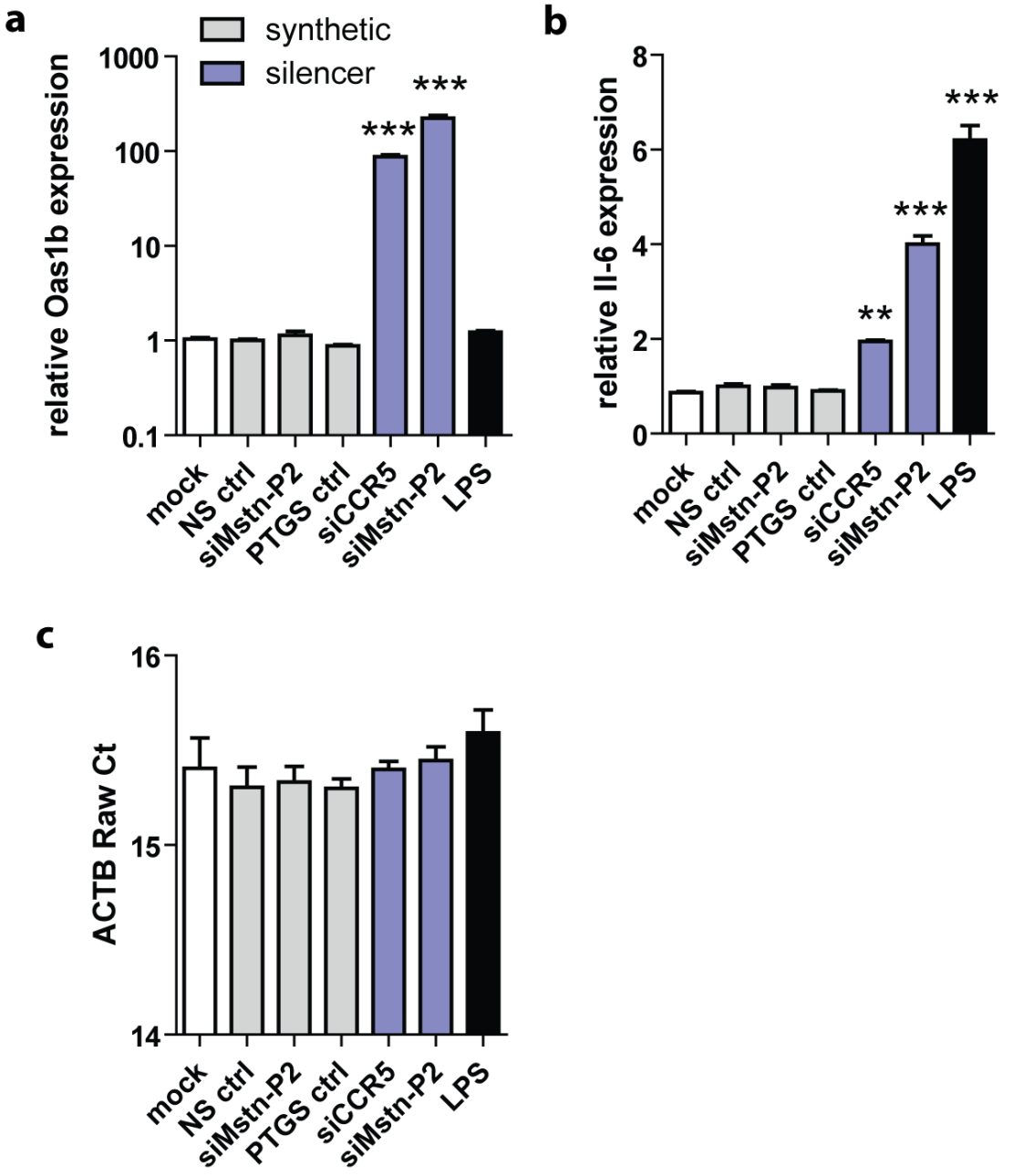
a
synthetic
silencer
relative Oas1b expression
1000
100
10
1
0.1
***
***
mock
NS ctrl
siMstn-P2
PTGS ctrl
siCCR5
siMstn-P2
LPS
b
relative Il-6 expression
8
6
4
2
0
**
***
***
mock
NS ctrl
siMstn-P2
PTGS ctrl
siCCR5
siMstn-P2
LPS
c
ACTB Raw Ct
16
15
14
mock
NS ctrl
siMstn-P2
PTGS ctrl
siCCR5
siMstn-P2
LPS

Figure 4.8 Myostatin silencing is independent of interferon induction.

Treatment of C2C12 MT cultures with *in vitro* transcribed, Silencer^{TM} siRNAs (blue bars), induces expression of (a) Oas1b and (b) Il-6, whereas chemically synthesised siRNAs (grey bars) do not. Values are mean + SEM, n=3, **p<0.01, ***p<0.001. (c) Raw cycle threshold (Ct) values for β-Actin (ACTB) for the experiment depicted in (a) and (b) indicating high reference gene stability. Values are mean Ct + SD, n=3. LPS, lipopolysaccharide.

4.2.6 Myostatin Silencing is Sensitive to Dexamethasone

Dexamethasone has previously been shown to induce expression of myostatin via a glucocorticoid receptor-mediated mechanism [364]. We confirmed this result in differentiated C2C12 myotubes, however, dexamethasone did not induce myostatin expression in undifferentiated C2C12 myoblasts (**Fig. 4.9a**). As dexamethasone treatment induces transcriptional activation of myostatin we hypothesised that this effect would antagonise silencing by a promoter-targeting siRNA. Pre-treatment of C2C12 cultures with dexamethasone for 1 week pre-transfection resulted in abrogation of silencing by siMstn-P2 relative to cultures that were not dexamethasone treated (**Fig. 4.9b**). The positive control PTGS siRNA was unaffected by dexamethasone treatment. Taken together these data suggest that myostatin silencing by the promoter-targeting siRNA occurs at the level of transcription and operates by a mechanism distinct from conventional RNA interference.

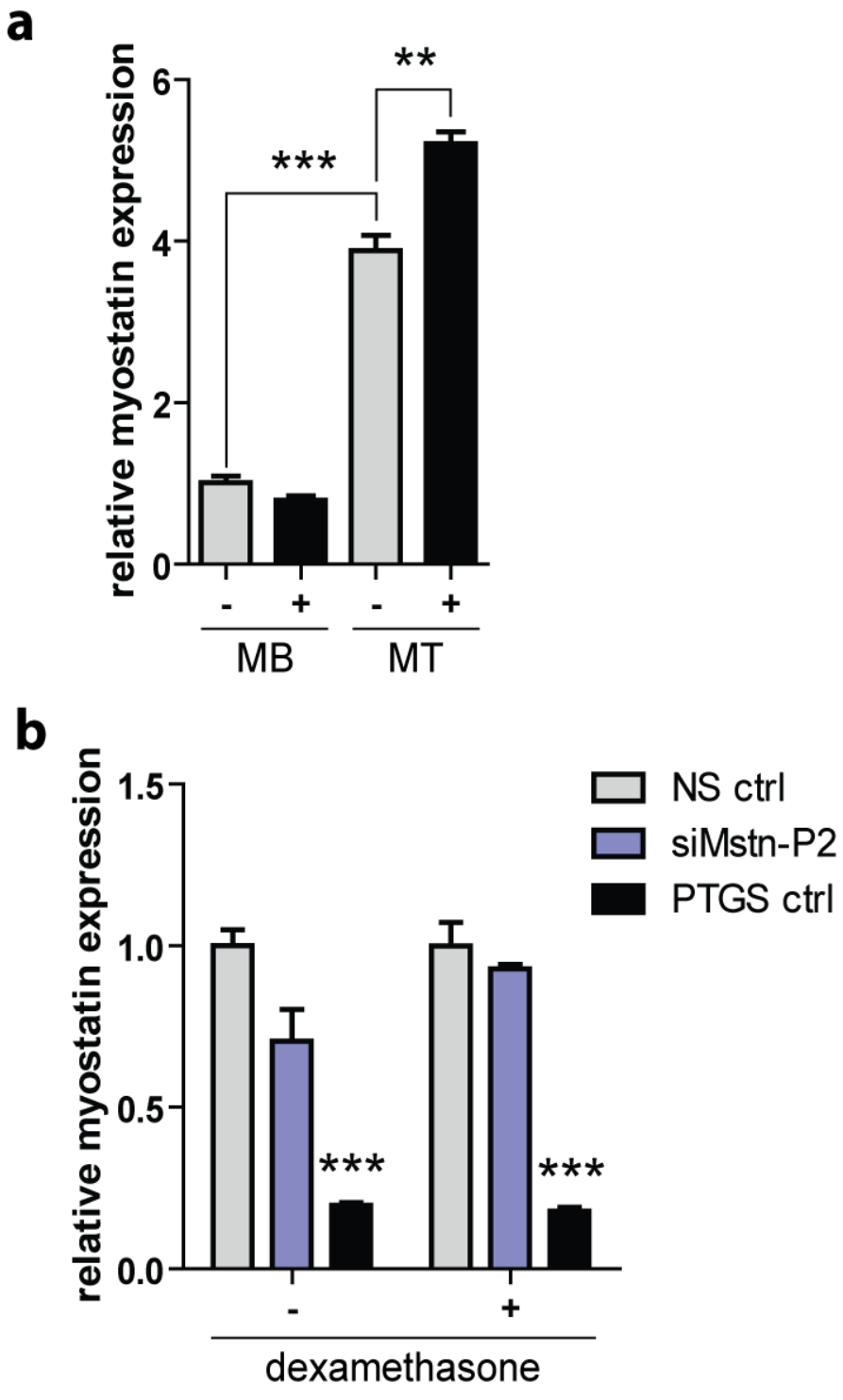
a
relative myostatin expression
6
4
2
0
**
***
-
+
-
+
MB
MT
b
relative myostatin expression
1.5
1.0
0.5
0.0
NS ctrl
siMstn-P2
PTGS ctrl
***
***
-
+
dexamethasone

Figure 4.9 Myostatin silencing: sensitivity to dexamethasone treatment.

(a) C2C12 MB and MT cultures were treated with dexamethasone for 24 hours or 7 days respectively and myostatin expression measured by RT-qPCR. (b) Effect of dexamethasone treatment on silencing by siMstn-P2 in C2C12 MT. All values are mean + SEM, n=3, **p<0.01, ***p<0.001, + = 100 nM. MB, myoblasts. MT, myotubes.

4.2.7 Epigenetic Myostatin Silencing

Acetylation of Histone H3 lysine residues 9 and 27 is associated with transcriptionally active chromatin. Consequently, deacetylation of these residues is a necessary first step in the process of silent state chromatin formation. In order to determine whether siMstn-P2 induces epigenetic gene silencing, transfections were performed in the presence of the histone deacetylase (HDAC) inhibitor trichostatin A (TSA). siRNA transfected cultures were treated with a range of TSA concentrations (50 nM to 5 μM) and for each experimental condition myostatin expression was normalised to the non-specific control. Silencing by siMstn-P2 was found to be sensitive to TSA concentrations above 500 nM whereas silencing by the PTGS control siRNA was largely unaffected (**Fig. 4.10a**). Treatment with TSA was found to activate basal myostatin expression at low concentrations and was toxic at high concentrations, which is consistent with other reports [362] (**Fig. 4.10b,c**). The observation that myostatin silencing by siMstn-P2 was abrogated by treatment with TSA at concentrations that activate myostatin expression in one case (500 nM) and are highly toxic in another (5 μM) is evidence that these factors are not confounding the results.

To investigate whether changes in chromatin structure are involved in myostatin silencing we performed chromatin immunoprecipitation analysis (ChIP) using antibodies against the silent state histone modifications; dimethyl-Histone H3 lysine9 (H3K9me2) and trimethyl-Histone H3 lysine27 (H3K27me3). Enrichment of H3K9me2 was detected at the myostatin promoter following treatment with siMstn-P2 although no change in H3K27me3 was detected (**Fig. 4.10d**). Sensitivity of silencing to TSA treatment and

changes in H3K9 methylation suggest that epigenetic remodelling at the myostatin promoter underlies the observed silencing effect. ChIP qPCR primers were validated by amplifying serial dilution of input chromatin DNA to perform a standard curve (**Fig. 4.11a**) and dissociation curve analysis confirmed that only a single amplification product was generated by the PCR reaction (**Fig. 4.11b**).

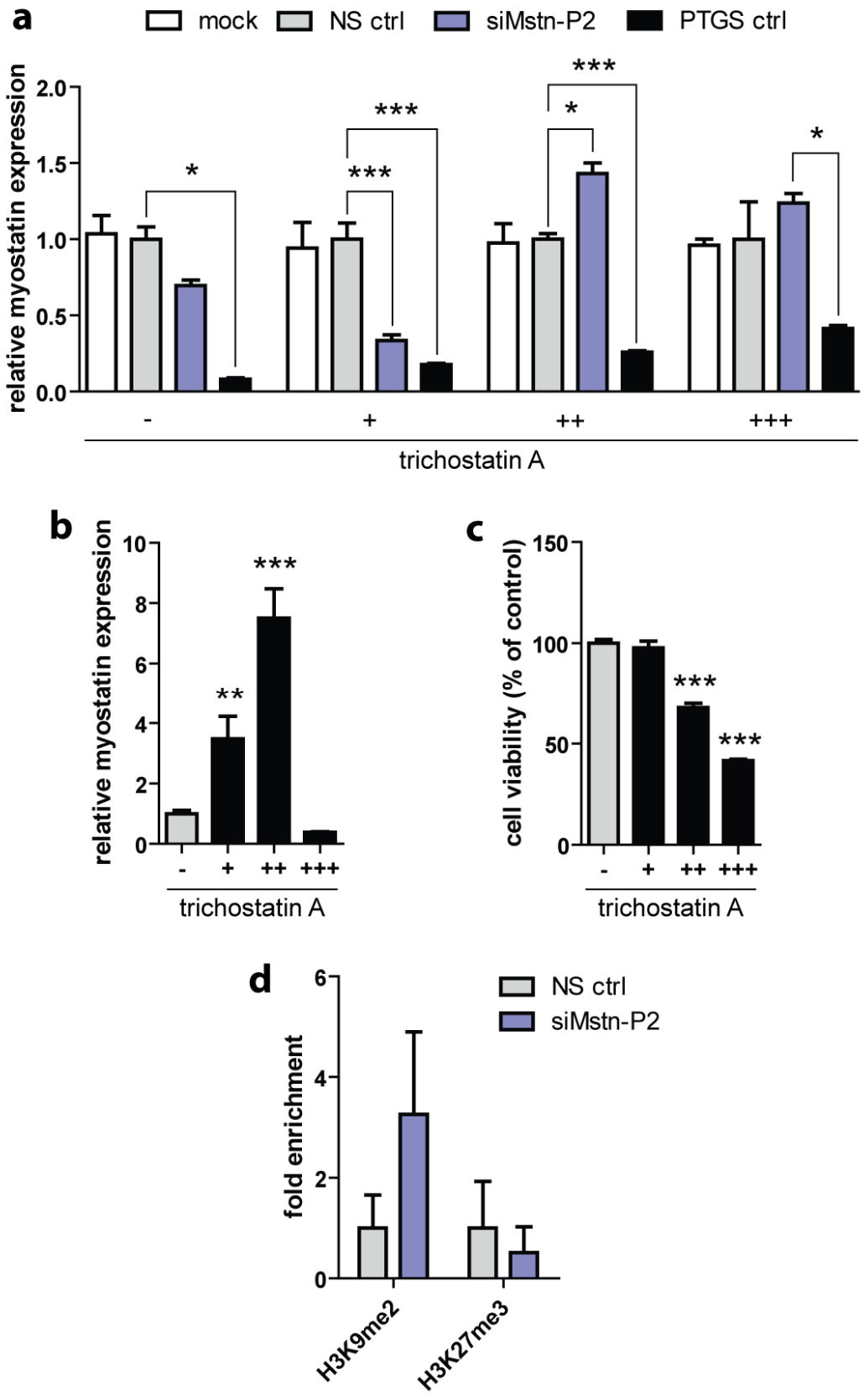
a
mock
NS ctrl
siMstn-P2
PTGS ctrl
relative myostatin expression
2.0
1.5
1.0
0.5
0.0
*
***
***
*
***
*
-
+
++
+++
trichostatin A
b
relative myostatin expression
10
8
6
4
2
0
**
***
-
+
++
+++
trichostatin A
c
cell viability (% of control)
150
100
50
0
***
***
-
+
++
+++
trichostatin A
d
NS ctrl
siMstn-P2
fold enrichment
6
4
2
0
H3K9me2
H3K27me3

Figure 4.10 Epigenetic effects are involved in myostatin transcriptional gene silencing. (a) C2C12 MTs were transfected with siRNAs in the presence or absence of trichostatin A and myostatin expression measured by RT-qPCR. Effects of increasing trichostatin A concentration on (b) basal myostatin transcription as measured by RT-qPCR and (c) cell viability as measured by MTS assay. (d) Chromatin immunoprecipitation with antibodies against H3K9me2 and H3K27me3 of C2C12 MT cultures transfected with siMstn-P2 or non-specific control siRNA. All values are mean + SEM, n=3 for (a),(b) and (d) and n=6 for (c). *$p<0.05$, **$p<0.01$, ***$p<0.001$. + = 50 nM, ++ = 500 nM, +++ = 5 μM.

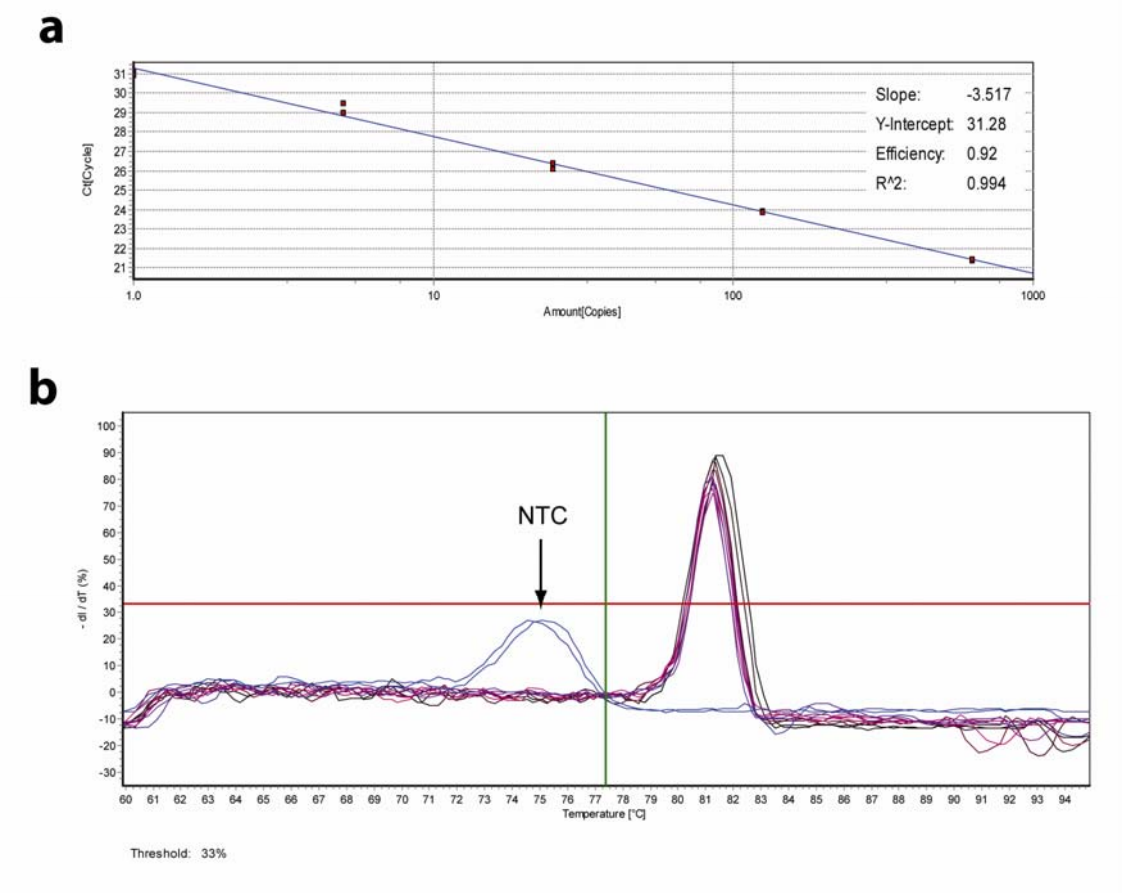

Figure 4.11 Validation of qPCR for chromatin immunoprecipitation analysis.

(a) Standard curve and (b) melt curve analysis for myostatin promoter ChIP qPCR assay. NTC, no template control.

4.3 Discussion

This study has demonstrated that siRNAs complementary to the myostatin promoter induce silencing of myostatin mRNA expression. Promoter-associated RNAs were detected at the myostatin locus and the sense-orientation transcript is the predicted target for the siRNA (although we have not shown a direct association between these two RNA species). Silencing was abrogated by treatment with the histone deacetylase inhibitor, TSA. Conversely, the PTGS control siRNA, which silences myostatin by acting upon the mature mRNA, was unaffected by TSA treatment. These results suggest that silencing with a promoter-targeting siRNA occurs by a different gene silencing pathway from conventional RNA interference. The results are consistent with other studies of TGS although we have not shown direct evidence of silencing at the level of transcription.

Interestingly, the combination of TGS and PTGS siRNAs resulted in higher levels of silencing than either strategy alone suggesting that the two silencing pathways can operate in a complementary manner. We and others have shown that, following transient transfection of TGS effectors, target genes are typically silenced by ~50% which is considerably less than with conventional RNAi. However, the level of silencing is expected to increase over time as the chromatin at the target locus becomes progressively more compacted and the promoter DNA methylated. These silencing kinetics were observed in studies that looked at long-term knockdown by TGS [170,172,183]. However, in the case of myostatin, even relatively low levels of silencing (27% protein reduction) have been shown to result in significant functional changes in muscle mass (10% increase) suggesting that high levels of silencing are not required for a

therapeutically relevant effect [355]. The demonstration of protein level silencing will be required to advance TGS as a therapy although, in this study, we were unable to consistently detect myostatin protein in cultured cells by western blot.

Several of the early studies to report TGS in mammalian cells utilised siRNAs produced by *in vitro* transcription [168,169,180]. siRNAs produced in this manner have the potential to elicit off-target gene silencing via induction of the interferon response [269]. These non-specific events are either due to a gene being directly regulated by interferons, or as a result of global mRNA down-regulation, following activation of RNase L. We investigated this phenomenon by measuring expression of two interferon-induced genes (Oas1b and Il-6) following siRNA transfections in order to ensure specific myostatin silencing by siMstn-P2. We have shown that *in vitro* transcribed siRNAs induce highly statistically significant increases in expression of interferon-stimulated genes. However, the findings that; (1) silencing is observed with a synthetic siMstn-P2 in the absence of induction of the interferon-stimulated genes, (2) silencing occurs relative to an *in vitro* transcribed control siRNA (siCCR5) and (3) the stability of the housekeeping transcript (β-Actin) is unaffected by transfection with *in vitro* transcribed siRNAs, suggests that myostatin silencing is not the result of off-target silencing due to interferon induction and activation of RNase L, but is rather a target-specific silencing effect.

Treatment of cultures with dexamethasone abrogated the effects of promoter-targeting siRNAs suggesting that silencing occurs at the level of transcription. As expected, the PTGS control siRNA was unaffected by dexamethasone treatment. Given that the

majority of DMD sufferers receive corticosteroid treatments this may limit the effectiveness of a TGS approach to silencing myostatin in patients.

Promoter-specific silencing was reversed in the presence of the HDAC inhibitor, TSA, consistent with previous studies that have shown that HDAC1 is required for TGS [170,183]. Similarly, we have detected a modest enrichment of the silent state chromatin modification, H3K9me2, following transfection with a myostatin promoter-targeting siRNA as reported previously [169,170,172,180,183]. These results are indicative of an epigenetic silencing process. Interestingly, enrichment of H3K27me3 was not detected. Hawkins *et al.* have shown by RNAi depletion experiments that Enhancer of zeste homologue 2 (EZH2), a histone methyltransferase that methylates histone H3 lysine27, is not essential for TGS. This suggests that epigenetic silencing can occur in the absence of H3K27 methylation and that there is a degree of redundancy between silent state histone modifications [170].

The detection of a promoter transcript involved in epigenetic regulation of the myostatin locus suggests that this may constitute part of an endogenous mechanism of gene regulation. Several studies have identified endogenous small RNAs (microRNAs) with complementarity to target gene promoters that induce TGS [322,220,221]. Long antisense RNAs have also been linked to epigenetic control of gene expression [249,363] and have been found to bind chromatin-remodelling factors [365]. Recently, a long non-coding RNA (lncRNA) has also been implicated in myogenesis by acting as a competitive

inhibitor for microRNAs involved in muscle differentiation [297]. However, the role of lncRNAs, microRNAs and pRNAs in epigenetic silencing is still not well understood.

This study adds to the growing literature that suggests small RNAs can direct TGS in mammalian cells and confirms that TGS occurs in mouse cells consistent with previous reports [205]. Several studies have demonstrated TGS in the absence of epigenetic changes, so-called antigene TGS [227,233]. These studies generally utilise oligonucleotides targeting transcriptional start sites and are speculated to involve direct interaction between the oligonucleotide and chromosomal DNA. Our data are more consistent with studies which have found a role for epigenetic changes involved in silencing and therefore lend credence to the idea that there are at least two distinct TGS mechanisms (epigenetic-TGS and antigene-TGS).

The use of TGS in animal models has so far been limited to three studies. Turunen *et al.* demonstrated that TGS of vascular endothelial growth factor (*Vegfa*) is possible in mouse muscle following lentiviral transduction [205]. Similarly, local injection of promoter-targeting siRNAs against the human papillomavirus (HPV) E6/E7 and thioredoxin-interacting protein (*Txnip*) promoters results in TGS in mouse xenograft tumors [280] and rat retina [206] respectively. Although these studies are highly promising, the general application of TGS *in vivo* has not yet been fully explored and may present its own unique obstacles. For instance, the relative abundance of promoter transcripts is likely to differ between cell culture models and live animals and may affect the efficacy of a TGS approach. Despite the paucity of *in vivo* studies the therapeutic application of TGS is a

promising alternative to RNAi, which is dependent on the presence of RNAi effectors that are gradually degraded within the cell or dispersed between daughter cells following cell division (effectively halving their concentration). Repeat administration is therefore required to elicit long-term silencing by siRNAs. Conversely, TGS effectors induce long-term silencing that is inherited following cell division and maintenance of silencing is not dependent on the presence of effector molecules [170]. A single treatment (or short course of treatments) may be sufficient to induce long-term gene silencing, hence repeat administration of TGS effectors is not required [170,171]. Consequently, TGS based therapies may require a small number of high doses to elicit an effect. The overall dose will thus be lower with TGS-based therapies as opposed to conventional RNAi, meaning lower toxicity of treatments and greatly reduced material costs. In addition, it has been shown that saturation of endogenous RNA processing pathways can lead to acute toxicity *in vivo* [366]. As TGS does not require repeat administration this risk is greatly reduced. Epigenetic silencing of myostatin by TGS is therefore a promising novel therapeutic strategy in the treatment of muscle wasting disorders.

5 Discussion

5.1 Summary of Results

The work presented in this thesis has explored aspects of small RNA biology in the context of DMD pathophysiology and therapeutics. Small RNAs are regulators of gene expression and, as such, they modulate the gene networks underlying cellular pathologies and can potentially be exploited as novel therapeutics. Firstly, we have performed the most thorough investigation of differential miRNA expression in the *mdx* mouse to date which improves upon previous studies. Through the use of high density miRNA microarray technology we have been able to detect differentially expressed miRNAs that were not identified previously. Similarly, we have provided evidence that some of the conflicting results reported in previous studies are due to inter-muscle variations and differences in methodology. Our results have confirmed that miR-31 is highly expressed in all *mdx* skeletal muscles investigated, which bodes well for anti-miR-31 therapeutics. We have also observed a stark contrast in the miRNA expression profiles of *mdx* muscles and serum which is evidence against the passive release of miRNAs as a result of muscle damage. Consistent with previous reports, we have shown that the dystromirs miR-1, miR-133a and miR-206 are highly abundant in the serum of *mdx* mice. Furthermore, this study is the first to demonstrate that effective peptide-PMO conjugate-mediated dystrophin exon-skipping results in partial normalisation of circulating dystromir abundance, suggesting that they are promising non-invasive disease biomarkers. This work has also explored a novel therapeutic approach to the treatment of muscle wasting disorders such as DMD. We have shown that an siRNA complementary to the myostatin

promoter induces silencing of myostatin expression in C2C12 and H2K *mdx* myotubes. We have demonstrated the reproducibility, specificity and dose dependence of this silencing effect. We have also investigated, and ruled out, off-target silencing as a result of induction of the interferon response. Sensitivity of the silencing effect to the histone deacetylase inhibitor trichostatin A and enrichment of the silent state chromatin mark H3K9me2 at the myostatin promoter following treatment implicate epigenetic remodelling as the cause of silencing consistent with numerous reports of TGS in mammalian cells. This study has demonstrated the feasibility of myostatin TGS as a novel therapeutic strategy targeting myostatin in cell culture.

5.2 MicroRNA Biology of DMD

One aspect of miRNA biology that we did not explore in this study is how differential miRNA expression varies with time. We have proposed that differential degeneration between tissues is an explanation for the differences in muscle miRNA expression profiles. For example, relatively few changes were observed in the heart, which shows little degeneration at this stage in the progression of *mdx* pathology. Future studies of *mdx* miRNA expression should address this issue by performing analyses at various stages in the natural history of disease progression. Future studies will also investigate the relationship between differential miRNA expression and histopathology in order to further understand the role of miRNAs in *mdx* pathophysiology. The differences observed between quadriceps, diaphragm and heart suggest that differential miRNA expression is likely to reflect pathophysiological processes rather than as a direct result of loss of dystrophin itself. This is supported by the normalisation of serum dystromirs following dystrophin restoration. Consequently, it is likely that these results may also provide

insights into the process of muscle regeneration in the context of other myopathies, muscle injury and aging.

This work constitutes part of the first step in understanding the role of miRNAs in DMD pathophysiology. We, and others, have identified numerous miRNAs that are differentially expressed in the *mdx* mouse and DMD patients [332,333]. However, as yet, the functions of these miRNAs are not well understood. As miRNAs can potentially influence the expression of many target mRNAs [367] it will be important for future studies to identify the relevant target genes which are mediating disease processes. Several miRNA target prediction algorithms are available online, although these typically return thousands of potential miRNA:mRNA targets [368–370]. As yet there is no consensus as to which algorithm performs best [371] and the number of experimentally validated targets in TarBase is relatively small [372]. Determining which miRNA:mRNA interactions are contributing to disease pathology is also not trivial. Studies which validate miRNA targets typically focus on a small number of targets and so potentially miss the 'bigger picture'. There is therefore a need to investigate the effects of differential miRNA expression on a global scale. High-throughput Sequencing of RNA – Cross-linking Immunoprecipitation (HITS-CLIP) has been shown to one method of directly determining miRNA:mRNA interactions [373]. Similarly, proteomics approaches using mass spectrometry might also be used to determine all of the target genes regulated by specific miRNAs.

The function of miR-29c, a dystromir investigated in this work, has been relatively well studied. The work of van Rooij *et al*. has shown that miR-29 regulates cardiac fibrosis through the repression of fibrogenic mRNAs (i.e. collagens, fibrillins and elastin) [130]. In the dystrophic condition, miR-29c expression decreases and repression of genes that promote fibrogenesis is lost. Consequently, a miRNA replacement therapy using a synthetic miR-29 oligonucleotide mimic was recently shown to inhibit fibrogenesis and alleviate pathology in the *mdx* mouse [374]. This study underlines the importance of miRNAs in disease pathology and how their manipulation can be exploited by for therapy. miRNA-based therapies are currently in development for a wide variety of diseases with some in late stage clinical trials (e.g. inhibition of miR-122 as a therapy for chronic HCV infection [122]) and it is likely that the resulting technological advances will have direct relevance for the anti-miRNA therapies for DMD (e.g. inhibition of miR-31 to improve exon skipping-mediated dystrophin restoration [126]). Similarly, miRNA mimics of miR-29 and miR-486 are also potential therapeutic approaches to DMD by inhibiting fibrosis or promoting myogenesis respectively [347]. A thorough understanding of the role of miRNA expression in DMD pathophysiology is likely to reveal other novel therapeutic targets. It is also possible that miRNA therapies targeting pathological processes in DMD may be also be relevant to other diseases. For example, fibrosis and inflammation are common features of multiple disease conditions.

5.3 MicroRNAs as Serum Biomarkers for DMD

Exon skipping therapies are steadily advancing towards the clinic with early clinical trial results looking highly promising [56,375]. However, the current methods for determining the efficacy of experimental therapies require biopsy of patient muscles, which is highly invasive. In addition, repeated patient biopsies will be required in order to monitor dystrophin restoration over time. Consequently, there is an urgent need for non-invasive disease biomarkers for DMD. This study, and others, have shown that the extracellular dystromirs miR-1, miR-133a and miR-206 show promise as DMD biomarkers as they are strongly up-regulated in *mdx* mice and DMD patient sera and show normalisation following dystrophin restoration [329]. Interestingly, only modest dystrophin restoration was observed in muscle (i.e. 5-13% of WT dystrophin protein levels in Pip6e-PMO treated tibialias anterior). This may go some way to explain why only partial normalisation of serum dystromirs was observed. Additionally, these results suggest that serum miRNAs may be highly sensitive biomarkers given their large changes in abundance in response to low level dystrophin restoration (and at only 2 weeks post-injection). Importantly, although extracellular miRNAs have previously been shown to be promising cancer biomarkers [376,377] they are not currently in clinical usage.

It remains to be seen as to whether these extracellular miRNAs are involved in regulating muscle physiology. I propose a model in which active secretion of these dystromirs promotes muscle regeneration following muscle damage. The role of these dystromirs in myogenesis is already well established [137,144]. In addition, miR-1 and miR-133a are primarily expressed in skeletal and cardiac muscle, and miR-206 restricted to skeletal

muscle [137], suggesting that these extracellular dystromirs are unlikely to originate in non-muscle tissues. It has also been reported that these miRNAs are expressed at very low levels in undifferentiated myoblasts and that their expression increases as these cultures progressively differentiate [332]. This suggests that extracellular dystromirs probably originate from mature muscle rather than from the satellite cells. This is supported by Yuasa *et al*. who showed that miR-206 is primarily expressed in regenerating fibres by fluorescence *in situ* hybridisation [334].

miRNAs are readily detectable in serum and plasma and show remarkable stability considering the RNase activity present in these fluids [376,377]. Extracellular miRNAs are known to be released in lipid membrane-bound vesicles (e.g. microvesicles, exosomes, [378,379] apoptopic bodies [380]), protein complexes (e.g. Argonaute 2 [350], nucleophosmin-1 [381]) or in lipoprotein complexes (e.g. high-density lipoprotein) [382]. The sequestration of extracellular miRNAs in lipid vesicles or in complex with (lipo)proteins provides an explanation for their insensitivity to RNase-mediated degradation.

Whether or not these miRNAs are able to silence target mRNAs in recipient cells is an open question. Several reports have shown that circulating miRNAs are taken up by target cells where they are biologically active [20,21,26], and exosomes have recently been shown to deliver exogenous siRNA cargoes [384]. Similarly, Kuwabara *et al*. showed that cell-to-cell transfer of miR-1 and miR-133 can induce silencing of luciferase miRNA sensors in cell culture [385]. Interestingly, local injection of muscle-specific

miRNAs has been shown to enhance muscle regeneration in injured rat muscle [154]. Furthermore, forced expression of miR-1 in HeLa (non-muscle) cells alters their transcriptional profile to become more muscle-like [145]. Taken together, these studies suggest that extracellular miRNAs can induce phenotypic changes in recipient cells.

In summary, I hypothesise that: (1) Dystromirs are actively secreted from dystrophic muscle. (2) Extracellular dsytromirs originate from mature muscle cells. (3) Encapsulation in exosomes or formation of protein/lipoprotein complexes protects extracellular dystromirs from RNase-mediated degradation. (4) Circulating dystromirs can influence gene expression in recipient cells. (5) Cell-to-cell transfer of dystromirs promotes muscle regeneration. Future work must test these predictions.

Aside from miR-1, miR-133a and miR-206, none of the other 9 dystromirs studied were suitable as serum biomarkers in *mdx* mice. Interestingly, miR-1 and miR-133 have also been found to be enriched in patient serum following myocardial infarction suggesting they are also biomarkers of cardiac damage [385]. It will be interesting to see if cardiac specific miRNA biomarkers can be identified such that skeletal muscle degeneration and dystrophic cardiomyopathy can be monitored independently.

5.4 Myostatin Transcriptional Silencing

An appraisal of recent discoveries reveals a new vision of genome biology in which RNA plays a central role. ncRNA transcripts are found throughout the genome and act to regulate the expression of genes at the epigenetic level. Targeting these transcripts with small RNAs presents exciting opportunities for the development of molecular therapies

and the study of gene function. Consequently, the development of epigenetic-TGS and TGA approaches has opened up the epigenome to molecular medicine.

Inhibition of myostatin signalling is a promising therapeutic approach in the treatment of muscle wasting disorders. In contrast with other studies, we have targeted myostatin for epigenetic silencing which is theoretically permanent. The combination of myostatin TGS with dystrophin exon skipping has the potential to expand the effectiveness of current experimental therapies. Indeed, proof-of-principle combination of myostatin blockade by RNAi with exon skipping has already been demonstrated [126]. Additional future work includes studies to determine whether promoter-targeting siRNAs can indeed induce long-term silencing of myostatin expression. Determination of long-term silencing in the case of myostatin would be a logical next step to the work presented in this thesis. Previous studies that have demonstrated long-term TGS have passaged cultured cells over a period of one month or one year [170,172,183]. As we have used differentiated C2C12 myotubes, passage of cells is not possible. In order to demonstrate long-term silencing of myostatin cultures would need to be maintained for ~45 days with resulting technical difficulties.

At time of writing only a handful of studies have reported *in vivo* transcriptional modulation although the results are highly promising [205,206,239,280]. The successful translation of transcriptional modulation from cell culture studies to the *in vivo* setting may be dependent on similar expression levels of the ncRNA target transcripts between cultured cells and tissues. The low abundance of these target RNAs may be a limiting

factor for treatment efficacy given that many are highly unstable [198]. Similarly, the delivery of charged oligonucleotides (i.e. siRNAs) to skeletal muscle is a significant obstacle to the development of TGS therapeutics for muscle wasting disorders.

While myostatin is an attractive therapeutic target, cell culture studies targeting myostatin are subject to a number of other technical difficulties. Myostatin is expressed at very low levels in undifferentiated myoblasts. In order to consistently detect myostatin C2C12 cells were switched to differentiation medium for 7 days. In this study we were unable to consistently detect myostatin protein in cultured cells by western blot. Antibodies against myostatin are notoriously poor. These difficulties relate to the low expression levels of myostatin (particularly in cultured cells), the secretory nature of the protein and its close homology with other TGF-β superfamily transcription factors. Similarly, low levels of myostatin expression meant that levels of nascent myostatin RNA could only be detected at background levels and so nuclear run-on analysis and direct determination of silencing at the levels of transcription was not possible.

Mechanistic details of TGS have not been fully elucidated. These include the relative kinetics of histone remodelling and promoter methylation, the differential roles of Argonaute proteins and a complete description of RITS components. However, due to the difficulties associated with working with myostatin it is likely that these questions will be best answered using other experimental systems.

5.5 Further Therapeutic Targets for Transcriptional Modulation

A number of other genes are promising targets for transcriptional modulation. Transgenic mouse models in which the expression of other components in the myostatin pathway were modulated resulted in animals with phenotypes similar to the myostatin null mouse thereby identifying them as potential therapeutic targets. Transgenic expression of a dominant negative mutant of the myostatin receptor, Acvr2b, resulted in an increase in skeletal muscle mass of up to 125% [353]. Acvr2b acts as an integration point for other signals relating to the repression of myocyte proliferation (e.g. GDF-11) [386] and so targeting Acvr2b by TGS might provide advantages over and above myostatin inhibition. Conversely, a combinatorial approach targeting both myostatin and Acrv2b may provide additional functional correction. In addition to FLRG and GASP-1, follistatin also acts as an endogenous myostatin antagonist [387]. Up-regulation of follistatin is therefore an alternate means of inhibiting myostatin signalling [387]. Follistatin is known to inhibit the signalling function of a wide range of TGF-β ligands. Over-expression of follistatin in transgenic mice resulted in an increase in muscle mass of up to 327% [353]. This massive increase is likely to be the result of perturbing multiple ligands involved in regulating myogenesis which is encouraging in that a large increase in muscle mass can be obtained using a single strategy but discouraging in that the risk of potentially harmful off-target effects is increased. Similarly, up-regulation of utrophin is an established therapeutic strategy for the treatment of DMD [65,66]. Current utrophin up-regulation studies have focused on the use of small molecules although TGA is another potential approach.

5.6 Concluding Remarks

The work in this thesis has contributed to our understanding of the miRNA biology of DMD. It has identified novel differentially expressed miRNAs in the *mdx* mouse which may be involved in pathophysiological processes or potential therapeutic targets. I have demonstrated the potential of circulating dystromirs as disease biomarkers as they are highly up-regulated in *mdx* serum and are normalised by antisense oligonucleotide-mediated exon-skipping. Additionally, I have demonstrated the feasibility of epigenetic silencing of myostatin by transcriptional gene silencing. This novel approach expands the possible experimental molecular therapies for DMD.

6 References

1. Hoffman, E.P., Brown, R.H. & Kunkel, L.M. (1987). Dystrophin: the protein product of the Duchenne muscular dystrophy locus. *Cell*; **51**: 919–928.
2. Monaco, A.P., Bertelson, C.J., Liechti-Gallati, S., Moser, H. & Kunkel, L.M. (1988). An explanation for the phenotypic differences between patients bearing partial deletions of the DMD locus. *Genomics*; **2**: 90–95.
3. Aartsma-Rus, A., Van Deutekom, J.C.T., Fokkema, I.F., Van Ommen, G.-J.B. & Den Dunnen, J.T. (2006). Entries in the Leiden Duchenne muscular dystrophy mutation database: an overview of mutation types and paradoxical cases that confirm the reading-frame rule. *Muscle Nerve*; **34**: 135–144.
4. Koenig, M., Hoffman, E.P., Bertelson, C.J., Monaco, A.P., Feener, C. & Kunkel, L.M. (1987). Complete cloning of the Duchenne muscular dystrophy (DMD) cDNA and preliminary genomic organization of the DMD gene in normal and affected individuals. *Cell*; **50**: 509–517.
5. Koenig, M., Monaco, A.P. & Kunkel, L.M. (1988). The complete sequence of dystrophin predicts a rod-shaped cytoskeletal protein. *Cell*; **53**: 219–228.
6. Levine, B.A., Moir, A.J., Patchell, V.B. & Perry, S.V. (1990). The interaction of actin with dystrophin. *FEBS Lett.*; **263**: 159–162.
7. Amann, K.J., Renley, B.A. & Ervasti, J.M. (1998). A cluster of basic repeats in the dystrophin rod domain binds F-actin through an electrostatic interaction. *J. Biol. Chem.*; **273**: 28419–28423.
8. Lai, Y., Thomas, G.D., Yue, Y., Yang, H.T., Li, D., Long, C., *et al.* (2009). Dystrophins carrying spectrin-like repeats 16 and 17 anchor nNOS to the sarcolemma and enhance exercise performance in a mouse model of muscular dystrophy. *J. Clin. Invest*; **119**: 624–635.
9. Koenig, M. & Kunkel, L.M. (1990). Detailed analysis of the repeat domain of dystrophin reveals four potential hinge segments that may confer flexibility. *J. Biol. Chem.*; **265**: 4560–4566.
10. Ishikawa-Sakurai, M., Yoshida, M., Imamura, M., Davies, K.E. & Ozawa, E. (2004). ZZ domain is essentially required for the physiological binding of dystrophin and utrophin to beta-dystroglycan. *Hum. Mol. Genet.*; **13**: 693–702.
11. Adams, M.E., Butler, M.H., Dwyer, T.M., Peters, M.F., Murnane, A.A. & Froehner, S.C. (1993). Two forms of mouse syntrophin, a 58 kd dystrophin-associated protein, differ in primary structure and tissue distribution. *Neuron*; **11**: 531–540.
12. Ahn, A.H. & Kunkel, L.M. (1995). Syntrophin binds to an alternatively spliced exon of dystrophin. *J. Cell Biol.*; **128**: 363–371.
13. Adams, M.E., Mueller, H.A. & Froehner, S.C. (2001). In vivo requirement of the alpha-syntrophin PDZ domain for the sarcolemmal localization of nNOS and aquaporin-4. *J. Cell Biol.*; **155**: 113–122.
14. Ervasti, J.M. & Campbell, K.P. (1991). Membrane organization of the dystrophin-glycoprotein complex. *Cell*; **66**: 1121–1131.
15. Venema, V.J., Ju, H., Zou, R. & Venema, R.C. (1997). Interaction of neuronal nitric-oxide synthase with caveolin-3 in skeletal muscle. Identification of a novel caveolin scaffolding/inhibitory domain. *J. Biol. Chem.*; **272**: 28187–28190.

16. Rybakova, I.N., Patel, J.R. & Ervasti, J.M. (2000). The dystrophin complex forms a mechanically strong link between the sarcolemma and costameric actin. *J. Cell Biol.*; **150**: 1209–1214.
17. Ervasti, J.M. & Campbell, K.P. (1993). A role for the dystrophin-glycoprotein complex as a transmembrane linker between laminin and actin. *J. Cell Biol*; **122**: 809–823.
18. Winder, S.J. (1997). The membrane-cytoskeleton interface: the role of dystrophin and utrophin. *J. Muscle Res. Cell. Motil*; **18**: 617–629.
19. Brenman, J.E., Chao, D.S., Xia, H., Aldape, K. & Bredt, D.S. (1995). Nitric oxide synthase complexed with dystrophin and absent from skeletal muscle sarcolemma in Duchenne muscular dystrophy. *Cell*; **82**: 743–752.
20. Sander, M., Chavoshan, B., Harris, S.A., Iannaccone, S.T., Stull, J.T., Thomas, G.D., *et al.* (2000). Functional muscle ischemia in neuronal nitric oxide synthase-deficient skeletal muscle of children with Duchenne muscular dystrophy. *Proc. Natl. Acad. Sci. U.S.A*; **97**: 13818–13823.
21. Deconinck, N. & Dan, B. (2007). Pathophysiology of duchenne muscular dystrophy: current hypotheses. *Pediatr. Neurol*; **36**: 1–7.
22. Ervasti, J.M., Ohlendieck, K., Kahl, S.D., Gaver, M.G. & Campbell, K.P. (1990). Deficiency of a glycoprotein component of the dystrophin complex in dystrophic muscle. *Nature*; **345**: 315–319.
23. Petrof, B.J. (1998). The molecular basis of activity-induced muscle injury in Duchenne muscular dystrophy. *Mol. Cell. Biochem*; **179**: 111–123.
24. Morandi, L., Mora, M., Gussoni, E., Tedeschi, S. & Cornelio, F. (1990). Dystrophin analysis in Duchenne and Becker muscular dystrophy carriers: correlation with intracellular calcium and albumin. *Ann. Neurol*; **28**: 674–679.
25. Bodensteiner, J.B. & Engel, A.G. (1978). Intracellular calcium accumulation in Duchenne dystrophy and other myopathies: a study of 567,000 muscle fibers in 114 biopsies. *Neurology*; **28**: 439–446.
26. Imbert, N., Vandebrouck, C., Duport, G., Raymond, G., Hassoni, A.A., Constantin, B., *et al.* (2001). Calcium currents and transients in co-cultured contracting normal and Duchenne muscular dystrophy human myotubes. *J. Physiol. (Lond.)*; **534**: 343–355.
27. Arthur, P.G., Grounds, M.D. & Shavlakadze, T. (2008). Oxidative stress as a therapeutic target during muscle wasting: considering the complex interactions. *Curr Opin Clin Nutr Metab Care*; **11**: 408–416.
28. Heslop, L., Morgan, J.E. & Partridge, T.A. (2000). Evidence for a myogenic stem cell that is exhausted in dystrophic muscle. *J. Cell. Sci*; **113 (Pt 12)**: 2299–2308.
29. Spencer, M.J., Montecino-Rodriguez, E., Dorshkind, K. & Tidball, J.G. (2001). Helper (CD4(+)) and cytotoxic (CD8(+)) T cells promote the pathology of dystrophin-deficient muscle. *Clin. Immunol*; **98**: 235–243.
30. Sicinski, P., Geng, Y., Ryder-Cook, A.S., Barnard, E.A., Darlison, M.G. & Barnard, P.J. (1989). The molecular basis of muscular dystrophy in the mdx mouse: a point mutation. *Science*; **244**: 1578–1580.
31. Mendell, J.R., Moxley, R.T., Griggs, R.C., Brooke, M.H., Fenichel, G.M., Miller, J.P., *et al.* (1989). Randomized, double-blind six-month trial of prednisone in Duchenne's muscular dystrophy. *N. Engl. J. Med.*; **320**: 1592–1597.

32. Biggar, W.D., Gingras, M., Fehlings, D.L., Harris, V.A. & Steele, C.A. (2001). Deflazacort treatment of Duchenne muscular dystrophy. *J. Pediatr.*; **138**: 45–50.
33. King, W.M., Ruttencutter, R., Nagaraja, H.N., Matkovic, V., Landoll, J., Hoyle, C., *et al.* (2007). Orthopedic outcomes of long-term daily corticosteroid treatment in Duchenne muscular dystrophy. *Neurology*; **68**: 1607–1613.
34. Pichavant, C., Aartsma-Rus, A., Clemens, P.R., Davies, K.E., Dickson, G., Takeda, S., *et al.* (2011). Current status of pharmaceutical and genetic therapeutic approaches to treat DMD. *Mol. Ther.*; **19**: 830–840.
35. Aartsma-Rus, A., Fokkema, I., Verschuuren, J., Ginjaar, I., van Deutekom, J., van Ommen, G.-J., *et al.* (2009). Theoretic applicability of antisense-mediated exon skipping for Duchenne muscular dystrophy mutations. *Hum. Mutat.*; **30**: 293–299.
36. Malik, V., Rodino-Klapac, L.R., Viollet, L., Wall, C., King, W., Al-Dahhak, R., *et al.* (2010). Gentamicin-induced readthrough of stop codons in Duchenne muscular dystrophy. *Ann. Neurol.*; **67**: 771–780.
37. Welch, E.M., Barton, E.R., Zhuo, J., Tomizawa, Y., Friesen, W.J., Trifillis, P., *et al.* (2007). PTC124 targets genetic disorders caused by nonsense mutations. *Nature*; **447**: 87–91.
38. Partridge, T.A., Morgan, J.E., Coulton, G.R., Hoffman, E.P. & Kunkel, L.M. (1989). Conversion of mdx myofibres from dystrophin-negative to -positive by injection of normal myoblasts. *Nature*; **337**: 176–179.
39. Mendell, J.R., Kissel, J.T., Amato, A.A., King, W., Signore, L., Prior, T.W., *et al.* (1995). Myoblast transfer in the treatment of Duchenne's muscular dystrophy. *N. Engl. J. Med.*; **333**: 832–838.
40. Rouger, K., Larcher, T., Dubreil, L., Deschamps, J.-Y., Le Guiner, C., Jouvion, G., *et al.* (2011). Systemic delivery of allogenic muscle stem cells induces long-term muscle repair and clinical efficacy in duchenne muscular dystrophy dogs. *Am. J. Pathol.*; **179**: 2501–2518.
41. Gussoni, E., Soneoka, Y., Strickland, C.D., Buzney, E.A., Khan, M.K., Flint, A.F., *et al.* (1999). Dystrophin expression in the mdx mouse restored by stem cell transplantation. *Nature*; **401**: 390–394.
42. Jackson, K.A., Mi, T. & Goodell, M.A. (1999). Hematopoietic potential of stem cells isolated from murine skeletal muscle. *Proc. Natl. Acad. Sci. U.S.A.*; **96**: 14482–14486.
43. Sampaolesi, M., Torrente, Y., Innocenzi, A., Tonlorenzi, R., D'Antona, G., Pellegrino, M.A., *et al.* (2003). Cell therapy of alpha-sarcoglycan null dystrophic mice through intra-arterial delivery of mesoangioblasts. *Science*; **301**: 487–492.
44. Sampaolesi, M., Blot, S., D'Antona, G., Granger, N., Tonlorenzi, R., Innocenzi, A., *et al.* (2006). Mesoangioblast stem cells ameliorate muscle function in dystrophic dogs. *Nature*; **444**: 574–579.
45. Torrente, Y., Belicchi, M., Marchesi, C., Dantona, G., Cogiamanian, F., Pisati, F., *et al.* (2007). Autologous transplantation of muscle-derived CD133+ stem cells in Duchenne muscle patients. *Cell Transplant*; **16**: 563–577.
46. Torrente, Y., Belicchi, M., Sampaolesi, M., Pisati, F., Meregalli, M., D'Antona, G., *et al.* (2004). Human circulating AC133(+) stem cells restore dystrophin expression and ameliorate function in dystrophic skeletal muscle. *J. Clin. Invest.*; **114**: 182–195.

47. Wang, B., Li, J. & Xiao, X. (2000). Adeno-associated virus vector carrying human minidystrophin genes effectively ameliorates muscular dystrophy in mdx mouse model. *Proc. Natl. Acad. Sci. U.S.A.*; **97**: 13714–13719.
48. Harper, S.Q., Hauser, M.A., DelloRusso, C., Duan, D., Crawford, R.W., Phelps, S.F., *et al.* (2002). Modular flexibility of dystrophin: implications for gene therapy of Duchenne muscular dystrophy. *Nat. Med.*; **8**: 253–261.
49. Wells, D.J., Wells, K.E., Asante, E.A., Turner, G., Sunada, Y., Campbell, K.P., *et al.* (1995). Expression of human full-length and minidystrophin in transgenic mdx mice: implications for gene therapy of Duchenne muscular dystrophy. *Hum. Mol. Genet.*; **4**: 1245–1250.
50. Phelps, S.F., Hauser, M.A., Cole, N.M., Rafael, J.A., Hinkle, R.T., Faulkner, J.A., *et al.* (1995). Expression of full-length and truncated dystrophin mini-genes in transgenic mdx mice. *Hum. Mol. Genet.*; **4**: 1251–1258.
51. Wang, B., Li, J., Qiao, C., Chen, C., Hu, P., Zhu, X., *et al.* (2008). A canine minidystrophin is functional and therapeutic in mdx mice. *Gene Ther.*; **15**: 1099–1106.
52. Wang, Z., Storb, R., Lee, D., Kushmerick, M.J., Chu, B., Berger, C., *et al.* (2010). Immune responses to AAV in canine muscle monitored by cellular assays and noninvasive imaging. *Mol. Ther.*; **18**: 617–624.
53. Rodino-Klapac, L.R., Montgomery, C.L., Bremer, W.G., Shontz, K.M., Malik, V., Davis, N., *et al.* (2010). Persistent expression of FLAG-tagged micro dystrophin in nonhuman primates following intramuscular and vascular delivery. *Mol. Ther.*; **18**: 109–117.
54. Mendell, J.R., Campbell, K., Rodino-Klapac, L., Sahenk, Z., Shilling, C., Lewis, S., *et al.* (2010). Dystrophin immunity in Duchenne's muscular dystrophy. *N. Engl. J. Med.*; **363**: 1429–1437.
55. England, S.B., Nicholson, L.V., Johnson, M.A., Forrest, S.M., Love, D.R., Zubrzycka-Gaarn, E.E., *et al.* (1990). Very mild muscular dystrophy associated with the deletion of 46% of dystrophin. *Nature*; **343**: 180–182.
56. Kinali, M., Arechavala-Gomeza, V., Feng, L., Cirak, S., Hunt, D., Adkin, C., *et al.* (2009). Local restoration of dystrophin expression with the morpholino oligomer AVI-4658 in Duchenne muscular dystrophy: a single-blind, placebo-controlled, dose-escalation, proof-of-concept study. *Lancet Neurol*; **8**: 918–928.
57. van Deutekom, J.C., Janson, A.A., Ginjaar, I.B., Frankhuizen, W.S., Aartsma-Rus, A., Bremmer-Bout, M., *et al.* (2007). Local dystrophin restoration with antisense oligonucleotide PRO051. *N. Engl. J. Med.*; **357**: 2677–2686.
58. Yin, H., Moulton, H.M., Betts, C., Seow, Y., Boutilier, J., Iverson, P.L., *et al.* (2009). A fusion peptide directs enhanced systemic dystrophin exon skipping and functional restoration in dystrophin-deficient mdx mice. *Hum. Mol. Genet*; **18**: 4405–4414.
59. Yin, H., Saleh, A.F., Betts, C., Camelliti, P., Seow, Y., Ashraf, S., *et al.* (2011). Pip5 transduction peptides direct high efficiency oligonucleotide-mediated dystrophin exon skipping in heart and phenotypic correction in mdx mice. *Mol. Ther.*; **19**: 1295–1303.

60. Goyenvalle, A., Vulin, A., Fougerousse, F., Leturcq, F., Kaplan, J.-C., Garcia, L., *et al.* (2004). Rescue of dystrophic muscle through U7 snRNA-mediated exon skipping. *Science*; **306**: 1796–1799.
61. Denti, M.A., Incitti, T., Sthandier, O., Nicoletti, C., De Angelis, F.G., Rizzuto, E., *et al.* (2008). Long-term benefit of adeno-associated virus/antisense-mediated exon skipping in dystrophic mice. *Hum. Gene Ther.*; **19**: 601–608.
62. Béroud, C., Tuffery-Giraud, S., Matsuo, M., Hamroun, D., Humbertclaude, V., Monnier, N., *et al.* (2007). Multiexon skipping leading to an artificial DMD protein lacking amino acids from exons 45 through 55 could rescue up to 63% of patients with Duchenne muscular dystrophy. *Hum. Mutat.*; **28**: 196–202.
63. van Vliet, L., de Winter, C.L., van Deutekom, J.C.T., van Ommen, G.-J.B. & Aartsma-Rus, A. (2008). Assessment of the feasibility of exon 45-55 multiexon skipping for Duchenne muscular dystrophy. *BMC Med. Genet.*; **9**: 105.
64. Tinsley, J.M., Blake, D.J., Roche, A., Fairbrother, U., Riss, J., Byth, B.C., *et al.* (1992). Primary structure of dystrophin-related protein. *Nature*; **360**: 591–593.
65. Tanaka, H., Ishiguro, T., Eguchi, C., Saito, K. & Ozawa, E. (1991). Expression of a dystrophin-related protein associated with the skeletal muscle cell membrane. *Histochemistry*; **96**: 1–5.
66. Mizuno, Y., Nonaka, I., Hirai, S. & Ozawa, E. (1993). Reciprocal expression of dystrophin and utrophin in muscles of Duchenne muscular dystrophy patients, female DMD-carriers and control subjects. *J. Neurol. Sci.*; **119**: 43–52.
67. Tinsley, J., Deconinck, N., Fisher, R., Kahn, D., Phelps, S., Gillis, J.M., *et al.* (1998). Expression of full-length utrophin prevents muscular dystrophy in mdx mice. *Nat. Med.*; **4**: 1441–1444.
68. Goyenvalle, A., Babbs, A., Powell, D., Kole, R., Fletcher, S., Wilton, S.D., *et al.* (2010). Prevention of dystrophic pathology in severely affected dystrophin/utrophin-deficient mice by morpholino-oligomer-mediated exon-skipping. *Mol. Ther*; **18**: 198–205.
69. Krag, T.O.B., Bogdanovich, S., Jensen, C.J., Fischer, M.D., Hansen-Schwartz, J., Javazon, E.H., *et al.* (2004). Heregulin ameliorates the dystrophic phenotype in mdx mice. *Proc. Natl. Acad. Sci. U.S.A.*; **101**: 13856–13860.
70. Chaubourt, E., Fossier, P., Baux, G., Leprince, C., Israël, M. & De La Porte, S. (1999). Nitric oxide and l-arginine cause an accumulation of utrophin at the sarcolemma: a possible compensation for dystrophin loss in Duchenne muscular dystrophy. *Neurobiol. Dis.*; **6**: 499–507.
71. Sonnemann, K.J., Heun-Johnson, H., Turner, A.J., Baltgalvis, K.A., Lowe, D.A. & Ervasti, J.M. (2009). Functional substitution by TAT-utrophin in dystrophin-deficient mice. *PLoS Med.*; **6**: e1000083.
72. Squire, S., Raymackers, J.M., Vandebrouck, C., Potter, A., Tinsley, J., Fisher, R., *et al.* (2002). Prevention of pathology in mdx mice by expression of utrophin: analysis using an inducible transgenic expression system. *Hum. Mol. Genet.*; **11**: 3333–3344.
73. McPherron AC, Lawler, A.M. & Lee, S.J. (1997). Regulation of skeletal muscle mass in mice by a new TGF-beta superfamily member. *Nature*; **387**: 83–90.
74. Zhu X, Hadhazy M, Wehling M, Tidball JG & McNally EM (2000). Dominant negative myostatin produces hypertrophy without hyperplasia in muscle. *FEBS Lett*; **474**: 71–5.

75. Reisz-Porszasz, S., Bhasin, S., Artaza, J.N., Shen, R., Sinha-Hikim, I., Hogue, A., *et al.* (2003). Lower skeletal muscle mass in male transgenic mice with muscle-specific overexpression of myostatin. *Am J Physiol Endocrinol Metab*; **285**: E876–E888.
76. Grobet, L., Martin, L.J., Poncelet, D., Pirottin, D., Brouwers, B., Riquet, J., *et al.* (1997). A deletion in the bovine myostatin gene causes the double-muscled phenotype in cattle. *Nat. Genet*; **17**: 71–74.
77. Kambadur, R., Sharma, M., Smith, T.P. & Bass, J.J. (1997). Mutations in myostatin (GDF8) in double-muscled Belgian Blue and Piedmontese cattle. *Genome Res*; **7**: 910–916.
78. McPherron, A.C. & Lee, S.J. (1997). Double muscling in cattle due to mutations in the myostatin gene. *Proc. Natl. Acad. Sci. U.S.A*; **94**: 12457–12461.
79. Schuelke M, Wagner KR, Stolz LE, Hubner C, Riebel T, Komen W, *et al.* (2004). Myostatin mutation associated with gross muscle hypertrophy in a child. *N Engl J Med*; **350**: 2682–8.
80. Sharma, M., Langley, B., Bass, J. & Kambadur, R. (2001). Myostatin in muscle growth and repair. *Exerc Sport Sci Rev*; **29**: 155–158.
81. Hill, J.J., Davies, M.V., Pearson, A.A., Wang, J.H., Hewick, R.M., Wolfman, N.M., *et al.* (2002). The myostatin propeptide and the follistatin-related gene are inhibitory binding proteins of myostatin in normal serum. *J. Biol. Chem*; **277**: 40735–40741.
82. Hill, J.J., Qiu, Y., Hewick, R.M. & Wolfman, N.M. (2003). Regulation of myostatin in vivo by growth and differentiation factor-associated serum protein-1: a novel protein with protease inhibitor and follistatin domains. *Mol. Endocrinol*; **17**: 1144–1154.
83. Wolfman, N.M., McPherron, A.C., Pappano, W.N., Davies, M.V., Song, K., Tomkinson, K.N., *et al.* (2003). Activation of latent myostatin by the BMP-1/tolloid family of metalloproteinases. *Proc. Natl. Acad. Sci. U.S.A*; **100**: 15842–15846.
84. Benabdallah, B.F., Bouchentouf, M., Rousseau, J., Bigey, P., Michaud, A., Chapdelaine, P., *et al.* (2008). Inhibiting myostatin with follistatin improves the success of myoblast transplantation in dystrophic mice. *Cell Transplant*; **17**: 337–50.
85. Thies, R.S., Chen, T., Davies, M.V., Tomkinson, K.N., Pearson, A.A., Shakey, Q.A., *et al.* (2001). GDF-8 propeptide binds to GDF-8 and antagonizes biological activity by inhibiting GDF-8 receptor binding. *Growth Factors*; **18**: 251–259.
86. Langley, B., Thomas, M., Bishop, A., Sharma, M., Gilmour, S. & Kambadur, R. (2002). Myostatin inhibits myoblast differentiation by down-regulating MyoD expression. *J. Biol. Chem*; **277**: 49831–49840.
87. Bogdanovich S, Perkins KJ, Krag TO, Whittemore LA & Khurana TS (2005). Myostatin propeptide-mediated amelioration of dystrophic pathophysiology. *FASEB J*; **19**: 543–9.
88. Whittemore LA, Song K, Li X, Aghajanian J, Davies M, Girgenrath S, *et al.* (2003). Inhibition of myostatin in adult mice increases skeletal muscle mass and strength. *Biochem Biophys Res Commun*; **300**: 965–71.
89. Nakatani, M., Takehara, Y., Sugino, H., Matsumoto, M., Hashimoto, O., Hasegawa, Y., *et al.* (2008). Transgenic expression of a myostatin inhibitor derived from

follistatin increases skeletal muscle mass and ameliorates dystrophic pathology in mdx mice. *FASEB J*; **22**: 477–87.
90. Qiao, C., Li, J., Jiang, J., Zhu, X., Wang, B., Li, J., *et al.* (2008). Myostatin propeptide gene delivery by adeno-associated virus serotype 8 vectors enhances muscle growth and ameliorates dystrophic phenotypes in mdx mice. *Hum Gene Ther*; **19**: 241–54.
91. Bogdanovich, S., McNally, E.M. & Khurana, T.S. (2008). Myostatin blockade improves function but not histopathology in a murine model of limb-girdle muscular dystrophy 2C. *Muscle Nerve*; **37**: 308–16.
92. Bogdanovich S, Krag TO, Barton ER, Morris LD, Whittemore LA, Ahima RS, *et al.* (2002). Functional improvement of dystrophic muscle by myostatin blockade. *Nature*; **420**: 418–21.
93. Wagner, K.R., McPherron, A.C., Winik, N. & Lee, S.-J. (2002). Loss of myostatin attenuates severity of muscular dystrophy in mdx mice. *Ann. Neurol*; **52**: 832–836.
94. Carlson, C.J., Booth, F.W. & Gordon, S.E. (1999). Skeletal muscle myostatin mRNA expression is fiber-type specific and increases during hindlimb unloading. *Am. J. Physiol*; **277**: R601–606.
95. Gilson, H., Schakman, O., Kalista, S., Lause, P., Tsuchida, K. & Thissen, J.-P. (2009). Follistatin induces muscle hypertrophy through satellite cell proliferation and inhibition of both myostatin and activin. *Am. J. Physiol. Endocrinol. Metab*; **297**: E157–164.
96. McCroskery, S., Thomas, M., Maxwell, L., Sharma, M. & Kambadur, R. (2003). Myostatin negatively regulates satellite cell activation and self-renewal. *J. Cell Biol*; **162**: 1135–1147.
97. McCroskery, S., Thomas, M., Platt, L., Hennebry, A., Nishimura, T., McLeay, L., *et al.* (2005). Improved muscle healing through enhanced regeneration and reduced fibrosis in myostatin-null mice. *J. Cell. Sci*; **118**: 3531–3541.
98. Amthor, H., Otto, A., Vulin, A., Rochat, A., Dumonceaux, J., Garcia, L., *et al.* (2009). Muscle hypertrophy driven by myostatin blockade does not require stem/precursor-cell activity. *Proc. Natl. Acad. Sci. U.S.A*; **106**: 7479–7484.
99. Liu, J., Carmell, M.A., Rivas, F.V., Marsden, C.G., Thomson, J.M., Song, J.-J., *et al.* (2004). Argonaute2 is the catalytic engine of mammalian RNAi. *Science*; **305**: 1437–1441.
100. Filipowicz, W. (2005). RNAi: the nuts and bolts of the RISC machine. *Cell*; **122**: 17–20.
101. Meister, G., Landthaler, M., Patkaniowska, A., Dorsett, Y., Teng, G. & Tuschl, T. (2004). Human Argonaute2 mediates RNA cleavage targeted by miRNAs and siRNAs. *Mol. Cell*; **15**: 185–197.
102. Dykxhoorn, D.M., Novina, C.D. & Sharp, P.A. (2003). Killing the messenger: short RNAs that silence gene expression. *Nat. Rev. Mol. Cell Biol*; **4**: 457–467.
103. Capodici, J., Karikó, K. & Weissman, D. (2002). Inhibition of HIV-1 infection by small interfering RNA-mediated RNA interference. *J. Immunol*; **169**: 5196–5201.
104. Filipowicz, W., Jaskiewicz, L., Kolb, F.A. & Pillai, R.S. (2005). Post-transcriptional gene silencing by siRNAs and miRNAs. *Curr. Opin. Struct. Biol*; **15**: 331–341.

105. Olsen, P.H. & Ambros, V. (1999). The lin-4 regulatory RNA controls developmental timing in Caenorhabditis elegans by blocking LIN-14 protein synthesis after the initiation of translation. *Dev. Biol*; **216**: 671–680.
106. Doench, J.G. & Sharp, P.A. (2004). Specificity of microRNA target selection in translational repression. *Genes Dev*; **18**: 504–511.
107. Ohler, U., Yekta, S., Lim, L.P., Bartel, D.P. & Burge, C.B. (2004). Patterns of flanking sequence conservation and a characteristic upstream motif for microRNA gene identification. *RNA*; **10**: 1309–1322.
108. Guo, H., Ingolia, N.T., Weissman, J.S. & Bartel, D.P. (2010). Mammalian microRNAs predominantly act to decrease target mRNA levels. *Nature*; **466**: 835–840.
109. Zeng, Y., Yi, R. & Cullen, B.R. (2003). MicroRNAs and small interfering RNAs can inhibit mRNA expression by similar mechanisms. *Proc. Natl. Acad. Sci. U.S.A.*; **100**: 9779–9784.
110. Grimson, A., Farh, K.K.-H., Johnston, W.K., Garrett-Engele, P., Lim, L.P. & Bartel, D.P. (2007). MicroRNA targeting specificity in mammals: determinants beyond seed pairing. *Mol. Cell*; **27**: 91–105.
111. Jiang, Q., Wang, Y., Hao, Y., Juan, L., Teng, M., Zhang, X., *et al.* (2009). miR2Disease: a manually curated database for microRNA deregulation in human disease. *Nucleic Acids Res.*; **37**: D98–104.
112. Pfeffer, S., Zavolan, M., Grässer, F.A., Chien, M., Russo, J.J., Ju, J., *et al.* (2004). Identification of virus-encoded microRNAs. *Science*; **304**: 734–736.
113. Jopling, C.L., Yi, M., Lancaster, A.M., Lemon, S.M. & Sarnow, P. (2005). Modulation of hepatitis C virus RNA abundance by a liver-specific MicroRNA. *Science*; **309**: 1577–1581.
114. Esquela-Kerscher, A. & Slack, F.J. (2006). Oncomirs - microRNAs with a role in cancer. *Nat. Rev. Cancer*; **6**: 259–269.
115. Ma, L., Reinhardt, F., Pan, E., Soutschek, J., Bhat, B., Marcusson, E.G., *et al.* (2010). Therapeutic silencing of miR-10b inhibits metastasis in a mouse mammary tumor model. *Nat. Biotechnol.*; **28**: 341–347.
116. Choi, W.-Y., Giraldez, A.J. & Schier, A.F. (2007). Target protectors reveal dampening and balancing of Nodal agonist and antagonist by miR-430. *Science*; **318**: 271–274.
117. Veedu, R.N. & Wengel, J. (2009). Locked nucleic acid as a novel class of therapeutic agents. *RNA Biol*; **6**: 321–323.
118. Fabani, M.M. & Gait, M.J. (2008). miR-122 targeting with LNA/2'-O-methyl oligonucleotide mixmers, peptide nucleic acids (PNA), and PNA-peptide conjugates. *RNA*; **14**: 336–346.
119. Fabani, M.M., Abreu-Goodger, C., Williams, D., Lyons, P.A., Torres, A.G., Smith, K.G.C., *et al.* (2010). Efficient inhibition of miR-155 function in vivo by peptide nucleic acids. *Nucl. Acids Res.*; **38**: 4466–4475.
120. Krützfeldt, J., Rajewsky, N., Braich, R., Rajeev, K.G., Tuschl, T., Manoharan, M., *et al.* (2005). Silencing of microRNAs in vivo with 'antagomirs'. *Nature*; **438**: 685–689.

121. Krützfeldt, J., Kuwajima, S., Braich, R., Rajeev, K.G., Pena, J., Tuschl, T., *et al.* (2007). Specificity, duplex degradation and subcellular localization of antagomirs. *Nucleic Acids Res.*; **35**: 2885–2892.
122. Lanford, R.E., Hildebrandt-Eriksen, E.S., Petri, A., Persson, R., Lindow, M., Munk, M.E., *et al.* (2010). Therapeutic silencing of microRNA-122 in primates with chronic hepatitis C virus infection. *Science*; **327**: 198–201.
123. Ebert, M.S., Neilson, J.R. & Sharp, P.A. (2007). MicroRNA sponges: competitive inhibitors of small RNAs in mammalian cells. *Nat. Methods*; **4**: 721–726.
124. Ma, L., Young, J., Prabhala, H., Pan, E., Mestdagh, P., Muth, D., *et al.* (2010). miR-9, a MYC/MYCN-activated microRNA, regulates E-cadherin and cancer metastasis. *Nat. Cell Biol.*; **12**: 247–256.
125. Kay, M.A. (2011). State-of-the-art gene-based therapies: the road ahead. *Nat. Rev. Genet.*; **12**: 316–328.
126. Cacchiarelli, D., Incitti, T., Martone, J., Cesana, M., Cazzella, V., Santini, T., *et al.* (2011). miR-31 modulates dystrophin expression: new implications for Duchenne muscular dystrophy therapy. *EMBO Rep.*; **12**: 136–141.
127. Calin, G.A. & Croce, C.M. (2006). MicroRNA signatures in human cancers. *Nat. Rev. Cancer*; **6**: 857–866.
128. Hammond, S.M. (2007). MicroRNAs as tumor suppressors. *Nat. Genet.*; **39**: 582–583.
129. Kota, J., Chivukula, R.R., O'Donnell, K.A., Wentzel, E.A., Montgomery, C.L., Hwang, H.-W., *et al.* (2009). Therapeutic microRNA delivery suppresses tumorigenesis in a murine liver cancer model. *Cell*; **137**: 1005–1017.
130. van Rooij, E., Sutherland, L.B., Thatcher, J.E., DiMaio, J.M., Naseem, R.H., Marshall, W.S., *et al.* (2008). Dysregulation of microRNAs after myocardial infarction reveals a role of miR-29 in cardiac fibrosis. *Proc. Natl. Acad. Sci. U.S.A.*; **105**: 13027–13032.
131. Wang, L., Zhou, L., Jiang, P., Lu, L., Chen, X., Lan, H., *et al.* (2012). Loss of miR-29 in Myoblasts Contributes to Dystrophic Muscle Pathogenesis. *Molecular Therapy*; **20**: 1222–1233.
132. Rettig, G.R. & Behlke, M.A. (2012). Progress toward in vivo use of siRNAs-II. *Mol. Ther.*; **20**: 483–512.
133. Brown, B.D., Venneri, M.A., Zingale, A., Sergi Sergi, L. & Naldini, L. (2006). Endogenous microRNA regulation suppresses transgene expression in hematopoietic lineages and enables stable gene transfer. *Nat. Med.*; **12**: 585–591.
134. Cawood, R., Chen, H.H., Carroll, F., Bazan-Peregrino, M., van Rooijen, N. & Seymour, L.W. (2009). Use of tissue-specific microRNA to control pathology of wild-type adenovirus without attenuation of its ability to kill cancer cells. *PLoS Pathog.*; **5**: e1000440.
135. Lagos-Quintana, M., Rauhut, R., Yalcin, A., Meyer, J., Lendeckel, W. & Tuschl, T. (2002). Identification of tissue-specific microRNAs from mouse. *Curr. Biol*; **12**: 735–739.
136. Chen, J.-F., Mandel, E.M., Thomson, J.M., Wu, Q., Callis, T.E., Hammond, S.M., *et al.* (2006). The role of microRNA-1 and microRNA-133 in skeletal muscle proliferation and differentiation. *Nat. Genet*; **38**: 228–233.

137. Kim, H.K., Lee, Y.S., Sivaprasad, U., Malhotra, A. & Dutta, A. (2006). Muscle-specific microRNA miR-206 promotes muscle differentiation. *J. Cell Biol*; **174**: 677–687.
138. Boutz, P.L., Chawla, G., Stoilov, P. & Black, D.L. (2007). MicroRNAs regulate the expression of the alternative splicing factor nPTB during muscle development. *Genes Dev*; **21**: 71–84.
139. Koutsoulidou, A., Mastroyiannopoulos, N.P., Furling, D., Uney, J.B. & Phylactou, L.A. (2011). Expression of miR-1, miR-133a, miR-133b and miR-206 increases during development of human skeletal muscle. *BMC Dev. Biol.*; **11**: 34.
140. Rao, P.K., Kumar, R.M., Farkhondeh, M., Baskerville, S. & Lodish, H.F. (2006). Myogenic factors that regulate expression of muscle-specific microRNAs. *Proc. Natl. Acad. Sci. U.S.A.*; **103**: 8721–8726.
141. Liu, N., Williams, A.H., Kim, Y., McAnally, J., Bezprozvannaya, S., Sutherland, L.B., *et al.* (2007). An intragenic MEF2-dependent enhancer directs muscle-specific expression of microRNAs 1 and 133. *Proc. Natl. Acad. Sci. U.S.A.*; **104**: 20844–20849.
142. Sweetman, D., Goljanek, K., Rathjen, T., Oustanina, S., Braun, T., Dalmay, T., *et al.* (2008). Specific requirements of MRFs for the expression of muscle specific microRNAs, miR-1, miR-206 and miR-133. *Dev. Biol.*; **321**: 491–499.
143. Zhao, Y., Samal, E. & Srivastava, D. (2005). Serum response factor regulates a muscle-specific microRNA that targets Hand2 during cardiogenesis. *Nature*; **436**: 214–220.
144. Chen, J.-F., Mandel, E.M., Thomson, J.M., Wu, Q., Callis, T.E., Hammond, S.M., *et al.* (2006). The role of microRNA-1 and microRNA-133 in skeletal muscle proliferation and differentiation. *Nat. Genet.*; **38**: 228–233.
145. Lim, L.P., Lau, N.C., Garrett-Engele, P., Grimson, A., Schelter, J.M., Castle, J., *et al.* (2005). Microarray analysis shows that some microRNAs downregulate large numbers of target mRNAs. *Nature*; **433**: 769–773.
146. Miska, E.A., Langley, E., Wolf, D., Karlsson, C., Pines, J. & Kouzarides, T. (2001). Differential localization of HDAC4 orchestrates muscle differentiation. *Nucleic Acids Res.*; **29**: 3439–3447.
147. Glass, C. & Singla, D.K. (2011). MicroRNA-1 transfected embryonic stem cells enhance cardiac myocyte differentiation and inhibit apoptosis by modulating the PTEN/Akt pathway in the infarcted heart. *Am. J. Physiol. Heart Circ. Physiol.*; **301**: H2038–2049.
148. Taulli, R., Bersani, F., Foglizzo, V., Linari, A., Vigna, E., Ladanyi, M., *et al.* (2009). The muscle-specific microRNA miR-206 blocks human rhabdomyosarcoma growth in xenotransplanted mice by promoting myogenic differentiation. *J. Clin. Invest.*; **119**: 2366–2378.
149. Williams, A.H., Valdez, G., Moresi, V., Qi, X., McAnally, J., Elliott, J.L., *et al.* (2009). MicroRNA-206 delays ALS progression and promotes regeneration of neuromuscular synapses in mice. *Science*; **326**: 1549–1554.
150. Chen, J.-F., Tao, Y., Li, J., Deng, Z., Yan, Z., Xiao, X., *et al.* (2010). microRNA-1 and microRNA-206 regulate skeletal muscle satellite cell proliferation and differentiation by repressing Pax7. *J. Cell Biol.*; **190**: 867–879.

151. Hirai, H., Verma, M., Watanabe, S., Tastad, C., Asakura, Y. & Asakura, A. (2010). MyoD regulates apoptosis of myoblasts through microRNA-mediated down-regulation of Pax3. *J. Cell Biol.*; **191**: 347–365.
152. Goljanek-Whysall, K., Sweetman, D., Abu-Elmagd, M., Chapnik, E., Dalmay, T., Hornstein, E., *et al.* (2011). MicroRNA regulation of the paired-box transcription factor Pax3 confers robustness to developmental timing of myogenesis. *Proc. Natl. Acad. Sci. U.S.A.*; **108**: 11936–11941.
153. Rosenberg, M.I., Georges, S.A., Asawachaicharn, A., Analau, E. & Tapscott, S.J. (2006). MyoD inhibits Fstl1 and Utrn expression by inducing transcription of miR-206. *J. Cell Biol.*; **175**: 77–85.
154. Nakasa, T., Ishikawa, M., Shi, M., Shibuya, H., Adachi, N. & Ochi, M. (2010). Acceleration of muscle regeneration by local injection of muscle-specific microRNAs in rat skeletal muscle injury model. *J. Cell. Mol. Med.*; **14**: 2495–2505.
155. Naguibneva, I., Ameyar-Zazoua, M., Polesskaya, A., Ait-Si-Ali, S., Groisman, R., Souidi, M., *et al.* (2006). The microRNA miR-181 targets the homeobox protein Hox-A11 during mammalian myoblast differentiation. *Nat. Cell Biol*; **8**: 278–284.
156. Small, E.M., O'Rourke, J.R., Moresi, V., Sutherland, L.B., McAnally, J., Gerard, R.D., *et al.* (2010). Regulation of PI3-kinase/Akt signaling by muscle-enriched microRNA-486. *Proc. Natl. Acad. Sci. U.S.A.*; **107**: 4218–4223.
157. Seok, H.Y., Tatsuguchi, M., Callis, T.E., He, A., Pu, W.T. & Wang, D.-Z. (2011). miR-155 inhibits expression of the MEF2A protein to repress skeletal muscle differentiation. *J. Biol. Chem.*; **286**: 35339–35346.
158. Creamer, K.M. & Partridge, J.F. (2011). RITS-connecting transcription, RNA interference, and heterochromatin assembly in fission yeast. *Wiley Interdiscip Rev RNA*; **2**: 632–646.
159. Verdel, A., Vavasseur, A., Le Gorrec, M. & Touat-Todeschini, L. (2009). Common themes in siRNA-mediated epigenetic silencing pathways. *Int. J. Dev. Biol*; **53**: 245–257.
160. Grewal, S.I.S. & Elgin, S.C.R. (2007). Transcription and RNA interference in the formation of heterochromatin. *Nature*; **447**: 399–406.
161. Matzke, M.A., Matzke, A.J., Pruss, G.J. & Vance, V.B. (2001). RNA-based silencing strategies in plants. *Curr. Opin. Genet. Dev.*; **11**: 221–227.
162. Egger, G., Liang, G., Aparicio, A. & Jones, P.A. (2004). Epigenetics in human disease and prospects for epigenetic therapy. *Nature*; **429**: 457–463.
163. Strahl, B.D. & Allis, C.D. (2000). The language of covalent histone modifications. *Nature*; **403**: 41–45.
164. Jenuwein, T. & Allis, C.D. (2001). Translating the histone code. *Science*; **293**: 1074–1080.
165. Lehnertz, B., Ueda, Y., Derijck, A.A.H.A., Braunschweig, U., Perez-Burgos, L., Kubicek, S., *et al.* (2003). Suv39h-mediated histone H3 lysine 9 methylation directs DNA methylation to major satellite repeats at pericentric heterochromatin. *Curr. Biol*; **13**: 1192–1200.
166. Viré, E., Brenner, C., Deplus, R., Blanchon, L., Fraga, M., Didelot, C., *et al.* (2006). The Polycomb group protein EZH2 directly controls DNA methylation. *Nature*; **439**: 871–874.

167. Paro, R. (1995). Propagating memory of transcriptional states. *Trends Genet.*; **11**: 295–297.
168. Morris, K.V., Chan, S.W.-L., Jacobsen, S.E. & Looney, D.J. (2004). Small interfering RNA-induced transcriptional gene silencing in human cells. *Science*; **305**: 1289–92.
169. Weinberg, M.S., Villeneuve, L.M., Ehsani, A., Amarzguioui, M., Aagaard, L., Chen, Z.-X., *et al.* (2006). The antisense strand of small interfering RNAs directs histone methylation and transcriptional gene silencing in human cells. *RNA*; **12**: 256–62.
170. Hawkins, P.G., Santoso, S., Adams, C., Anest, V. & Morris, K.V. (2009). Promoter targeted small RNAs induce long-term transcriptional gene silencing in human cells. *Nucleic Acids Res*; **37**: 2984–95.
171. Suzuki, K., Shijuuku, T., Fukamachi, T., Zaunders, J., Guillemin, G., Cooper, D., *et al.* (2005). Prolonged transcriptional silencing and CpG methylation induced by siRNAs targeted to the HIV-1 promoter region. *J RNAi Gene Silencing*; **1**: 66–78.
172. Yamagishi, M., Ishida, T., Miyake, A., Cooper, D.A., Kelleher, A.D., Suzuki, K., *et al.* (2009). Retroviral delivery of promoter-targeted shRNA induces long-term silencing of HIV-1 transcription. *Microbes Infect.*; **11**: 500–508.
173. Kim, J.-W., Zhang, Y.-H., Zern, M.A., Rossi, J.J. & Wu, J. (2007). Short hairpin RNA causes the methylation of transforming growth factor-beta receptor II promoter and silencing of the target gene in rat hepatic stellate cells. *Biochem. Biophys. Res. Commun*; **359**: 292–297.
174. Pulukuri, S.M.K. & Rao, J.S. (2007). Small interfering RNA directed reversal of urokinase plasminogen activator demethylation inhibits prostate tumor growth and metastasis. *Cancer Res*; **67**: 6637–6646.
175. Turner, A.-M.W., De La Cruz, J. & Morris, K.V. (2009). Mobilization-competent Lentiviral Vector-mediated Sustained Transcriptional Modulation of HIV-1 Expression. *Mol. Ther*; **17**: 360–368.
176. Ting, A.H., Schuebel, K.E., Herman, J.G. & Baylin, S.B. (2005). Short double-stranded RNA induces transcriptional gene silencing in human cancer cells in the absence of DNA methylation. *Nat Genet*; **37**: 906–10.
177. Liu, J., Carmell, M.A., Rivas, F.V., Marsden, C.G., Thomson, J.M., Song, J.-J., *et al.* (2004). Argonaute2 is the catalytic engine of mammalian RNAi. *Science*; **305**: 1437–1441.
178. Lippman, Z., May, B., Yordan, C., Singer, T. & Martienssen, R. (2003). Distinct mechanisms determine transposon inheritance and methylation via small interfering RNA and histone modification. *PLoS Biol*; **1**: E67.
179. Verdel, A., Jia, S., Gerber, S., Sugiyama, T., Gygi, S., Grewal, S.I.S., *et al.* (2004). RNAi-mediated targeting of heterochromatin by the RITS complex. *Science*; **303**: 672–676.
180. Kim, D.H., Villeneuve, L.M., Morris, K.V. & Rossi, J.J. (2006). Argonaute-1 directs siRNA-mediated transcriptional gene silencing in human cells. *Nat. Struct. Mol. Biol*; **13**: 793–797.
181. Rivas, F.V., Tolia, N.H., Song, J.-J., Aragon, J.P., Liu, J., Hannon, G.J., *et al.* (2005). Purified Argonaute2 and an siRNA form recombinant human RISC. *Nat. Struct. Mol. Biol*; **12**: 340–349.

182. Tolia, N.H. & Joshua-Tor, L. (2007). Slicer and the argonautes. *Nat. Chem. Biol.*; **3**: 36–43.
183. Suzuki, K., Juelich, T., Lim, H., Ishida, T., Watanebe, T., Cooper, D.A., *et al.* (2008). Closed chromatin architecture is induced by an RNA duplex targeting the HIV-1 promoter region. *J. Biol. Chem*; **283**: 23353–23363.
184. Fuks, F., Burgers, W.A., Godin, N., Kasai, M. & Kouzarides, T. (2001). Dnmt3a binds deacetylases and is recruited by a sequence-specific repressor to silence transcription. *EMBO J*; **20**: 2536–2544.
185. Datta, J., Ghoshal, K., Sharma, S.M., Tajima, S. & Jacob, S.T. (2003). Biochemical fractionation reveals association of DNA methyltransferase (Dnmt) 3b with Dnmt1 and that of Dnmt 3a with a histone H3 methyltransferase and Hdac1. *J. Cell. Biochem*; **88**: 855–864.
186. Fuks, F., Hurd, P.J., Deplus, R. & Kouzarides, T. (2003). The DNA methyltransferases associate with HP1 and the SUV39H1 histone methyltransferase. *Nucleic Acids Res*; **31**: 2305–2312.
187. Viré, E., Brenner, C., Deplus, R., Blanchon, L., Fraga, M., Didelot, C., *et al.* (2006). The Polycomb group protein EZH2 directly controls DNA methylation. *Nature*; **439**: 871–874.
188. Jeffery, L. & Nakielny, S. (2004). Components of the DNA methylation system of chromatin control are RNA-binding proteins. *J. Biol. Chem*; **279**: 49479–49487.
189. Castanotto, D., Tommasi, S., Li, M., Li, H., Yanow, S., Pfeifer, G.P., *et al.* (2005). Short hairpin RNA-directed cytosine (CpG) methylation of the RASSF1A gene promoter in HeLa cells. *Mol Ther*; **12**: 179–83.
190. Mehndiratta, M., Palanichamy, J.K., Pal, A., Bhagat, M., Singh, A., Sinha, S., *et al.* (2011). CpG Hypermethylation of the C-myc Promoter by dsRNA Results in Growth Suppression. *Mol. Pharm.*; **8**: 2302–2309.
191. Clark, M.B., Amaral, P.P., Schlesinger, F.J., Dinger, M.E., Taft, R.J., Rinn, J.L., *et al.* (2011). The reality of pervasive transcription. *PLoS Biol.*; **9**: e1000625; discussion e1001102.
192. Kapranov, P., Drenkow, J., Cheng, J., Long, J., Helt, G., Dike, S., *et al.* (2005). Examples of the complex architecture of the human transcriptome revealed by RACE and high-density tiling arrays. *Genome Res*; **15**: 987–997.
193. Dahary, D., Elroy-Stein, O. & Sorek, R. (2005). Naturally occurring antisense: transcriptional leakage or real overlap? *Genome Res*; **15**: 364–368.
194. Lapidot, M. & Pilpel, Y. (2006). Genome-wide natural antisense transcription: coupling its regulation to its different regulatory mechanisms. *EMBO Rep*; **7**: 1216–1222.
195. Katayama, S., Tomaru, Y., Kasukawa, T., Waki, K., Nakanishi, M., Nakamura, M., *et al.* (2005). Antisense transcription in the mammalian transcriptome. *Science*; **309**: 1564–1566.
196. Seila, A.C., Core, L.J., Lis, J.T. & Sharp, P.A. (2009). Divergent transcription: a new feature of active promoters. *Cell Cycle*; **8**: 2557–2564.
197. Kapranov, P., Cheng, J., Dike, S., Nix, D.A., Duttagupta, R., Willingham, A.T., *et al.* (2007). RNA maps reveal new RNA classes and a possible function for pervasive transcription. *Science*; **316**: 1484–1488.

198. Preker, P., Nielsen, J., Kammler, S., Lykke-Andersen, S., Christensen, M.S., Mapendano, C.K., *et al.* (2008). RNA exosome depletion reveals transcription upstream of active human promoters. *Science*; **322**: 1851–1854.
199. Han, J., Kim, D. & Morris, K.V. (2007). Promoter-associated RNA is required for RNA-directed transcriptional gene silencing in human cells. *Proc. Natl. Acad. Sci. U.S.A*; **104**: 12422–12427.
200. Schmitz, K.-M., Mayer, C., Postepska, A. & Grummt, I. (2010). Interaction of noncoding RNA with the rDNA promoter mediates recruitment of DNMT3b and silencing of rRNA genes. *Genes Dev.*; **24**: 2264–2269.
201. Martianov, I., Ramadass, A., Serra Barros, A., Chow, N. & Akoulitchev, A. (2007). Repression of the human dihydrofolate reductase gene by a non-coding interfering transcript. *Nature*; **445**: 666–670.
202. Sun, B.K., Deaton, A.M. & Lee, J.T. (2006). A transient heterochromatic state in Xist preempts X inactivation choice without RNA stabilization. *Mol. Cell*; **21**: 617–628.
203. Klase, Z., Kale, P., Winograd, R., Gupta, M.V., Heydarian, M., Berro, R., *et al.* (2007). HIV-1 TAR element is processed by Dicer to yield a viral micro-RNA involved in chromatin remodeling of the viral LTR. *BMC Mol. Biol.*; **8**: 63.
204. Lim, H.G.W., Suzuki, K., Cooper, D.A. & Kelleher, A.D. (2008). Promoter-targeted siRNAs induce gene silencing of simian immunodeficiency virus (SIV) infection in vitro. *Mol. Ther*; **16**: 565–570.
205. Turunen, M.P., Lehtola, T., Heinonen, S.E., Assefa, G.S., Korpisalo, P., Girnary, R., *et al.* (2009). Efficient regulation of VEGF expression by promoter-targeted lentiviral shRNAs based on epigenetic mechanism: a novel example of epigenetherapy. *Circ. Res*; **105**: 604–609.
206. Perrone, L., Devi, T.S., Hosoya, K.-I., Terasaki, T. & Singh, L.P. (2010). Inhibition of TXNIP expression in vivo blocks early pathologies of diabetic retinopathy. *Cell Death Dis*; **1**: e65.
207. Hong, D., Lu, W., Ye, F., Hu, Y. & Xie, X. (2009). Gene silencing of HPV16 E6/E7 induced by promoter-targeting siRNA in SiHa cells. *Br. J. Cancer*; **101**: 1798–1804.
208. Palanichamy, J.K., Mehndiratta, M., Bhagat, M., Ramalingam, P., Das, B., Das, P., *et al.* (2010). Silencing of integrated human papillomavirus-16 oncogenes by small interfering RNA-mediated heterochromatization. *Mol. Cancer Ther.*; **9**: 2114–2122.
209. Zhou, J., Peng, C., Li, B., Wang, F., Zhou, C., Hong, D., *et al.* (2012). Transcriptional gene silencing of HPV16 E6/E7 induces growth inhibition via apoptosis in vitro and in vivo. *Gynecol. Oncol.*; **124**: 296–302.
210. Murayama, A., Sakura, K., Nakama, M., Yasuzawa-Tanaka, K., Fujita, E., Tateishi, Y., *et al.* (2006). A specific CpG site demethylation in the human interleukin 2 gene promoter is an epigenetic memory. *EMBO J*; **25**: 1081–1092.
211. Zhang, M.-X., Ou, H., Shen, Y.H., Wang, J., Wang, J., Coselli, J., *et al.* (2005). Regulation of endothelial nitric oxide synthase by small RNA. *Proc. Natl. Acad. Sci. U.S.A*; **102**: 16967–16972.
212. Bühler, M., Mohn, F., Stalder, L. & Mühlemann, O. (2005). Transcriptional silencing of nonsense codon-containing immunoglobulin minigenes. *Mol. Cell*; **18**: 307–317.

213. Gonzalez, S., Pisano, D.G. & Serrano, M. (2008). Mechanistic principles of chromatin remodeling guided by siRNAs and miRNAs. *Cell Cycle*; **7**: 2601–2608.
214. Gonzalez, S., Klatt, P., Delgado, S., Conde, E., Lopez-Rios, F., Sanchez-Cespedes, M., *et al.* (2006). Oncogenic activity of Cdc6 through repression of the INK4/ARF locus. *Nature*; **440**: 702–706.
215. Wang, X., Feng, Y., Pan, L., Wang, Y., Xu, X., Lu, J., *et al.* (2007). The proximal GC-rich region of p16(INK4a) gene promoter plays a role in its transcriptional regulation. *Mol. Cell. Biochem*; **301**: 259–266.
216. Feng, X.-Z., He, X.-S., Zhuang, Y.-Z., Luo, Q., Jiang, J.-H., Yang, S., *et al.* (2008). Investigation of transcriptional gene silencing and mechanism induced by shRNAs targeted to RUNX3 in vitro. *World J. Gastroenterol.*; **14**: 3006–3014.
217. Taft, R.J., Hawkins, P.G., Mattick, J.S. & Morris, K.V. (2011). The relationship between transcription initiation RNAs and CCCTC-binding factor (CTCF) localization. *Epigenetics Chromatin*; **4**: 13.
218. Younger, S.T. & Corey, D.R. (2011). Transcriptional regulation by miRNA mimics that target sequences downstream of gene termini. *Mol Biosyst*; **7**: 2383–2388.
219. Alló, M., Buggiano, V., Fededa, J.P., Petrillo, E., Schor, I., de la Mata, M., *et al.* (2009). Control of alternative splicing through siRNA-mediated transcriptional gene silencing. *Nat. Struct. Mol. Biol*; **16**: 717–724.
220. Kim, D.H., Saetrom, P., Snøve, O. & Rossi, J.J. (2008). MicroRNA-directed transcriptional gene silencing in mammalian cells. *Proc. Natl. Acad. Sci. U.S.A*; **105**: 16230–16235.
221. Tan, Y., Zhang, B., Wu, T., Skogerbø, G., Zhu, X., Guo, X., *et al.* (2009). Transcriptional inhibiton of Hoxd4 expression by miRNA-10a in human breast cancer cells. *BMC Mol. Biol.*; **10**: 12.
222. Benhamed, M., Herbig, U., Ye, T., Dejean, A. & Bischof, O. (2012). Senescence is an endogenous trigger for microRNA-directed transcriptional gene silencing in human cells. *Nat. Cell Biol.*; **14**: 266–275.
223. Dean, A. (2011). In the loop: long range chromatin interactions and gene regulation. *Brief Funct Genomics*; **10**: 3–10.
224. Yue, X., Schwartz, J.C., Chu, Y., Younger, S.T., Gagnon, K.T., Elbashir, S., *et al.* (2010). Transcriptional regulation by small RNAs at sequences downstream from 3' gene termini. *Nat. Chem. Biol*; **6**: 621–629.
225. Holstege, F.C., Fiedler, U. & Timmers, H.T. (1997). Three transitions in the RNA polymerase II transcription complex during initiation. *EMBO J.*; **16**: 7468–7480.
226. Milne, L., Xu, Y., Perrin, D.M. & Sigman, D.S. (2000). An approach to gene-specific transcription inhibition using oligonucleotides complementary to the template strand of the open complex. *Proc. Natl. Acad. Sci. U.S.A.*; **97**: 3136–3141.
227. Janowski, B.A., Huffman, K.E., Schwartz, J.C., Ram, R., Hardy, D., Shames, D.S., *et al.* (2005). Inhibiting gene expression at transcription start sites in chromosomal DNA with antigene RNAs. *Nat. Chem. Biol*; **1**: 216–222.
228. Janowski, B.A., Huffman, K.E., Schwartz, J.C., Ram, R., Nordsell, R., Shames, D.S., *et al.* (2006). Involvement of AGO1 and AGO2 in mammalian transcriptional silencing. *Nat. Struct. Mol. Biol*; **13**: 787–792.

229. Janowski, B.A., Kaihatsu, K., Huffman, K.E., Schwartz, J.C., Ram, R., Hardy, D., *et al.* (2005). Inhibiting transcription of chromosomal DNA with antigene peptide nucleic acids. *Nat. Chem. Biol*; **1**: 210–215.
230. Beane, R.L., Ram, R., Gabillet, S., Arar, K., Monia, B.P. & Corey, D.R. (2007). Inhibiting gene expression with locked nucleic acids (LNAs) that target chromosomal DNA. *Biochemistry*; **46**: 7572–7580.
231. Beane, R., Gabillet, S., Montaillier, C., Arar, K. & Corey, D.R. (2008). Recognition of chromosomal DNA inside cells by locked nucleic acids. *Biochemistry*; **47**: 13147–13149.
232. Watts, J.K., Yu, D., Charisse, K., Montaillier, C., Potier, P., Manoharan, M., *et al.* (2010). Effect of chemical modifications on modulation of gene expression by duplex antigene RNAs that are complementary to non-coding transcripts at gene promoters. *Nucleic Acids Res*; **38**: 5242–5259.
233. Napoli, S., Pastori, C., Magistri, M., Carbone, G.M. & Catapano, C.V. (2009). Promoter-specific transcriptional interference and c-myc gene silencing by siRNAs in human cells. *EMBO J*; **28**: 1708–1719.
234. Schwartz, J.C., Younger, S.T., Nguyen, N.-B., Hardy, D.B., Monia, B.P., Corey, D.R., *et al.* (2008). Antisense transcripts are targets for activating small RNAs. *Nat Struct Mol Biol*; **15**: 842–8.
235. Chu, Y., Yue, X., Younger, S.T., Janowski, B.A. & Corey, D.R. (2010). Involvement of argonaute proteins in gene silencing and activation by RNAs complementary to a non-coding transcript at the progesterone receptor promoter. *Nucleic Acids Res*; **38**: 7736–7748.
236. Jiang, G., Zheng, L., Pu, J., Mei, H., Zhao, J., Huang, K., *et al.* (2012). Small RNAs targeting transcription start site induce heparanase silencing through interference with transcription initiation in human cancer cells. *PLoS ONE*; **7**: e31379.
237. Li, L.-C., Okino, S.T., Zhao, H., Pookot, D., Place, R.F., Urakami, S., *et al.* (2006). Small dsRNAs induce transcriptional activation in human cells. *Proc Natl Acad Sci U S A*; **103**: 17337–42.
238. Morris, K.V., Santoso, S., Turner, A.-M., Pastori, C. & Hawkins, P.G. (2008). Bidirectional transcription directs both transcriptional gene activation and suppression in human cells. *PLoS Genet*; **4**: e1000258.
239. Modarresi, F., Faghihi, M.A., Lopez-Toledano, M.A., Fatemi, R.P., Magistri, M., Brothers, S.P., *et al.* (2012). Inhibition of natural antisense transcripts in vivo results in gene-specific transcriptional upregulation. *Nat. Biotechnol.*; **30**: 453–459.
240. Mao, Q., Li, Y., Zheng, X., Yang, K., Shen, H., Qin, J., *et al.* (2008). Up-regulation of E-cadherin by small activating RNA inhibits cell invasion and migration in 5637 human bladder cancer cells. *Biochem. Biophys. Res. Commun.*; **375**: 566–570.
241. Huang, V., Qin, Y., Wang, J., Wang, X., Place, R.F., Lin, G., *et al.* (2010). RNAa is conserved in mammalian cells. *PLoS ONE*; **5**: e8848.
242. Junxia, W., Ping, G., Yuan, H., Lijun, Z., Jihong, R., Fang, L., *et al.* (2010). Double strand RNA-guided endogeneous E-cadherin up-regulation induces the apoptosis and inhibits proliferation of breast carcinoma cells in vitro and in vivo. *Cancer Sci.*; **101**: 1790–1796.

243. Janowski, B.A., Younger, S.T., Hardy, D.B., Ram, R., Huffman, K.E. & Corey, D.R. (2007). Activating gene expression in mammalian cells with promoter-targeted duplex RNAs. *Nat Chem Biol*; **3**: 166–73.
244. Matsui, M., Sakurai, F., Elbashir, S., Foster, D.J., Manoharan, M. & Corey, D.R. (2010). Activation of LDL receptor expression by small RNAs complementary to a noncoding transcript that overlaps the LDLR promoter. *Chem. Biol.*; **17**: 1344–1355.
245. Chen, R., Wang, T., Rao, K., Yang, J., Zhang, S., Wang, S., *et al.* (2011). Up-regulation of VEGF by small activator RNA in human corpus cavernosum smooth muscle cells. *J Sex Med*; **8**: 2773–2780.
246. Matilainen, J.M., Husso, T., Toropainen, S., Seuter, S., Turunen, M.P., Gynther, P., *et al.* (2010). Primary effect of 1α,25$(OH)_2D_3$ on IL-10 expression in monocytes is short-term down-regulation. *Biochim. Biophys. Acta*; **1803**: 1276–1286.
247. Majid, S., Dar, A.A., Saini, S., Yamamura, S., Hirata, H., Tanaka, Y., *et al.* (2010). MicroRNA-205-directed transcriptional activation of tumor suppressor genes in prostate cancer. *Cancer*; **116**: 5637–5649.
248. Place, R.F., Li, L.-C., Pookot, D., Noonan, E.J. & Dahiya, R. (2008). MicroRNA-373 induces expression of genes with complementary promoter sequences. *Proc. Natl. Acad. Sci. U.S.A*; **105**: 1608–1613.
249. Hawkins, P.G. & Morris, K.V. (2010). Transcriptional regulation of Oct4 by a long non-coding RNA antisense to Oct4-pseudogene 5. *Transcription*; **1**: 165–175.
250. Huang, V., Place, R.F., Portnoy, V., Wang, J., Qi, Z., Jia, Z., *et al.* (2012). Upregulation of Cyclin B1 by miRNA and its implications in cancer. *Nucleic Acids Res.*; **40**: 1695–1707.
251. Wang, J., Place, R.F., Huang, V., Wang, X., Noonan, E.J., Magyar, C.E., *et al.* (2010). Prognostic value and function of KLF4 in prostate cancer: RNAa and vector-mediated overexpression identify KLF4 as an inhibitor of tumor cell growth and migration. *Cancer Res.*; **70**: 10182–10191.
252. Wang, X., Wang, J., Huang, V., Place, R.F. & Li, L.-C. (2012). Induction of NANOG expression by targeting promoter sequence with small activating RNA antagonizes retinoic acid-induced differentiation. *Biochem. J.*; **443**: 821–828.
253. Qin, Q., Lin, Y.-W., Zheng, X.-Y., Chen, H., Mao, Q.-Q., Yang, K., *et al.* (2012). RNAa-mediated overexpression of WT1 induces apoptosis in HepG2 cells. *World J Surg Oncol*; **10**: 11.
254. Turner, A.-M.W. & Morris, K.V. (2010). Controlling transcription with noncoding RNAs in mammalian cells. *BioTechniques*; **48**: ix–xvi.
255. Janowski, B.A., Hu, J. & Corey, D.R. (2006). Silencing gene expression by targeting chromosomal DNA with antigene peptide nucleic acids and duplex RNAs. *Nat Protoc*; **1**: 436–443.
256. Reynolds, A., Leake, D., Boese, Q., Scaringe, S., Marshall, W.S. & Khvorova, A. (2004). Rational siRNA design for RNA interference. *Nat Biotechnol*; **22**: 326–30.
257. Sherman, M.P. & Greene, W.C. (2002). Slipping through the door: HIV entry into the nucleus. *Microbes Infect*; **4**: 67–73.
258. Morris, K.V. (2005). siRNA-mediated transcriptional gene silencing: the potential mechanism and a possible role in the histone code. *Cell. Mol. Life Sci*; **62**: 3057–3066.

259. Hwang, H.-W., Wentzel, E.A. & Mendell, J.T. (2007). A hexanucleotide element directs microRNA nuclear import. *Science*; **315**: 97–100.
260. Liao, J.-Y., Ma, L.-M., Guo, Y.-H., Zhang, Y.-C., Zhou, H., Shao, P., *et al.* (2010). Deep sequencing of human nuclear and cytoplasmic small RNAs reveals an unexpectedly complex subcellular distribution of miRNAs and tRNA 3' trailers. *PLoS ONE*; **5**: e10563.
261. Braasch, D.A., Jensen, S., Liu, Y., Kaur, K., Arar, K., White, M.A., *et al.* (2003). RNA interference in mammalian cells by chemically-modified RNA. *Biochemistry*; **42**: 7967–7975.
262. Moreno, P.M.D., Wenska, M., Lundin, K.E., Wrange, O., Strömberg, R. & Smith, C.I.E. (2009). A synthetic snRNA m3G-CAP enhances nuclear delivery of exogenous proteins and nucleic acids. *Nucleic Acids Res*; **37**: 1925–1935.
263. Jackson, A.L., Burchard, J., Schelter, J., Chau, B.N., Cleary, M., Lim, L., *et al.* (2006). Widespread siRNA 'off-target' transcript silencing mediated by seed region sequence complementarity. *RNA*; **12**: 1179–1187.
264. Bridge, A.J., Pebernard, S., Ducraux, A., Nicoulaz, A.-L. & Iggo, R. (2003). Induction of an interferon response by RNAi vectors in mammalian cells. *Nat. Genet*; **34**: 263–264.
265. Sledz, C.A., Holko, M., de Veer, M.J., Silverman, R.H. & Williams, B.R.G. (2003). Activation of the interferon system by short-interfering RNAs. *Nat. Cell Biol.*; **5**: 834–839.
266. Elbashir, S.M., Harborth, J., Lendeckel, W., Yalcin, A., Weber, K. & Tuschl, T. (2001). Duplexes of 21-nucleotide RNAs mediate RNA interference in cultured mammalian cells. *Nature*; **411**: 494–498.
267. Hornung, V., Guenthner-Biller, M., Bourquin, C., Ablasser, A., Schlee, M., Uematsu, S., *et al.* (2005). Sequence-specific potent induction of IFN-alpha by short interfering RNA in plasmacytoid dendritic cells through TLR7. *Nat. Med.*; **11**: 263–270.
268. Judge, A.D., Sood, V., Shaw, J.R., Fang, D., McClintock, K. & MacLachlan, I. (2005). Sequence-dependent stimulation of the mammalian innate immune response by synthetic siRNA. *Nat. Biotechnol*; **23**: 457–462.
269. Kim, D.-H., Longo, M., Han, Y., Lundberg, P., Cantin, E. & Rossi, J.J. (2004). Interferon induction by siRNAs and ssRNAs synthesized by phage polymerase. *Nat. Biotechnol*; **22**: 321–325.
270. Weinberg, M.S., Barichievy, S., Schaffer, L., Han, J. & Morris, K.V. (2007). An RNA targeted to the HIV-1 LTR promoter modulates indiscriminate off-target gene activation. *Nucleic Acids Res*; **35**: 7303–7312.
271. Moses, J., Goodchild, A. & Rivory, L.P. (2010). Intended transcriptional silencing with siRNA results in gene repression through sequence-specific off-targeting. *RNA*; **16**: 430–441.
272. Suzuki, K., Ishida, T., Yamagishi, M., Ahlenstiel, C., Swaminathan, S., Marks, K., *et al.* (2011). Transcriptional gene silencing of HIV-1 through promoter targeted RNA is highly specific. *RNA Biol*; **8**: 1035–1046.
273. Das, A.T., Brummelkamp, T.R., Westerhout, E.M., Vink, M., Madiredjo, M., Bernards, R., *et al.* (2004). Human immunodeficiency virus type 1 escapes from RNA interference-mediated inhibition. *J. Virol*; **78**: 2601–2605.

274. Boden, D., Pusch, O., Lee, F., Tucker, L. & Ramratnam, B. (2003). Human immunodeficiency virus type 1 escape from RNA interference. *J. Virol*; **77**: 11531–11535.
275. Westerhout, E.M., Ooms, M., Vink, M., Das, A.T. & Berkhout, B. (2005). HIV-1 can escape from RNA interference by evolving an alternative structure in its RNA genome. *Nucleic Acids Res*; **33**: 796–804.
276. von Eije, K.J., ter Brake, O. & Berkhout, B. (2008). Human immunodeficiency virus type 1 escape is restricted when conserved genome sequences are targeted by RNA interference. *J. Virol*; **82**: 2895–2903.
277. Li, M.-J., Kim, J., Li, S., Zaia, J., Yee, J.-K., Anderson, J., *et al.* (2005). Long-term inhibition of HIV-1 infection in primary hematopoietic cells by lentiviral vector delivery of a triple combination of anti-HIV shRNA, anti-CCR5 ribozyme, and a nucleolar-localizing TAR decoy. *Mol. Ther*; **12**: 900–909.
278. Aguilar-Cordova, E., Chinen, J., Donehower, L., Lewis, D.E. & Belmont, J.W. (1994). A sensitive reporter cell line for HIV-1 tat activity, HIV-1 inhibitors, and T cell activation effects. *AIDS Res. Hum. Retroviruses*; **10**: 295–301.
279. Wu, X. & Pandolfi, P.P. (2001). Mouse models for multistep tumorigenesis. *Trends Cell Biol.*; **11**: S2–9.
280. Zhou, J., Peng, C., Li, B., Wang, F., Zhou, C., Hong, D., *et al.* (2011). Transcriptional gene silencing of HPV16 E6/E7 induces growth inhibition via apoptosis in vitro and in vivo. *Gynecologic Oncology*; **in press**
281. Pulukuri, S.M.K., Estes, N., Patel, J. & Rao, J.S. (2007). Demethylation-linked activation of urokinase plasminogen activator is involved in progression of prostate cancer. *Cancer Res.*; **67**: 930–939.
282. Ylä-Herttuala, S. & Alitalo, K. (2003). Gene transfer as a tool to induce therapeutic vascular growth. *Nat. Med.*; **9**: 694–701.
283. Mercer, T.R., Dinger, M.E., Sunkin, S.M., Mehler, M.F. & Mattick, J.S. (2008). Specific expression of long noncoding RNAs in the mouse brain. *Proc. Natl. Acad. Sci. U.S.A.*; **105**: 716–721.
284. Dinger, M.E., Amaral, P.P., Mercer, T.R., Pang, K.C., Bruce, S.J., Gardiner, B.B., *et al.* (2008). Long noncoding RNAs in mouse embryonic stem cell pluripotency and differentiation. *Genome Res.*; **18**: 1433–1445.
285. Guttman, M., Amit, I., Garber, M., French, C., Lin, M.F., Feldser, D., *et al.* (2009). Chromatin signature reveals over a thousand highly conserved large non-coding RNAs in mammals. *Nature*; **458**: 223–227.
286. Yu, W., Gius, D., Onyango, P., Muldoon-Jacobs, K., Karp, J., Feinberg, A.P., *et al.* (2008). Epigenetic silencing of tumour suppressor gene p15 by its antisense RNA. *Nature*; **451**: 202–206.
287. Bonasio, R., Tu, S. & Reinberg, D. (2010). Molecular signals of epigenetic states. *Science*; **330**: 612–616.
288. Mayer, C., Schmitz, K.-M., Li, J., Grummt, I. & Santoro, R. (2006). Intergenic transcripts regulate the epigenetic state of rRNA genes. *Mol. Cell*; **22**: 351–361.
289. Huarte, M., Guttman, M., Feldser, D., Garber, M., Koziol, M.J., Kenzelmann-Broz, D., *et al.* (2010). A large intergenic noncoding RNA induced by p53 mediates global gene repression in the p53 response. *Cell*; **142**: 409–419.

290. Rinn, J.L., Kertesz, M., Wang, J.K., Squazzo, S.L., Xu, X., Brugmann, S.A., *et al.* (2007). Functional demarcation of active and silent chromatin domains in human HOX loci by noncoding RNAs. *Cell*; **129**: 1311–1323.
291. Tsai, M.-C., Manor, O., Wan, Y., Mosammaparast, N., Wang, J.K., Lan, F., *et al.* (2010). Long noncoding RNA as modular scaffold of histone modification complexes. *Science*; **329**: 689–693.
292. Maison, C., Bailly, D., Roche, D., Montes de Oca, R., Probst, A.V., Vassias, I., *et al.* (2011). SUMOylation promotes de novo targeting of HP1α to pericentric heterochromatin. *Nat. Genet.*; **43**: 220–227.
293. Khalil, A.M., Guttman, M., Huarte, M., Garber, M., Raj, A., Rivea Morales, D., *et al.* (2009). Many human large intergenic noncoding RNAs associate with chromatin-modifying complexes and affect gene expression. *Proc. Natl. Acad. Sci. U.S.A.*; **106**: 11667–11672.
294. Wang, K.C., Yang, Y.W., Liu, B., Sanyal, A., Corces-Zimmerman, R., Chen, Y., *et al.* (2011). A long noncoding RNA maintains active chromatin to coordinate homeotic gene expression. *Nature*; **472**: 120–124.
295. Yang, L., Lin, C., Liu, W., Zhang, J., Ohgi, K.A., Grinstein, J.D., *et al.* (2011). ncRNA- and Pc2 methylation-dependent gene relocation between nuclear structures mediates gene activation programs. *Cell*; **147**: 773–788.
296. Kino, T., Hurt, D.E., Ichijo, T., Nader, N. & Chrousos, G.P. (2010). Noncoding RNA gas5 is a growth arrest- and starvation-associated repressor of the glucocorticoid receptor. *Sci Signal*; **3**: ra8.
297. Cesana, M., Cacchiarelli, D., Legnini, I., Santini, T., Sthandier, O., Chinappi, M., *et al.* (2011). A long noncoding RNA controls muscle differentiation by functioning as a competing endogenous RNA. *Cell*; **147**: 358–369.
298. Poliseno, L., Salmena, L., Zhang, J., Carver, B., Haveman, W.J. & Pandolfi, P.P. (2010). A coding-independent function of gene and pseudogene mRNAs regulates tumour biology. *Nature*; **465**: 1033–1038.
299. Faghihi, M.A., Zhang, M., Huang, J., Modarresi, F., Van der Brug, M.P., Nalls, M.A., *et al.* (2010). Evidence for natural antisense transcript-mediated inhibition of microRNA function. *Genome Biol.*; **11**: R56.
300. Bernard, D., Prasanth, K.V., Tripathi, V., Colasse, S., Nakamura, T., Xuan, Z., *et al.* (2010). A long nuclear-retained non-coding RNA regulates synaptogenesis by modulating gene expression. *EMBO J.*; **29**: 3082–3093.
301. Tripathi, V., Ellis, J.D., Shen, Z., Song, D.Y., Pan, Q., Watt, A.T., *et al.* (2010). The nuclear-retained noncoding RNA MALAT1 regulates alternative splicing by modulating SR splicing factor phosphorylation. *Mol. Cell*; **39**: 925–938.
302. Petruk, S., Sedkov, Y., Riley, K.M., Hodgson, J., Schweisguth, F., Hirose, S., *et al.* (2006). Transcription of bxd noncoding RNAs promoted by trithorax represses Ubx in cis by transcriptional interference. *Cell*; **127**: 1209–1221.
303. Faghihi, M.A., Modarresi, F., Khalil, A.M., Wood, D.E., Sahagan, B.G., Morgan, T.E., *et al.* (2008). Expression of a noncoding RNA is elevated in Alzheimer's disease and drives rapid feed-forward regulation of beta-secretase. *Nat. Med.*; **14**: 723–730.
304. Modarresi, F., Faghihi, M.A., Patel, N.S., Sahagan, B.G., Wahlestedt, C. & Lopez-Toledano, M.A. (2011). Knockdown of BACE1-AS Nonprotein-Coding Transcript

Modulates Beta-Amyloid-Related Hippocampal Neurogenesis. *Int J Alzheimers Dis*; **2011**: 929042.
305. Yang, N. & Kazazian, H.H., Jr (2006). L1 retrotransposition is suppressed by endogenously encoded small interfering RNAs in human cultured cells. *Nat. Struct. Mol. Biol.*; **13**: 763–771.
306. Kawaji, H., Nakamura, M., Takahashi, Y., Sandelin, A., Katayama, S., Fukuda, S., *et al.* (2008). Hidden layers of human small RNAs. *BMC Genomics*; **9**: 157.
307. Qureshi, I.A., Mattick, J.S. & Mehler, M.F. (2010). Long non-coding RNAs in nervous system function and disease. *Brain Res.*; **1338**: 20–35.
308. Guttman, M., Donaghey, J., Carey, B.W., Garber, M., Grenier, J.K., Munson, G., *et al.* (2011). lincRNAs act in the circuitry controlling pluripotency and differentiation. *Nature*; **477**: 295–300.
309. Panning, B. & Jaenisch, R. (1998). RNA and the epigenetic regulation of X chromosome inactivation. *Cell*; **93**: 305–308.
310. Rougeulle, C. & Heard, E. (2002). Antisense RNA in imprinting: spreading silence through Air. *Trends Genet.*; **18**: 434–437.
311. Halvorsen, M., Martin, J.S., Broadaway, S. & Laederach, A. (2010). Disease-associated mutations that alter the RNA structural ensemble. *PLoS Genet.*; **6**: e1001074.
312. Glinskii, A.B., Ma, J., Ma, S., Grant, D., Lim, C.-U., Sell, S., *et al.* (2009). Identification of intergenic trans-regulatory RNAs containing a disease-linked SNP sequence and targeting cell cycle progression/differentiation pathways in multiple common human disorders. *Cell Cycle*; **8**: 3925–3942.
313. Wojcik, S.E., Rossi, S., Shimizu, M., Nicoloso, M.S., Cimmino, A., Alder, H., *et al.* (2010). Non-codingRNA sequence variations in human chronic lymphocytic leukemia and colorectal cancer. *Carcinogenesis*; **31**: 208–215.
314. Gupta, R.A., Shah, N., Wang, K.C., Kim, J., Horlings, H.M., Wong, D.J., *et al.* (2010). Long non-coding RNA HOTAIR reprograms chromatin state to promote cancer metastasis. *Nature*; **464**: 1071–1076.
315. Ji, P., Diederichs, S., Wang, W., Böing, S., Metzger, R., Schneider, P.M., *et al.* (2003). MALAT-1, a novel noncoding RNA, and thymosin beta4 predict metastasis and survival in early-stage non-small cell lung cancer. *Oncogene*; **22**: 8031–8041.
316. Tufarelli, C., Stanley, J.A.S., Garrick, D., Sharpe, J.A., Ayyub, H., Wood, W.G., *et al.* (2003). Transcription of antisense RNA leading to gene silencing and methylation as a novel cause of human genetic disease. *Nat. Genet*; **34**: 157–165.
317. Lewejohann, L., Skryabin, B.V., Sachser, N., Prehn, C., Heiduschka, P., Thanos, S., *et al.* (2004). Role of a neuronal small non-messenger RNA: behavioural alterations in BC1 RNA-deleted mice. *Behav. Brain Res.*; **154**: 273–289.
318. Mus, E., Hof, P.R. & Tiedge, H. (2007). Dendritic BC200 RNA in aging and in Alzheimer's disease. *Proc. Natl. Acad. Sci. U.S.A.*; **104**: 10679–10684.
319. Ponjavic, J. & Ponting, C.P. (2007). The long and the short of RNA maps. *Bioessays*; **29**: 1077–1080.
320. Ørom, U.A. & Shiekhattar, R. (2011). Long non-coding RNAs and enhancers. *Curr. Opin. Genet. Dev.*; **21**: 194–198.

321. Schwartz, J.C., Younger, S.T., Nguyen, N.-B., Hardy, D.B., Monia, B.P., Corey, D.R., *et al.* (2008). Antisense transcripts are targets for activating small RNAs. *Nat. Struct. Mol. Biol*; **15**: 842–848.
322. Younger, S.T., Pertsemlidis, A. & Corey, D.R. (2009). Predicting potential miRNA target sites within gene promoters. *Bioorg. Med. Chem. Lett*; **19**: 3791–3794.
323. Hawkins, P.G., Santoso, S., Adams, C., Anest, V. & Morris, K.V. (2009). Promoter targeted small RNAs induce long-term transcriptional gene silencing in human cells. *Nucleic Acids Res*; **37**: 2984–2995.
324. Brazma, A., Hingamp, P., Quackenbush, J., Sherlock, G., Spellman, P., Stoeckert, C., *et al.* (2001). Minimum information about a microarray experiment (MIAME)[mdash]toward standards for microarray data. *Nat Genet*; **29**: 365–371.
325. Edgar, R., Domrachev, M. & Lash, A.E. (2002). Gene Expression Omnibus: NCBI gene expression and hybridization array data repository. *Nucleic Acids Res.*; **30**: 207–210.
326. Bustin, S.A., Benes, V., Garson, J.A., Hellemans, J., Huggett, J., Kubista, M., *et al.* (2009). The MIQE guidelines: minimum information for publication of quantitative real-time PCR experiments. *Clin. Chem*; **55**: 611–622.
327. Taylor, S., Wakem, M., Dijkman, G., Alsarraj, M. & Nguyen, M. (2010). A practical approach to RT-qPCR-Publishing data that conform to the MIQE guidelines. *Methods*; **50**: S1–5.
328. Pfaffl, M.W. (2001). A new mathematical model for relative quantification in real-time RT-PCR. *Nucleic Acids Res.*; **29**: e45.
329. Cacchiarelli, D., Legnini, I., Martone, J., Cazzella, V., D'Amico, A., Bertini, E., *et al.* (2011). miRNAs as serum biomarkers for Duchenne muscular dystrophy. *EMBO Mol Med*; **3**: 258–265.
330. Sharp, P.S., Bye-a-Jee, H. & Wells, D.J. (2011). Physiological characterization of muscle strength with variable levels of dystrophin restoration in mdx mice following local antisense therapy. *Mol. Ther.*; **19**: 165–171.
331. Morgan, J.E., Beauchamp, J.R., Pagel, C.N., Peckham, M., Ataliotis, P., Jat, P.S., *et al.* (1994). Myogenic cell lines derived from transgenic mice carrying a thermolabile T antigen: a model system for the derivation of tissue-specific and mutation-specific cell lines. *Dev. Biol*; **162**: 486–498.
332. Greco, S., De Simone, M., Colussi, C., Zaccagnini, G., Fasanaro, P., Pescatori, M., *et al.* (2009). Common micro-RNA signature in skeletal muscle damage and regeneration induced by Duchenne muscular dystrophy and acute ischemia. *FASEB J*; **23**: 3335–3346.
333. Eisenberg, I., Eran, A., Nishino, I., Moggio, M., Lamperti, C., Amato, A.A., *et al.* (2007). Distinctive patterns of microRNA expression in primary muscular disorders. *Proc. Natl. Acad. Sci. U.S.A*; **104**: 17016–17021.
334. Yuasa, K., Hagiwara, Y., Ando, M., Nakamura, A., Takeda, S. & Hijikata, T. (2008). MicroRNA-206 is highly expressed in newly formed muscle fibers: implications regarding potential for muscle regeneration and maturation in muscular dystrophy. *Cell Struct. Funct*; **33**: 163–169.
335. Cacchiarelli, D., Martone, J., Girardi, E., Cesana, M., Incitti, T., Morlando, M., *et al.* (2010). MicroRNAs involved in molecular circuitries relevant for the Duchenne

muscular dystrophy pathogenesis are controlled by the dystrophin/nNOS pathway. *Cell Metab*; **12**: 341–351.
336. Mizuno, H., Nakamura, A., Aoki, Y., Ito, N., Kishi, S., Yamamoto, K., *et al.* (2011). Identification of muscle-specific microRNAs in serum of muscular dystrophy animal models: promising novel blood-based markers for muscular dystrophy. *PLoS ONE*; **6**: e18388.
337. McCarthy, J.J., Esser, K.A. & Andrade, F.H. (2007). MicroRNA-206 is overexpressed in the diaphragm but not the hindlimb muscle of mdx mouse. *Am. J. Physiol., Cell Physiol*; **293**: C451–457.
338. Ardite, E., Perdiguero, E., Vidal, B., Gutarra, S., Serrano, A.L. & Muñoz-Cánoves, P. (2012). PAI-1-regulated miR-21 defines a novel age-associated fibrogenic pathway in muscular dystrophy. *J. Cell Biol.*; **196**: 163–175.
339. Corney, D.C., Flesken-Nikitin, A., Godwin, A.K., Wang, W. & Nikitin, A.Y. (2007). MicroRNA-34b and MicroRNA-34c are targets of p53 and cooperate in control of cell proliferation and adhesion-independent growth. *Cancer Res.*; **67**: 8433–8438.
340. Kuang, W., Tan, J., Duan, Y., Duan, J., Wang, W., Jin, F., *et al.* (2009). Cyclic stretch induced miR-146a upregulation delays C2C12 myogenic differentiation through inhibition of Numb. *Biochem. Biophys. Res. Commun.*; **378**: 259–263.
341. Cardinali, B., Castellani, L., Fasanaro, P., Basso, A., Alemà, S., Martelli, F., *et al.* (2009). Microrna-221 and microrna-222 modulate differentiation and maturation of skeletal muscle cells. *PLoS ONE*; **4**: e7607.
342. Johnnidis, J.B., Harris, M.H., Wheeler, R.T., Stehling-Sun, S., Lam, M.H., Kirak, O., *et al.* (2008). Regulation of progenitor cell proliferation and granulocyte function by microRNA-223. *Nature*; **451**: 1125–1129.
343. Dangain, J. & Vrbova, G. (1984). Muscle development in mdx mutant mice. *Muscle Nerve*; **7**: 700–704.
344. Tanabe, Y., Esaki, K. & Nomura, T. (1986). Skeletal muscle pathology in X chromosome-linked muscular dystrophy (mdx) mouse. *Acta Neuropathologica*; **69**: 91–95.
345. Megraw, M., Sethupathy, P., Corda, B. & Hatzigeorgiou, A.G. (2007). miRGen: a database for the study of animal microRNA genomic organization and function. *Nucleic Acids Res.*; **35**: D149–155.
346. Stedman, H.H., Sweeney, H.L., Shrager, J.B., Maguire, H.C., Panettieri, R.A., Petrof, B., *et al.* (1991). The mdx mouse diaphragm reproduces the degenerative changes of Duchenne muscular dystrophy. *Nature*; **352**: 536–539.
347. Alexander, M.S., Casar, J.C., Motohashi, N., Myers, J.A., Eisenberg, I., Gonzalez, R.T., *et al.* (2011). Regulation of DMD pathology by an ankyrin-encoded miRNA. *Skelet Muscle*; **1**: 27.
348. Livak, K.J. & Schmittgen, T.D. (2001). Analysis of relative gene expression data using real-time quantitative PCR and the 2(-Delta Delta C(T)) Method. *Methods*; **25**: 402–408.
349. Hunter, M.P., Ismail, N., Zhang, X., Aguda, B.D., Lee, E.J., Yu, L., *et al.* (2008). Detection of microRNA expression in human peripheral blood microvesicles. *PLoS ONE*; **3**: e3694.

350. Arroyo, J.D., Chevillet, J.R., Kroh, E.M., Ruf, I.K., Pritchard, C.C., Gibson, D.F., *et al.* (2011). Argonaute2 complexes carry a population of circulating microRNAs independent of vesicles in human plasma. *Proc. Natl. Acad. Sci. U.S.A.*; **108**: 5003–5008.
351. Dumonceaux, J., Marie, S., Beley, C., Trollet, C., Vignaud, A., Ferry, A., *et al.* (2010). Combination of myostatin pathway interference and dystrophin rescue enhances tetanic and specific force in dystrophic mdx mice. *Mol. Ther*; **18**: 881–887.
352. Wagner, K.R., Fleckenstein, J.L., Amato, A.A., Barohn, R.J., Bushby, K., Escolar, D.M., *et al.* (2008). A phase I/IItrial of MYO-029 in adult subjects with muscular dystrophy. *Ann Neurol*; **63**: 561–71.
353. Lee, S.J. & McPherron, A.C. (2001). Regulation of myostatin activity and muscle growth. *Proc. Natl. Acad. Sci. U.S.A*; **98**: 9306–9311.
354. Kang, J.K., Malerba, A., Popplewell, L., Foster, K. & Dickson, G. (2011). Antisense-induced myostatin exon skipping leads to muscle hypertrophy in mice following octa-guanidine morpholino oligomer treatment. *Mol. Ther.*; **19**: 159–164.
355. Magee TR, Artaza JN, Ferrini MG, Vernet D, Zuniga FI, Cantini L, *et al.* (2006). Myostatin short interfering hairpin RNA gene transfer increases skeletal muscle mass. *J Gene Med*; **8**: 1171–81.
356. Wakaguri, H., Yamashita, R., Suzuki, Y., Sugano, S. & Nakai, K. (2008). DBTSS: database of transcription start sites, progress report 2008. *Nucleic Acids Res*; **36**: D97–101.
357. Karolchik, D., Hinrichs, A.S. & Kent, W.J. (2011). The UCSC Genome Browser. *Curr Protoc Hum Genet*; **18**: Unit18.6.
358. Larionov, A., Krause, A. & Miller, W. (2005). A standard curve based method for relative real time PCR data processing. *BMC Bioinformatics*; **6**: 62.
359. Ezzat, K., El Andaloussi, S., Zaghloul, E.M., Lehto, T., Lindberg, S., Moreno, P.M.D., *et al.* (2011). PepFect 14, a novel cell-penetrating peptide for oligonucleotide delivery in solution and as solid formulation. *Nucleic Acids Res*; **39**: 5284–98.
360. Khvorova, A., Reynolds, A. & Jayasena, S.D. (2003). Functional siRNAs and miRNAs exhibit strand bias. *Cell*; **115**: 209–216.
361. Schwarz, D.S., Hutvágner, G., Du, T., Xu, Z., Aronin, N. & Zamore, P.D. (2003). Asymmetry in the assembly of the RNAi enzyme complex. *Cell*; **115**: 199–208.
362. Landthaler, M., Gaidatzis, D., Rothballer, A., Chen, P.Y., Soll, S.J., Dinic, L., *et al.* (2008). Molecular characterization of human Argonaute-containing ribonucleoprotein complexes and their bound target mRNAs. *RNA*; **14**: 2580–2596.
363. Morris, K.V., Santoso, S., Turner, A.-M., Pastori, C. & Hawkins, P.G. (2008). Bidirectional transcription directs both transcriptional gene activation and suppression in human cells. *PLoS Genet*; **4**: e1000258.
364. Ma, K., Mallidis, C., Artaza, J., Taylor, W., Gonzalez-Cadavid, N. & Bhasin, S. (2001). Characterization of 5'-regulatory region of human myostatin gene: regulation by dexamethasone in vitro. *Am. J. Physiol. Endocrinol. Metab*; **281**: E1128–1136.
365. Khalil, A.M., Guttman, M., Huarte, M., Garber, M., Raj, A., Rivea Morales, D., *et al.* (2009). Many human large intergenic noncoding RNAs associate with

chromatin-modifying complexes and affect gene expression. *Proc. Natl. Acad. Sci. U.S.A.*; **106**: 11667–11672.
366. Grimm D, Streetz KL, Jopling CL, Storm TA, Pandey K, Davis CR, *et al.* (2009). Fatality in mice due to oversaturation of cellular microRNA. *Nature.*; **441**: 537–41.
367. Lim, L.P., Lau, N.C., Garrett-Engele, P., Grimson, A., Schelter, J.M., Castle, J., *et al.* (2005). Microarray analysis shows that some microRNAs downregulate large numbers of target mRNAs. *Nature*; **433**: 769–773.
368. John, B., Enright, A.J., Aravin, A., Tuschl, T., Sander, C. & Marks, D.S. (2004). Human MicroRNA targets. *PLoS Biol.*; **2**: e363.
369. Lewis, B.P., Burge, C.B. & Bartel, D.P. (2005). Conserved seed pairing, often flanked by adenosines, indicates that thousands of human genes are microRNA targets. *Cell*; **120**: 15–20.
370. Kiriakidou, M., Nelson, P.T., Kouranov, A., Fitziev, P., Bouyioukos, C., Mourelatos, Z., *et al.* (2004). A combined computational-experimental approach predicts human microRNA targets. *Genes Dev*; **18**: 1165–1178.
371. Alexiou, P., Maragkakis, M., Papadopoulos, G.L., Reczko, M. & Hatzigeorgiou, A.G. (2009). Lost in translation: an assessment and perspective for computational microRNA target identification. *Bioinformatics*; **25**: 3049–3055.
372. Papadopoulos, G.L., Reczko, M., Simossis, V.A., Sethupathy, P. & Hatzigeorgiou, A.G. (2009). The database of experimentally supported targets: a functional update of TarBase. *Nucleic Acids Res*; **37**: D155–158.
373. Chi, S.W., Zang, J.B., Mele, A. & Darnell, R.B. (2009). Argonaute HITS-CLIP decodes microRNA-mRNA interaction maps. *Nature*; **460**: 479–486.
374. Wang, L., Zhou, L., Jiang, P., Lu, L., Chen, X., Lan, H., *et al.* (2012). Loss of miR-29 in Myoblasts Contributes to Dystrophic Muscle Pathogenesis. *Molecular Therapy: The Journal of the American Society of Gene Therapy*;
375. Cirak, S., Feng, L., Anthony, K., Arechavala-Gomeza, V., Torelli, S., Sewry, C., *et al.* (2012). Restoration of the dystrophin-associated glycoprotein complex after exon skipping therapy in Duchenne muscular dystrophy. *Mol. Ther.*; **20**: 462–467.
376. Mitchell, P.S., Parkin, R.K., Kroh, E.M., Fritz, B.R., Wyman, S.K., Pogosova-Agadjanyan, E.L., *et al.* (2008). Circulating microRNAs as stable blood-based markers for cancer detection. *Proc. Natl. Acad. Sci. U.S.A*; **105**: 10513–10518.
377. Gilad, S., Meiri, E., Yogev, Y., Benjamin, S., Lebanony, D., Yerushalmi, N., *et al.* (2008). Serum microRNAs are promising novel biomarkers. *PLoS ONE*; **3**: e3148.
378. Kosaka, N., Iguchi, H., Yoshioka, Y., Takeshita, F., Matsuki, Y. & Ochiya, T. (2010). Secretory mechanisms and intercellular transfer of microRNAs in living cells. *J. Biol. Chem.*; **285**: 17442–17452.
379. Valadi, H., Ekström, K., Bossios, A., Sjöstrand, M., Lee, J.J. & Lötvall, J.O. (2007). Exosome-mediated transfer of mRNAs and microRNAs is a novel mechanism of genetic exchange between cells. *Nat. Cell Biol.*; **9**: 654–659.
380. Zernecke, A., Bidzhekov, K., Noels, H., Shagdarsuren, E., Gan, L., Denecke, B., *et al.* (2009). Delivery of microRNA-126 by apoptotic bodies induces CXCL12-dependent vascular protection. *Sci Signal*; **2**: ra81.
381. Wang, K., Zhang, S., Weber, J., Baxter, D. & Galas, D.J. (2010). Export of microRNAs and microRNA-protective protein by mammalian cells. *Nucleic Acids Res.*; **38**: 7248–7259.

382. Vickers, K.C., Palmisano, B.T., Shoucri, B.M., Shamburek, R.D. & Remaley, A.T. (2011). MicroRNAs are transported in plasma and delivered to recipient cells by high-density lipoproteins. *Nat. Cell Biol.*; **13**: 423–433.
383. Zhang, L., Hou, D., Chen, X., Li, D., Zhu, L., Zhang, Y., *et al.* (2012). Exogenous plant MIR168a specifically targets mammalian LDLRAP1: evidence of cross-kingdom regulation by microRNA. *Cell Res.*; **22**: 107–126.
384. Alvarez-Erviti, L., Seow, Y., Yin, H., Betts, C., Lakhal, S. & Wood, M.J.A. (2011). Delivery of siRNA to the mouse brain by systemic injection of targeted exosomes. *Nat. Biotechnol.*; **29**: 341–345.
385. Kuwabara, Y., Ono, K., Horie, T., Nishi, H., Nagao, K., Kinoshita, M., *et al.* (2011). Increased microRNA-1 and microRNA-133a levels in serum of patients with cardiovascular disease indicate myocardial damage. *Circ Cardiovasc Genet*; **4**: 446–454.
386. Lee, S.-J., Reed, L.A., Davies, M.V., Girgenrath, S., Goad, M.E.P., Tomkinson, K.N., *et al.* (2005). Regulation of muscle growth by multiple ligands signaling through activin type II receptors. *Proc. Natl. Acad. Sci. U.S.A.*; **102**: 18117–18122.
387. Amthor, H., Nicholas, G., McKinnell, I., Kemp, C.F., Sharma, M., Kambadur, R., *et al.* (2004). Follistatin complexes Myostatin and antagonises Myostatin-mediated inhibition of myogenesis. *Dev Biol*; **270**: 19–30.